REPORT DOCUMENTATION PAGE

READ INSTRUCTIONS BEFORE COMPLETING FORM

1. REPORT NUMBER: DTNSRDC-82/011	2. GOVT ACCESSION NO.: AD-A118688
3. RECIPIENT'S CATALOG NUMBER:	
4. TITLE (and Subtitle): THE SPECTRAL OCEAN WAVE MODEL (SOWM), A NORTHERN HEMISPHERE COMPUTER MODEL FOR SPECIFYING AND FORECASTING OCEAN WAVE SPECTRA	5. TYPE OF REPORT & PERIOD COVERED: Final Report
	6. PERFORMING ORG. REPORT NUMBER:
7. AUTHOR(s): Willard J. Pierson	8. CONTRACT OR GRANT NUMBER(s): N00167-80-M-4781
9. PERFORMING ORGANIZATION NAME AND ADDRESS: CUNY Institute of Marine and Atmospheric Sciences, The City College of the City University of New York, New York, N.Y. 10031	10. PROGRAM ELEMENT, PROJECT, TASK AREA & WORK UNIT NUMBERS: (See reverse side)
11. CONTROLLING OFFICE NAME AND ADDRESS: Ship Performance Department (1568) Bethesda, Maryland 20084	12. REPORT DATE: July 1982
	13. NUMBER OF PAGES: 201
14. MONITORING AGENCY NAME & ADDRESS (if different from Controlling Office)	15. SECURITY CLASS. (of this report): UNCLASSIFIED
	15a. DECLASSIFICATION/DOWNGRADING SCHEDULE:

16. DISTRIBUTION STATEMENT (of this Report)

APPROVED FOR PUBLIC RELEASE: DISTRIBUTION UNLIMITED.

17. DISTRIBUTION STATEMENT (of the abstract entered in Block 20, if different from Report)

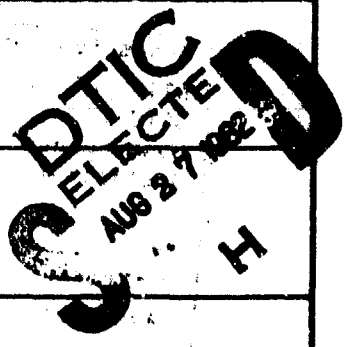

18. SUPPLEMENTARY NOTES

19. KEY WORDS (Continue on reverse side if necessary and identify by block number)

Ocean Waves
Spectral Ocean Wave Model
Hindcast
Forecast
Seakeeping
Ship Design

20. ABSTRACT (Continue on reverse side if necessary and identify by block number)

The Spectral Ocean Wave Model (SOWM) in use at the Fleet Numerical Oceanography Center since 1974 has been used to produce spectra for a 20-year ocean wave climatology for the Northern Hemisphere oceans. The data sources and concepts used to develop the computer model are described; and the equations and computer program structure for the model are given in this report. The accuracy of the model is evaluated by analysis of

(Continued on reverse side)

(Block 10)

Project Element 62759N
Block Number SF-59-557
Work Unit Numbers 1500-382, 1500-300, and 1568-838

Work Request Number NA80DA-G00215 (NOCD-Asheville, N.C.)
Work Unit Number 1568-844

(Block 20 continued)

studies that used spacecraft radar altimeter measurements of significant wave height and by comparison of predicted and estimated frequency spectra and significant wave heights. This report also describes sampling variability effects and incorporates them into the interpretation of the accuracy of the model specifications. In addition, rapid spatial and temporal variations of actual waves that are not reproduced by the model are documented; and possible errors in the specification of swell are suggested. With care in interpretation, a SOWM wave climatology, which is in preparation, should prove to be more accurate than those based on conventional ship reports.

TABLE OF CONTENTS

LIST OF FIGURES

Page

Page

Page

LIST OF TABLES

Page

ABSTRACT

The Spectral Ocean Wave Model (SOWM) in use at the Fleet Numerical Oceanography Center since 1974 has been used to produce spectra for a 20-year ocean wave climatology for the Northern Hemisphere oceans. The data sources and concepts used to develop the computer model are described; and the equations and computer program structure for the model are given in this report. The accuracy of the model is evaluated by analysis of studies that used spacecraft radar altimeter measurements of significant wave height and by comparison of predicted and estimated frequency spectra and significant wave heights. This report also describes sampling variability effects and incorporates them into the interpretation of the accuracy of the model specifications. In addition, rapid spatial and temporal variations of actual waves that are not reproduced by the model are documented; and possible errors in the specification of swell are suggested. With care in interpretation, a SOWM wave climatology, which is in preparation, should prove to be more accurate than those based on conventional ship reports.

ADMINISTRATIVE INFORMATION

The work reported herein was conducted in support of the David W. Taylor Naval Ship Research and Development Center (DTNSRDC) under Contract No. N00167-80-M-4781. It was funded under Program Element 62759N through the Surface Wave Spectra for Ship Design Block Program SF-59-557 for which DTNSRDC is the lead laboratory and under the Naval Oceanography Command Detachment (Asheville, N.C.) Work Request Number NA80DA-G00215. At DTNSRDC it is identified with Work Unit Numbers 1500-382, 1500-300, 1568-838, and 1568-844, respectively.

METRIC EQUIVALENCY TABLE

Throughout this report, those values given in the original source in non-metric units have usually been provided with their metric equivalents in parentheses or by means of duplicate scales. For completeness, this brief conversion table is provided.

To convert from	To	Multiply by
degrees latitude	kilometers	111.1
feet	meters	0.3048
knots	meters per second	0.514
millibars	kilo Pascals	0.1
nautical miles	kilometers	1.852

INTRODUCTION

The Spectral Ocean Wave Model (SOWM) is a computer-based procedure for forecasting and specifying (hindcasting) the spectra of ocean waves in deep water at a stated angular and frequency resolution for a grid of points on a global scale.[1,2,3*] Its three precursors were Hydrographic Office Pub 603,[4] which was the first (hand graphical) spectral wave forecasting model; an attempt to computerize the techniques of Hydrographic Office Pub 603;[5] and parallel research in France which evolved in steps to the DSA 5 model for the North Atlantic.[6] Presently, the SOWM, which became operational[3] in December 1974, is used daily at the Fleet Numerical Oceanography Center (FNOC) to nowcast (specify) the waves on the basis of observed winds every 6 hours and to forecast the waves every 12 hours for up to 72 hours by means of forecasted winds. Forecasts and nowcasts are made for the Northern Hempsphere oceans only and do not include swell that has propagated into the Northern Hemisphere from the Southern Hemisphere. The winds of the Southern Hemisphere are not known with sufficient accuracy to permit either hindcasts or forecasts.

Wave spectra have been produced by means of the presently operational SOWM at FNOC. Meteorological data on winds and weather for some of the years in the data base over the Northern Hemisphere were reanalyzed and used to compute improved wind fields over the ocean.[7] These winds were, in turn, used to compute wave spectra for the grid of points of the SOWM.[7]

The final product of this activity is to be a spectral wave climatology for the Northern Hemisphere, which is to be published and disseminated by the Naval Oceanography Command Detachment (Asheville, North Carolina). In anticipation of the publication of this climatology, one purpose of this report is to provide a description of the SOWM in terms of the theories and programs that are available. Another purpose is to provide quantitative information on how well the model specified the waves. The comparison of the data from the climatology with wave observations is limited to only a few examples. Other examples of the comp... of other wave model data to wave observations are given to suggest ways to cor... the wave climatology to actual data for additional verification purposes.

*A complete listing of references is given on page 179.

DEVELOPMENT OF THE SPECTRAL OCEAN WAVE MODEL

GENERAL COMMENTS

The development of the SOWM required as a precursor an adequate description, based on observation, experiment, and reasoning, of the waves on the ocean. A description of waves based on observation and reasoning is a theory;[8] and a wave forecasting model based on experiment and observation is empirical.[8] The SOWM has been called "a physical-empirical model,"[9] and a "semi-empirical (model) in which the theoretical developments can be accommodated in the best tradition of engineering."*[10] There do not seem to be any theories about the physical world that are not based on observation and experiment, and, thus, all theories are ultimately empirical.

If observations and experiments do not agree with a theory, one possibility is that the theory is incorrect. The other is that the observations were incorrect and that the experiment was not properly designed. One might wish to derive an entire theory of waves starting with the (empirical) hydrodynamic equations of motion; however, a theory derived from this basis will be a long term effort.

MEASUREMENTS AND ANALYSES

The ability to estimate the spectrum of the waves from an ocean wave record was the essential first requirement for the development of the SOWM.[11,12] The concepts that: (1) a wave record is a sample from a population, (2) the frequency spectrum resolves the total variance of the random process into frequency bands, (3) it is an "estimate" of the true spectrum, and (4) sampling variability can be substantial are all essential in understanding waves, wave forecasting, and verification of wave forecasts.

Wave records and spectral analysis techniques for these records were also needed. It was recognized that conventional ship reports of wave height and period were virtually useless,[1] as confirmed in recent studies,[9] and so the SOWM was based upon the only high quality data then available, which were waves measured by the Tucker Shipborne Wave Recorder,[13] as archived by the National Institute of Oceanography in Great Britain (now the Institute of Oceanographic Sciences). The data that were used were spectrally analyzed, corrected for high frequency response, and published as a series of three reports.[14] Each of the spectra that were analyzed were also provided with upper and lower 90 percent fiducial confidence intervals,

---

*"Engineering: science, work or profession of an engineer".[8]

with the total degrees of freedom of the estimate of the variance, and with confidence intervals on the significant wave height. (See Figure 12.9 of Reference 15). These data have been used in numerous studies at DTNSRDC.

The spectra hindcasted, specified, and predicted by the SOWM have never been verified. The handful of scientifically measured wave properties from which directional spectra can be estimated are too few to permit attempts to verify the SOWM. There have been no direct quantitative comparisons of directional spectra estimated from wave data with SOWM spectra, but this may soon become possible because some properties of directional spectra may become available from the National Data Buoy Network.

Time histories of measured waves yield estimates of frequency spectra to be compared with the SOWM product summed over direction. A 20 minute wave record does not provide precise information on the wave spectrum. Typically, a spectral estimate is not known to within a factor of two. The significant wave height, estimated from a 20 minute wave record, is typically unknown to within ± 10 percent to ± 20 percent. Verification of the significant wave heights and the frequency spectra from the SOWM require the careful consideration of sampling variability effects. Random effects cannot be predicted; only averages of random effects can be interpreted by means of statistical procedures. If frequency spectra estimated from wave data agree within sampling variability effects with a corresponding SOWM frequency spectrum, then the model is only partially verified. Many different directional spectra could have produced the same frequency spectrum. Conversely, if the model frequency spectra and the estimated frequency spectrum do not agree, then some part of the model is incorrect.

BOUNDARY LAYER WINDS

Forecasting ocean waves has always required knowledge of the winds over the ocean. In general, prior to the SOWM, these winds were both inadequately measured and inadequately analyzed. Efforts to define the winds more accurately over the ocean received new insight in the work of Thomasell and Welsh,[16] who first corrected wind fields for the wide variation in the heights of anemometers on weather ships. The development of an adequate planetary boundary layer model to specify and predict the winds as a function of height above the ocean with greater accuracy was an integral part of the development of the SOWM.[17] Among its accomplishments was the correction of all wind speeds to an effective neutral wind

at 64 feet* for all ship reports where the anemometer heights were known. The SOWM requires winds measured at 64 feet* above the sea surface corrected for the effects of atmospheric stability.

The improved boundary layer models that resulted from this research contribute to the improved wave specifications and forecasts of the SOWM. However, errors in the wind fields used by the SOWM both for wave specification and forecasting and for this wave climatology are probably the greatest source of errors in the wave specifications and forecasts. Recent studies of this problem have provided new insight and perhaps better observational and analysis techniques will be forthcoming soon.

THE GAUSSIAN WAVE MODEL

The theories upon which the SOWM is based are those with a short-crested gaussian sea surface as a model as summarized by Kinsman[18] and Neumann and Pierson.[15] This requires the description of the waves by means of either a spectrum as a function of frequency and direction or a vector wave number spectrum.[19] Nonlinear, and hence nongaussian,[20,21,22] wave properties have been studied in some detail and corrections to both the spectrum and the form of the waves are possible to a certain extent by means of these results.

FULLY DEVELOPED SEAS

One of the concepts in the SOWM is that of a fully developed, wind-generated sea for which the wave spectrum is independent of fetch and duration and is a function of the wind speed only. The form of the spectrum is based on the analysis of the shipborne wave recorder data described above.[14] The fully developed spectrum[23] is defined as a function of the speed of the wind for a neutrally stratified atmosphere as measured at 19.5 meters because this was the height of the anemometers on the ships that measured the waves.[24] This definition avoided the problem of referring the wind to 10 meters by means of a boundary layer model at the time; however, the problem has not gone away. Careful attention to the fact that the height of a fully developed sea had been related to winds measured at different anemometer heights partially reconciled the differences that were present at the time.[24,25] The spectrum for a fully developed sea used in the SOWM has been verified by numerous investigators as to its general form, but some slight differences in the constants can be found in the literature.

*64 feet = 19.5 meters.

There have been a number of investigations that show that the high frequency gravity wave spectrum is wind speed dependent.[26,27] The very short gravity waves measured in tropical storms for example are much higher than would be modeled by the spectrum originally used for the SOWM.[2] Corrections for the high frequencies have been incorporated in the present SOWM.

WAVE GENERATION

Also needed for the SOWM were improved theories for the generation of waves by winds and those of Phillips,[28] Miles,[29] and Phillips[30] were experimentally modified to agree with observed spectral growths.[31] This particular aspect of the SOWM has been questioned from the very beginning, and the fact that the SOWM does not incorporate the theoretical effects of third order nonlinear wave interactions is one of the major differences between it and more recent spectral wave forecasting models.[32,33]

SWELL

It has been thoroughly demonstrated that waves generated by an area of high winds are dispersive as they propagate as swell into areas of relative calm.[34,35] The kinetic and potential energy in a wave system propagates at the group velocities of the spectral components. Even the most casual observation of wind-generated waves on the deep ocean will convince one that an individual wave cannot be followed for very long. Debatable at the time of the development of the first wave forecasting methods was whether or not frequency and angular dispersion were all that was needed to forecast swell. If additional attenuation was needed, it was difficult to quantify, and in fact, one of the most careful studies found little, or no, effect.[35]

DISSIPATION

As extratropical cyclones pass a given point on the ocean, the waves seem to be traveling in the direction of the wind, even as the wind shifts continuously to all points of the compass. Conversely, in areas of light winds, wave trains traveling in many different directions can be seen. The SOWM required some way to keep the wave spectrum from becoming isotropic in areas of rapidly changing high winds and wind directions. There was very little theoretical guidance (and even today, there is still not much), so this effect was modeled by the dissipation term in the SOWM described later on in this report.

COMPUTER EXPERIMENTS

The SOWM is also based upon experiment. These experiments were computer experiments with the model to see how different assumptions about initial conditions affected the growth of the spectrum and computer tests using the winds over the North Atlantic generated by a boundary layer wind field to see how well the model specified the waves measured at a British weather ship and the frequency spectra computed from these measured waves. Figures 3, 4, and 5 of Pierson, Tick, and Baer[1] illustrate some of the first experiments to study the effect of dissipation in the model and various growth equations.

There have been numerous changes in the SOWM since it was first described in 1966. The equations actually used at present will be documented in the following sections.

DATA FROM SPACECRAFT

At the time the SOWM was developed, the techniques for measuring winds and waves from a spacecraft were in their first stages of formulation[1] and the concepts were ambiguous.[36] An experiment on SKYLAB demonstrated that wind speed could be determined by measuring the roughness of the ocean with a radar on a spacecraft.[37] SEASAT demonstrated that wind speed and direction could be accurately determined from sea surface roughness measurements.[38,39,40] The altimeters on GEOS-3 and SEASAT measured changes in the return altimeter wave form from which significant wave height could be computed along the subsatellite track.[41,42,9] The Synthetic Aperture Radar (SAR) on SEASAT obtained images of low waves that were processed to yield something like, but not exactly, directional wave spectra.[43] These data (to be discussed in a later section) have been used to see how well various wave forecasting models compare with Northern Hemisphere wave measurements.[9,42,44,45]

The sparsity of high quality data on waves and winds on a global scale, so that waves can be described more accurately and climatologies of <u>actual</u> wave measurements can be generated, may end in the decade of the 1980s. By the year 2000, the waves on the ocean may be much better understood. Until then, the products of the SOWM can help to fill the present void.

DESIGN OF THE SPECTRAL OCEAN WAVE MODEL

There are many different computer based models of the atmosphere in existence for forecasting the atmospheric circulation.[46] A few are operational at the national centers for weather forecasting. There have been many different wave forecasting

models developed other than the SOWM, such as the sequence of DSA models,[6] and a large number of newer ones for limited areas.[47,48,49,50*] There are even special modifications of the SOWM.[51] None of these were designed from the beginning to be global in nature. No two weather forecasting models are alike, yet they all perform fairly well. The lifetime of a weather forecasting model is typically only a few years before it is superseded by an improved model. There are ways to improve the SOWM by means of higher spectral resolution, additional wave measurements, an improved treatment of island effects, and computer experiments. The comparison of different models with each other without, at the same time, comparing them with actual wave data is not as productive as comparing various models with actual wave measurements.

The SOWM was designed with definite objectives, and, at the same time, substantial restrictions on the allotted computer facilities and the time available for an update and a forecast. As originally planned, there were to have been four times as many grid points and twice the angular resolution for the spectra. The computer program for this higher resolution model exists, but it is not operational. Running time and memory allocation constraints made it necessary to reduce the number of grid points and decrease the angular resolution.

The design of the SOWM can be stated as a set of objectives to be met by the final computer program for the wave specification and forecasting model. The statement would be as follows:

Within certain computer resources and within assigned time constraints, develop a wave specification and forecasting procedure that will describe the frequency-direction spectrum of the waves in deep water, with a reasonable resolution on a grid of points over the oceans of the world, given the winds and forecasts of the winds, by using physically realistic equations that account for the growth of the waves, under the action of the wind, dissipation effects, and wave propagation on a sphere.

The grid of points was laid out on gnomonic subprojections on an isosohedron so as to allow great circle propagation. The spectrum was resolved into 15 frequency bands of different band widths and 12 thirty-degree direction bands. The time step was finally chosen to be 3 hours consistent with the availability of synoptic scale wind information over the Northern Hemisphere (at least).

---

*As examples.

Once the grid, the spectral resolution, and the time step are chosen, the rest of the problem can be stated in a simpler way: given that the spectrum is correct at all grid points at the time $t = t_o$, and given the winds at each grid point for the next 3 hours (each a constant speed and direction), compute what the spectrum will be at each grid point 3 hours later.

In the SOWM, this is accomplished (1) by computing how much the wind generated sea will increase or grow (if at all) during the next 3 hours at each grid point, (2) by computing by how much the waves traveling against the wind (± 90 degrees) will be dissipated, and (3) by computing how far each spectral component will propagate at a representative group velocity along a great circle path in 3 hours and then reassembling the spectra for the end of the time step.

For brevity, these steps are called "Grow, Dissipate, and Propagate." At the end of the 3 hour time step, within the resolution of the model, the new spectra at the grid points now represent the waves at $t = t_o + 3$ hours; new winds can be used, and the processes of Grow, Dissipate, and Propagate can be repeated.

The SOWM has to be started up at some time. At that time, the spectra are not known, nor for that matter are they even known as observed (computed from measured wave properties) functions at all of the grid points of the model. For this climatology, the SOWM was started up in the summer with zero values for all spectral components. After a week or so, (real time), the spectra become believable and were used in the climatology. The run for a preceeding year would, of course, overlap in time the start up for a following year since the wind fields did not become available in chronological order.

For wave forecasts, the SOWM is reinitialized every 6 hours by using 6 hour-old spectral data and computing how the spectra changed on the basis of wind fields computed from the available synoptic weather reports. Then, wave forecasts are made by means of forecasted wind fields. Each wave forecast depends upon both the accuracy of the past wind fields used to reinitialize the model and on the accuracy of the wind field forecasts. Wind field forecasting errors do not enter as an error source for the SOWM wave climatology given in this document.

UNITS

The units of the SOWM, used more or less consistently throughout, are feet for wave height; $feet^2$ for variances; $feet^2$-seconds for frequency spectra; $feet^2$-seconds-$radians^{-1}$ for directional spectra; knots for wind speed and the group

velocity of spectral components; nautical miles and degrees of latitude for distance; seconds, minutes, and hours for time; and seconds^{-1} for frequency. Conversion to metric units would be facilitated if angles were expressed in "grads" for latitude and longitude.

THE MAP PROJECTION AND THE GRID

The SOWM grid is constructed upon an icosahedron, which is a solid bounded by 20 equilateral triangles.[52] For each of the 20 triangles, a gnomonic projection is used. Thus, a straight line with any orientation on any of the 20 subprojections is a great circle. On the sphere, the sides of the equilateral spherical triangle intersect at an angle of 72 degrees, and, thus, 5 triangles meet at a common point. On a map, the sides of the equilateral triangle meet at an angle of 60 degrees.* Table 1 gives the pertinent data for the triangles.[2]

The triangles are not oriented in a simple way relative to the latitudes and longitudes on the earth. Instead, the icosahedron was located so as to maximize the number of vertices on land. Figure 1 shows the 20 triangles as their vertices and edges appear on a Mercator projection. Each triangle covers exactly the same area, and the marked area distortion of a Mercator projection is evident.

Two sides of a triangle form a natural set of axes for each subprojection and the grid of points at which the SOWM spectra are computed is formed by the intersections of equally spaced lines drawn parallel to the two chosen sides of each subprojection (as shown in Figure 2).[1] Each grid point, in principle, ought to be representative of wave spectra anywhere within the hexagon surrounding the grid point.

The great circle property is indicated by the fact that waves can travel to a given grid point along a great circle path from any one of the six surrounding grid points, thus accounting for six of the 12 direction bands in the model. The other six direction bands have directions of travel halfway between those for each of the primary directions. These spectral components are effectively treated as if they come from a source on the inner hexagon surrounding each grid point at a point halfway between two grid points. The distance involved is thus only about 85 percent of the primary distance (as shown in Figure 3).[2]

---

*If each triangle is plotted as a gnomonic projection.

TABLE 1 - PROPERTIES OF THE GNOMONIC PROJECTION ON A FACE OF AN ICOSAHEDRON*

Area, 1/20th of the Earth's surface	7.45×10^6 square nautical miles (25.55×10^6 square kilometers)
On the Earth:	
Length of side	63°26.1' or 3806 nautical miles (7068 kilometers)
Length of altitude	58°16.9' or 3497 nautical miles (6476 kilometers)
Vertex angle (spherical)	72 degrees
On the Plane:	
Length of side	4552 nautical miles (8430 kilometers)
Length of altitude	3942 nautical miles (7300 kilometers)
Vertex angle	60 degrees
Distortion relative to 1.00 at the tangent point:	
Radial - maximum (at vertices)	1.58
- mean (midpoints of sides)	1.15
Transverse - maximum	1.26
- mean	1.07
Areal - maximum	1.99
- mean	1.23
Distortion relative to 1.00 at the midpoints of the sides (location of mean distortion):	
Radial - maximum (at vertices)	1.37
- minimum (at tangent point)	0.87
Transverse - maximum	1.18
- minimum	0.93
Areal - maximum	1.62
- minimum	0.81

*Assumes spherical Earth of radius 3440.19 nautical miles (6370.66 kilometers).

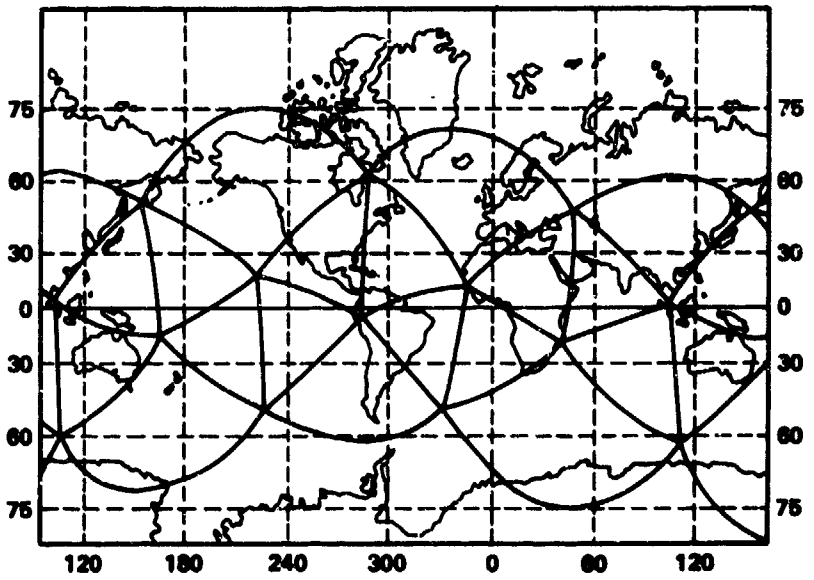

NOTE: All triangles are the same size on the Earth, but the Mercator projection distorts them. Portions of the Earth are repeated twice. The triangles that cover the poles actually have only three sides. (From Reference 2.)

Figure 1 - The Twenty Equilateral Triangles of the Icosahedral Gnomonic Projection of the Spectral Ocean Wave Model

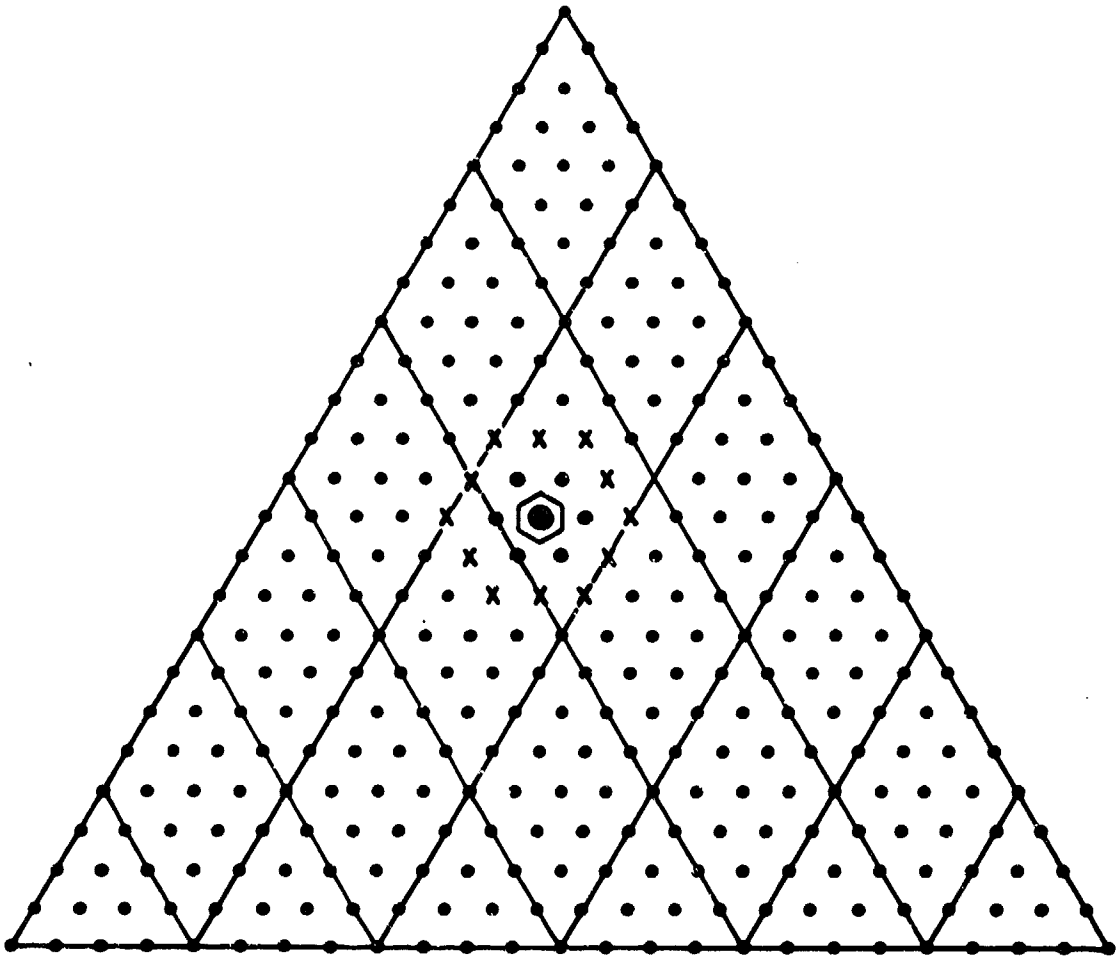

NOTE: Any straight line is a great circle. The hexagon around the circled dot shows the area represented by a grid point. The inner hexagon of heavy dots and the outer hexagon of X's show those grid points required to treat wave propagation effects at the circled point.

Figure 2 - The 325 Grid Points on a Triangular Gnomonic Subprojection for the Spectral Ocean Wave Model

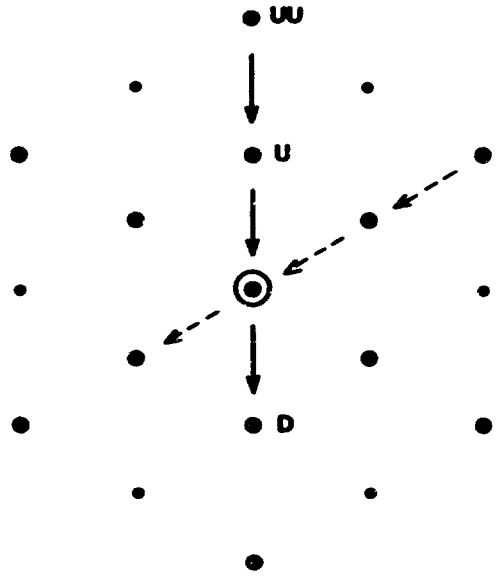

Figure 3a - Six Primary Directions

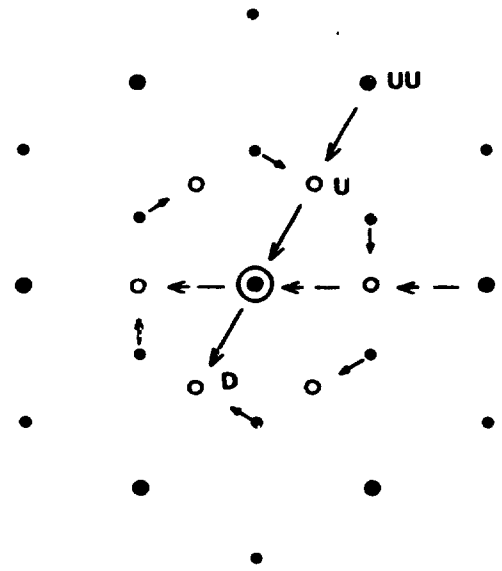

Figure 3b - Six Secondary Directions

NOTE: The large dots on the left are for the six primary directions. For the circled point a downward propagating spectral component requiring an upstream point, an upper upstream point and a downstream point are shown. For secondary directions, the points on the inner hexagon are treated as if located at the open circles for one time step. The shift is reversed for the next time step.

Figure 3 - Grid Points Involved in Propagation

The great circle propagation property is not without its price, which has to be paid in the rather complicated details of the propagation subroutine of the model. The distances from one grid point to its neighbors vary as a function of the location of the grid point on the subprojection. The true Earth distances between grid points are smaller near the vertices and farther apart near the centers of the subprojection. These varying distances must be accounted for in the propagation of each spectral component.

Also, the great circle orientation of the grid points changes from one triangle to the next. This property of the grid requires some complicated steps so that the waves can cross over the edge from one triangle to an adjacent triangle.

Figure 4 shows some of the grid points of the SOWM that were used for the production of this wave climatology. The triangular subprojection that covers the Indian Ocean (not shown in Figure 4) has been relocated for the operational version so as to cover more evenly that part of the Indian Ocean north of the Equator. For the Northern Hemisphere, the Indian Ocean is isolated from the other oceans so that the change has no effect on the model. (See Figure 1.)

Rows of points along the six primary directions can easily be identified. Rows of points along the six secondary directions can also be identified. Some interesting features of great circle propagation and of the way the triangular subprojections interact can be seen. As examples, waves that approach Scotland coming from the west-northwest could have been generated in an area of high winds south of Greenland and due west of Ireland and could have started out traveling toward the east-northeast. The lines of points that cross a triangle near the center of one of the sides do not change direction from one subprojection to the other by very much. Thus, swell approaching the border between Washington and Oregon from due west could have started out from a typhoon to the east of the Phillipines and north of New Guinea. One row of grid points lies just to the east of the 180th meridian. It runs as practically a straight line north-south along a longitude line, which, of course, is a great circle. A study of the grid point patterns in this figure illustrate many other interesting features of great circle propagation over long distances.

Many of the hand-graphical analyses of wind fields and fetches are made on polar stereographic map projections. The above material suggests that sources of waves identified by such analyses may be incorrect.

Figure 4 - Spectral Ocean Wave Model Grid Points Plotted on a Mercator Projection

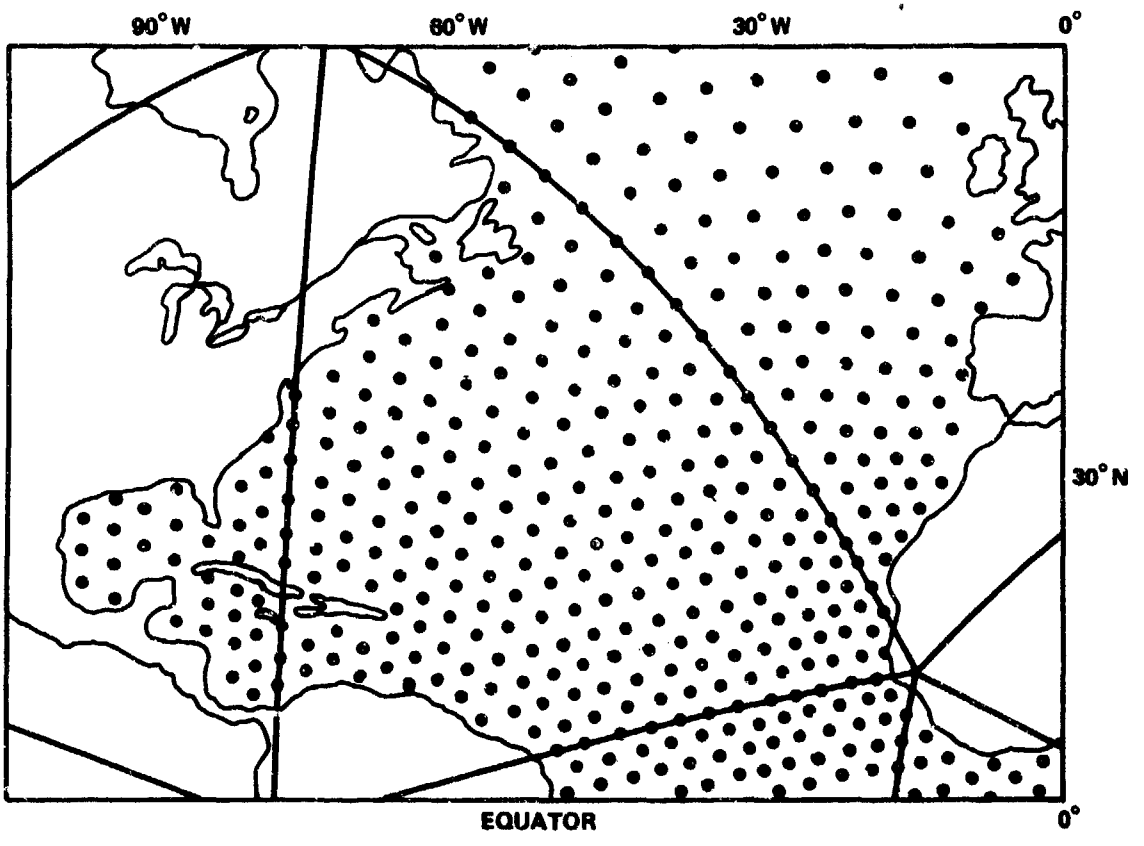

Figure 4a - Spectral Ocean Wave Model Grid Points for a Portion of the North Atlantic Ocean Plotted on a Mercator Projection Showing the Boundaries of the Triangular Subprojections

Figure 4 (Continued)

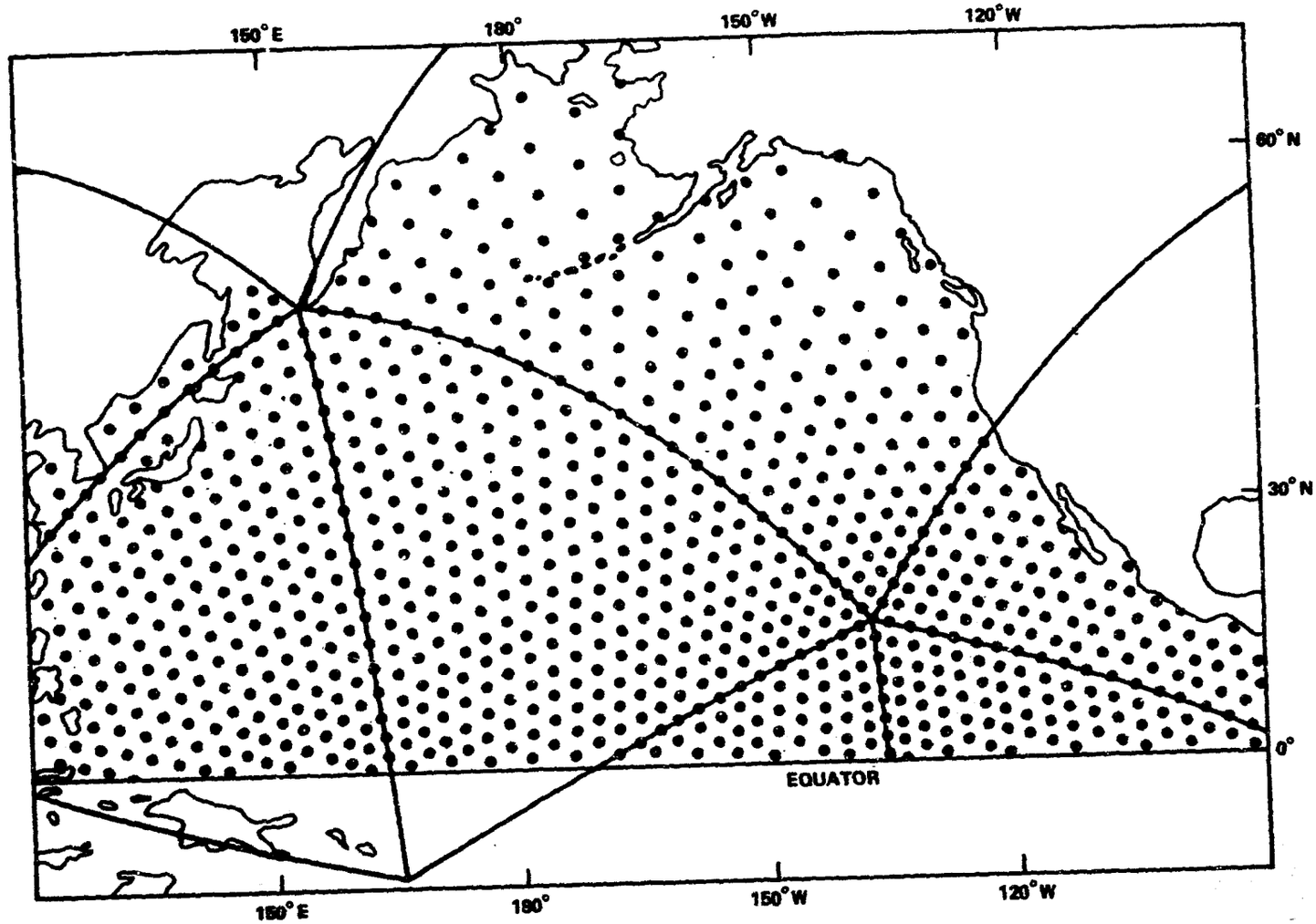

Figure 4b - Spectral Ocean Wave Model Grid Points for Part of the North Pacific Plotted on a Mercator Projection Showing the Boundaries of the Triangular Subprojections

Each triangular subprojection in the SOWM has 25 grid points, equally spaced on the gnomonic projection, along each side. There are a total of 325 (25(25 + 1)/2) grid points in the triangle, of which 72 are on the edges. Those on the edges are used twice, and information about the waves in midocean is repeated for five different triangles at their common point. There are about 1,575 grid points for the Northern Hemisphere for which the spectra are computed. The land points within each subprojection are assigned a coded flag to identify them. Grid points just south of the Equator are treated as an artificial land boundary to provide appropriate sinks for southbound spectral components and artifically fetch limited waves for southerly winds at the Equator. No swell from the Southern Hemisphere exists in the model, although it could actually be appreciable just north of the Equator during the Southern Hemisphere winter.[35]

THE SPECTRAL OCEAN WAVE MODEL SPECTRA

THE FREQUENCY-DIRECTION ARRAY

The spectra in the SOWM represent integrals over certain frequency and direction bands of a continuous function of frequency and direction, $S(f,\theta)$, that would be the spectrum with infinite resolution (unattainable) at each grid point. There are 15 frequency bands and 12 direction bands so that the spectrum at each grid point is represented by 180 numbers with units of $(\text{feet})^2$ as in Equation (1).*

$$S(f_i,\theta_j) = \int_{f_i - \Delta f_i/2}^{f_i + \Delta f_i/2} \int_{\theta_j - \Delta\theta_j/2}^{\theta_j + \Delta\theta_j/2} S(f,\theta)\, d\theta df \qquad (1)$$

The values of f_i are not equally spaced on the frequency axis. More resolution is provided for lower frequencies than for intermediate and higher frequencies. The θ_j are 30 degrees apart and the $\Delta\theta_j$, are all 30 degrees. On the gnomonic grid, the angles are constant, but in Earth coordinates, the angular bounds for the direction bands change continuously as a component propagates along.

The wave data that were analyzed in developing the SOWM were digitized every 1.5 seconds and the spectra were estimated for 60 bands between zero frequency and a Nyquist frequency of 1/3. The elemental frequency band was therefore 1/180

*To convert to $(\text{meters})^2$, multiply by 0.0929.

second^{-1}. The center frequencies for the bands are simply integers, or integers plus one half, times this elemental band.[14]

Table 2 shows the band number assigned to each frequency, the bandwidth (x180), the central frequency (as a fraction and in decimal form), and the frequency range covered by the particular band. The contribution to the spectrum for frequencies above 0.375 hertz is negligible for wave height calculations.

Earlier versions of the SOWM had different frequency bands. Also, the highest frequency band was carried to infinity at the high frequency end. In both the current model and the past model, the highest frequency band is in instantaneous equilibrium with the local wind speed and direction and is not propagated.[2*]

For many applications, it is necessary to have the spectral values. The numbers in the output should be divided by the bandwidth, and if in directional form by $\pi/6$, to obtain spectral values in units of feet^2-second-radians^{-1}.

The lowest possible frequency in the model, corresponding to a period of 27.7 seconds, was chosen on the basis of frequency analyses of wave records reported to the National Institute of Oceanography (NIO). Frequencies this low, or periods this long, had not been detected in any of the wave data analyzed up to that time. Such low frequencies require extremely high winds, long durations, and large fetches for their generation.

THE FREQUENCY SPECTRA

The sum over all directions at a fixed frequency as in

$$S(f_i) = \sum_{\theta_j} S(f_i, \theta_j) \tag{2}$$

is the equivalent of

$$S(f_i) = \int_{f_i - \Delta f_i/2}^{f_i + \Delta f_i/2} \int_{-\pi}^{\pi} S(f_i, \theta)\, d\theta df \tag{3}$$

The frequency spectra can be compared with spectra estimated from wave recordings as a function of time at a fixed point. It is important to compare the spectra band

*Band 2, $f_i = 37.5/180$ is also treated this way.

TABLE 2 - BAND NUMBER, BAND WIDTH, CENTRAL FREQUENCY (AS A FRACTION AND A DECIMAL), PERIOD, AND BANDWIDTH BOUNDS

Band Number	Band Width x 180	Central Frequency	f_i	T_i	Lower Bound x 180	Upper Bound x 180
1	24	55.5/180	$0.30833\overline{3}$	3.24	43.5	67.5
2	12	37.5/180	$0.20833\overline{3}$	4.8	31.5	43.5
3	6	28.5/180	$0.15833\overline{3}$	6.32	25.5	31.5
4	3	24.0/180	$0.13333\overline{3}$	7.5	22.5	25.5
5	3	21.0/180	$0.11666\overline{6}$	8.57	19.5	22.5
6	2	18.5/180	$0.10277\overline{7}$	9.73	17.5	19.5
7	2	16.5/180	$0.09166\overline{6}$	10.91	15.5	17.5
8	2	14.5/180	$0.08055\overline{5}$	12.4	13.5	15.5
9	1	13.0/180	$0.07222\overline{2}$	13.85	12.5	13.5
10	1	12.0/180	$0.066\overline{6}$	15.0	11.5	12.5
11	1	11.0/180	$0.0611\overline{1}$	16.4	10.5	11.5
12	1	10.0/180	$0.055\overline{5}$	18.0	9.5	10.5
13	1	9.0/180	$0.050\overline{0}$	20.0	8.5	9.5
14	1	8.0/180	$0.044\overline{4}$	22.5	7.5	8.5
15	1	7.0/180	$0.038\overline{8}$	25.7	6.5	7.5

for band, as variances, for each band with the variable bandwidth that are used in the SOWM.[53]

For many practical applications, the SOWM spectra should be treated as a three dimensional histogram-like figure with the constant spectral value assigned over the polar co-ordinate plane in the region $f_i - \Delta f_i/2$ to $f_i + \Delta f_i/2$ and $\theta_j - \Delta\theta_j/2$ to $\theta_j + \Delta\theta_j/2$. It could be envisioned as being something like a cross between the giants causeway in Ireland and the ruins of a Roman ampitheater after an earthquake.

The values of the θ_j in the SOWM output represent the direction <u>from which</u> the spectral component came in degrees clockwise from north. Each subprojection of the SOWM has its own direction coordinate system and the output must be transformed to Earth directions.

SIGNIFICANT WAVE HEIGHT

A further summation of (3) over the 15 frequency bands yields, within a linear model, the variance of a time history of a wave record, or the area under the frequency spectrum, with units of feet^2. The "E" value in HO Pub 603 was twice the variance, and care should be taken to distinguish between the two.[4] With the further assumption that the spectrum is more or less narrow band and that the envelope of individual cycles in the wave record has a Rayleigh distribution, the significant wave height can be computed. The significant wave height is defined to be Equation (4).

$$H_{1/3} = 4.00 \ (\Sigma \ S(f_i))^{\frac{1}{2}} = 4 \ (m_o)^{\frac{1}{2}} \qquad (4)$$

The constant is not exactly four, differing from it at the fourth significant figure, but sampling variability effects for the estimation of the significant wave height from an ocean wave record so completely mask any calculation to four significant figures that the value of 4 can be used.[54]

By definition, the significant wave height is the average of the heights of the one-third highest waves in an ocean wave time history. The value, 4, is obtained by finding that value of the wave amplitude such that one third of the wave amplitudes exceed this value, normalizing the tail of the Rayleigh distribution to unity above this amplitude, calculating the expected value of the amplitude for this truncated distribution, and doubling it to get the significant wave height.

Recently some questions have arisen as to whether or not the significant wave height as defined above corresponds to the value that would be obtained by tabulating the wave heights in an actual wave record and computing the significant wave height from the one-third highest tabulated values. These questions in turn raise additional questions about whether or not the Rayleigh distribution actually fits wave data.[21,54,55]

These questions are far from being quantitatively resolved, and the above definition does fit most wave records reasonably well. In extreme seas, the high waves corresponding to the tail of the distribution may be reduced in height by breaking at the crests as they form. The significant wave height computed from Equation (4) would then be an over estimate of the significant wave height.

THE FULLY DEVELOPED SPECTRUM

DETERMINATION OF THE SPECTRUM

If the wind blows with constant speed and direction over a large enough area for a long enough time, the waves should be in equilibrium with the wind with generation and dissipation effects balanced. The spectrum of the waves should be a function of wind speed only, if the added condition that no waves can propagate into the area under analysis from some other part of the ocean is imposed. This condition is difficult to identify in nature. For light winds, waves from elsewhere are usually present; for high winds, the area may not be large enough and the wind may not have blown long enough.

Two subsets of data and wave spectral estimates from NIO were selected for further analysis.[24] One set was selected solely on the basis of the wind speed being near 20, 25, 30, 35, and 40 knots; and all spectra for the same wind speed were averaged. For the second set, the additional constraints that the wind direction could not shift by very much prior to the wave measurement, that the wind had to increase up to the speed used, that it had to have blown for a fairly long time, and that there were no obvious sources of swell present were imposed. All spectra for the same wind speed were averaged for this set also.

The averaged spectra for the two sets were quite different. The second set followed a u^2 law for wave height versus wind speed. The first had waves that were higher than this for low winds and lower for high winds.

If the population from which the samples were drawn is well defined, than all of the spectral estimates for a given frequency band ought to have come from some

chi-square distribution with a known number of degrees of freedom and with an unknown (but estimated from the average) expected value. Spectral estimates for the second set nearly fulfilled this criterion and almost had the correct chi-square distribution over the middle range of frequencies for which they were estimated. The spectra from the first set obviously were not a sample from a well defined population. The result of this study yielded averaged spectra for postulated fully developed seas for winds of 20, 25, 30, 35, and 40 knots.[24]

If the fully developed spectrum exists, it cannot be a function of fetch or duration and must therefore have a nondimensional form, which is a function of a nondimensional frequency as in Equation (5).[56]

$$\bar{f} = f\,u/g \tag{5}$$

A nondimensional spectrum must satisfy Equation (6).

$$\bar{S}(f) = F(\bar{f}) = S(f)g^3/u^5 \tag{6}$$

After an adjustment to account for the variability of the reported winds for each 5-knot class, a form for $F(\bar{f})$ was selected as Equation (7).[23]

$$F(\bar{f}) = ABe^{-B\bar{f}^{-4}}\bar{f}^{-5} \tag{7}$$

From Equations (6) and (5)

$$S(f) = \frac{u^5}{g^3}\,AB\,\frac{g^5}{f^5u^5}\,e^{-Bg^4(u^4f^4)^{-1}} = \frac{ABg^2}{f^5}\,e^{-Bg^4(u^4f^4)^{-1}} \tag{8}$$

Also from

$$f = \omega/2\pi \tag{9}$$

$$S(\omega)\,d\omega = \frac{ABg^2}{\omega^5}\,(2\pi)^4\,e^{-Bg^4(2\pi)^4(u^4\omega^4)^{-4}}\,d\omega$$

The final result is Equation (10).[23]

$$S(\omega)\, d\omega = \alpha g^2 \omega^{-5}\, e^{-\beta(\omega_o/\omega)^4}\, d\omega \tag{10}$$

where

$$\alpha = 8.1 \times 10^{-3} \text{ and } \beta = 0.74$$

and

$$\omega_o = g/u$$

PROPERTIES

This spectrum has many interesting properties. For examples,

$$\text{VAR} = \int_o^\infty S(\omega)\, d\omega = 2.809 \times 10^{-6}\, u^4 \tag{11}$$

and

$$H_{1/3} = 4.00\ (\text{VAR})^{1/2} = 2.12 \times 10^{-2}\, u^2 \tag{12}$$

with u in meters per second and $H_{1/3}$ in meters, where $H_{1/3}$ is the average of the heights of the one third highest waves.

The spectral peak occurs at

$$\omega_m = \frac{g}{u}\left(\frac{4\beta}{5}\right)^{1/4} = 0.877 g/u \tag{13}$$

and has the value

$$S(\omega_m) = 0.765\, \alpha u^5/g^3 \tag{14}$$

Thus, the frequency at the peak varies inversely as the wind speed, the significant wave height varies as the square of the wind speed, the area under the spectrum varies as the fourth power of the wind speed, and the peak of the spectrum increases as the fifth power of the wind speed. As proportionalities, thus,

$$\omega_m \sim u^{-1} \text{ and } d\omega_m \sim u^{-2}\, du$$

$$H_{1/3} \sim u^2 \text{ and } dH_{1/3} \sim u\, du$$

$$VAR \sim u^4 \text{ and } dVAR \sim u^3 du$$

and

$$S(\omega_m) \sim u^5 \text{ and } dS(\omega_m) \sim u^4 du \tag{15}$$

If wave forecasting, contrary to the fact, were to consist simply of relating a fully developed spectrum to the local wind speed at each grid point of a model, some interesting results can be found from Equation (15). For various wind speeds, if the error in the wind speed specification is +2 meters per second, for example, and for winds from 4.83 to 25 meters per second, the percentage errors in the various spectral properties can be very large (as shown in Table 3).

If, for example, the true wind is 4.83 meters per second, and if the spectrum for a 6.83 meters per second is forecasted instead, the wave height will be in error by a factor of two (100 percent error), the area under the spectrum will be four times too large (300 percent error), and the spectral peak will be 5.65 times too high. Similarly, for a true 10.57 meters per second wind, if 12.57 meters per second is forecast instead, the wave height will be 41 percent too high and the area under the spectrum will be twice what it should be. For 13.45 meters per second and 15.45 meters per second the spectral peak will be twice as high as it should be. The shapes of wave spectra and the variances computed from them are thus very sensitive to the accuracy of the winds that generate the waves.

As also shown in Equation (15), the actual errors for increasing wind speed, given the same wind speed error, are strongly wind speed dependent. The error in wind speed is masked as an error in the frequency of the spectral peak which is

TABLE 3 - THE EFFECT OF A 2-METER PER SECOND ERROR IN WIND SPEED ON WAVE SPECTRA AS A FUNCTION OF WIND SPEED

Wind Speed Meters Per Second	$H_{1/3}$ (meters)	Error +2 Meters Per Second	$H_{1/3}$ (meters)	Height Difference (meters)	Percentage Error For				
					Wind	ω_m	$H_{1/3}$	VAR	$S(\omega_m)$
4.83	0.50	6.83	1.00	0.50	41	- 29	100	300	465
5.00	0.53	7.00	1.04	0.51	40	- 28	96	284	437
10.00	2.12	12.00	3.05	0.93	20	- 17	44	107	149
10.57	2.37	12.57	3.35	0.98	19	- 16	41	100	138
13.45	3.84	15.45	5.06	1.22	15	- 13	32	74	100
15.00	4.77	17.00	6.12	1.35	13	- 12	28	65	87
20.00	8.48	22.00	10.26	1.78	10	- 9	21	46	61
25.00	13.25	27.00	15.45	2.20	8	- 7	17	36	47

insensitive to high winds. Height errors increase with wind speed; and spectral properties are very sensitive to wind speed errors.

Another way to show the effect of wind speed on the spectrum is to consider the ratios of ω_m, $H_{1/3}$, VAR and $S(\omega_m)$ for 25 meters per second and 10 meters per second. As the wind increases by a factor of 2.5, ω_m decreases by a factor of 0.4, the wave height increases by a factor of 6.25, the area under the spectrum increases by a factor of 39, and the peak of the spectrum increase by a factor of 97.7.

THE KITAIGORODSKII RANGE

There is some evidence that the saturation range given by $\alpha g^2 \omega^{-5}$ does not really exist at high frequencies. A spectral form given by Equation (16) then describes the gravity wave spectrum at the higher frequencies.[56]

$$S(f) \sim u_* / f^4 \tag{16}$$

For the SOWM with u_* in knots, the proportionality constant is 1.37×10^{-3}. This equation is evaluated for each frequency band; and if it exceeds the corresponding values from Equation (10) (in units of feet^2 with u_* in knots), it is used for the spectral value summed over direction.

Such a representation increases the wave height by very little. For wave slopes and wave curvature properties, these models are inadequate. Some results on wave slope and wave curvature at high frequencies and high wave numbers are available.[26,27]

THE ANGULAR SPREAD OF THE SPECTRUM

The fully developed SOWM spectrum is also a function of direction relative to the wind direction, θ^*. It is represented in full by Equation (17)

$$S(\omega, \theta, u) = \frac{\alpha g^2}{\omega^5} e^{-\beta(\omega_o/\omega)^4} [F(\omega, \theta, u)] \tag{17}$$

where

$$F(\omega, \theta, u) = \frac{1}{\pi}\left\{ 1 + \left[0.5 + 0.82\, e^{-(\omega v/g)^4/2}\right] \cos\left(2(\theta-\theta^*)\right) + 0.32\, e^{-(\omega u/g)^4/2} \cos\left(4(\theta-\theta^*)\right)\right\} \tag{18}$$

for

$$-\frac{\pi}{2} < \theta - \theta^* < \frac{\pi}{2} \text{ and zero otherwise.}$$

The integral of $F(\omega; \theta, u)$ for any ω and u over its range of definition for θ is clearly 1. For small values of ω, the value of F becomes

$$F(0, \theta) = \frac{1}{\pi}\left[1 + 1.32 \cos(2(\theta-\theta^*)) + 0.32 \cos(4(\theta-\theta^*))\right] \quad (19)$$

which is zero at $\theta-\theta^* = \pm \pi/2$; and, for large ω, it becomes

$$F(\infty, \theta) = \frac{1}{\pi}\left[1 + 0.5 \cos(2(\theta-\theta^*))\right] \quad (20)$$

which is $\frac{1}{2\pi}$ at $\theta-\theta^* = \pm \pi/2$.

It should be noted that

$$\frac{8}{3}(\cos\theta)^4 = 1 + \frac{4}{3}\cos 2\theta + \frac{1}{3}\cos 4\theta \quad (21)$$

so that, for low frequencies, Equation (18) varies as essentially as $[\cos(\theta-\theta^*)]^4$. The SOWM spectrum is more peaked for low frequencies.

As alternate form for the angular spread has occurred in the literature as

$$G(\theta) = G_o (\cos\theta/2)^p \quad (22)$$

properly normalized by G_o with values of p around 16 for low frequencies in the spectrum. These two angular spreading functions are compared in Table 4. The slight difference between these functions would be difficult to identify, especially with the resolution of the SOWM.

THE SPECTRAL OCEAN WAVE MODEL SPECTRUM FOR A FULLY DEVELOPED SEA

Equations (17) and (18) can be used to compute the 180 values in the SOWM spectrum exactly for a fully developed sea, as designated by $S_\infty(f_i, \theta_j, u)$ as defined by Equation (1), if the wind speed and direction are known. For example, from Equation (10) with

TABLE 4 - A COMPARISON OF TWO DIFFERENT ANGULAR SPREADING FUNCTIONS

θ (degrees)	$(\cos \theta)^4$	$(\cos \theta/2)^{16}$
0	1.0	1.0
30	0.56	0.57
45	0.25	0.28
60	0.0625	0.100
90	0.0	0.004

$$\omega_i + \Delta \frac{\omega_i}{2} = 2\pi\left(f_i + \Delta \frac{f_i}{2}\right) \text{ and so forth} \tag{23a}$$

$$S_\infty(f_i,u) = \int_{\omega_i - \Delta\,\omega_i/2}^{\omega_i + \Delta\,\omega_i/2} S(\omega)\, d\,\omega$$

$$S_\infty(f_i,u) = \frac{\alpha\, u^4}{4\beta g^2}\left\{\exp\left[-\beta\left(\frac{g}{u(\omega_i + \Delta\,\omega_i/2)}\right)^4\right]\right. \tag{23b}$$

$$\left. - \exp\left[-\beta\left(\frac{g}{u\,(\omega_i - \Delta\omega_i/2)}\right)^4\right]\right\}$$

which yields the values of $S_\infty(f_i,u)$ in feet^2, if g is in feet-seconds^{-2} and u is in feet-seconds^{-1}. The values of α, β, and g can be combined and a transformation so that u is in knots can be used so that Equation (23) can be computed directly. The Kitaigorodskii range at high frequencies can be computed in a similar way if it is needed.

From Equation (18), with angles in radians, and ϕ replacing θ as the variable of integration

$$\int_{-\frac{\pi}{2} + \theta^*}^{\theta} F(u,\omega,\phi)d\phi = G(u,\,\omega;\,\theta,\,\theta^*)$$

$$= \frac{1}{\pi}\left[(\theta + \tfrac{\pi}{2} - \theta^*) + H(\omega,\,u)\,\sin 2\,(\theta-\theta^*) + M(\omega,\,u)\,\sin 4\,(\theta-\theta^*)\right] \tag{24}$$

where $$H(\omega,\,u) = 0.25 + 0.41\,\exp\,[-(\omega u/g)^4/2] \tag{25}$$

and $$M(\omega,u) = 0.08\,\exp\,[-(\omega u/g)^4/2] \tag{26}$$

Suppose for example, that the wind direction is from 276 degrees and that the $\theta_j - \Delta\theta_j/2$ are given by 166 degrees, 196 degrees, 226 degrees, 256 degrees,

286 degrees, 316 degrees, 346 degrees and 6 degrees (+ 360 degrees), so that seven values of $S_\infty(f_i, \theta_j)$ are needed.

The value of $\frac{\pi}{2} - \theta^*$ is -186 degrees or $-\pi(186)/180$ radians. The value of $S_\infty(f_i, \theta_j)$ for the first angular band would be

$$S_\infty(f_i) \left[G(2\pi f_i, u, 196\pi/180, 276\pi/180)\right]$$

the next value would be

$$S_\infty(f_i) \left[G(2\pi f_i, u, 226\pi/180, 276\pi/180) - G(2\pi f_i, u, 196\pi/180, 276\pi/180)\right]$$

and so on. There would be 7 (x 15) = 105 nonzero values of $S_\infty(f_i, \theta_j)$ and 5 (x 15) = 75 zero values to define the spectrum. The significant wave height would almost equal the value from Equation (12), if evaluated in the correct units for the wind speed used, except that it would be slightly higher because of Equation (16).

GROW

INTRODUCTION

At the end of a complete cycle of Grow, Dissipate, and Propagate, each ocean grid point of the model contains 180 numbers that describe the spectrum at that point at that time. The wind speed and direction have changed to a new value for the next time step. The problem addressed by Grow is that of determining how much the wind-generated part of the wave spectrum will change during the next 3 hours for the new wind.

The theories available to explain the growth of a wind-generated sea were those that treated a turbulent wind field advected over an initially calm sea surface,[28] which explained how waves could be generated on an initially calm ocean, a theory on how the wind extracted energy from a boundary layer logarithmic wind profile to generate waves,[29] and an extension[29] of this second theory by means of turbulent effects that enhanced this second mechanism and made it stronger.[30]

This theory could be called the Phillips-Miles-Phillips theory of wave generation. It is essentially a linear theory in that the growth of each spectral component is independent of the growth of any other spectral component and in that the waves can grow to be infinitely high.

Tests, even to the present time, seem to indicate that the mechanisms proposed in this combined theory are too weak to account for the observed generation of waves. Alternate mechanisms involving a theory of third order, nonlinear wave interactions have been set forth to try to explain wave growth.[47] In the opinion of the writer (as partially expressed in Reference 57), there are many problems associated with these third order, nonlinear growth theories such that they do not offer a correct explanation for the growth of waves on the ocean. It would have been possible between 1966 and 1974 to have tried to paramaterize the nonlinear theory, but this was not done.

THEORETICAL MODIFICATIONS

Instead, the functional form of the Phillips-Miles-Phillips theory was used and the parameters and constants in it were adjusted, usually by making them quite a bit larger, so that the observed growth of the spectrum for a given frequency band would be reproduced by the growth equations. Because only frequency spectral estimates were available, only the integrated growth over all of the direction components could be studied and parameterized.[31] These functions went through several cycles of analysis and improvement as additional data became available. Each change was tested against actual synoptic scale wind fields and checked against actual wave height data for ocean conditions.

For a given frequency band in the SOWM spectrum with a given central frequency, one can consider

$$S_w(f_i) = \sum_{\theta_w} S(f_i,\theta_j) \tag{27}$$

This represents the sum over direction of all of the elements in the spectral array at a given frequency and within 90 degrees of the wind direction.

If there were no waves present in this spectral band at the time of the time step and, if there were some wind, the theory would say that

$$\frac{d\,S(f_i)}{dt} = A(f_i,u) + B(f_i,u)\,S(f_i) \tag{28}$$

with the initial condition $S(f_1) = 0$ at $t = 0$. The solution to this ordinary differential equation is

$$S = A(e^{Bt}-1)/B \tag{29}$$

where functional dependence on wind speed and frequency is understood from Equation (28). Note that

$$\frac{dS}{dt} = A\, e^{Bt} = A + BS \tag{30}$$

A solution to Equation (28) exists even if B is zero, as in Equation (31)

$$S = A\, t \tag{31}$$

Waves generated by this mechanism alone would take an extremely long time to grow to observed heights.

Equation (2) has the properties that, if A is zero, the waves will never grow and that it is asymptotically equal to Equation (31) for small values of t. It also predicts unbounded wave growth with increasing time. It would be possible to require that Equation (29) hold if

$$S(t) < S_\infty(f_1, u) \text{ where} \tag{32}$$

$S_\infty(f_1, u)$ is the fully developed spectral frequency band and that

$$S(t) = S_\infty(u) \tag{33}$$

if Equation (29) exceeds the fully developed value. The effects, if they exist, that limit a wind sea to the fully developed spectrum have an off-on property that may not be realistic.

In the SOWM, the growth of a spectral frequency component is modeled by Equation (34) in an effort to slow down the spectral growth during the last stages of the growth of each frequency component.

$$\frac{ds}{dt} = \{A[1 - (S/S_\infty)^2]^{1/2} + BS\}\cdot[1 - (S/S_\infty)^2] \tag{34}$$

where $S = S(t)$, $A = A(f_i,u)$, $B = B(f_i,u)$ and $S_\infty = S(f_i,u)$, which is the value of the spectral band for a fully developed sea for the present wind speed.

The solution of Equation (34) for $S = 0$ at $t = 0$ is given by Equation (35)

$$S(t) = A(e^{Bt}-1)/B[F(t)]^{1/2} \tag{35}$$

where

$$F(t) = 1 + \left[\frac{A(e^{Bt} - 1)}{B\, S_\infty}\right]^2 \tag{36}$$

For the early stage of the growth of the spectral component, the result of Equation (35) is similar to Equation (27), but as t approaches infinity

$$S(t)/_{t\to\infty} = S_\infty(u) \tag{37}$$

That Equation (35) is the solution of Equation (34) can be verified by a few simple calculations.

$$\frac{dS}{dt} = A\, e^{Bt}\, F^{-1/2} - \frac{A^3(e^{Bt} - 1)^2}{B^2\, S_\infty^2}\, F^{-3/2}$$

$$= A\, e^{Bt}\, F^{-1/2}\, [1 - (S/S_\infty)^2] \tag{38}$$

$$= \{A[1 - (S/S_\infty)^2]^{1/2} + BS\}\cdot[1 - (S/S_\infty)^2]$$

At the start of the time step, $t = t_o$, the spectral band has reached the value, $S_w(f_i)$. If the wind is too light, nothing at all is done in Grow, and the spectral bands remain unchanged. If $S_w(f_i)$ equals or exceeds $S_\infty(f_i,u)$, nothing is done and the spectral band remains unchanged.

If $0 < S_w(f_i) < 0.95\, S_\infty(f_i, u)$, that frequency component of the wind-generated sea must grow to a new value during the next 3 hours. The time, t_o, required for the spectral component to have grown to the value $S_w(f_i)$ needs first to be found. In Equation (35), everything is known except t_o since $S(t_o) = S_w(f_i)$. The value of

t_o is given by Equation (39).

$$e^{Bt_o} = 1 + \frac{B\,S_w}{A\left(1 - \left(\frac{S_w}{S_\infty}\right)^2\right)^{1/2}} = R\,(A, B, S_w, S_\infty) \tag{39}$$

The new value of the spectral component at $t_o + \Delta t$, where Δt is 3 hours is

$$S_{NEW} = A\left[e^{B(t_o + \Delta t)} - 1\right] / \left[B\,F(t_o + \Delta t)\right]^{1/2} \tag{40}$$

The right hand side of Equation (39) can be substituted into Equation (40) and the increase in the spectrum for 3 hours can be found.

$$\Delta\,S(f_i) = S(f_i)_{NEW} - S_w(f_i) \tag{41}$$

$$= \frac{A[e^{B\Delta t}\,R - 1]}{B\left[1 + \left(\frac{A(e^{B\Delta t}R - 1)}{B\,S_\infty}\right)^2\right]^{1/2}} - S_w$$

This equation is the one programmed for the SOWM for a fixed time step of 3 hours. It is seen that the increase in the spectral component is simply a known function of the 3-hour time step, $A(f_i,u)$, $B(f_i,u)$, $S_w(f_i)$, and $S_\infty(f_i,u)$. The time, t_o, can be quite different for each of the spectral bands that may be increased by Grow.

If $0.95\,S_\infty \leq S_w(f_i) < S_\infty$

then

$$\Delta\,S(f_i) = S_\infty(f_i,u) - S_w(f_i) \tag{42}$$

The increment in the frequency spectrum from either Equation (41) or (42) is then spread out in direction according to Equation (24) and the present wind direction. As illustrated above, the fractions of the total area in 30-degree steps,

properly aligned with the reported wind direction and the direction bounds of the frequency-direction components, are found for each frequency-direction band. These fractions, which add to one, times $\Delta S(f_i)$ are added to what is present in the spectrum for each frequency-direction component.

For each frequency band, either six or seven of the direction bands will be increased by this calculation. Only if the wind direction is exactly at the boundary between two angular bands, will six angular bands be changed. All angular bands for each frequency in the spectrum are treated in this way except that those for the highest two frequencies are always treated to be in instantaneous equilibrium with the local wind.

THE FUNCTION $A(f_i,u)$

The function, $A(f_i,u)$, is based upon the theory of Phillips[28,31] and is a modification of the equations and techniques used by Barnett[58] in that additional data on its relation to the wind at 6.1 meters have been used.[59,3] A neutral wind profile and an assumed relationship between the roughness length and the friction velocity are used to compute the wind at 6.1 meters (20 feet), from the wind at 19.5 meters (64 feet). Two different equations for $A(f_i,u)$ are used. Given a wind at 19.5 meters in knots, it is converted to a wind at 6.1 meters and to the units of meters per second.

Then

$$A(f_i,u_{6.1}) = \begin{cases} A_1(f_i,u_{6.1}) \text{ if } \omega_i\, u_{6.1}^{-1} \leq 0.02 \\ A_2(f_i,u_{6.1}) \text{ if } \omega_i\, u_{6.1}^{-1} > 0.02 \end{cases} \tag{43}$$

where

$$A_1(f_i,u_{6.1}) = 2(1.438\times10^{-14})\omega_i^4\, u_{6.1}^3 \int_0^{\pi/2} \frac{d\,\theta}{Q_1(\omega_i,u_{6.1},\theta)R_1(\omega_i,u_{6.1},\theta)} \tag{44}$$

$$A_2(f_i,u_{6.1}) = 2(4.3\times10^{-12})\omega_i^{5.25}u_{6.1}^{1.75} \int_0^{\pi/2} \frac{d\,\theta}{Q_2(\omega_i,u_{6.1},\theta)R_2(\omega_i,u_{6.1},\theta)} \tag{45}$$

and where

$$Q_1 = 0.2704(\omega_i u_{6.1}^{-1})^2 + ((\omega_i^2 g^{-1} \sin\theta)^2 \tag{46}$$

$$R_1 = 4.87\text{x}10^{-6} + (\omega_i^2 g^{-1} \cos\theta - \omega_i u_{6.1}^{-1})^2 \tag{47}$$

$$Q_2 = Q_1 \tag{48}$$

$$R_2 = 0.1089\omega_i^{2.5}\, u_{6.1}^{-2.5} + (\omega_i^2 g^{-1} \cos\theta - \omega_i u_{6.1}^{-1})^2 \tag{49}$$

and where

$\omega_i = 2\pi f_i$, $u_{6.1}$ is in meters per second and g is in meters second^{-2}.

This integral is evaluated by finite differences as a function of θ for a given f_i and $u_{6.1}$. If the integral is defined over $-\pi/2$ to $+\pi/2$, it must be defined as an even function of θ. The function, $A(f_i,u)$, is essentially continuous at $\omega_i\, u_{6.1}^{-1} = 0.02$.

THE FUNCTION $B(f_i,u_*)$

The function $B(f_i,u_*)$ was expressed as a function of u_* (the friction velocity*) and required an integration over θ for the appropriate equation.[29,30,31] The result was a rather simple function that could be expressed analytically as a function of f_i and u_*. This function is given by

$$B(f_i,u_*) = \frac{10^{-4} f_i}{1.08}\left[k_1\, e^{-k_2\left(\frac{u_*}{c_i} - k_3\right)^2} + k_4\left(\frac{u_*}{c_i}\right)^2 e^{-k_5\left(\frac{c_i}{u_*}\right)^2}\right] \tag{50}$$

where $k_1 = 15$, $k_2 = 7000$, $k_3 = 0.031$, $k_4 = 7836$ and $k_5 = 0.0004$ and where B is in

*The friction velocity is a quantity used to define the wind profile over the sea surface. It has the same direction as the wind and is defined by $u_* = (\tau/\rho)^{\frac{1}{2}}$ where τ is the stress of the wind on the sea surface and ρ is the density of the air.

seconds^{-1}. From Equation (39), $B(f_i,u_*)$ is multiplied by the number of seconds in 3 hours (i.e., 1.0800×10^4). In Equation (50), c_i is the phase speed of the spectral component with the frequency f_i in the same units as u_*.

DISCUSSION AND EXAMPLES

The value of $S_w(f)$ was the result of all previous time steps for Grow, Dissipate, and Propagate. It could have the value that it has from swell that reached the grid point from quite a distance away; or it could have traveled to the grid point from upwind over a large fetch of more or less constant wind.

The nature of Equation (35) is such that the early stages of spectral growth are very slow as a function of time. Then, the exponential term takes over, and the spectral component grows toward saturation, slowing down slightly just before saturation. A special feature of the SOWM is that very small values of $S(f_i,\theta_j)$ are carried in all calculations so that the time required for the early stages of the growth of a spectral component has already been accounted for in midocean. These low values are discarded in archiving the spectra, but they are essential for realistic growth in midocean.

With test values for the functions $A(f_i,u)$ and $B(f_i,u_*)$ at an early stage of the development of Equation (35), the growth of the frequency spectrum from calm to fully developed was computed for an infinite fetch with an instantaneously turned on constant wind.

One such result is given by Figure 5. Although each spectral band started to grow at $t = 0$, the high frequencies grow the quickest and the soonest, and rapidly reach the fully developed state. The duration-controlled spectrum grows from high frequency to low frequency in a way quite similar to the way waves were grown as a function of duration in HO Pub 603. In about 42 hours, this wind sea becomes fully developed.

Contrariwise, in midocean for the SOWM, the initial condition is rarely ($S_w(f_i) = 0$ for all frequencies. Some background spectral components are usually present for many diverse reasons from previous time steps. Figure 6 shows what happens when a white noise fairly low background is present. The spectrum grows very quickly to full development at that wind speed in 18 hours. This example is over simplified compared to the actual variability of $S_w(f_i)$ as a function of f_i.

A long standing area of debate in the 1950 to 1966 time frame was concerned with the fetch and duration required for a fully developed sea. For example, for a

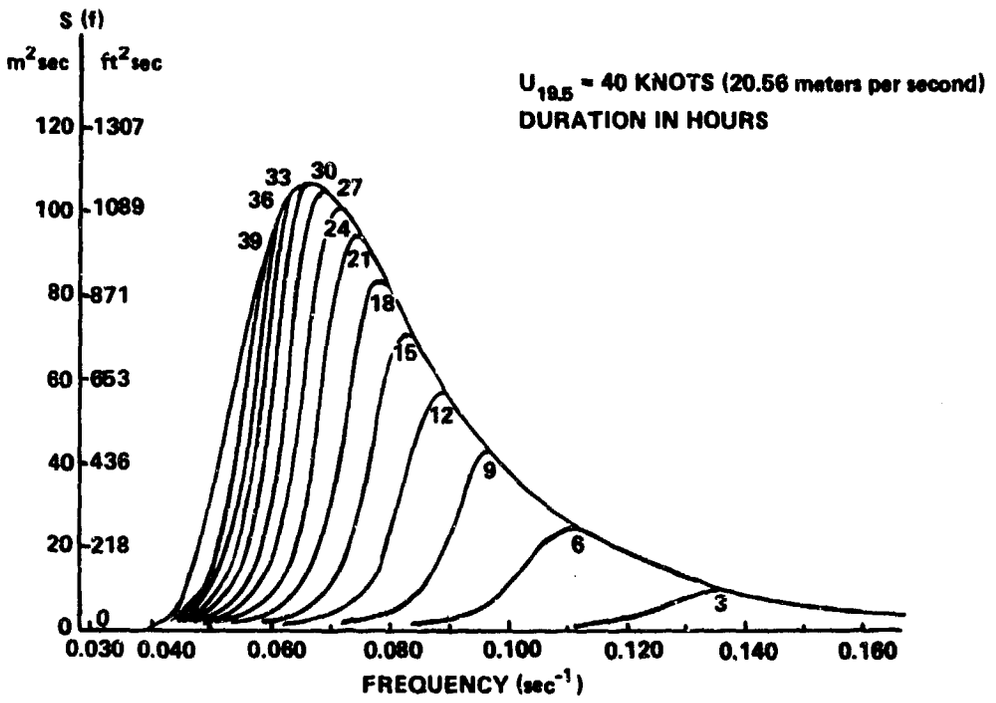

Figure 5 - Test Calculation of the Growth of the Spectrum as a Function of Time (Hours) for a 40-Knot Wind (20.56 meters per second) from a Zero Initial Condition at t = 0 (From Reference 1)

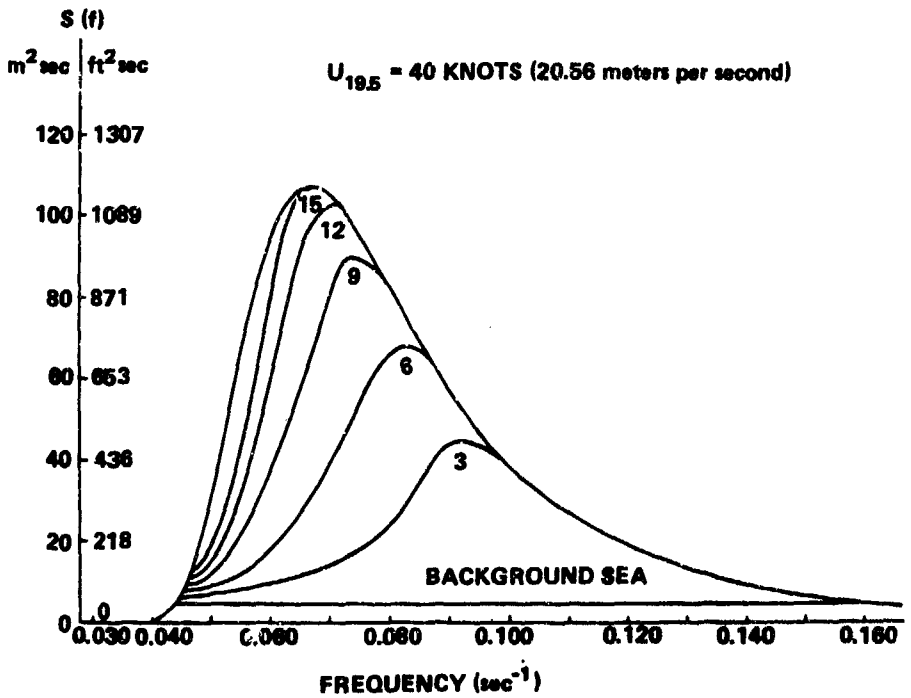

Figure 6 - Test Calculation of the Growth of the Spectrum as a Function of Time (Hours) for a 40-Knot Wind (20.56 meters per second) with a White Noise Background Sea at t = 0 (From Reference 1)

wind of 40 knots (20.56 meters per second), some data and analyses for the eastern side of the North Atlantic showed that only 18 to 24 hours were needed to reach full development.[60,61] Other data and other analyses on the western side of the North Atlantic suggested several days.[4] Corresponding differences were also evident for the required fetch. The suggestion[62] that different initial conditions with low background waves could account for such differences in the time for full development and the required fetch led to tests in which the very low components were carried along in the model as described above so as to result in this wave growth model.

A COMMENT

There is the possibility that $S(f_i,\theta_j)$ as a function of θ_j for a relatively high frequency would grow in such a way as to produce a bimodal function, if the resonance mechanism $A(f_i,u)$ dominated the growth, as suggested by the form of the second term in the denominator. Except for the slight hint of a bimodal form in the results of the Stereo Wave Observation Project, there are few data to support such a possibility.[19] For a locally generated wind sea, the lateral components of the mesoscale turbulence could conceivably blur a bimodal form to the unimodal form used in the SOWM.

DISSIPATE

For a SOWM spectrum at a grid point under analysis, there are often spectral components traveling against the wind sea. The Dissipate routine attenuates those spectral components traveling against the wind for each frequency direction component, $S(f_i,\theta_j)$, according to Equation (51)

$$S_D(f_i,\theta_j) = S_o(f_i,\theta_j)\left[e^{-C(S_w)^{\frac{1}{2}} f_i^4}\right]^{K(\theta_j)} \tag{51}$$

where S_D is spectral component after dissipation, S_w is defined by Equation (27), $C = 690$ is a constant with the dimensions of $[T^4 L^{-1}]$ that accounts for the total effect of 3 hours of attenuation when S_w is in $(\text{feet})^2$ and f_i is in seconds^{-1}. The power, $K(\theta_j)$, is dimensionless and equals 6 for the component that is traveling nearly opposite to the wind. It equals 4.5 for the next two direction components on each side of the one traveling opposite to the wind. It equals 3 for the last two that are involved and that are traveling nearly at right angles to the wind.

Equation (50) is based on Equation (8) of Section 348 of Chapter XI of Lamb (1932, 6th edition),[63] except that wave number has been expressed as frequency and molecular viscosity has been modeled by a wind-sea-dependent eddy viscosity, which in turn is wind-direction-dependent.

Thus, both the spectral growth equation and Equation (51) have treated breaking as the most important effect in limiting wave growth and in attenuating waves. That this effect is extremely important can be seen, at least qualitatively, in Figure 12.1 of Reference 15. Wave motion per se is dominantly irrotational, but the turbulence that occurs as waves break introduces dissipative effects by means of the interaction of a vorticity field with the wave motion. Being concentrated near the surface, these turbulent motions, must have their greatest effect on the short, high frequency waves, which partially justified the dependence on the fourth power of the frequency. The higher frequencies in the SOWM spectrum traveling against the wind are rapidly eliminated by this dissipation mechanism.

Also, wave breaking is controlled by the height of the wind-generated sea so that the exponential term in Equation (51) often varies as the square of the wind speed. The dissipation term becomes increasingly more effective as the speed of the wind increases and the local wind sea builds.

The wind direction dependence cannot be justified by the above analysis. It, in a sense, is partially based on the idea that dissipation could be similar to Equation (29) with a negative time dependent exponential term and with an angular spreading effect that would be most effective if the spectral component ran directly against a local wind sea.

The constant, 690 and the values of $K(\theta_j)$ were determined by numerical experiments in which a sequence of extratropical cyclones passed a British weather ship that had obtained wave records. Without the dissipation effect, the waves would die down after the passage of a cyclone to values that were too high. The next cyclone would cause the waves to increase to values that were much higher than those observed. After its passage the waves would be higher still after dying down.

For a third, and final cyclone, the waves at the height of the generation phase would be 20 to 30 percent too high. The values of C and $K(\theta_j)$ were adjusted until the model wave heights and spectra tracked the observed (estimated) wave heights and spectra for about a month.

The same Dissipate mechanism was also used in a tropical cyclone model as adapted to a 24-direction spectrum. Equally good results were obtained for wave height time histories and frequency spectra comparisons for this model.[51]

The winds over the ocean vary in both speed and direction for each time step of the SOWM. When combined with Dissipate and Propagate, the Grow part of each time step responds effectively and realistically to these changes in the wind. The wind sea spectrum at the start of the time step has virtually an infinite number of initial values. Each of these initial values is changed to a new set of values that are usually lined up more nearly in the local wind direction than they were at the start of the time step.

PROPAGATE

BEHAVIOR OF SWELL

Waves that leave an area in which they were generated and travel into an area of relative calm are called swell. The hand graphical methods for wave forecasting had difficulty with this concept in that the boundaries of the generation area were difficult to identify and were usually over-simplified in the analysis of the wind field and in that the swell emanating from the generation area was started toward a distant forecast point at a more or less arbitrary time. In the SOWM, the effects of fetch and the dispersion of swell are accounted for in the Propagate part of the model by translating the fields that result for each frequency-direction component in the known direction along a great circle path at the group velocity of the spectral component.

The choice of a gnomonic subprojection for each of the twenty triangles of the icosahedron was made bacause of the need to propagate waves correctly over oceanic distances. The difficulties inherent in any other grid system at that time seemed to be prohibitive.

A spectral component, as an example, with a frequency of 0.05 Hertz (a period of 20 seconds) travels at a group velocity of 30.3 knots (15.57 meters per second). In 3 hours, it moves 90.9 nautical miles (168.3 kilometers), and in one day, it moves 727.2 nautical miles (1346.7 kilometers), or about 12 degrees of arc along a great circle. Some of the components generated in extratropical cyclones rapidly (in a geophysical sense) reach the subtropical highs (where the winds are light), travel through the highs, and on to the Equator.

The process of dispersion, as a result of both the angular variation of the spectrum and the effect of group velocity, is an on-going, ever present, physical phenomenon. In the SOWM, the model never has to discriminate between sea and swell. Fetch and duration-limited waves are automatically accounted for the repeated application of Grow, Dissipate, and Propagate in contrast to more recent models for which hybrid procedures have been developed.[47,64,65,66]

THE FREQUENCY-DIRECTION FIELDS

After the operations of Grow and Dissipate, the spectral values that result from these two steps are rewritten into a different part of the memory in the form of frequency-direction fields. Since there are 180 values for the spectrum, of which 24 are treated to be in instantaneous equilibrium for two high frequency bands, this requires 156 separate frequency-direction fields for each of the icosahedral triangles that are involved in Propagate. To carry out the propagation step, it is necessary to know the values of the spectral component at the grid points for a given direction that are upstream of a particular grid point, downstream of a particular grid point, and upstream of the upstream grid point as described previously in the legend of Figure 3. This last grid point is called the upper upstream grid point.

At the edges of each main triangle of the icosahedron, there is no information on the downstream grid point for an outbound spectral component. In order to provide this information, an additional row of points is used to surround each of the subprojection triangles. The new, augmented triangle contains 28 points on each side for a total of 406 grid points to be used in the Propagate subroutine. The calculation of the spectral components for the rows of points on the augmented triangle takes into consideration the changes in direction of the great circle paths as the spectral components travel across the edge of a triangular subprojection and transforms them to the triangle being analyzed.

For a primary direction of propagation, there will be a row of grid points lined up along a great circle path in the direction of propagation of the particular frequency-direction spectral component under analysis. For a secondary direction of propagation, the upstream and downstream grid points relative to the grid point being analyzed are treated differently. The points on the inner hexagon are shifted, first one way and then another way, on alternate time steps as shown in Figure 3. The value of the spectral component at a grid point is assumed to be located on the

base of the triangle forming the inner hexagon of the grid, halfway between two points of this hexagon. The propagation distance is shortened to the value that would be calculated for a great circle path along this base. The points for the propagation scheme for the secondary directions of travel are closer together (in a sense) then those for the primary direction. The program knows which of the two shifts has been made, and they are alternated every 3 hours. It must be assumed that the frequency-direction field is smoothly varying enough to permit the toggling approximation.

The spectral values that lie along one of these great circle lines on the augmented triangle form an envelope of values that represent the spatial variation of the frequency-direction component. The problem for Propagate is to shift this envelope, without changing its form in the direction of wave propagation by an amount that would correspond to having each spectral component travel along a great circle path at its correct group velocity for 3 hours as given by the central frequency in Table 2.

THE DISCONTINUITY FIELD

One of the most interesting features of the arrival of swell at a distant point is that it often appears suddenly. A wave record taken at a particular time will contain no low frequencies, and a wave record taken 3 hours later will contain these low frequencies which then indicate the arrival of swell with a distinct arrival time from some distant source. The Propagate subroutine attempts to preserve this feature of the arrival of swell by not permitting the envelope to spread out and become flatter as the waves propagate across oceanic distances.

In order to preserve this particular feature of the arrival of swell and to model the effects of fetch as the spectral components propagate away from land, each spectral value in the spectrum has associated with it, for the last six bits of the word defining that spectral value, a number that varies between zero and one. This number is the discontinuity value. If it is slightly less than one and greater than zero, this number indicates that a discontinuity exists and has propagated that fraction of the distance from the grid point associated with the spectral value toward the downstream grid point. If this number is equal to one, it indicates that no discontinuity exists, and the envelope of the spectral values for this particular frequency-direction component is then translated in a different way because it is relatively smoothly varying.

The use of a discontinuity field is an attempt to treat various observed wave effects within the constraints of the current model. Wind shifts at fronts, shadowing by land features, and the relatively sudden deepening and filling of cyclones can all result in sudden changes in space and time of the waves.

Since the spectrum was changed at each grid point by the Grow and Dissipate operations, the discontinuity field that existed at the start of the time step is no longer applicable for the Propagate routine at some of the grid points. The first step in Propagate is to repair the discontinuity field.

Discontinuity values, other than one, are associated with a particular grid point for three different reasons. If that particular value in the spectrum is a local maximum (that is, if the spectral values upstream and downstream of the grid point are both less than the value at the grid point), there must be a discontinuity inserted for the upstream grid point and for the particular grid point being analyzed. Similarly, if there is a local minimum along this line of spectral values, a discontinuity must exist at the upper grid point and at the grid point being analyzed. The program checks to see if these local maxima and minima exist. Then it checks to see whether or not the discontinuity values are equal to one. If they are not equal to one, this particular feature existed for the prior time step and no changes are made. If the discontinuity values for either the upstream grid point or the grid point being analyzed, are equal to 1, the appropriate discontinuity value is set equal to 0.5.

Discontinuities are also inserted wherever the values of the spectral component change by more than 20 percent from one grid point to the next. If the absolute value of the difference between two spectral components along the great circle divided by their sum is greater than 0.4, a discontinuity value of 0.5 is inserted at the upstream grid point under consideration, if it did not exist from the previous time step.

For an offshore wind, the discontinuity field always ensures that there will be a discontinuity between a land point that is upstream of a water point in the model. This discontinuity value, if it does not exist at the start of the Propagate routine, will be inserted because of the rule just described as soon as the water grid point has a nonzero spectral value.

Changes in the spectral values caused by Grow and Dissipate can also produce conditions for which a discontinuity is no longer needed. These discontinuities are then removed by setting the discontinuity value equal to one.

The flow diagram for the Repair D Subroutine is shown in Figure 7. An error termination should not occur when the spectra are correct, and thus an error termination indicates something drastically wrong with the spectral field.

THE PROPAGATION OF EACH FREQUENCY-DIRECTION FIELD

After the operation of the subroutine that repairs the discontinuity field, each frequency-direction field will have associated with it both the values of the spectral component for that particular frequency and direction and an indication of the shape of the frequency-direction field along the great circle lines of propagation of that spectral component. Once the discontinuity field has been repaired, the steps that are taken to change the frequency-direction field to one appropriate for 3 hours later are as follows, as quoted with minor changes for Reference 2:

"Propagation of the spectral variance field is accomplished in a subroutine called MOVE3. The basic mode of propagation is by a linear velocity gradient technique. There are four possible discontinuity configurations, which are:

(1) no discontinuity,

(2) upstream discontinuities only,

(3) a downstream discontinuity only, and

(4) both upstream and downstream discontinuities.

Each frequency-direction field is propagated at group velocity depending on the value of the discontinuity attached to each frequency-direction component of the wave spectrum. If no discontinuity exists, then the field is assumed to be continuous and propagation can be done by means of an upstream velocity gradient; however, due to the great variation in distance between grid points discontinuities will exist at many points in the field.

"The propagation equations require the values of the spectral variances $S(f_i,\theta_j)$ and the discontinuity at the downstream, upstream, and upper-upstream grid points. If a discontinuity exists for a particular frequency-direction component, the value of the discontinuity indicates the fraction of the grid distance beyond the grid point that the component has traveled.

"For a given pattern of discontinuities, one of four methods of propagation can be used. They are the upstream gradient method, the downstream gradient method, the upper-upstream gradient method, and (the) pure jump.

"Since the spectrum at each border grid point is duplicated in two subprojections, and since it is necessary to have the wave spectrum at the upper-upstream

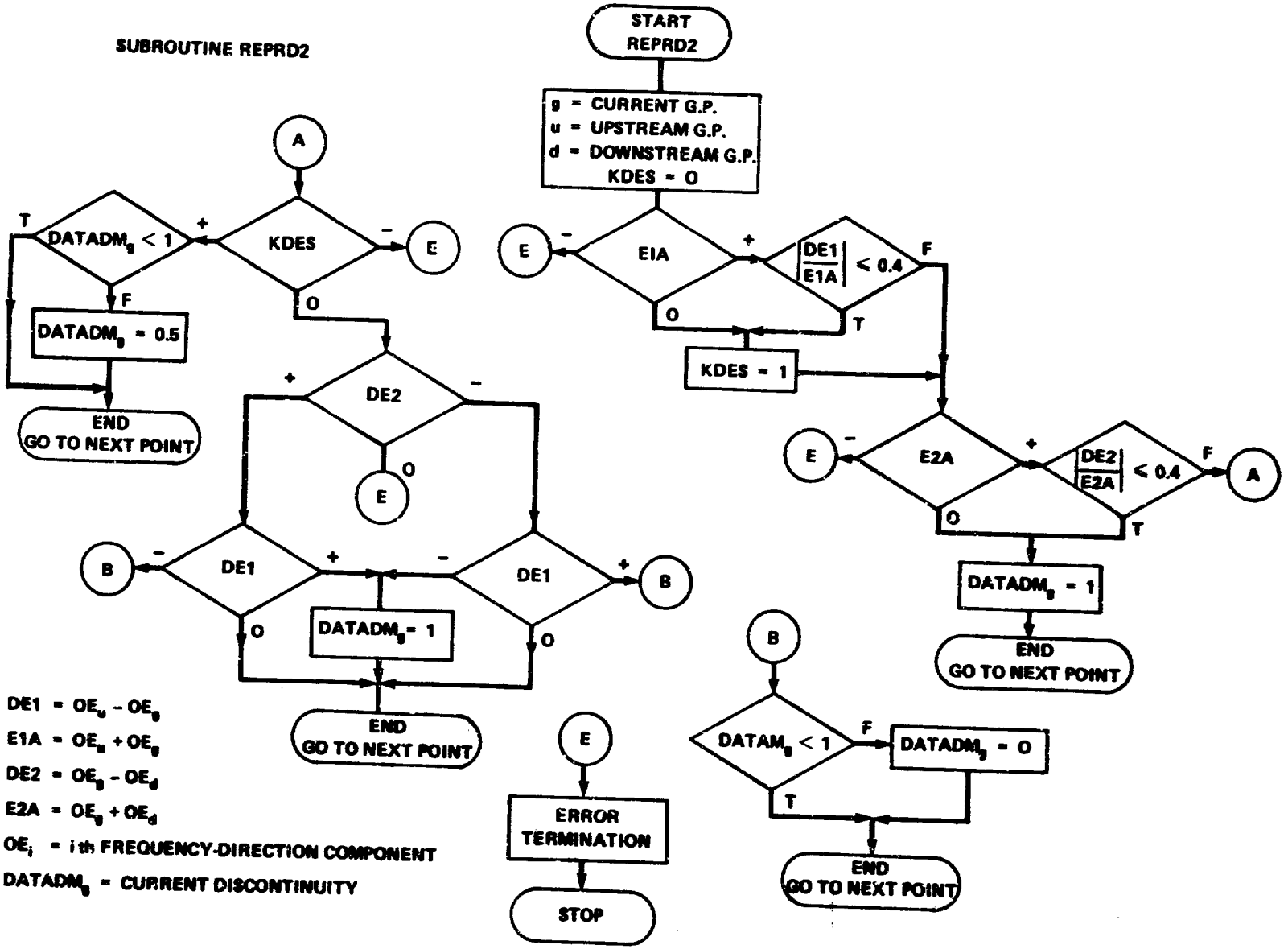

Figure 7 - Flow Diagram for Subroutine Repair D
(From Reference 2)

grid point in order to perform the propagation calculations, only the outbound directions on each side of a subprojection are propagated. It is then necessary to reconstitute the full spectrum (on the edges of) each sub-projection after the propagation calculations are complete before the next time step is started.

"The manner in which the spectrum is reconstructed is similar to the way in which the edges were bridged to construct the augmented triangle to start the propagation calculation. At each border grid point, the inbound directional components are, or course, the outbound components of the adjacent subprojection; each component is transformed to the local coordinate system of the sub-projection in which it will be used.

"The gnomonic projection presents severe problems regarding the areal distortion of the projection. In order to account for this distortion, each frequency-direction component is corrected by an areal distortion parameter for the hexagonal region represented by each grid point. (Parallel lines on a gnomonic projection actually converge or diverge on the globe, and this correction accounts for this effect.) In addition, the distances used in computing the various gradients are a function of position on the gnomonic plane.

"The (propagation scheme for secondary directions) must be modified in the vicinity of coasts. For example, for a secondary direction the grid points upstream are used on alternate time steps. If only one of these points is land, it is possible that the discontinuity from the land point may pass the target grid point on a toggle that is not used for the propagation computation at that time step. To account for this possibility, it is necessary to examine both upstream points at each time step. If the current upstream point is land, the computation proceeds normally; however, if the current upstream point is sea, it is necessary to check the value of the discontinuity at the alternate upstream point. If the discontinuity will pass the current point on this time step, then the zero from the upstream land point is jumped to the current grid point and the discontinuity reset to the corrected value. The effect of this procedure is to preserve the correct fetch effects along irregular coast lines as well as to model the turning behavior around headlands.

"Figures 8, 9, and 10 show the various methods used for wave propagation. Figure 8 shows the calculations used for the no discontinuity condition and the downstream only discontinuity condition. Figure 9 shows the method for an upstream

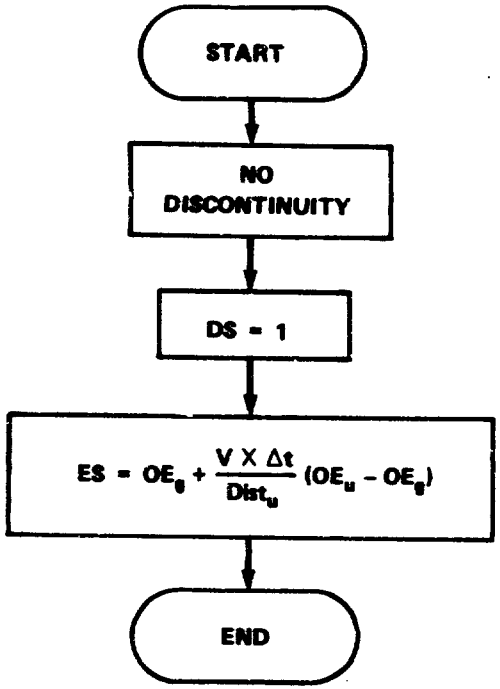

SUBROUTINE MOVE 3

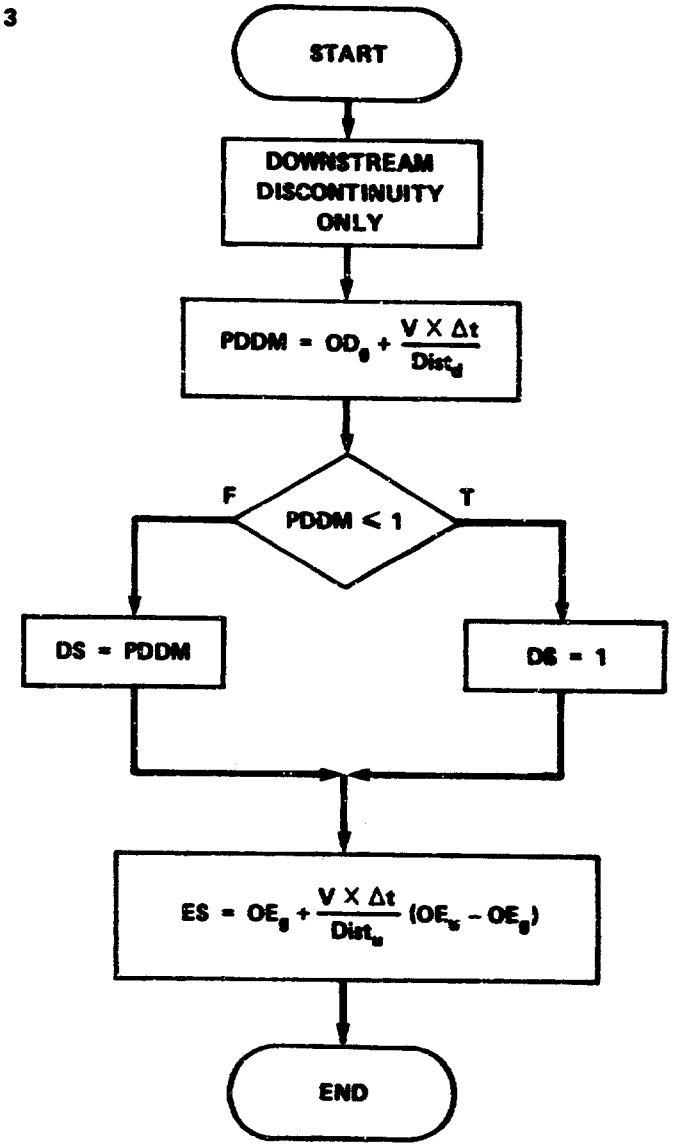

ES = NEW FREQUENCY-DIRECTION COMPONENT
DS = NEW DISCONTINUITY
OE_i = i th OLD FREQUENCY-DIRECTION COMPONENT
OD_i = i th OLD DISCONTINUITY
g = CURRENT GRID POINT
u = UPSTREAM G.P.
uu = UPPER-UPSTREAM G.P.
d = DOWNSTREAM G.P.
V = GROUP VELOCITY
Δt = TIME STEP
$Dist_i$ = DISTANCE TO i th GRID POINT

Figure 8 - Flow Diagrams for the Propagate Subroutine When No Discontinuity Is Present and When a Downstream Discontinuity Only Is Present (From Reference 2)

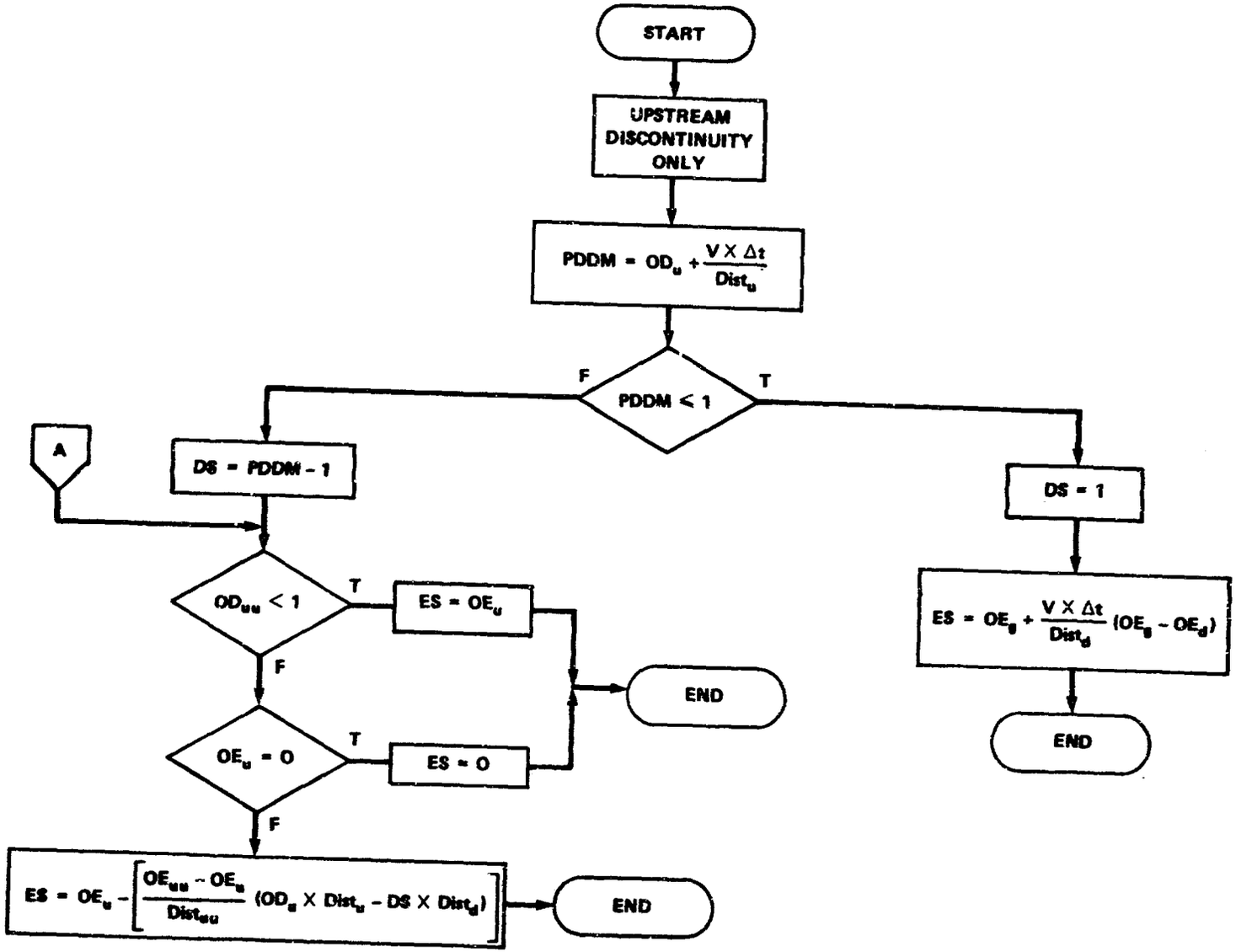

Figure 9 - Flow Diagram for the Propagate Subroutine When an Upstream Discontinuity Only Is Present
(From Reference 2)

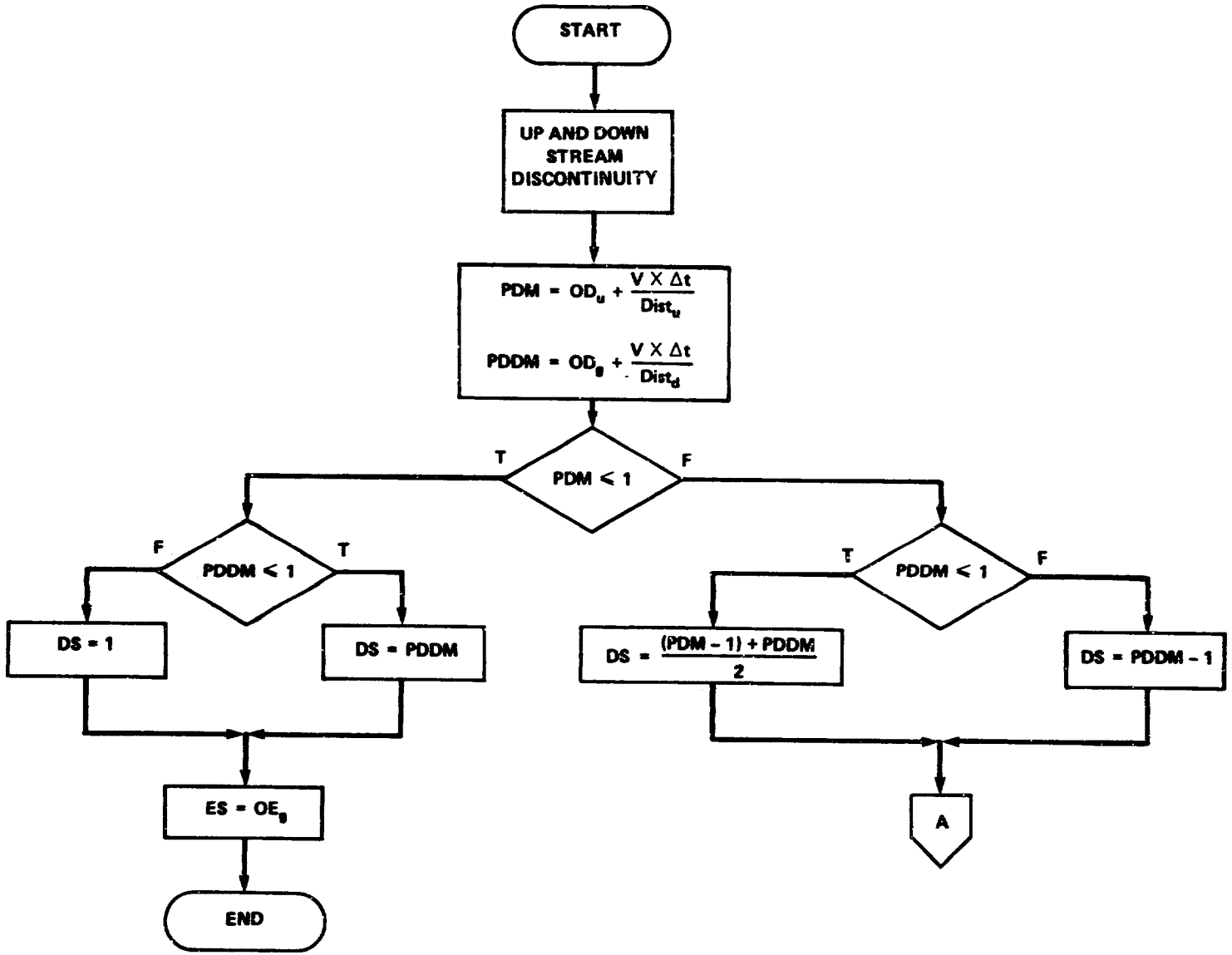

Figure 10 - Flow Diagram for the Propagate Subroutine When Both Upstream and Downstream Discontinuities Exist
(From Reference 2)

only discontinuity and Figure 10 shows the method for both upstream and downstream discontinuities."

Figure 11 is a schematic example of conditions that might exist after the discontinuity field has been repaired at the start of the propagation subroutine. As shown, it is hypothetically for the eleventh frequency band and the third direction component, which is a primary direction. The actual distances between grid points vary along the direction of propagation, but are shown as constant for the gnomonic projection. For the 22 grid points shown, there are two land points at each end. The spectral values are shown with an arbitrary scale as dots at each grid point. They are very small compared to all of the others at Grid Points 19 and 20. (In the actual SOWM, the grid points would have quite different values since they are numbered sequentially starting in one corner.)

Grid Points 4, 5, 6, 9, 14, 15, 16, 18, and 19 have no downstream discontinuities associated with them. The discontinuity is carried as a one in the computer program to indicate this fact.

Grid Point 1, a land point, has a discontinuity, D_1, that has propagated almost to Grid Point 2. The discontinuity has existed for at least one previous time step. Grid Point 2 has a discontinuity, D_2, that was just inserted halfway between it and Grid Point 3. Grid Point 3 has a previously existing discontinuity that has almost reached Grid Point 4.

Grid Point 8 shows a local maximum. It was just created by Grow and Dissipate; and D_7 and D_8 are halfway between Grid Points 7 and 8 and Grid Points 8 and 9. Grid Point 11 shows a local minimum that existed for at least one previous time step. The discontinuities D_{10} and D_{11} have almost reached their respective downstream grid points. Grid Point 13 is a new local maximum with new discontinuities D_{12} and D_{13}.

Finally, the discontinuity at Grid Point 17 has almost reached Grid Point 18. It will, in not too many hours, moving at a speed of 24.85 knots (12.77 meters per second), pass Grid Points 18 and 19 and reach 20, perhaps as swell with a period of 16.4 seconds.

Grid Point 2 has both an upstream and a downstream discontinuity. From Figure 10, D_1 (the upstream discontinuity) and D_2 (the downstream discontinuity) are increased by the fractional part of the distance they propagate at group velocity during one time step. The upstream discontinuity may be either less than or equal to one or greater than one.

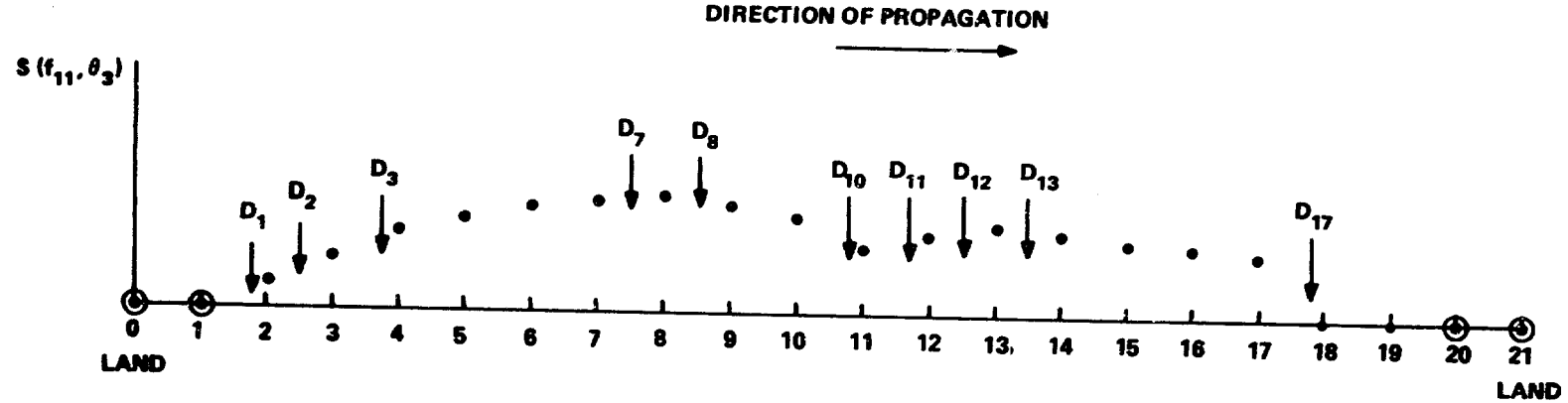

Figure 11 - Schematic Example of Spectral Values for a Given Direction of Propagation and Frequency Along a Great Circle and the Location of Discontinuities After They Have Been Repaired

Suppose that it is greater than one. The discontinuity has passed Grid Point 2. The first F branch in Figure 10 is taken. The downstream discontinuity D_2 has also moved; and, in time, it has either not reached Grid Point 3 or it has passed it. If D_2 has passed Grid Point 3, the discontinuity at Grid Point 2 is set equal to the amount by which D_1 has traveled past Grid Point 2. If both D_1 and D_2 lie between Grid Points 2 and 3, their average position is used.

The program continues to entry point A on Figure 9 and looks at the discontinuity at the upper upstream grid point (Grid Point 0 in the example). The discontinuity value for a land point surrounded by land points is one, and thus the spectral value at Grid Point 2 is set equal to the value at Grid Point 1 (a land point), which is zero.

On the other hand, suppose that D_1 did not move past Grid Point 2. If the upstream discontinuity D_1 moves past Grid Point 3, the discontinuity at Grid Point 2 is set equal to 1; if D_1 did not pass Grid Point 3, it is set equal to its new value. The value of the spectral component in either case is not changed and the program moves to Grid Point 3, still working with the original spectral values and discontinuities.

Incidentally, Grid Point 1 is treated in the same way as water points. If the downstream discontinuity moves past Grid Point 2, the new value of the discontinuity is set equal to one half.

Grid Point 4 has an upstream discontinuity only. Either it will move past Grid Point 4 during this time step or it will not. If it does not move past, the T branch in Figure 9 is followed, the discontinuity value for Grid Point 4 is kept equal to 1, and the new spectral value at Grid Point 4 would be decreased by means of the equation shown on the right hand side of Figure 9. In essence, a straight line through Grid Points 4 and 5 is extrapolated to upstream. The line is then translated as an envelope to the right at group velocity and the new value for the spectrum at Grid Point 4 is found.

Grid Point 5 has no upstream and no downstream discontinuity. The new spectral value at Grid Point 5 is found quite simply as shown on Figure 8.

The flow charts are slightly deceptive in that the spectral values are also corrected for the effect of convergence and divergence of the great circle paths during the propagate step. The spectral values are divided by an areal distortion term before the calculation is made and multiplied by that term after the calculation to obtain the new value.

The flow charts treat all possible contingencies exhaustively. The final result, after applying the above logic to every single grid point for every frequency and every direction, is a completely new set of spectral values and discontinuity values at each grid point as contained in the frequency direction arrays.

These arrays must then be reassembled into the 180 values for the spectrum at each grid point. The grid points on the sides of the triangular subprojection are treated differently, as described above; but the final result is such that the winds for the next 3 hour time step can be accessed and the processes of Grow, Dissipate, and Propagate repeated once again.

If the winds over the oceans were to cease completely, Grow and Dissipate would no longer change the spectrum. The row of grid points in the example is about 3045 nautical miles long. Repeated applications of Propagate would shift the envelope to the right. In about 5 days, the discontinuity D_1 would travel to Grid Point 20 and all spectral values along the section would be zero.

For those spectral components in a frequency-direction field that are traveling away from land, this Propagate routine effectively takes into account the effects of fetch within the time and space resolution of the model. As soon as a spectral component that is one grid point in from land becomes nonzero for an offshore wind, a discontinuity value will be inserted halfway between that grid point and the upstream land grid point. By the Propagate routine, the discontinuity will be shifted at group velocity toward the water grid point. As soon as it passes the water grid point, the spectral value will be set back to zero. A close inspection of the behavior of grid points near land shows an oscillation in the values of the higher frequencies as the spectra evolve from one time step to the next. Nevertheless, the particular spectral component can never get to be very high, because it is continuously being erased by a zero propagating to that grid point from land. The lower frequencies in the spectrum, as mentioned in the Grow section, take quite a while to reach appreciable values. The effect of zeros propagating from land is to limit the growth of the lower frequencies, farther and farther offshore, so that the high frequencies are found near shore, in an offshore wind, but not the low frequencies. One must look several grid points downstream during an offshore wind to find low frequencies in the spectrum with any appreciable amplitudes.

Moreover, an area of high winds over the ocean can itself translate along at a speed and direction equal to the group velocity of a spectral component. The effective duration of the wind under such circumstances will be much longer than

what would be calculated at some fixed point. The effective fetch would also be much larger. It is difficult to see how a hybrid model could treat this effect.

Conversely, spectral components that are propagated toward land will eventually reach a land grid point with this propagation scheme; and, when they do, they are set equal to zero. Wave dissipation is accomplished therefore by destroying the waves as they reach a coastline, just as if they were experiencing 100 percent breaking and dissipation. There is no reflection of the waves from the coastline. Similarly, for the Northern Hemisphere model, those parts of the triangles that comprise the Northern Hemisphere that extend into the Southern Hemisphere, are filled with land points, and any spectral component that reaches the Equator effectively disappears, because the Southern Hemisphere is not present in the model.

The propagate part of the SOWM, in contrast to Grow and Dissipate, where the continuous nature of the spectral function is preserved to a greater or lesser extent, treats the various spectral components in a somewhat unrealistic way, in that all of the spectral variance associated with a spectral component is propagated at a single frequency and in a particular direction. If the oceanic areas involved are too large, something similar to what was illustrated in HO Pub 603 (on page 79)[4] could occur to the frequency-direction fields that were generated in a particular area of high winds. The frequency resolution for the SOWM is probably good enough to prevent major discontinuities in the behavior of the frequencies, but the angular resolution probably allows certain spectral frequency-direction fields to spread apart and leave gaps between them after they have travelled a great distance from the source. For this reason, swell may be too high in some areas of the trade winds and too low in others. The effect may actually be systematic because of the fixed angles for the angular resolution possible within oceanic areas where high waves can be generated.

It is known that the Fleet Numerical Oceanography Center (FNOC) has been testing a new version of Propagate for the SOWM with grid system based on latitude and longitude that allows double the angular resolution of the currently operational model. This should improve the product substantially. Future models may include improvements that could make Propagate more realistic.

A FLEET NUMERICAL OCEANOGRAPHY CENTER MODIFICATION THAT AFFECTS PROPAGATE

The currently operational version of the SOWM at FNOC contains some additional programming in the Grow part of the program that actually modifies the way the

spectral components Propagate. For each frequency band during Grow, some further checks on the angular spread of the spectrum are made, if that frequency component, $S_w(f_i)$, for the thirteen lowest frequencies exceeds the fully developed spectrum, $S_\infty(f_i)$, for the current wind speed.

If the peak of the angular variation at that frequency lies within ± 60 degrees of the wind direction, and if it exceeds the sum of the two values of the spectrum one on each side, then the peak of the angular variation is reduced and the values on each side are increased, keeping the total over direction constant.

This modification affects any generated sea as soon as the wind speed decreases, so that the spectral component no longer grows, and any swell with a following wind within ± 60 degrees of its direction of travel. As soon as the angular variation at a particular frequency smooths out, the modification ceases to operate.

If a narrow band of swell, say of unit variance had no spectral variance on either side of it, as a function of direction, and if it extended over several grid points along its direction of propagation, then the application of this modification would change (for $S(f_i,\theta - 30)$, $S(f_i,\theta)$, and $S(f_i,\theta + 30)$ equal to 0, 1, and 0 respectively) the spectral values to 0.125, 0.75, 0.125 after one time step; to 0.203, 0.594, 0.203 after two time steps; to 0.252, 0.496, 0.252 after three time steps; and then cease to operate.

The objective of this modification is quite desirable along the lines of some of the points mentioned above. However, there are probably better ways to accomplish the desired features of the modification without such drastic changes in the direction of propagation of the spectral components.

THE COMPUTER PROGRAM

The SOWM was programmed for computing machines that were developed between 1955 and 1965 and are in use in the 1966 to 1981 time frame. The faster, larger capacity computers of today would permit shorter time steps, more grid points, and a higher spectral resolution in anticipation of vastly improved wind fields and wind field forecasts made possible by future remote sensing spacecraft. A great circle propagation routine for a conventional latitude-longitude grid under test at FNOC would result in a shorter computing time.

The present program at FNOC employs the equations and techniques described herein. The details have been modified since it was documented in Reference 2.

The (computer program for the) wave model is highly modular, consisting of a main program and 13 subroutines. Each routine performs a specific task of the computation. The program for the reduced resolution model was originally developed and tested on a Univac 1108. It was then modified so as to run on the computers at FNOC and made operational.[2,3] The details that follow are quoted, with minor changes, from Reference 2.

"The input is the file containing the wind field. The output consists of two files. The first file contains the complete two-dimensional wave spectra; the wind speed; direction and wind stress; the day, date, and time for the spectra; and their location. The second file contains the total variance at all grid points for each synoptic time of the calculation.

"Four files are required for the various tables used to describe the properties of the gnomonic projection and the land-sea tables for the ocean in question. Two files are used for the grid point adjacency tables and distance tables. Two tables are required because of the zig-zag method used to describe the paths of the secondary directions.

"Two files are required for the coefficients used by subroutines FIX 2 and RECNST. These coefficients are needed to perform the coordinate transformations from one subprojection to another.

"Finally, two files are used for land-sea tables. One file is used for the land-sea tables for the basic subprojection and the other is used for the land-sea tables for the augmented subprojections.

"Two scratch files are used for the wave spectra. The first file contains the result of the previous time step, which serves as input to the current time step; these spectra are input to the Grow and Dissipate phase of the program. The second scratch file is used for the result of the Grow-Dissipate phase and as input to the Propagate phase. The result of the Propagate phase is written back to the first file to be used as input to the next time step. In the normal operation of the program, the contents of this scratch file should be output as a forecast or for climatology (usually for every other time step) and saved to be used for the next time step. The size of the files for the wind field, the two output files, and the scratch files depends on the ocean for which the model is being run.

The program consists of the main program and the following subroutines:

1. INIT
2. GROW
3. CMPE12
4. LODTAB
5. ATERM
6. PACPRO
7. FIX2
8. REPRD2
9. MOVE3
10. RECNST
11. PRNT
12. SAVES
13. PRNTS

"The Main program provides overall control for all phases of the model. There are three modules to the program, the Grow module (which includes the Dissipate calculation), the Propagate module, and the Save module.

"Subroutine GROW is a driver for the growth phase. This includes reading in the wind field and the spectral fields, which are input to subroutine CMPE12, and writing out the resultant spectral fields which are input to the next module. Subroutine CMPE12 computes the new variance spectrum at each sea point based on the value of the wind at that point. Subroutine CMPE12 has one function type subprogram ATERM, which computes the "A" term for the spectral growth equations and subroutine LODTAB, which has several tables of constants used by CMPE12.

"The propagation module is controlled by subroutine PACPRO which is the driver for this section of the program. The first thing that must be determined is the toggle key for the zig-zag scheme. This determines which adjacency and direction tables will be used for this time step and which set of coefficients will be used for the edge coordinate transformation.

"Each subprojection is processed in turn. This means that, as each subprojection is processed, it is necessary to know which edges of other subprojections are adjacent to the current subprojection. In order to accomplish this, a table of subprojection and side number is used. Once the correct subprojection is established, another table is used to strip off the correct grid points to enable construction of the extended edge of the augmented subprojection used for the Propagate computation. The spectra at these grid points are then transformed into the correct coordinate system by subroutine FIX2.

"After all three sides of the subprojection have been processed, the results are then appended to the correct frequency-direction fields, in turn, as the actual Propagate calculations are performed.

"The Propagate calculations are done in two steps. First, the entire frequency-direction field is operated on by subroutine REPRD2 to make the necessary adjustments to the discontinuity field as described in the previous section on Propagate. Then, subroutine MOVE3 does the various velocity gradient calculations, or variations thereto.

"When all subprojections have been processed, the spectra at the grid points on the edges must be reconstructed, because only the outbound directions on an edge are propagated. This is done in much the same manner as the construction of the extended edges for the augmented subprojection, except that only the in-bound directions are used for any grid point. Subroutine RECNST is used for the reconstruction of the edges.

"The last section of subroutine PACPRO accumulates the total variance at each grid point, writes the total variance field to the output file and calls subroutine PRNT, which produces a printer plot of the significant wave height for each subprojection.

"The SAVES module is the last phase of the model. Subroutine SAVES constructs the two-dimensional wave spectrum at each sea point and writes the spectrum, all wind data at that point, and identification to the output file. Subroutine PRNTS prints the two-dimensional spectrum at selected grid points.

"A time step is completed after the propagation module is finished. It is only necessary to invoke the SAVES module for those time steps that are to be saved.

"The program is set up in such a way that only minor modifications at compile time are necessary to specify what ocean of the world is to be the subject of the computation. The layout of the icosahedral-gnomonic projection is such that the North Pacific and the North Atlantic can be worked as separate computations in parallel, rather than being run sequentially.

"One of the major problems in the implementation of the wave model is that the Grow-Dissipate phase requires the complete point spectrum at each grid point while the Propagate phase requires individual frequency-direction fields. The result is that between these phases of the program it is necessary to transpose arrays of the form A (325, 12, 15) to the form B (15, 12, 325). This procedure places a very heavy input-output load on the program, because any storage layout and file structure that would be optimal for one phase is the least optimal for the other phase. Currently, the data for each subprojection are organized as 15 records, each 325 x 12 in a random access file.

"In addition, in order to minimize the storage requirements for the model both the variance and the discontinuity value for a given frequency-direction component are stored in one computer word. This facilitates data handling and reduces the mass storage necessary for the model by a factor of two. The method used is not described in detail, because these routines are highly machine-dependent and should be designed according to the architecture of the computer on which the model is being implemented."

Flow charts and a program listing have been given in Reference 2 for a Univac 1108. For the North Atlantic, 94,000 words of main memory and 2,000,000 words of mass storage are needed for the various files.

The SOWM computer program is used four times each day at FNOC.[67] At 00z (or 00 GMT), the initial value specification is updated for the past 6 hours. Wave forecasts are generated out to 72 hours, with both oceans run concurrently. Each ocean requires about 3600 seconds of Central Processor Unit (CPU) time. At 06z, the initial value specification is updated. At 12z, the initial value specification is updated and forecasts to 72 hours are made. At 18z, the initial values are updated for the past 6 hours so as to be ready for the 00z forecast.*

DATA RECOVERY

THE DATA BASE

For this 20-year wave climatology, as generated by means of the SOWM, there are about 46,000,000 spectra. Each spectrum requires 180 numbers to describe it, plus about 10 items of additional information. The wave climatology in its raw form thus involves about 8,280,000,000 numbers, which is a incomprehensible amount. Whatever is done to analyze, summarize, and synthesize this mass of data must also simplify it. The climatology is really this full set of data, and the challenge is to produce a useful condensation of facts and data for practical applications.

---

*Meteorological and oceanographic analyses and forecasts are usually made for the nearest hour and referred to time as measured at Greenwich, England on the zeroth meridian. Thus, 06 GMT means 6 AM Greenwich Mean Time. Another convention is to use the abbreviation z for GMT. Consequently 0600 z, 06 z, 06 GMT and 0600 GMT all mean the same. The date and time, 1 January 1979 00z, corresponds to midnight Dec. 31, 1978. A 24 hour clock is also used so that 18 z corresponds to 6 PM. GMT and z are used interchangeably throughout. For time different from the nearest hour the minutes are given, as in 0637 z. For some spacecraft applications, a more detailed time is needed, as in 06 h 37 m 21.7 sec.

To do this, it is necessary to be able to retrieve subsets of these 46,000,000 spectra inexpensively. This is a nontrivial search problem that, once the data became available, proved to be difficult. It appeared to cost more to recover a particular spectrum from the archives than it did to compute them originally at FNOC.

A data retrieval program was developed by R.E. Salfi. It reduces the time and cost for retrieving spectra by a factor of about 10 compared to what was originally available. The retrieval program is described below, as quoted with minor changes from Reference 67.

GENERAL DESCRIPTION

"The Spectral Ocean Wave Model Data Base Management System (SOWM-DBMS) consists of two computer programs written in Fortran. The first program creates a set of random access files and associated directories from the SOWM data as delivered to David Taylor Naval Ship Research and Development Center (DTNSRDC) by FNOC; the second program accesses those files and provides the user with wave spectra for the specified time periods and locations in either the North Atlantic or North Pacific oceans. The SOWM wave data, as supplied to the DTNSRDC by FNOC, is in a highly compressed form and not readily useable in any practical sense, because the cost of retriving the data in its original form far exceeds what would normally be expected for everyday operational use of the data. The goal of this new system is to put the SOWM wave spectral data into a form that is readily accessible to the user at minimal cost, so that the staff of DTNSRDC can make routine use of the wave climatology without incurring prohibitive costs.

"The indexing algorithm, which is the heart of the retrival system, uses subprojection, month, day, and hour as keys to compute the record number for both the file that contains the spectral data and the associated directory file. The spectral data are in File 20 of the program; the directory is File 21. These are parallel indexed files that are used together to provide the shortest possible path length to an individual spectrum. When the data are retrived by the retrival program, the numbers in the spectrum are converted to the appropriate floating point format, and the associated identification, wind speed, direction, meteorological wind direction, the real earth directions of the spectral direction bands, and the one-dimensional density, are computed and provided to the user in either printed or Fortran file form, either formated or unformated.

DESIGN CONSIDERATIONS

"Several factors had to be considered in the design of the SOWM-DBMS. First, the system needed to be small, fast, and economical to operate. Second, due to the large volume of data, the system should use its storage medium efficiently. Third, because data are constantly being added to the data-base, the system needed to be open-ended.

"In order to accommodate the open-ended nature of the data-base, it was decided that a basic unit of one calendar year would be used. In this manner, new years can be continually added on as they become available. This decision also resulted in defining the file structure of the system, because all years are structurally the same. All years are of 366 days and date keys are of the form month, day, hour.

"Typically, the user desires that the data be retrieved for some time period at some set of locations. The data for each subprojection is stored as one record in a random access file whose indexing key is of the form month, day, hour, subprojection.

DATA DESCRIPTION AND FILE FORMAT

"The indexing is done on the keys of month, day, hour, and subprojection. One year for the larger ocean, that is the North Pacific, consists of seven subprojections of the icosahedral-gnomonic map; that is, 10,248 records of information. The data are stored in such a way that only the spectra at the active grid points in each subprojection are retained. This goes a long way toward minimizing the amount of space required. Furthermore, each individual spectrum is stored in a compressed form consisting of two words of identification plus 36 words of spectral values. Each of the 36 words consists of five 12-bit integers, which represent the values of the wave spectrum, scaled by 100 and converted to integer.

"The basic data unit of the system is a 38 x 325 word array. However, because no subprojection has the full set of 325 active points, the data are stored such that only the active points are put into the array, so that the actual record written to the file will be something less than 38 x 325. In order to accomplish this, the data are stored in the array, and a subindex, which associates grid point number to location in the data array, is created.

"The subindex is an array 326 words long. The 326th word is the actual number of spectra in the 38 x 325 array. The other 325 words of the subindex act as

pointers to individual wave spectra. That is, if one desires grid point 100, one looks at location 100 of the directory array for the pointer that indicates where the spectrum for grid point 100 resides in the 38 x whatever array, that was created. Such a lookup table allows the data to be compressed in a very efficient form. Each record written to the random access file contains the data for one subprojection for a given time point. The index keys to the random access file consist of subprojection, month, day, and hour. Year is an implicit index in that each file contains data for only one particular year or part of a year.

"The SOWM-DBMS takes into consideration and is set up in such a way as to keep storage space to a minimum, while providing as rapid direct access to the desired data as possible. To this end, the system is geared toward one year of basic data. That is, each file of the system consists of no more than 366 days, accounting for leap years."

PRODUCTS OF THE SPECTRAL OCEAN WAVE MODEL

INTRODUCTION

Various products of the SOWM have been made available to scientists by FNOC for studies involved with preliminary analyses of this climatological data, ship trials, wave measurement programs, the planning of experiments and comparisons with buoy and spacecraft measurements.[45,69,70,71*] Such products consist of significant wave-height-contoured fields for a given synoptic map time along with the associated wind and pressure fields, time histories of significant wave height at selected grid points, the full frequency-direction spectra for selected grid points, and the frequency spectra derived therefrom.

WAVE HEIGHT VARIABILITY

A time history of the 6-hour variability of the significant wave height at some selected grid point reveals the variability of wave conditions with time.[69,70] Figure 12 shows the significant wave height in meters and the wind speed in knots for the month of March 1968 at 58.3° N 12.3° W in the North Atlantic.[69] It represents one of eight extreme wave conditions for the 10-year period from the summer of 1959 to the summer of 1969. The significant wave height ranged from about 2 meters to 17.5 meters. The area under the spectrum would be about 76 times greater

*As examples.

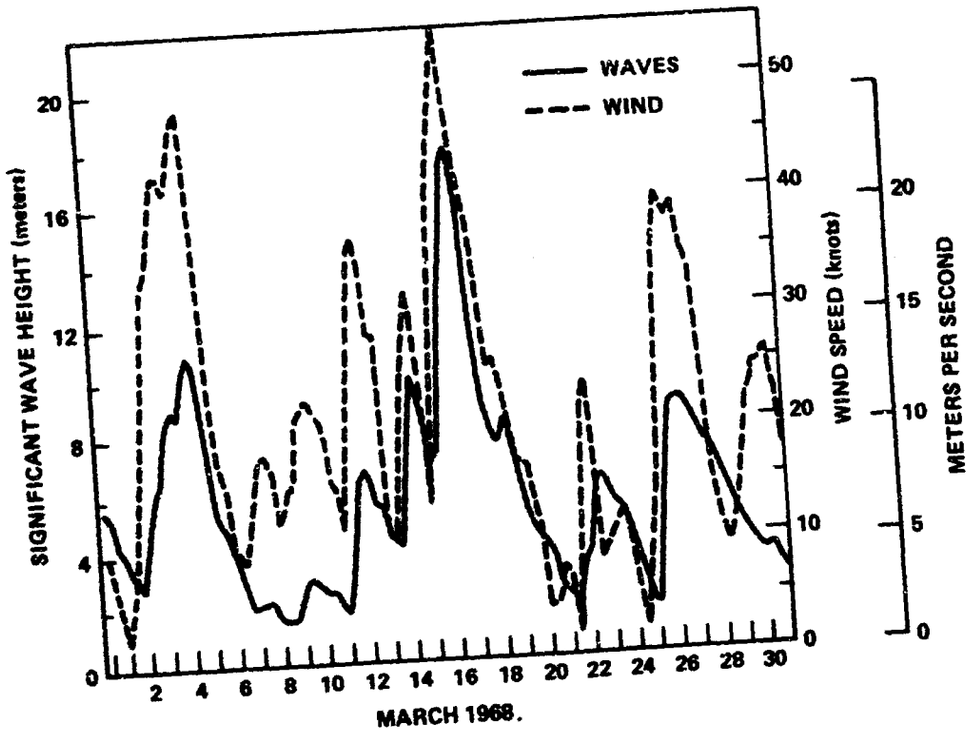

Figure 12 - Sample Storm Growth and Decay at Grid Point 127
(From Reference 69)

for the highest waves compared to the lowest waves during this period. From 17 March to 21 March, the wave height at this grid point went from 17.5 meters to 2 meters in 4 days according to the model. The wind speeds during the month varied from 55 knots (28.3 meters per second) to 0.5 knot (26 centimeters per second) when this occurred. From 11 March to 17 March, there appears to be a succession of cyclones, each of which builds up the waves to a higher point than its predecessor.

Similar graphs for parts of November and December 1966 are shown for a grid point near Weather Ship I (Station India) in Figure 13. Measurements of wave height and wind speed at this weather ship are shown by the X's to be compared with the SOWM specifications. The winds reached nearly 60 knots (30 meters per second); and there is one 22-knot (11.3 meters per second) difference between the weather ship wind and the SOWM wind which is not reflected in a large SOWM wave height error. The peak waves are a little more than 12.5 meters high and the SOWM heights appear to verify fairly well.

SIGNIFICANT WAVE HEIGHT FIELDS AND VECTOR WIND FIELDS

A sequence of 11 significant wave height fields and 11 sea surface pressure and wind fields are shown in pairs in Figure 14 through 35 as produced at FNOC[68] with dates and times during October 1977. Except for 25 October 1977, there are two wave height and two wind field and sea surface pressure charts each day for most of the North Pacific.

The first pair of charts, Figures 14 and 15 for 00z 25 October 1977, show three extratropical cyclones for the wind and pressure fields. Each full barb is 10 knots (5.14 meters per second) and a flag is 50 knots (25.7 meters per second), so that two of the cyclones have 50 knot winds with a southerly component. Waves with significant heights of 28.9 feet, 25.4 feet, and 48.2 feet (8.8, 7.7 and 14.7 meters) are associated with the areas of high winds. The height contours are drawn for every 3 feet on these charts. The cyclone near 48° N and 168° E is the one of interest in the sequence to follow.

The following day at 00z (26 October 1977) (Figures 16 and 17), the low off Canada has disappeared and the one in the Central Pacific has moved north of the Aleutian Islands. Westerly winds of 70 knots (36 meters per second) are shown to the south of the Aleutian Islands. The SOWM shows 48-foot (14.6 meters) waves in an area where they had been 12 and 15 feet (3.7 and 4.6 meters) 24 hours before.

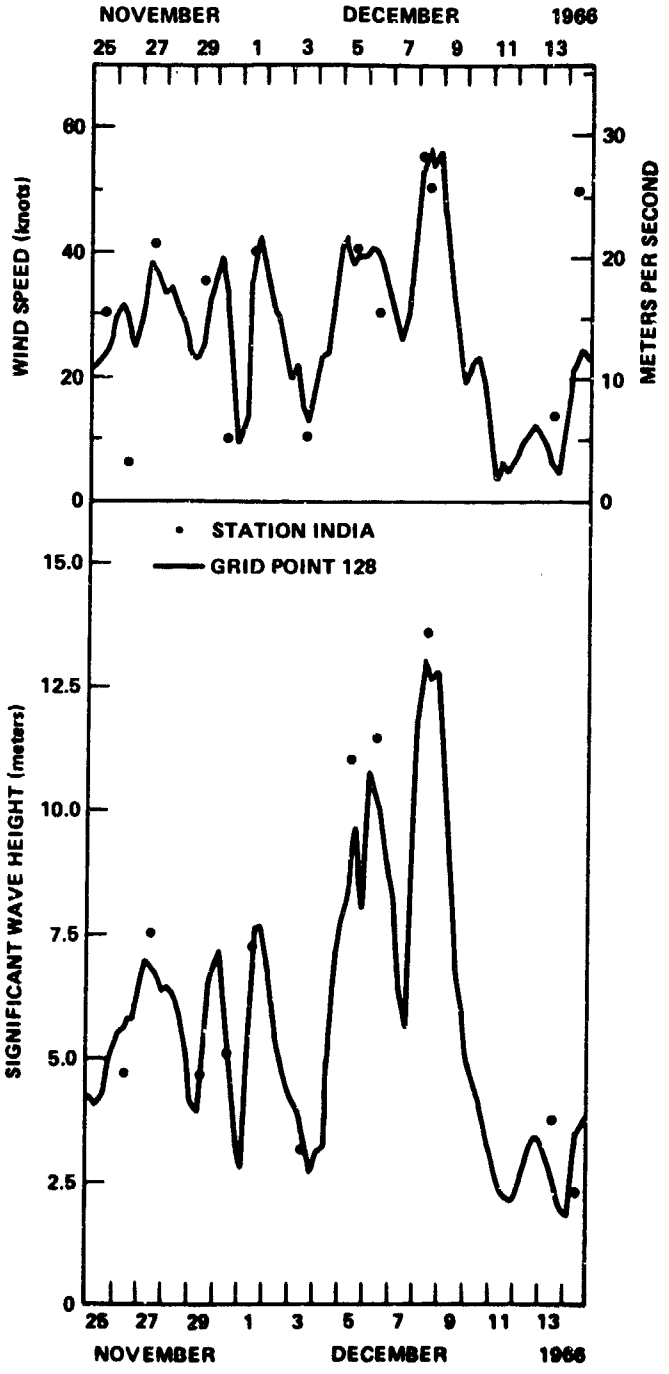

Figure 13 - Comparison of Station India and Grid Point 128 Winds and Waves for Storm of 25 November to 14 December 1966 (From Reference 70)

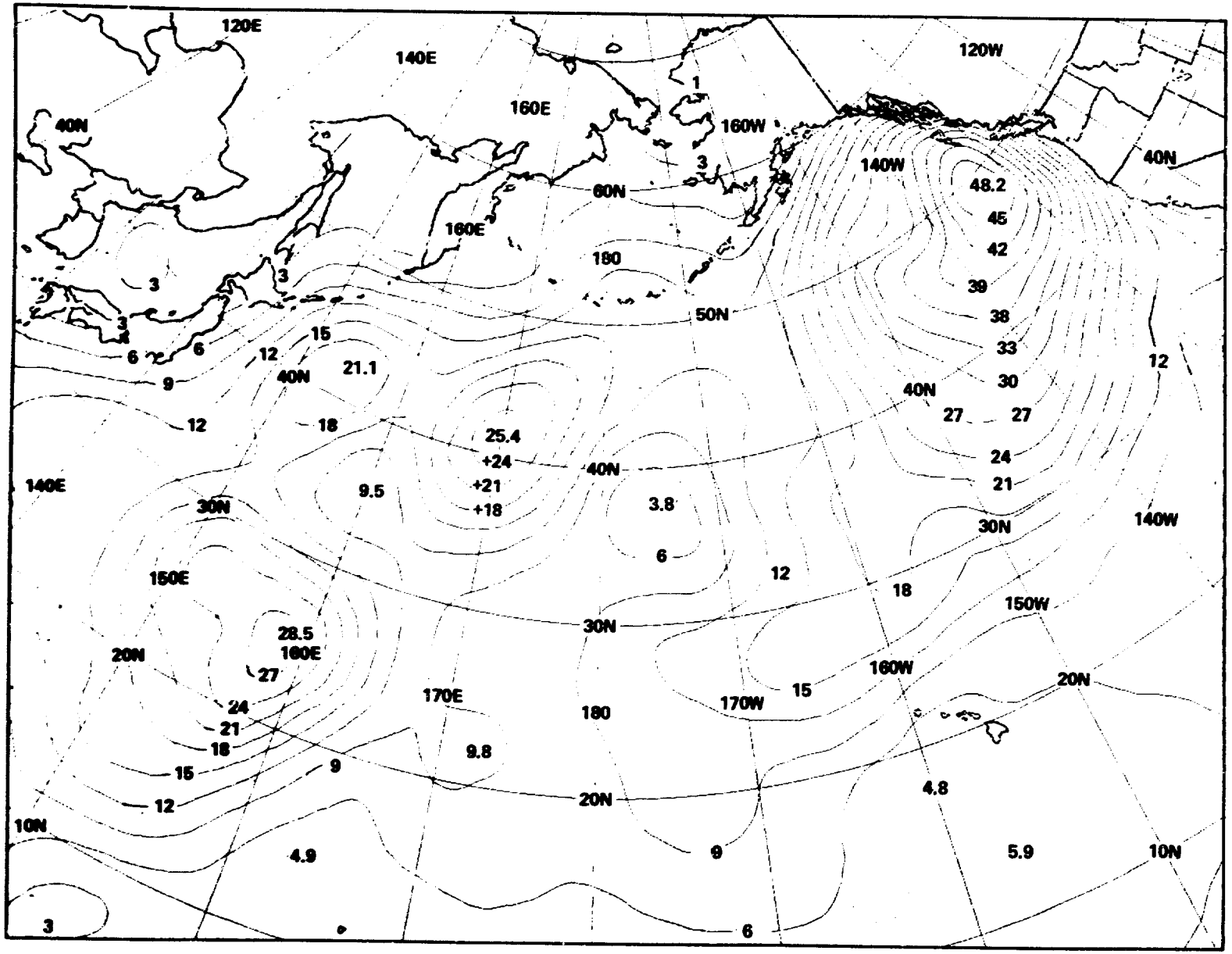

Figure 14 - Significant Wave Height Field (Feet) for 00z 25 October 1977

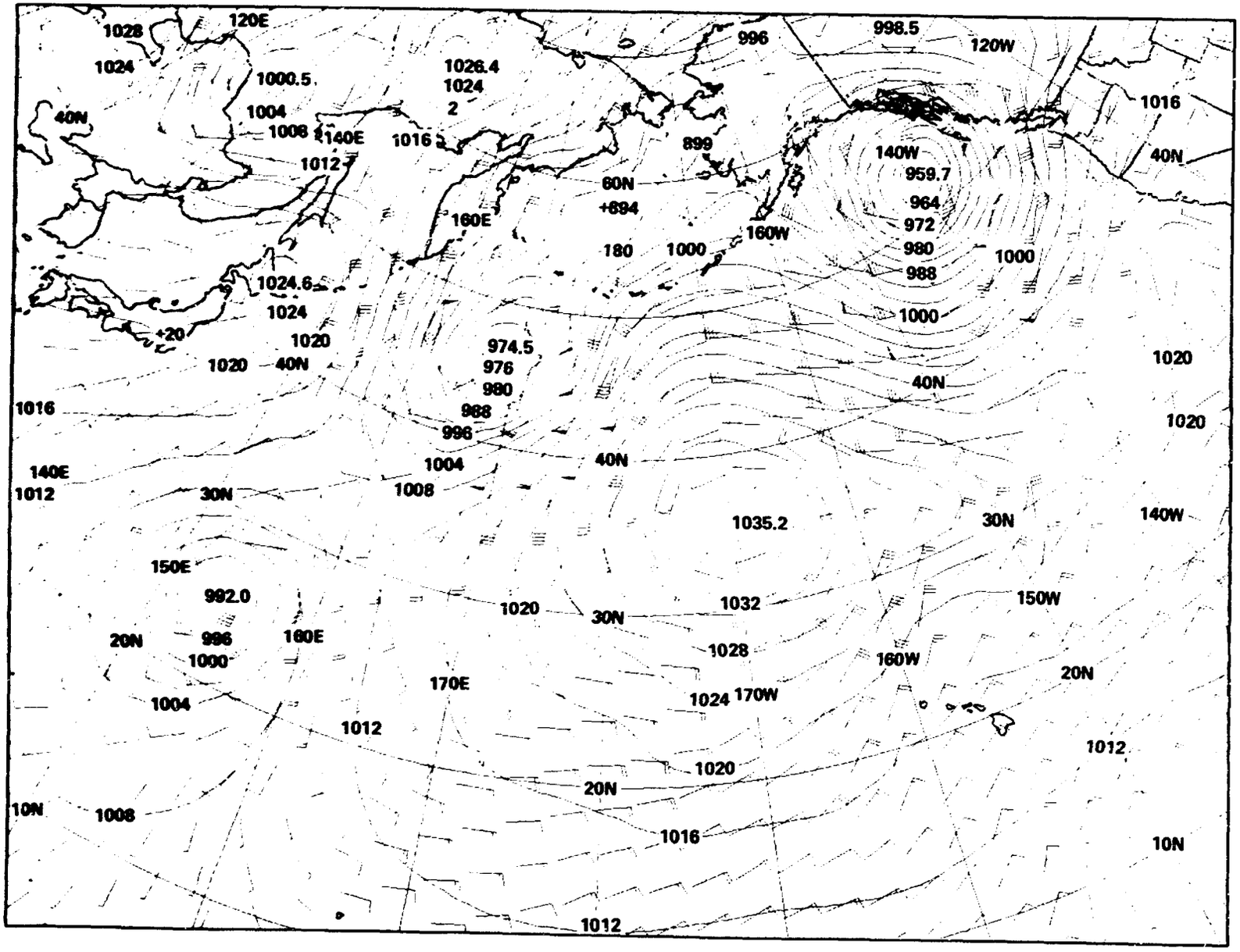

Figure 15 - Vector Winds (Knots) and Sea Surface Pressure Field (Millibars) for 00z 25 October 1977

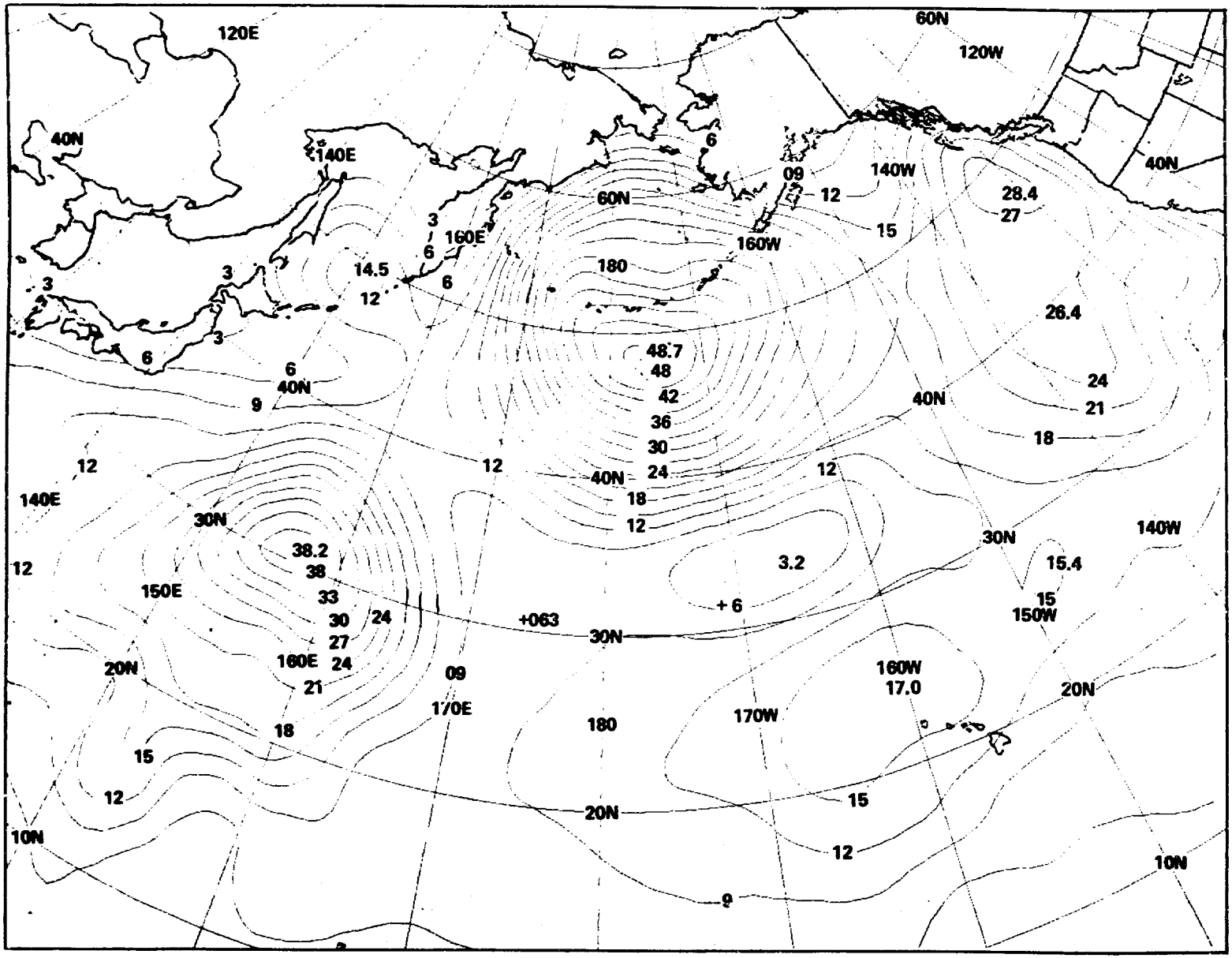

Figure 16 - Significant Wave Height Field (Feet) for 00z 26 October 1977

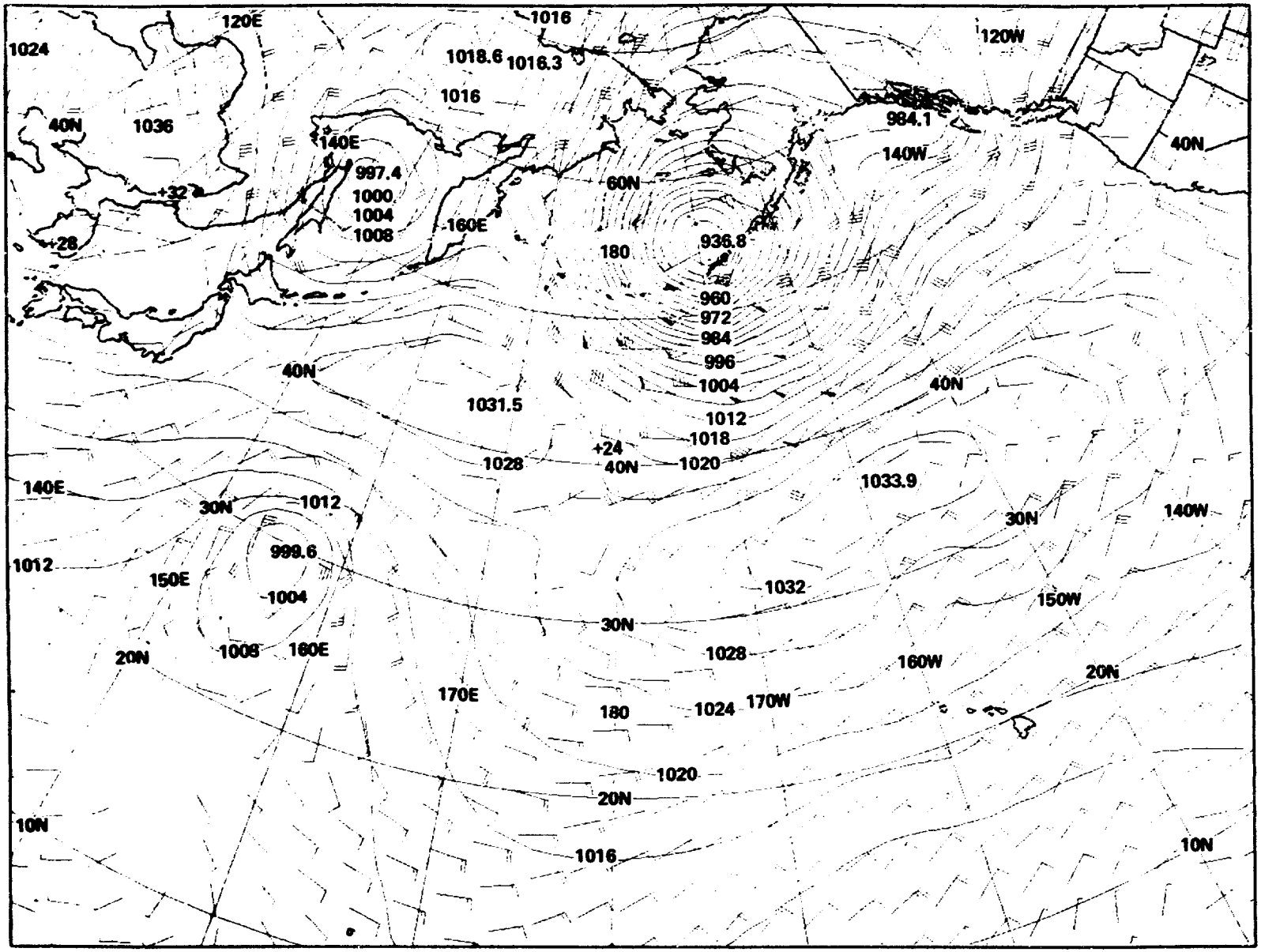

Figure 17 - Vector Winds (Knots) and Sea Surface Pressure Field (Millibars) for 00z 26 October 1977

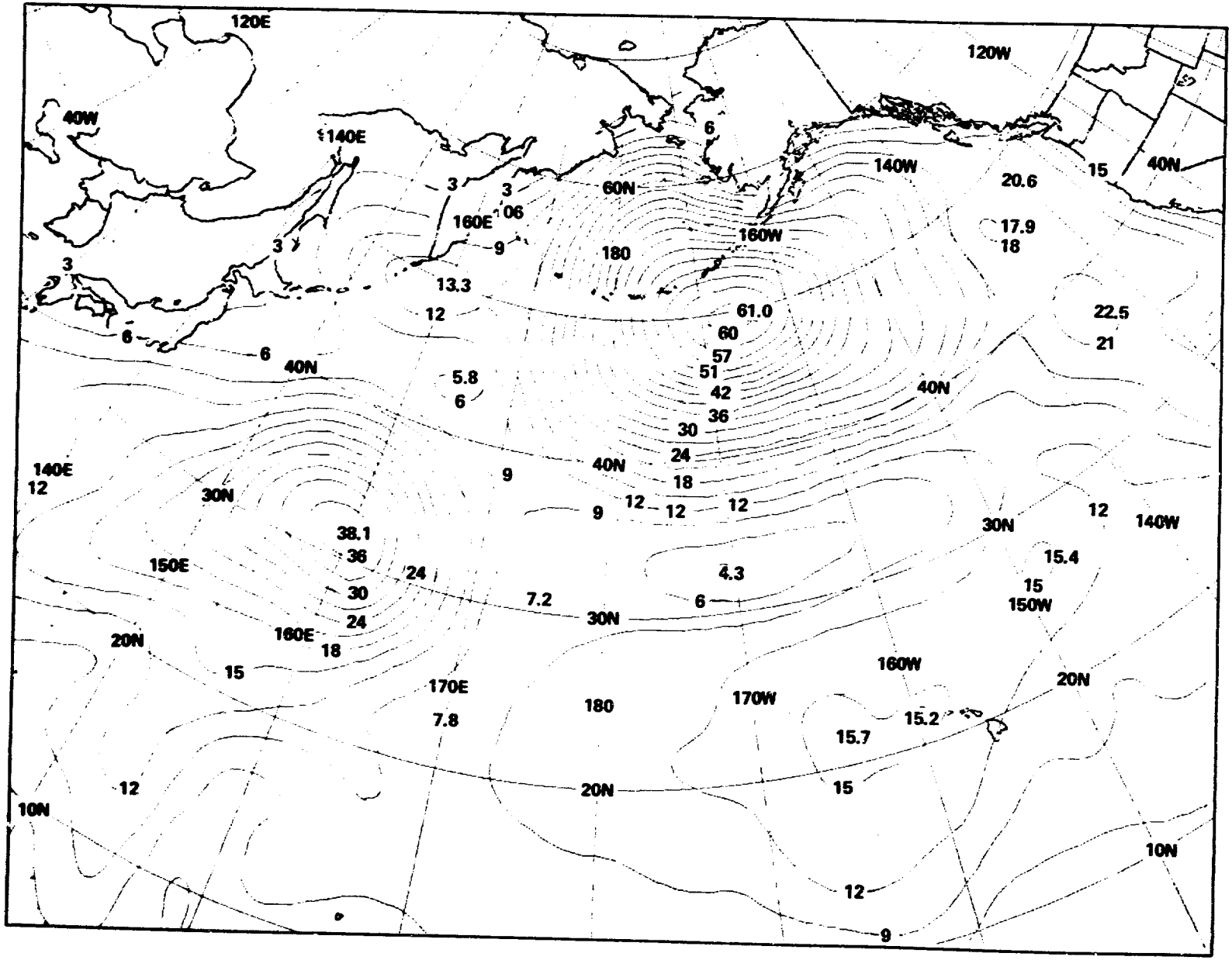

Figure 18 - Significant Wave Height Field (Feet) for 12z 26 October 1977

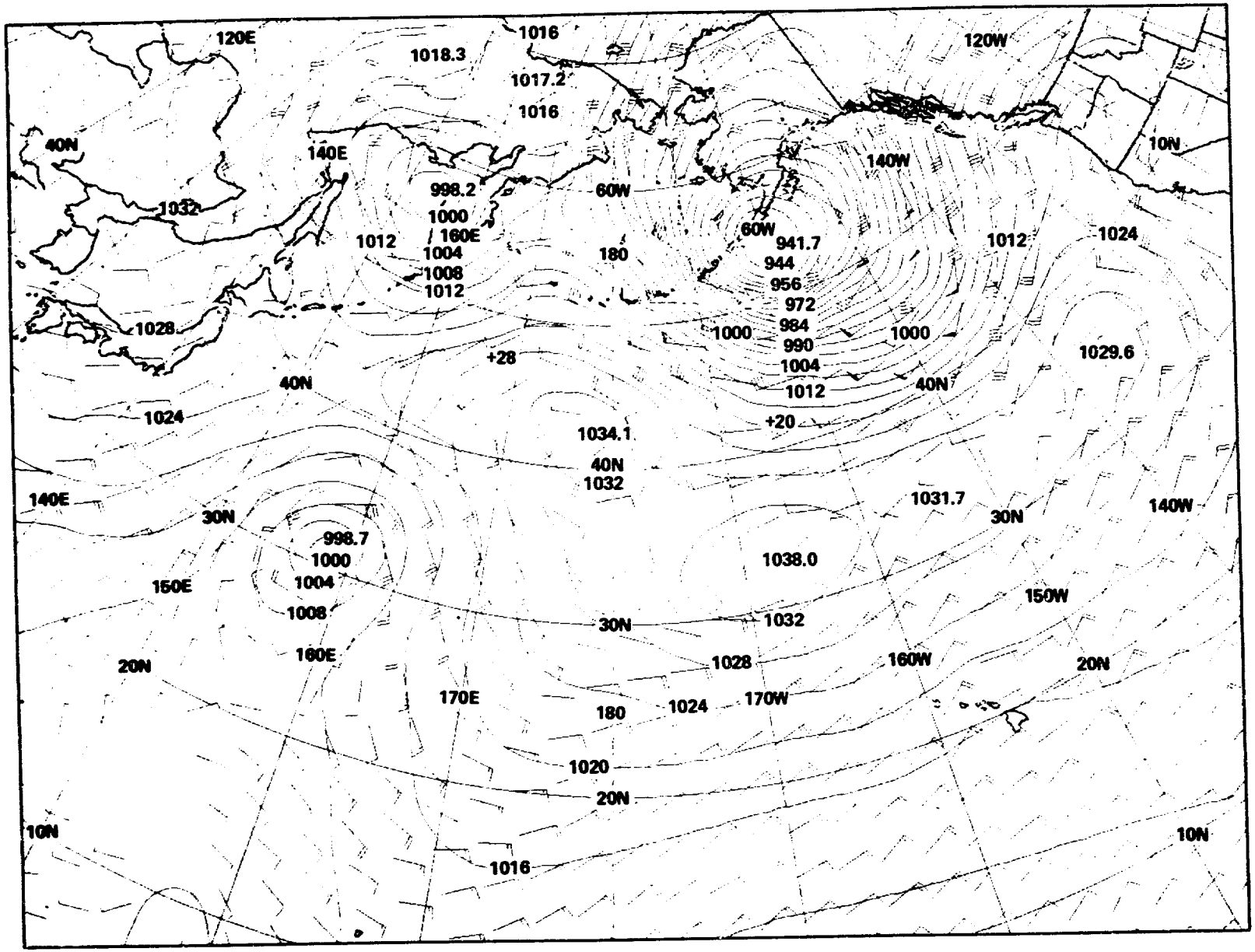

Figure 19 - Vector Winds (Knots) and Sea Surface Pressure Field (Millibars) for 12z 26 October 1977

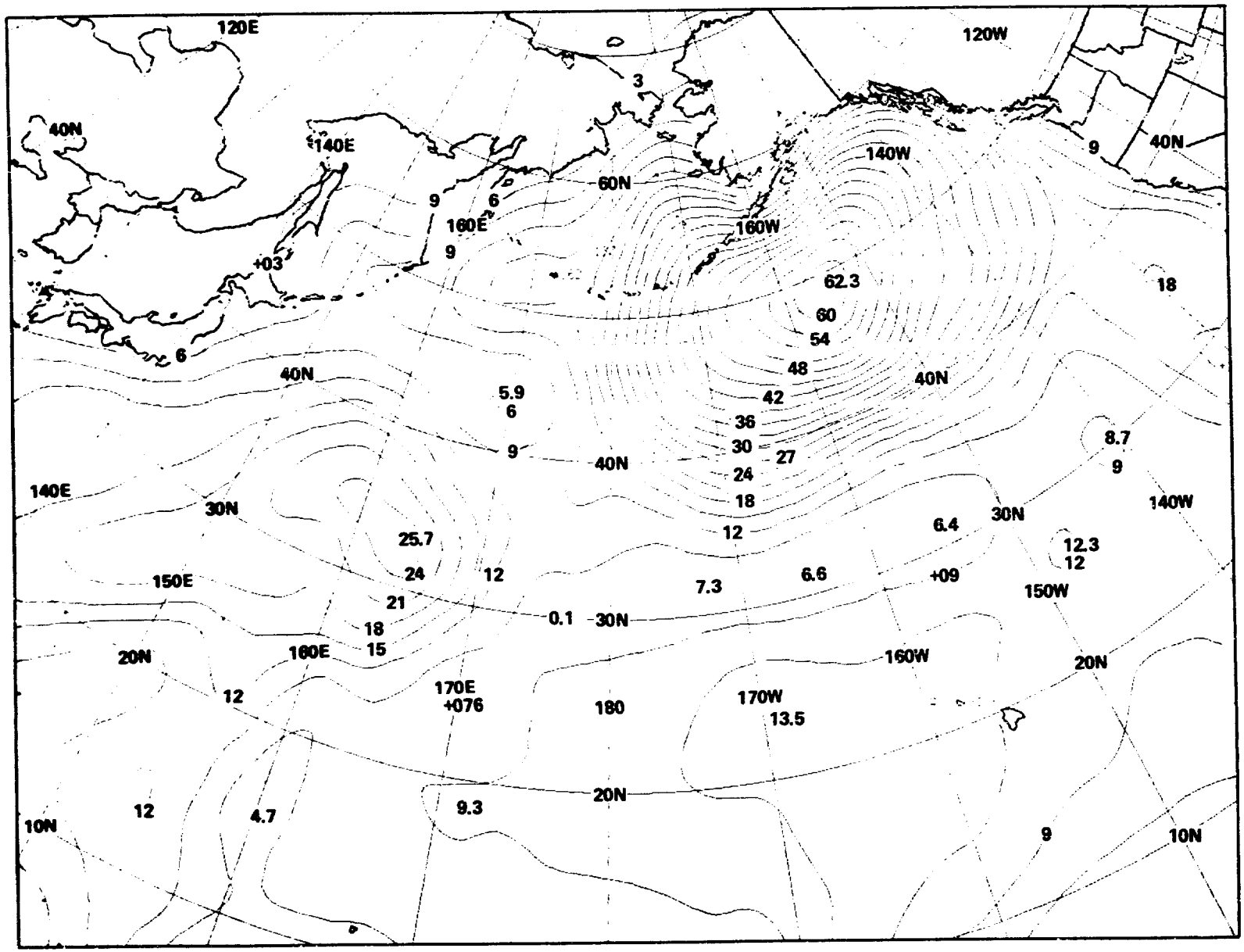

Figure 20 - Significant Wave Height Field (Feet) for 00z 27 October 1977

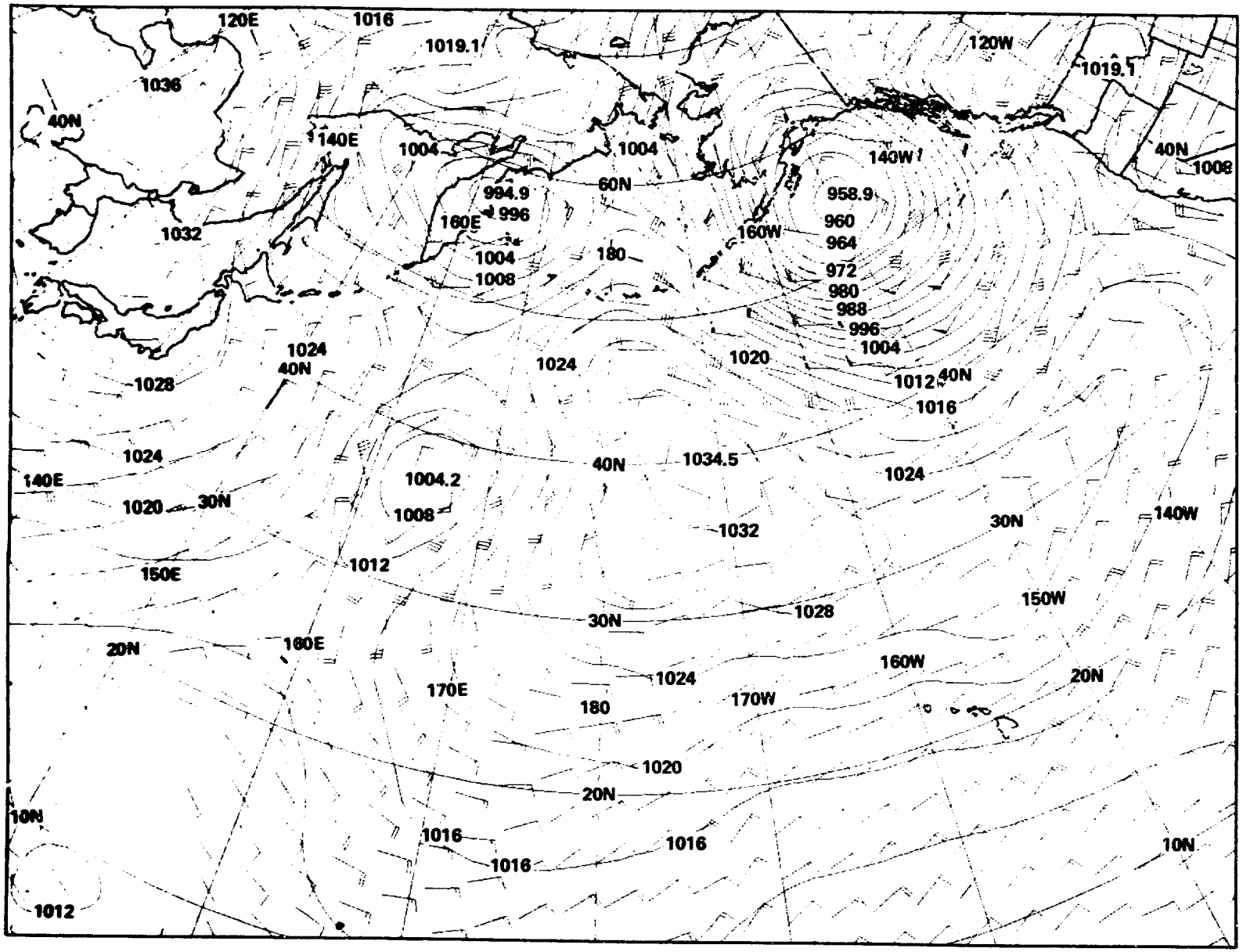

Figure 21 - Vector Winds (Knots) and Sea Surface Pressure Field (Millibars) for 00z 27 October 1977

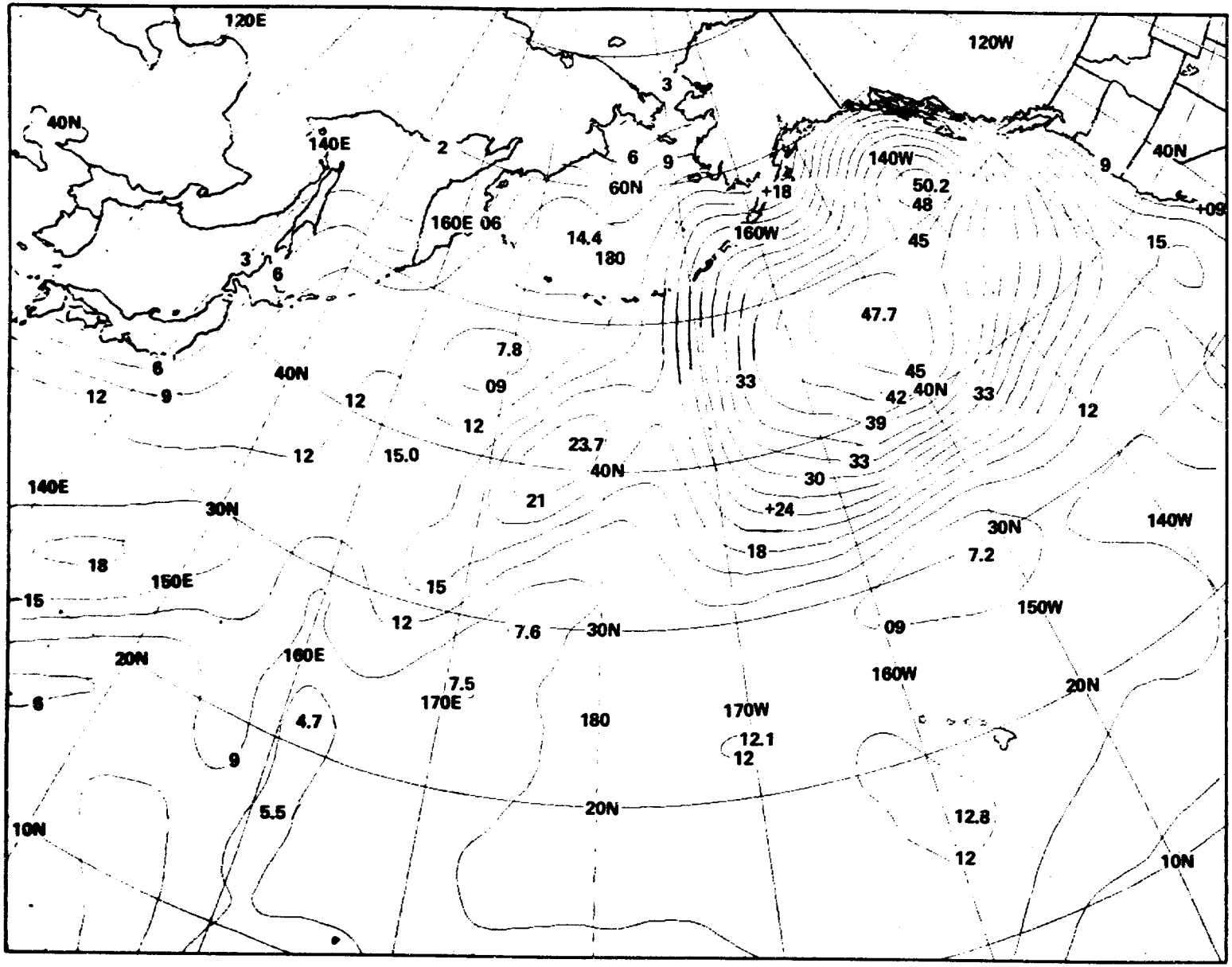

Figure 22 - Significant Wave Height Field (Feet) for 12z 27 October 1977

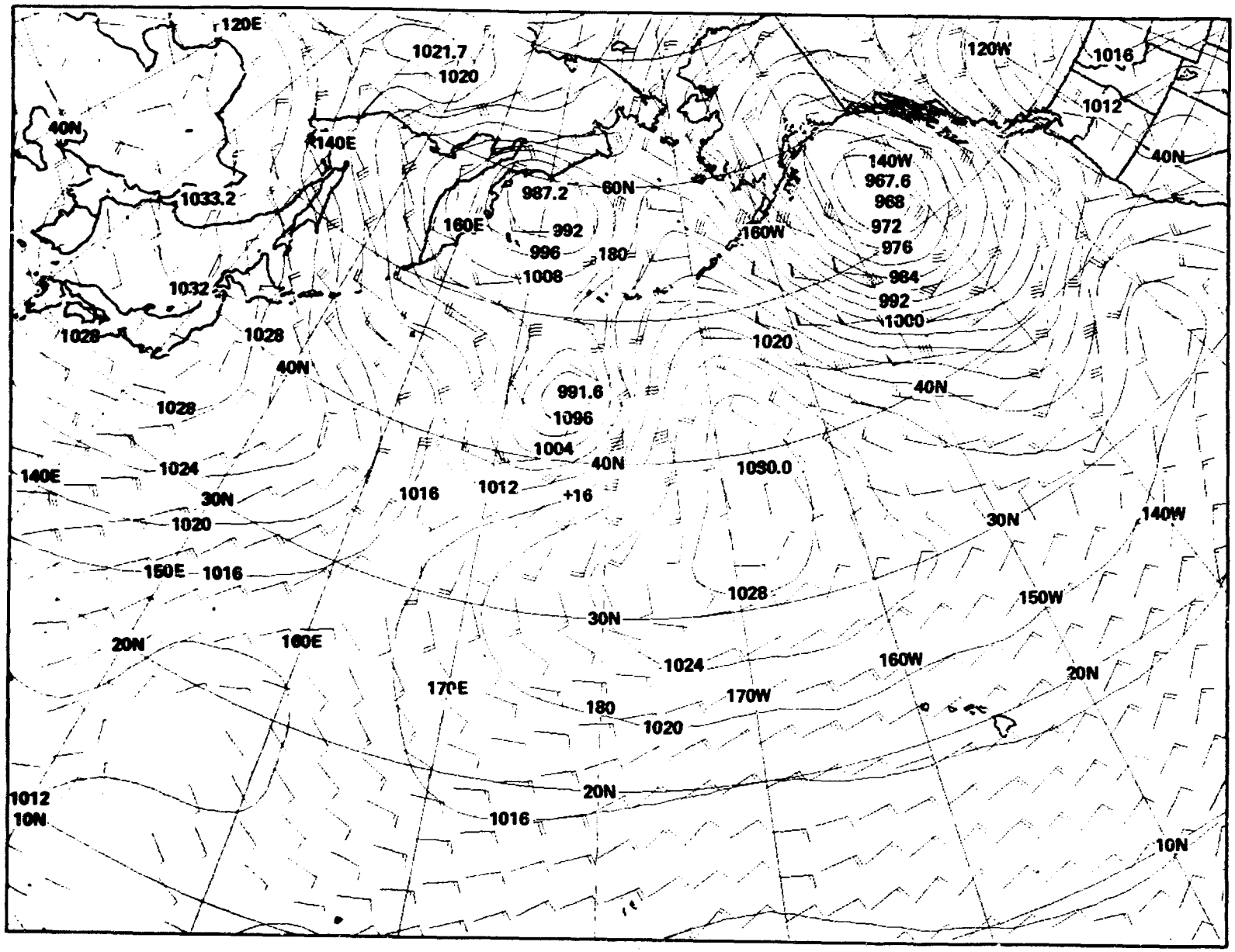

Figure 23 - Vector Winds (Knots) and Sea Surface Pressure Field (Millibars) for 12z 27 October 1977

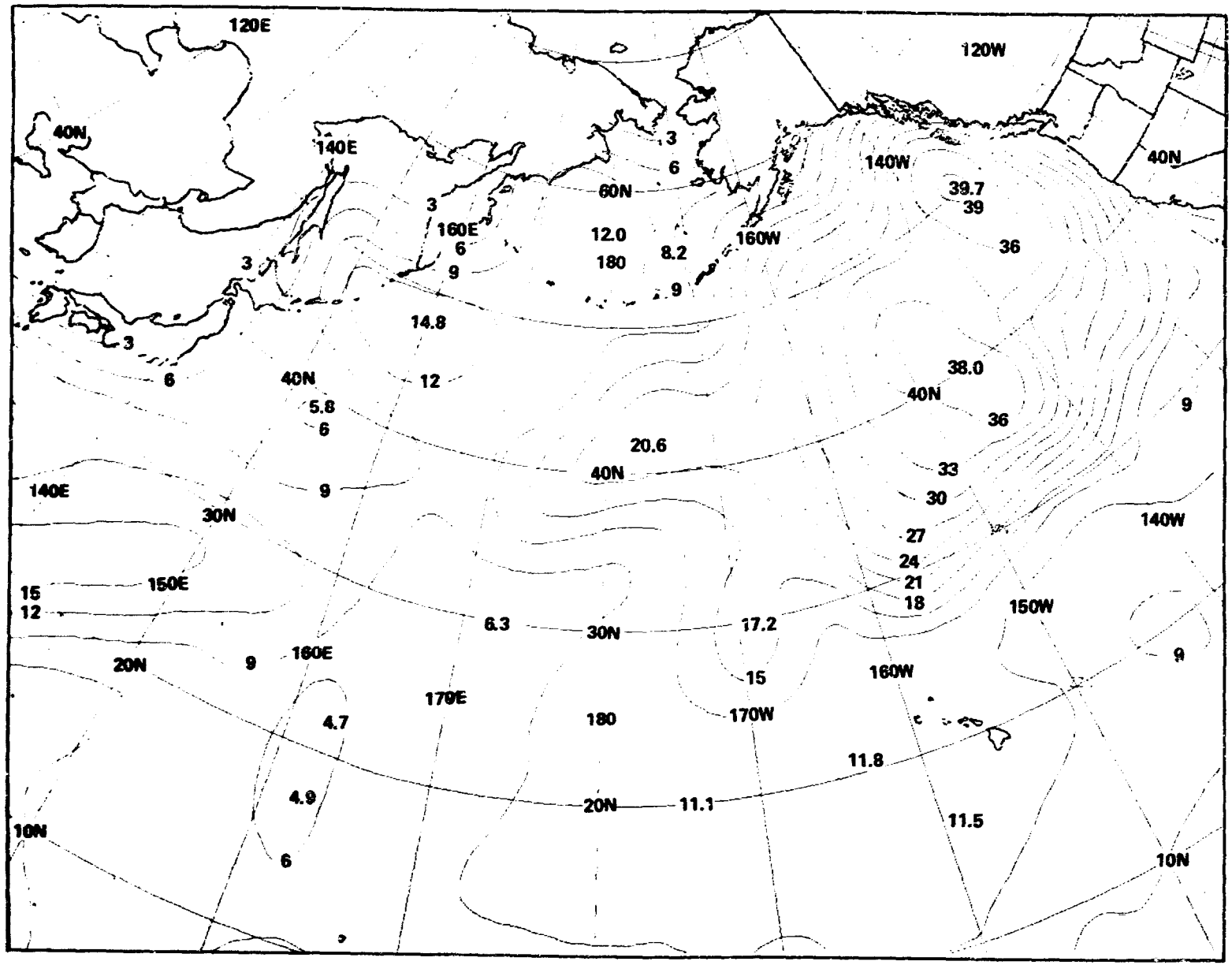

Figure 24 - Significant Wave Height Field (Feet) for 00z 28 October 1977

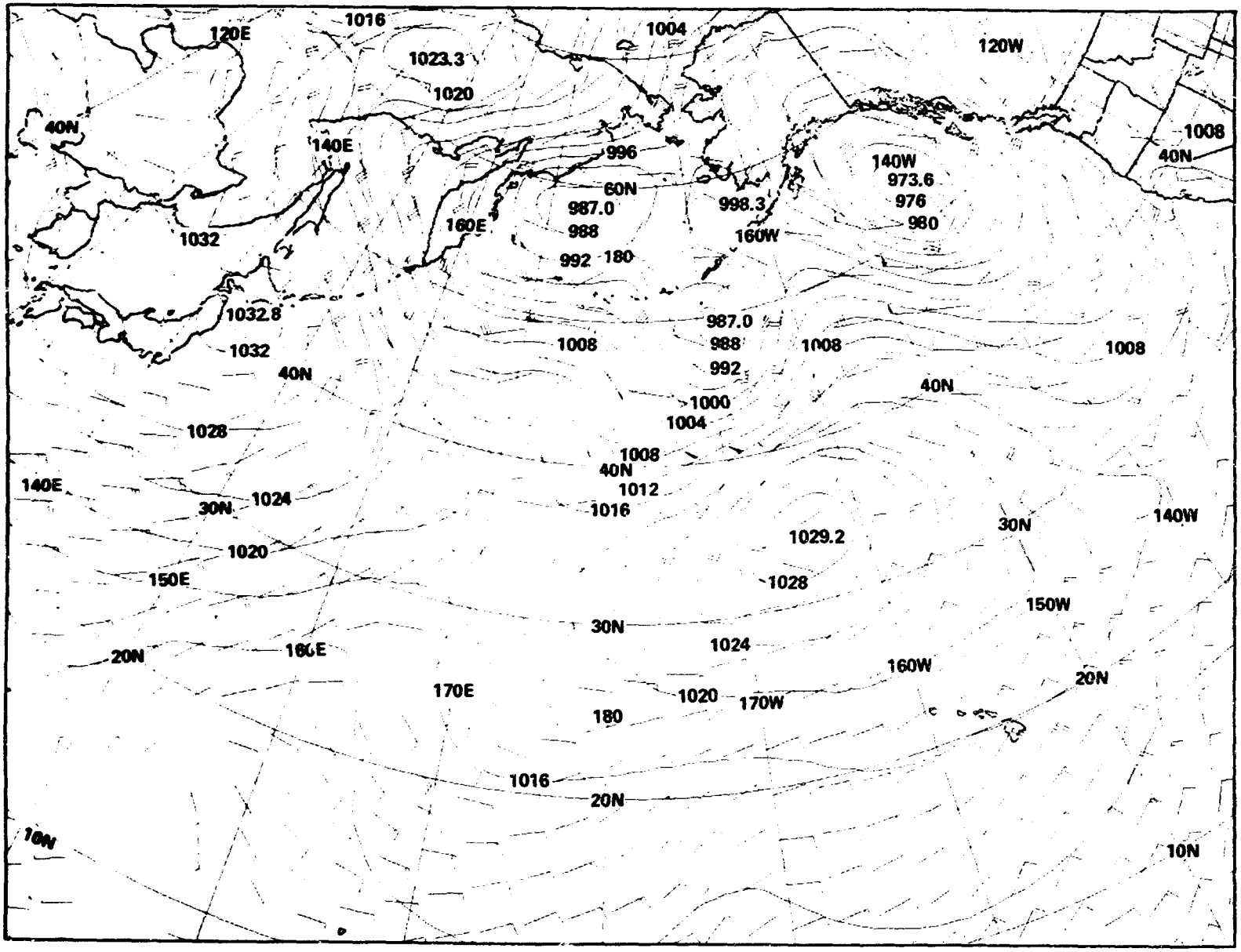

Figure 25 - Vector Winds (Knots) and Sea Surface Pressure Field (Millibars) for 00z 28 October 1977

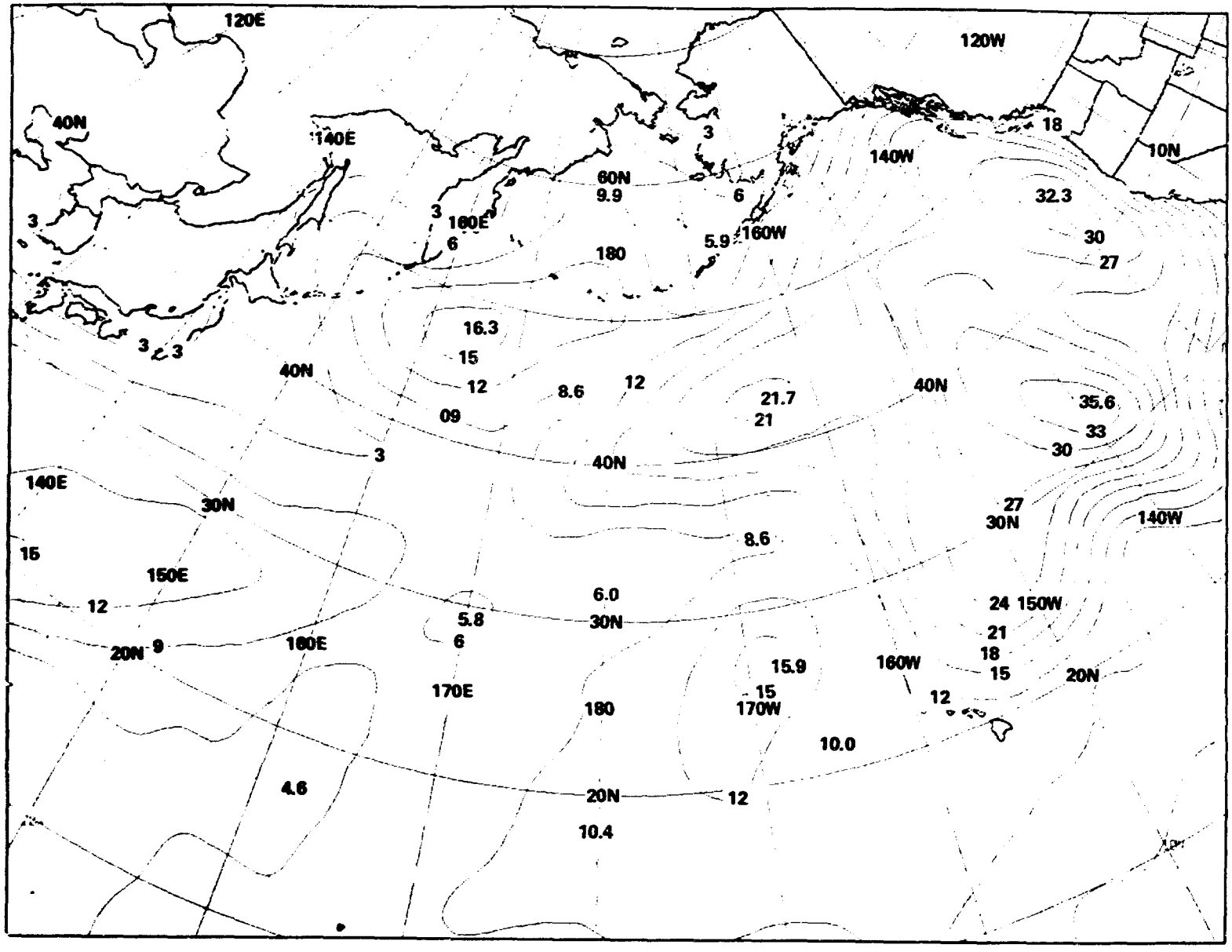

Figure 26 - Significant Wave Height Field (Feet) for 12z 28 October 1977

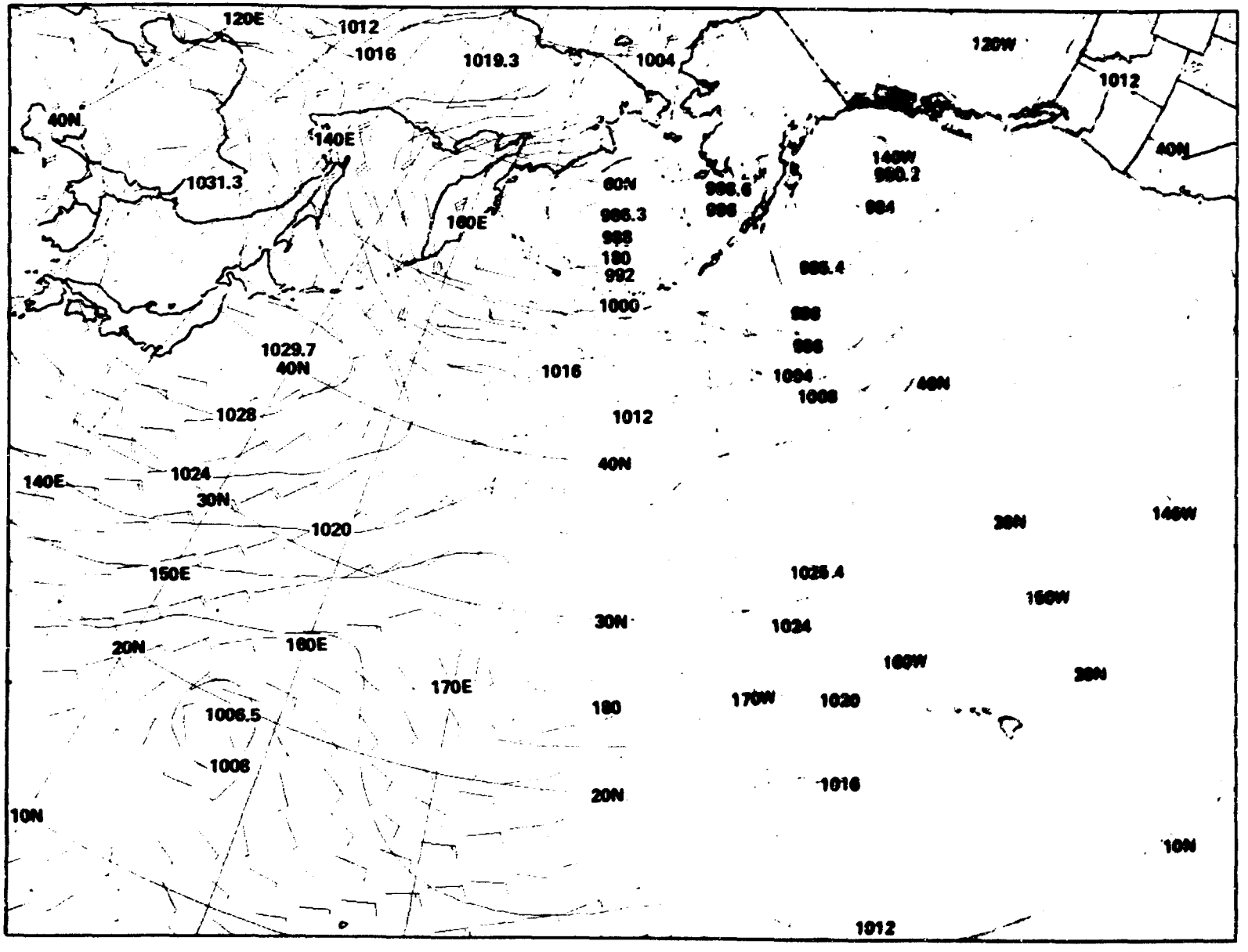

Figure 27 - Vector Winds (Knots) and Sea Surface Pressure Field (Millibars) for 12z 28 October 1977

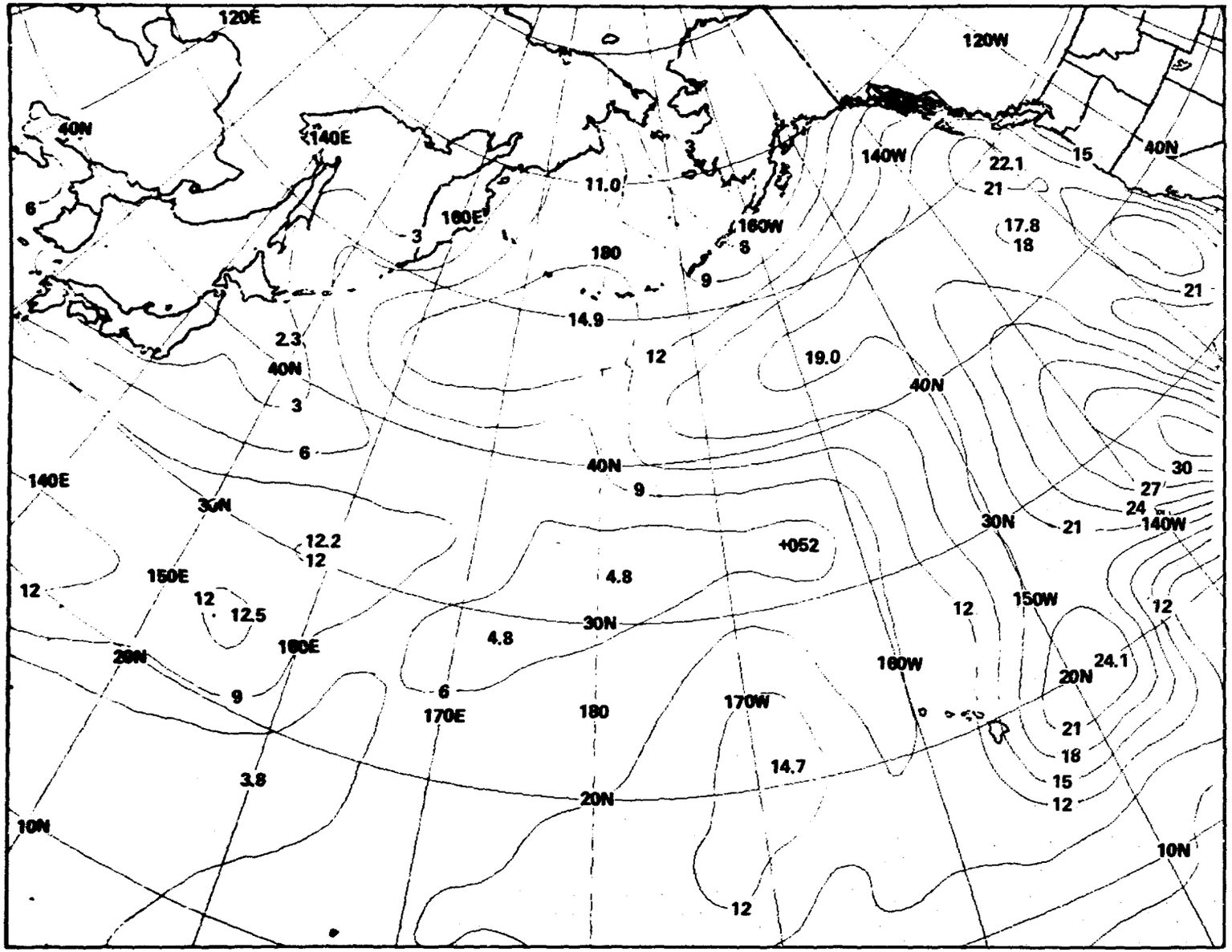

Figure 28 - Significant Wave Height Field (Feet) for 00z 29 October 1977

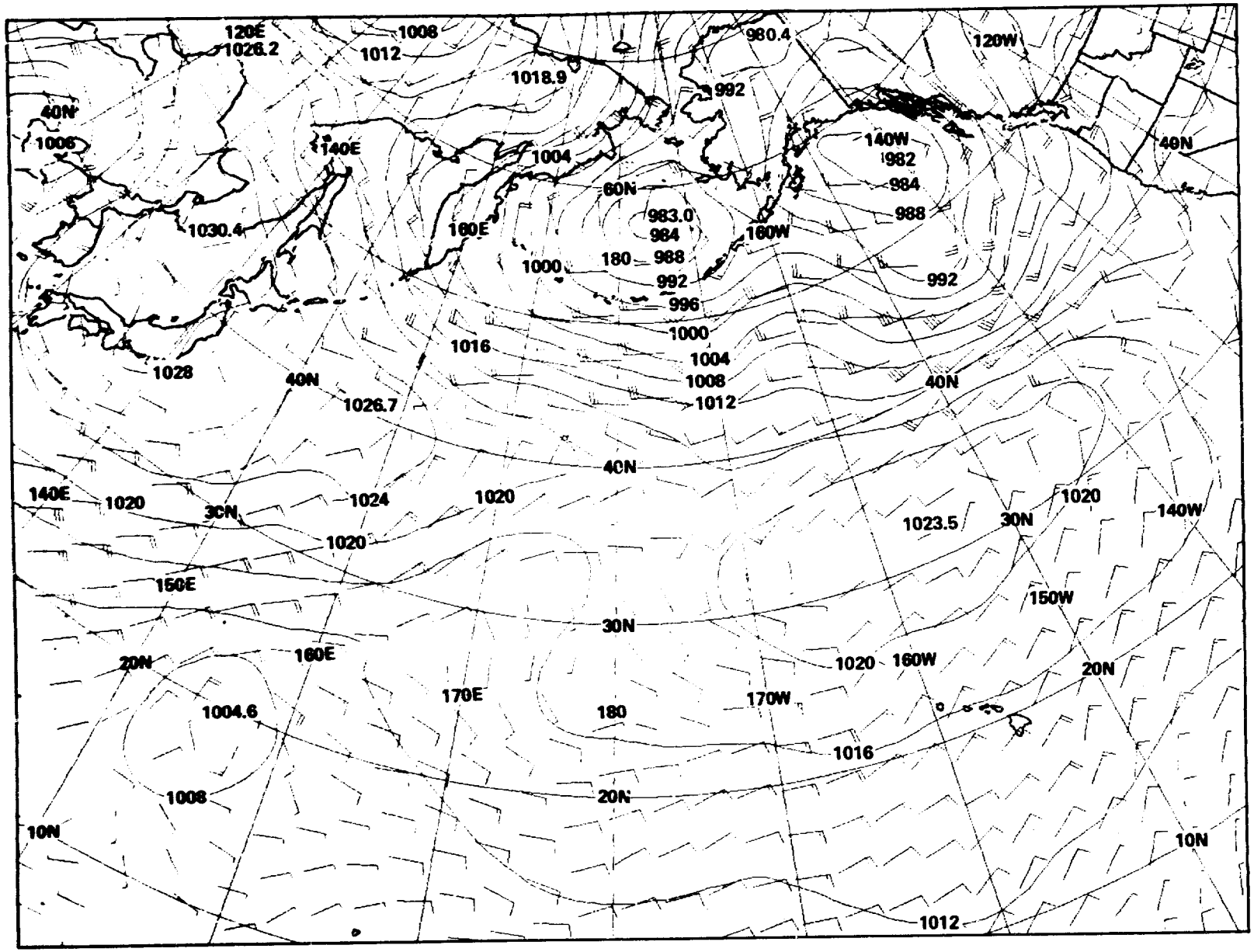

Figure 29 - Vector Wind (Knots) and Sea Surface Pressure Field (Millibars) for 00z 29 October 1977

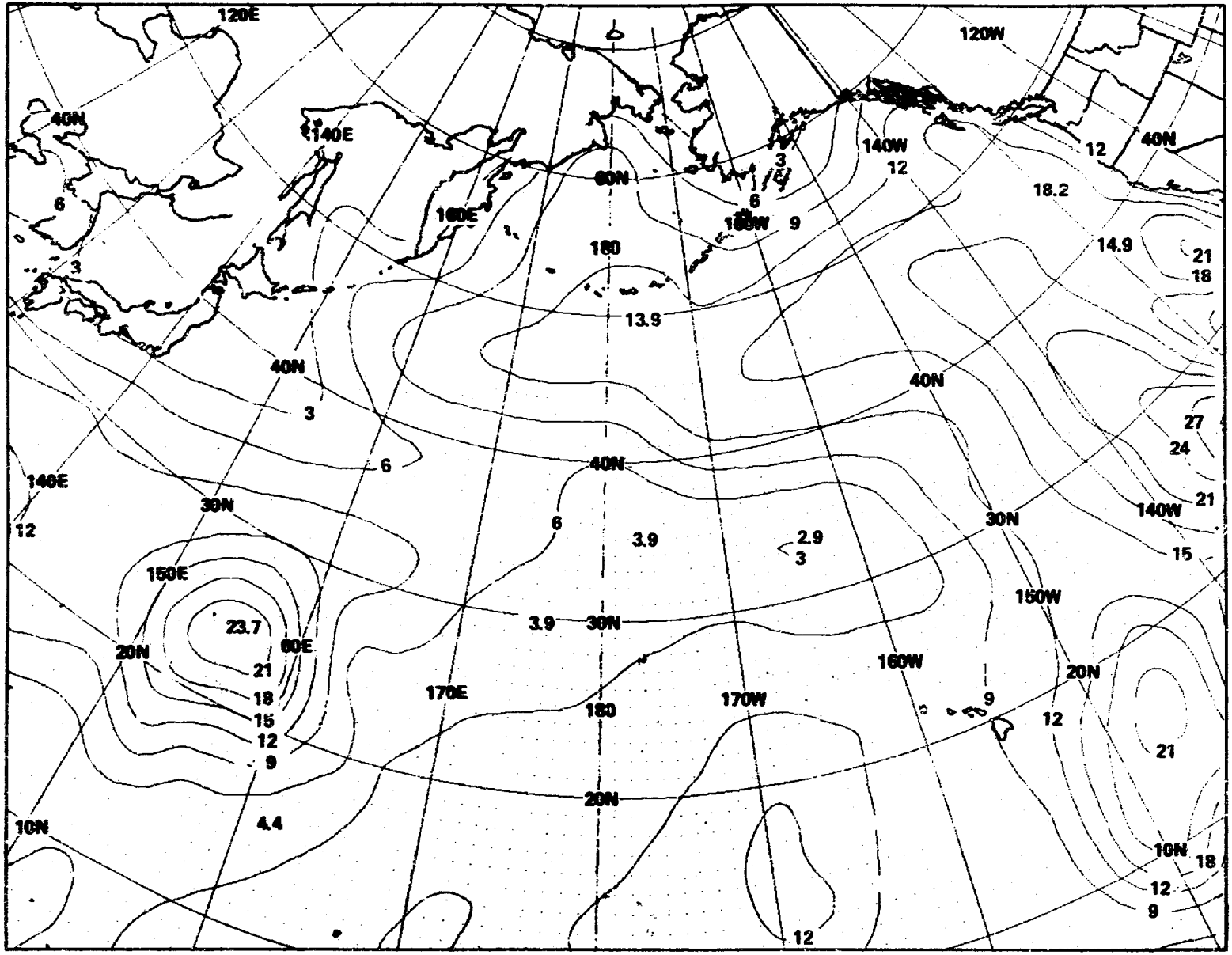

Figure 30 - Significant Wave Height Field (Feet) for 12z 29 October 1977

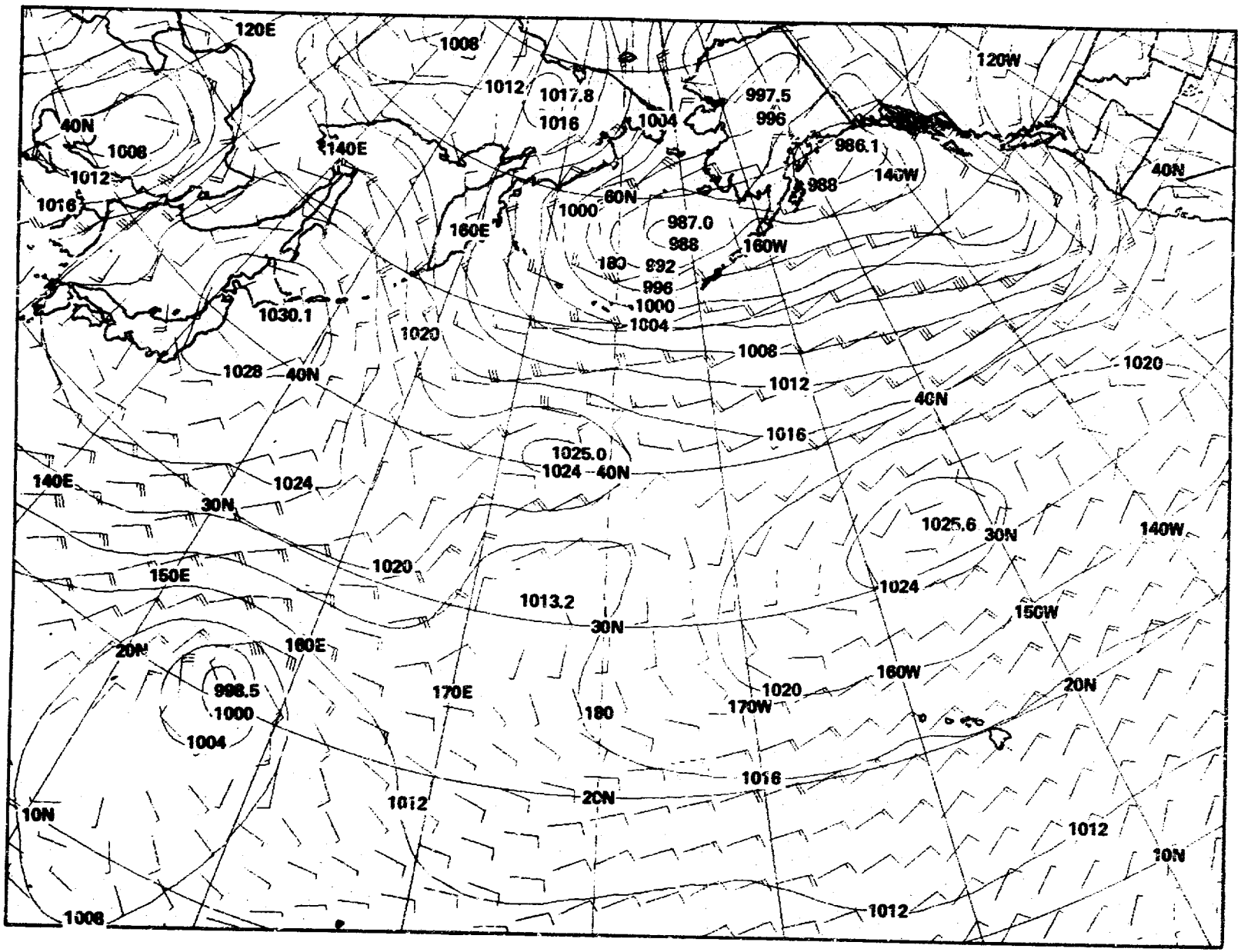

Figure 31 - Vector Wind (Knots) and Sea Surface Pressure Field (Millibars) for 12z 29 October 1977

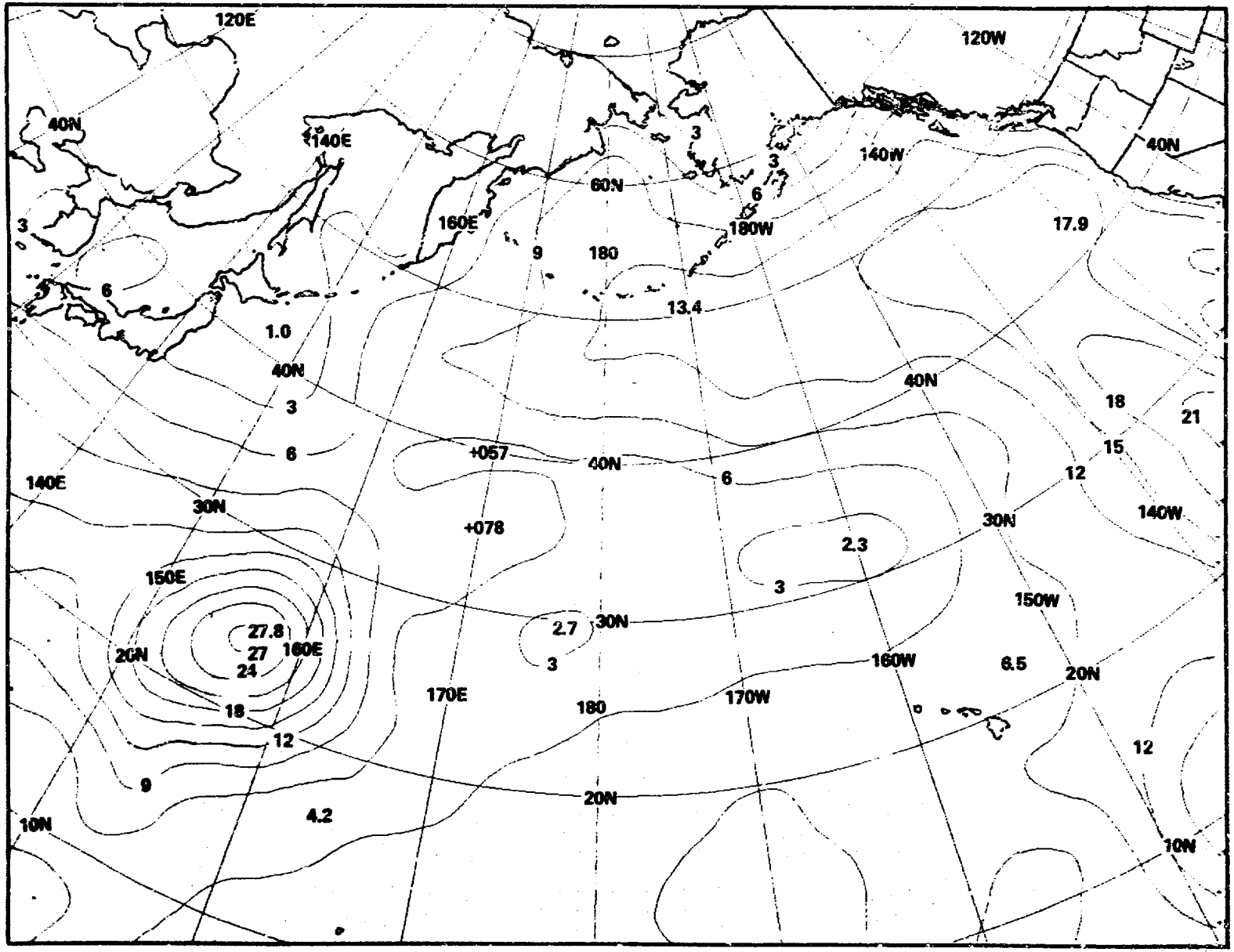

Figure 32 - Significant Wave Height Field (Feet) for 00Z 30 October 1977

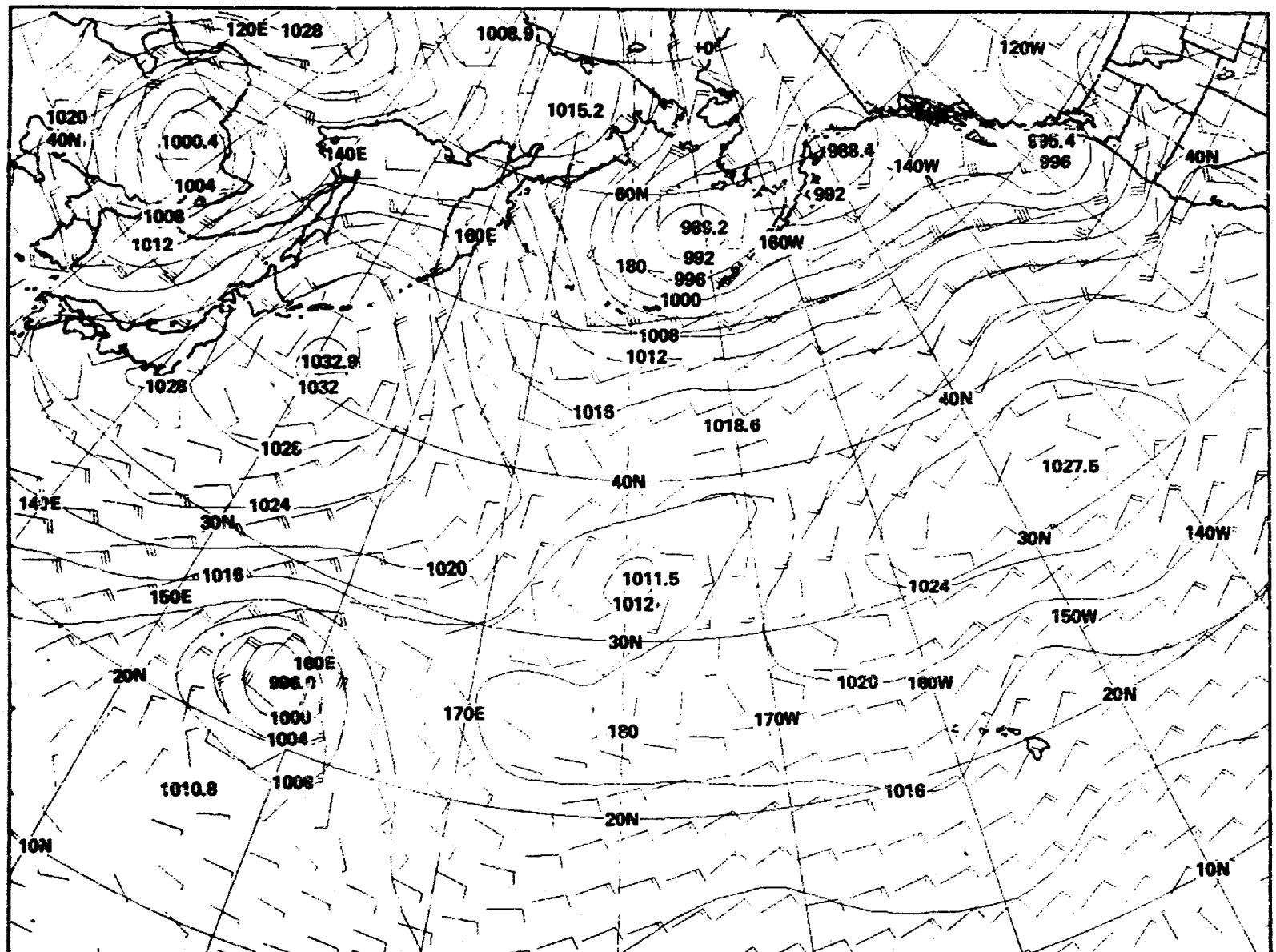

Figure 33 - Vector Wind (Knots) and Sea Surface Pressure Field (Millibars) for 00z 30 October 1977

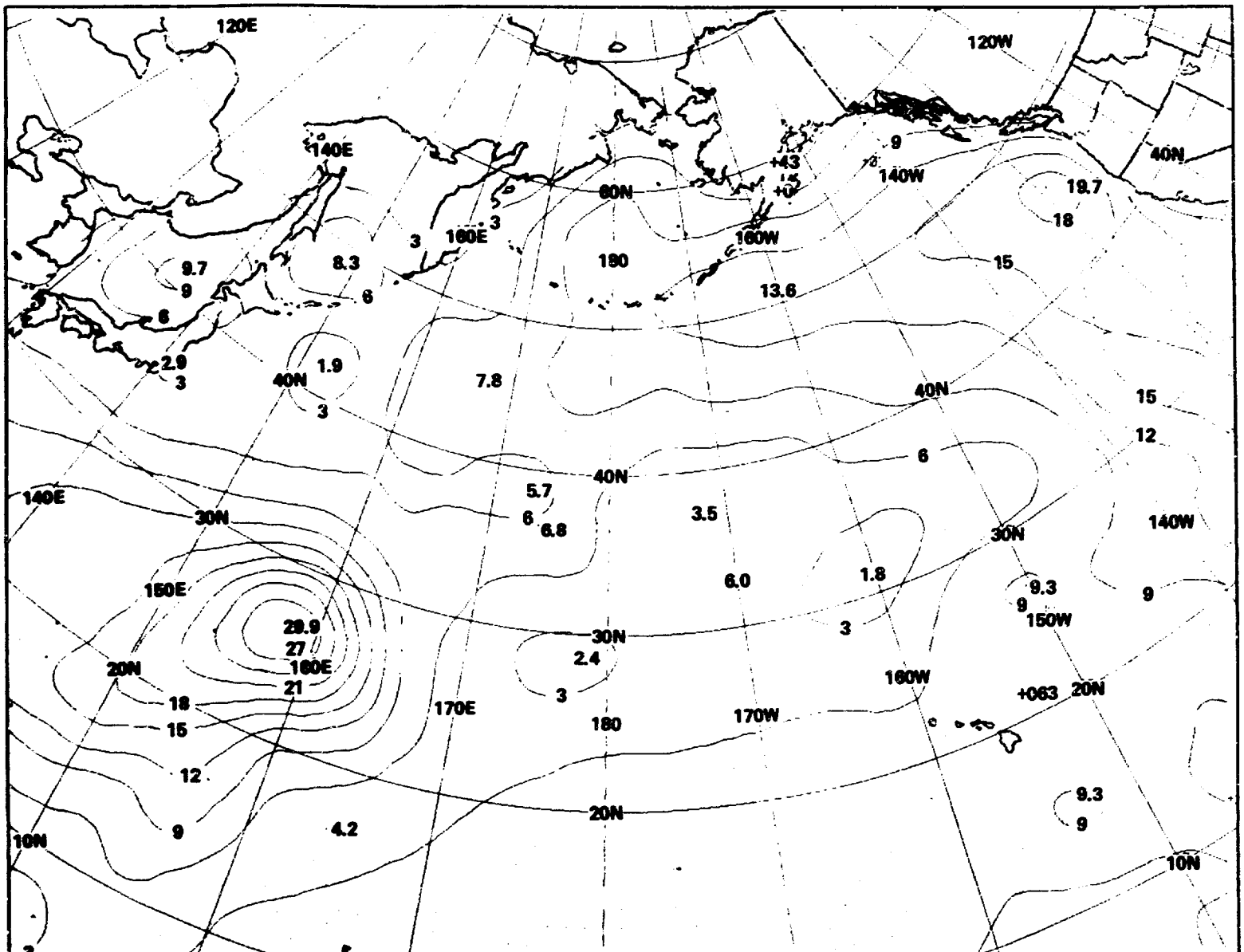

Figure 34 - Significant Wave Height Field (Feet) for 12z 30 October 1977

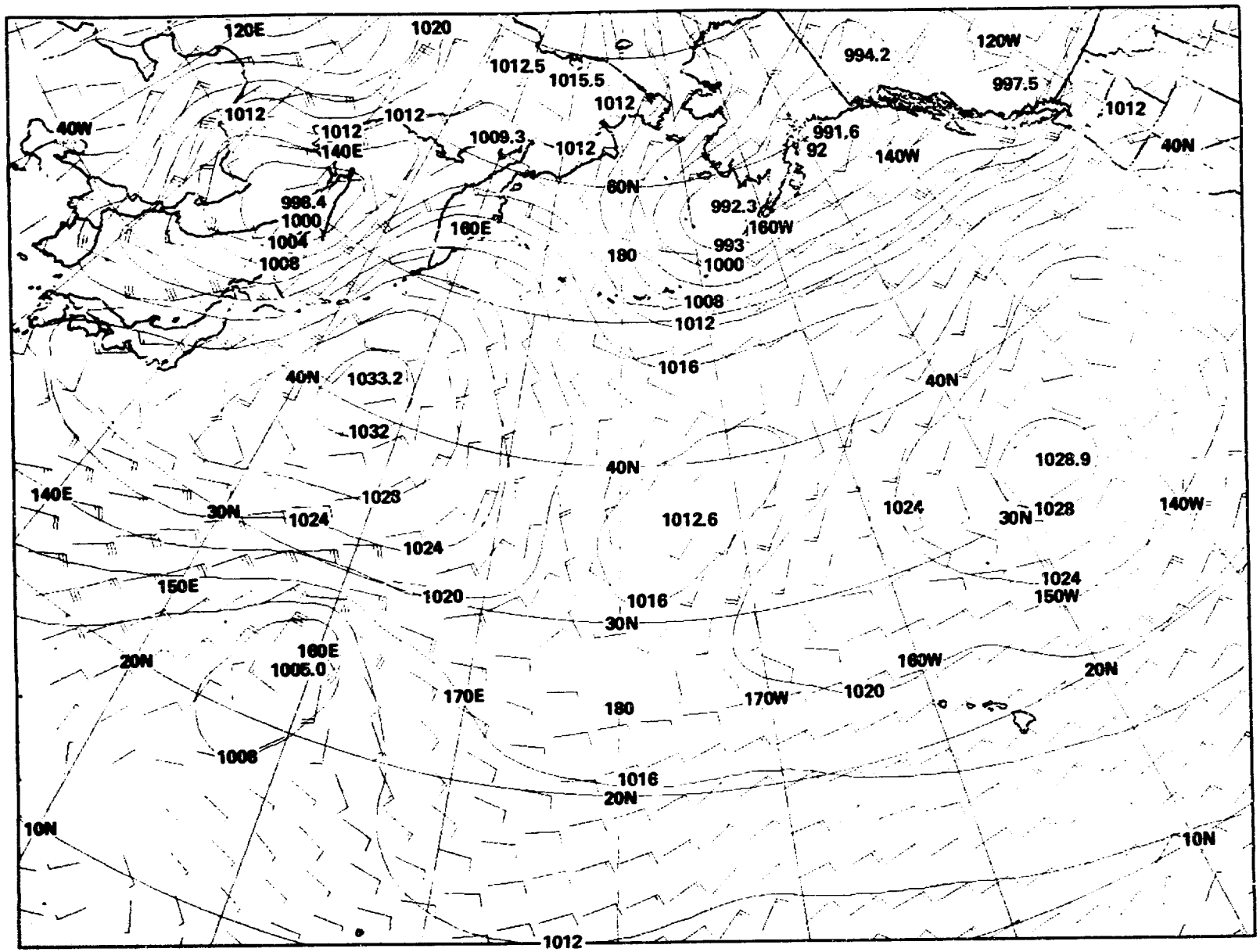

Figure 35 - Vector Wind (Knots) and Sea Surface Pressure Field (Millibars) for 12z 30 October 1977

In 12 more hours, (Figure 18 and 19) the cyclone crosses the Aleutian Islands. A wind of 85 knots (43.7 meters per second) is shown. The SOWM shows waves 60 feet high (18.3 meters) for this cyclone. The highest waves have moved eastnortheastward about 300 nautical miles (550 kilometers).

At 00z on 27 October 1977, Figures 20 and 21, the high waves are still 60 feet high (18.3 meters) and have moved farther eastward. Winds of 80 knots (41 meters per second) are still shown in the cyclone.

Twelve hours later the cyclone has weakened (12z 27 October 77, Figures 22 and 23). Two areas of high waves (50 and 48 feet, about 15 meters) have formed, but the highest waves have decreased 10 feet (3 meters) in height.

On 28 October 1977 at 00z (Figures 24 and 25), only a few winds are near 50 knots (25.7 meters per second). One area of high waves is off the coast of Canada. Another has started to move southward.

The low center continues to weaken and eventually vanishes during the next five pairs of charts with westerly winds in the Gulf of Alaska dying down to 30 knots (15 meters per second), or so, by the end of the series. On 12z 28 October, 33-foot (10 meters) swell has moved into an area with 15-knot (7.7 meters per second) winds and 24-foot (7.3 meters) swell is only a few hundred nautical miles northeast of the Hawaiian Islands. The 24-foot high swell passes to the east of the Hawaiian Islands on 00z 29 October, reaching 10° N as 15-foot (4.5 meters) swell on 30 October with little or no trace of swell by 12z on 15 October.

Whether or not some of the details of the pattern shown for the swell are real or an artifact of the angular resolution of the model could be determined by using the new higher resolution model under development for this same intense storm and by tracking some of the individual frequency-direction fields during this period.

These wave height fields are produced by a computer program that contours the values of the significant wave height located at each of the grid points of the model as given in Figure 4b. The actual SOWM heights appear to vary more erratically from grid point to grid point.[45] Also at times, the height contours do not appear to be very realistic near land. The contoured product may have lost some of the information in the original SOWM product on rapid gradients of wave height. It might make a useful study to experiment with ways to improve the significant height fields by varying the closeness of fit to grid point values and accounting for the presence of land more realistically.

SPECTRAL OCEAN WAVE MODEL SPECTRAL PRINTOUTS

Two examples of a SOWM spectral printout are shown in Table 5. The time, date, latitude, and longitude of the grid point are shown first, followed on the next line by the wind direction (from which in degrees clockwise from north), wind speed in knots, the white cap production index, and the friction velocity in knots (as defined in the subsection on $B(f_1 u_*)$).

The spectrum is a 15 by 12 array of numbers. The next row across the top is the spectral central frequency from Table 2 in seconds^{-1}. The far right column shows the directions from which the spectral components are coming. The zeros in the 180-element array have been suppressed, but in the first spectrum tabulated, there are 88 nonzero values to describe the frequency direction spectrum. The entries in the table are the values of Equation (1).

The column to the left of the direction column, and just to the right of the array, is the sum over frequency for a particular direction band. For this example, the peak waves were coming from a band centered on 268.29 degrees. The sum of this column is 192.48 (feet^2) (17.88 (meters)^2), which represents the total area under the spectrum. The significant wave height, which is the last quantity listed, is 55.49 feet (16.9 meters) for this first example.

The sums of the columns are also listed directly under the array. When properly plotted, these represent the frequency spectrum that might be obtained from a wave record of the rise and fall of the sea surface at a point. The sum of the values in this row is also, of course, 192.48 feet^2.

The frequency spectrum is shown in Figure 36. For one scale, the area under a unit frequency interval ($\Delta f = 1/180$) is shown in units of feet^2. When these values are multiplied by 180, they then have the proper dimensions of a spectrum; i.e., feet^2-seconds. The first seven values from low to high frequency are plotted as tabulated. The next three are halved and plotted over twice the Δf range. The next two would be divided by three and plotted over three times the Δf range, except that the high frequency tail of the spectrum is not shown.

The spectrum is shown in the form of a histogram. It contains exactly the correct area for each frequency band. If the dots at the center of each band are connected by straight lines, the resulting curve is misleading because (1) the area under the curve is no longer correct, (2) some of the variance has been shifted incorrectly into other frequency bands, and (3) the false impression is created that the spectrum has a peak at 0.05 Hertz.

TABLE 5 - SAMPLE SPECTRAL OCEAN WAVE MODEL* SPECTRA

Time, Date - 9z, 12 Dec 78, Location - 45.229N / 25.952W

WDDR - 261.3, WDSP - 66.3, White Caps - 14, USTR - 3.65

Frequencies	.308	.208	.158	.133	.117	.103	.092	.081	.072	.067	.061	.056	.050	.044	.039		Directions (From)
																	88.29
																	58.29
																	28.29
							0.02	0.10	0.11	0.18	0.17	0.19	0.10	0.05		0.92	358.29
	0.09	0.20	0.30	0.31	0.54	0.66	1.14	1.96	1.44	1.83	2.21	2.30	2.12	1.13	0.04	16.27	328.29
	0.15	0.33	0.47	0.47	0.87	1.04	1.84	3.42	2.85	4.00	5.64	7.78	8.06	5.53	0.20	42.65	298.29
	0.19	0.43	0.61	0.59	1.03	1.22	2.13	3.97	3.37	4.97	7.37	10.77	14.58	13.77	0.54	65.54	268.29
	0.18	0.40	0.55	0.53	0.96	1.13	1.96	3.57	2.93	4.14	5.78	8.04	13.04	7.05	0.33	50.57	238.29
	0.12	0.26	0.37	0.36	0.65	0.78	1.33	2.37	1.34	1.91	2.45			2.64	0.02	14.60	208.29
						0.01	0.05	0.18	0.24	0.35	0.50			0.56		1.89	178.29
																	148.29
																	118.29
Total	0.73	1.62	2.30	2.26	4.03	4.84	8.47	15.57	12.28	17.38	24.12	29.08	37.90	30.73	1.13	192.48	

H1/3 = 55.49 ft

Time, Date - 9z, 12 Dec 78, Location - 45.103N / 30.152W

WDDR - 264.3, WDSP - 61.5, White Caps - 30, USTR - 3.28

Frequencies	.308	.208	.158	.133	.117	.103	.092	.081	.072	.067	.061	.056	.050	.044	.039		Directions (From)
																	85.34
																	55.34
																	25.34
						0.01	0.07	0.35	0.07	0.05	0.17	0.13	0.10	0.30		0.98	355.34
	0.07	0.15	0.35	0.33	0.59	0.64	1.11	2.22	1.50	1.78	2.01	1.82	1.07	0.55	0.02	14.21	325.34
	0.11	0.25	0.52	0.50	0.91	1.05	1.88	3.32	2.83	3.89	5.14	6.21	5.86	2.74	0.12	35.33	295.34
	0.15	0.32	0.58	0.56	0.98	1.18	2.05	3.76	3.09	4.41	5.89	7.09	7.20	4.30	0.03	41.59	265.34
	0.13	0.30	0.46	0.48	0.90	1.12	1.90	3.30	2.50	3.18	3.51	3.92	5.08	0.21	0.01	27.00	235.34
	0.09	0.20	0.29	0.32	0.59	0.72	1.19	1.37	1.29	0.00	0.83	1.12	0.85	0.67		9.53	205.34
							0.04	0.04	0.05	0.04	0.01	0.07	0.05			0.30	175.34
																	145.34
																	115.34
Total	0.55	1.22	2.20	2.19	3.97	4.72	8.24	14.36	11.33	13.35	17.56	20.36	20.21	8.50	0.18	128.94	

H1/3 = 45.42 ft

*See text for units.

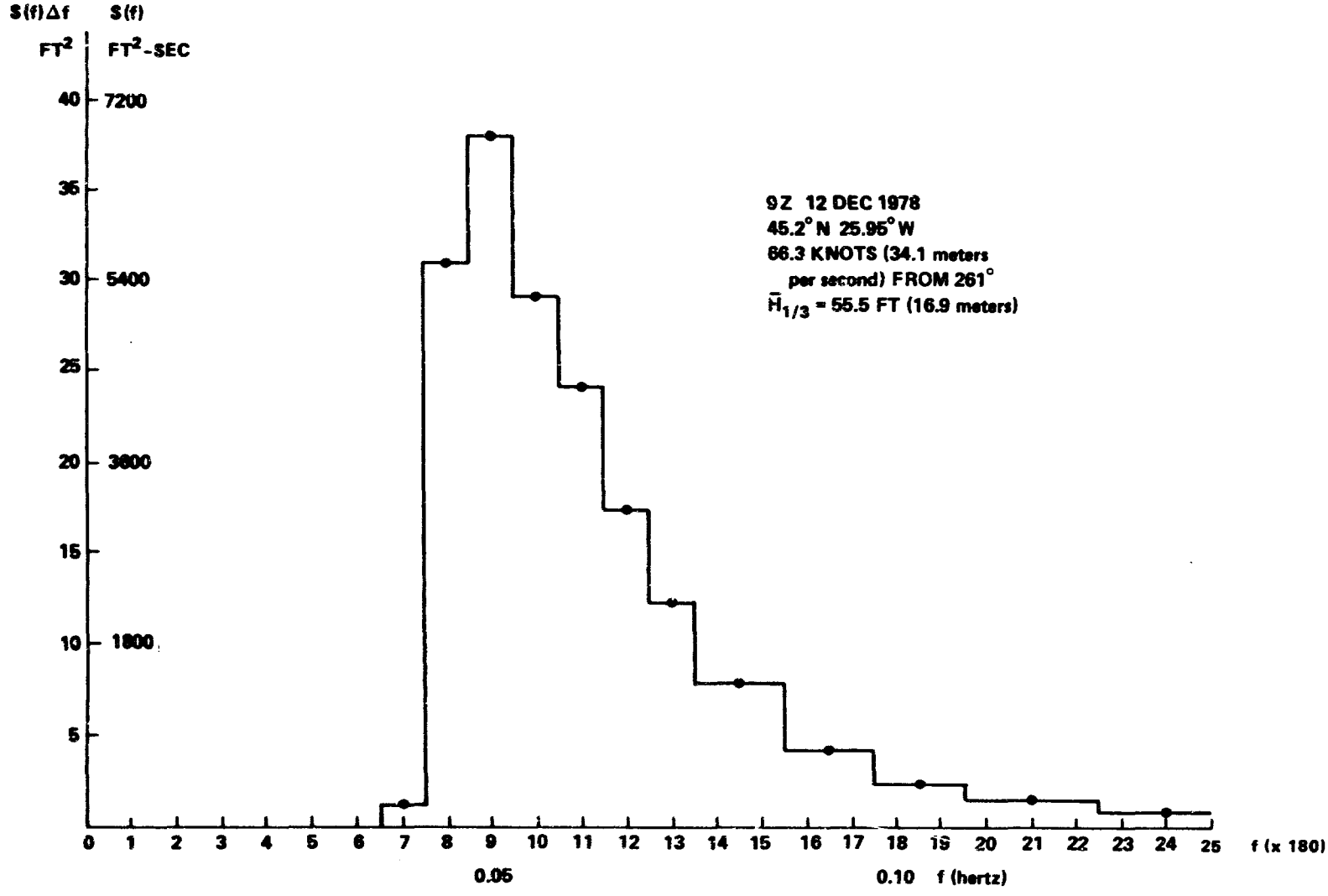

Figure 36 - A Frequency Spectrum from the Spectral Ocean Wave Model

The detailed variation of the spectra over each frequency band is not known. As an extreme example, the band from 6.5/180 seconds^{-1} to 7.5/180 seconds^{-1} shown to be 1.13 x 180 feet^2-seconds high might actually be zero from 6.5/180 to 7.45/180 and have the spectral value of 1.13 x 180 x 20 over the frequency range from 7.45/180 to 7.5/180.

The peak of a spectrum with four times the spectral resolution could actually be in the range from 7.5/180 to 8.5/180, although it is more likely to be in the next highest band and to correspond to a wave period between 21.17 and 18.95 seconds.

The angular variability of the first spectrum in Table 5 can be studied in terms of plots such as the one in Figure 37, which is again area preserving. Only the lowest 9 of the 15 frequency bands are plotted as a function of θ for each frequency band. The highest two frequencies have been appropriately halved. The vertical scales are in feet^2 and should in principal be multiplied by 180 and divided by $\pi/6$ to obtain the spectral values with units of feet^2-seconds-radians^{-1}.

As a second example a spectrum for 09z 8 December 1966 at 58.59° N and 18.18° W is shown in Table 6.[70] The significant wave height is 42.9 feet. The 180 spectral values have been partially converted to spectral values by multiplying the numbers corresponding to the previous table by 180 or by 180/2, 180/3, 180/6, and so on as required. The variance summed over frequencies is in feet^2 for each direction and the total variance for the entire spectrum is 115 feet^2.

The frequency spectra are given in three different forms. Had the entries in the 15 x 12 array been divided by $\pi/6$ the sums of each column would be multipled by $\pi/6$ to get the frequency spectrum in the first row. The first is S(f) in units of feet^2-seconds. The second is $S(\omega)$ in units of feet^2-seconds-radians^{-1}. The second row is simply the first row divided by 2π to convert frequency to circular frequency and $\Delta f = 180^{-1}$ becomes $\Delta\omega = 2\pi\ (180^{-1})$ so the integral is invariant. In the last row the length unit has been converted to meters from feet by dividing by the square of 3.281.

For many applications, the frequency-direction spectrum is multiplied by some kind of transfer function that is a function of frequency and direction. Division of the original SOWM spectral listing by Δf and $\Delta\theta$ to get it into proper units, then multiplying by Δf and $\Delta\theta$ after the transfer function is applied, and then summing to integrate seems to require a number of useless calculations. The spectral output of the SOWM can usually be used directly without going through this process.

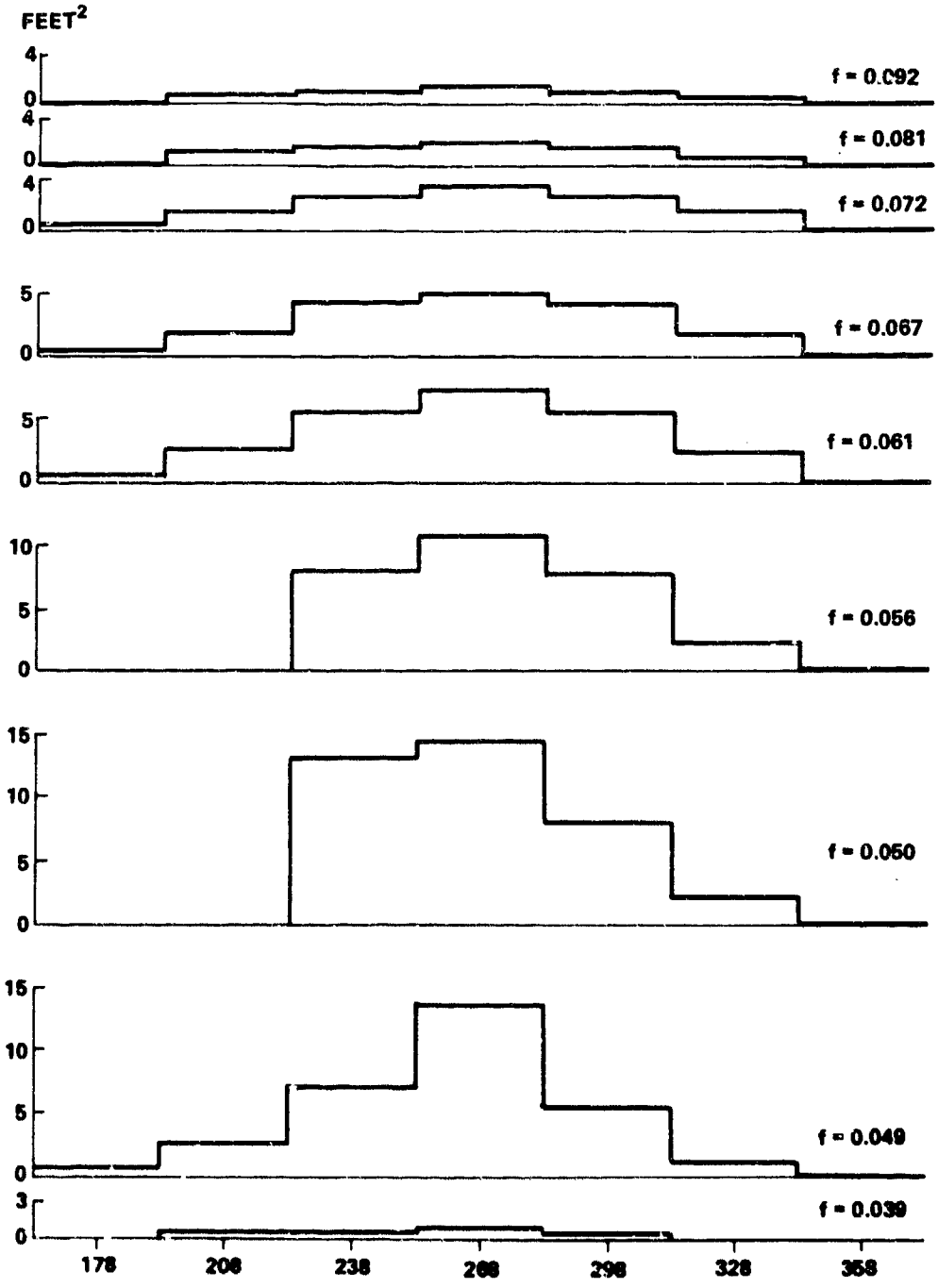

Figure 37 - The Directional Bands for the Eight Lower Frequencies in Table 5

TABLE 6 - TYPICAL HINDCAST DIRECTIONAL SPECTRUM (CONVERTED TO DENSITIES)

Time, Date - 9z, 8 Dec 66, Location - 58.579N / 18.175W

WDDR - 280.565, WDSP - 56.386 (knots), White Caps - 28, USTR 2.936 (Friction Velocity knots)

Wave Frequencies (Hertz)	.308	.208	.158	.133	.117	.103	.092	.081	.072	.067	.061	.056	.050	.044	.039	Total Variance From Each Direction	Wave Directions (From)
Spectral Densities	0.00	0.00	0.00	0.00	0.00	0.00	0.00	0.00	0.00	0.00	0.00	0.00	0.00	0.00	0.00	0.00	91.56
	0.00	0.00	0.00	0.00	0.00	0.00	0.00	0.00	0.00	0.00	0.00	0.00	0.00	0.00	0.00	0.00	61.56
	0.00	0.00	0.00	0.00	0.00	0.00	0.00	0.00	0.00	0.00	0.00	0.00	0.00	0.00	0.00	0.00	31.56
	0.00	0.00	0.00	0.00	0.00	2.70	126.80	38.74	78.85	114.13	128.57	21.82	1.78	0.00	0.00	13.79	1.56
	0.67	3.15	9.00	19.21	37.19	69.31	118.71	214.41	336.92	456.52	582.14	803.64	21.35	5.45	3.57	18.26	331.56
	1.05	4.65	13.80	28.81	55.79	102.61	178.96	337.84	571.68	838.77	1201.79	1745.45	62.28	21.82	8.93	83.87	301.56
	1.12	5.10	14.40	30.01	57.59	106.21	185.25	348.65	587.81	856.88	1208.93	1707.27	58.72	21.82	8.93	34.21	271.56
	0.90	3.90	12.00	25.81	45.59	79.21	133.09	231.53	351.25	460.14	533.93	538.18	23.13	9.09	3.57	17.55	241.56
	0.52	3.15	11.10	21.61	33.59	45.00	62.95	101.80	137.99	116.74	155.36	121.82	3.56	1.82	0.00	7.05	211.56
	0.00	0.00	0.00	0.00	0.00	0.90	2.70	8.11	10.75	7.25	5.36	1.82	0.00	0.00	0.00	0.27	181.56
	0.00	0.00	0.00	0.00	0.00	0.00	0.00	0.00	0.00	0.00	0.00	0.00	0.00	0.00	0.00	0.00	151.56
	0.00	0.00	0.00	0.00	0.00	0.00	0.00	0.00	0.00	0.00	0.00	0.00	0.00	0.00	0.00	0.00	121.56
Frequency Spectrum*																	
$S_1(f)$	4.27	19.94	60.29	125.45	229.75	405.94	838.45	1281.08	2075.27	2880.43	3816.07	4940.00	170.82	60.00	25.00	115.00	
$S_2(\omega)$	0.68	3.17	9.60	19.97	36.57	64.61	128.67	203.89	330.29	458.44	607.35	786.23	27.19	9.55	3.98	Total Variance (feet^2)	
$S_3(\omega)$	0.06	0.29	0.89	1.85	3.40	6.00	11.95	18.94	30.68	42.59	56.42	73.04	2.53	0.89	0.37		

Significant Wave Height = 42.9 ft (13.1 m)

*$S_1(f)$ in feet^2-seconds, $S_2(\omega)$ in feet^2-seconds-radians^{-1}, $S_3(\omega)$ in meters^2-seconds-radians^{-1}

THE VERIFICATION OF SPECTRAL OCEAN WAVE MODEL WAVE HEIGHTS AND WINDS

THE WINDS OF THE SPECTRAL OCEAN WAVE MODEL

In order to produce this SOWM wave climatology, it was necessary to reanalyze the meteorological data base of ship and land reports of surface pressure and wind speed and direction for the years involved.[7,72] The SOWM can only be as good as the wind fields that drive it. Wind speed errors as illustrated in Table 3 can cause large errors in wave height forecasts and even larger errors in wave spectra. The true situation is much more complicated for the SOWM (or for that matter for any wave forecasting model), than is indicated in the discussion of Table 3.

Ships report winds for too short a time average, and there are additional complications even in the "simple" problem of correctly measuring the wind near the surface of the ocean. The wind measurements that were used to produce the SOWM climatology are "state of the art," but improvements in the future are to be expected.

A comparison of the wind speeds measured at ocean station PAPA, a Canadian weather station in the North Pacific, and the winds that went into the operational SOWM model prior to 1978 in order to generate the wave spectra, has been made. A sample for this ship shows that the actual winds were, on the average, three meters per second higher than the analysis yielded at that point; that the mean square difference between the measured winds at PAPA and the winds of the model was seven meters per second; and that, if the bias was removed, there would still be a standard deviation of six meters per second.[7]

These large discrepancies have been removed by reprocessing most of the climatological wind fields so that they agree more closely with observed winds. With the waves growing as the square of the wind speed, in a sense, one would imagine that the wave forecast would be quite poor. However, on comparing the wave heights produced by the model at a grid point near the ocean station vessel, it was found that, for this particular sample, the waves were biased 0.1 meters too high that the root mean square difference was 2.3 meters; and that the standard deviation (obviously) was also essentially 2.3 meters. Further analysis suggested that an interpolation to the location of PAPA would be desirable in comparing wave height statistics for this study. The interpolated SOWM waves were biased 0.3 meter too high, the root mean square difference was 1.5 meters, and the standard deviation was essentially 1.5 meters.

These results clearly indicate that the winds are an important part of the SOWM. Unless they are correct, the spectra will not be very good. FNOC's efforts to upgrade the quality of the wind fields used in the 20-year wave climatology to generate the SOWM spectral wave hindcasts are an important part of the production of this climatology. The starting point is a file of sea surface pressure fields for the year under consideration. These sea surface pressure fields were reanalyzed by means of more modern boundary layer theories and the ship report and land report data on winds from the United States National Climatic Center. A substantial improvement and an increase in the pressure gradients for the wind fields analyzed for a particular day in the series was illustrated.[71]

A scatter diagram of the verification of the wind speeds that were used to drive the SOWM model for this climatology, as compared to measured wind speeds for 328 points for a number of different observing platforms for the North Atlantic and the North Pacific oceans, has been published.[72] This scatter diagram illustrates the fact that the actual winds were about 2.4 knots higher than the winds used by the SOWM, that the root mean square difference between the SOWM wind and the actual winds was 8.5 knots, and that the standard deviation with the bias removed (which is not done) was 8.2 knots.*

The reduced root mean square error, compared to the winds used on a day-to-day basis at FNOC for operational forecasts above, is an important improvement. Nevertheless, the actual wind was at times stronger by a factor of three than the wind used in the SOWM model; and, at other times, the actual wind was four or five times weaker than the wind used in the SOWM model.

Both of the studies are involved with the specification of the winds over the ocean on the basis of observations; and, in a sense, the data used for verification were not applied to the specification of the winds. Most analysis techniques for the description of the wind fields over the ocean do a considerable amount of smoothing. The density of the reports over the oceans from ships and from data buoys leaves much to be desired in the specification of the winds over vast areas of the ocean.

---

*1.2 meters/second, 4.4 meters/second and 4.2 meters/second respectively compared to the 3 meters/second, 7 meters/second and 6 meters/second values before correction.

COMPARISON WITH DATA BUOY WAVE HEIGHT MEASUREMENTS

The large scatter in the specification of the winds is not reflected in a comparably large scatter in the specification of ocean wave heights, contrary to what might be concluded from Table 3. Three hundred and twenty-five observations of wave height by various instruments were compared with the wave heights specified by the SOWM.[72] The SOWM waves tended to be 0.8-foot (0.2 meters) lower than the waves that were measured (estimated) at the various locations. The root mean square difference between the SOWM wave heights and the measured wave heights was 3.9 feet (1.2 meters); and the standard deviation with the bias removed was 3.8 feet (1.2 meters).*

VERIFICATION OF SIGNIFICANT WAVE HEIGHTS BY MEANS OF WAVE HEIGHTS MEASURED WITH A RADAR ALTIMETER ON GEOS-3

A short 15 (GEOS-3) or 3 (SEASAT) nanosecond radar pulse transmitted from a spacecraft has a return pulse form that can be used to determine the location of the sea surface relative to the center of the earth for geodetic and oceanographic applications.[73,74] The shape of the return pulse contains information from which the significant wave height can be found. It is possible to produce continuous graphs of the significant wave height along the subsatellite track of the orbiting spacecraft.

Those who have been active in describing, measuring, hindcasting (or specifying), and forecasting ocean waves well understand the impact that the capability demonstrated by GEOS-3 and SEASAT to measure waves will have and the tremendous scientific advances that will be possible, once these data are used routinely in an operational way. Simply to obtain a set of data comparable to one single orbit pass that requires only 10 or 15 minutes to travel from the Equator to landfall by any other means would be prohibitively difficult. Without remote sensing techniques from a spacecraft, the only other way to obtain such a data set would have been to position ships at every degree of latitude with ocean wave recorders on them along a line such as in Figure 38, extending from the Equator to a continent in either the Atlantic or the Pacific, and have them all make wave recordings of approximately 20-minutes duration simultaneously on a particular day at an agreed upon time. The cost would be prohibitive. If it were done, however, by the time the ships got

*This result was obtained after correcting the wind fields and compares to 0.3 meters, 1.5 meters and 1.5 meters before correction.

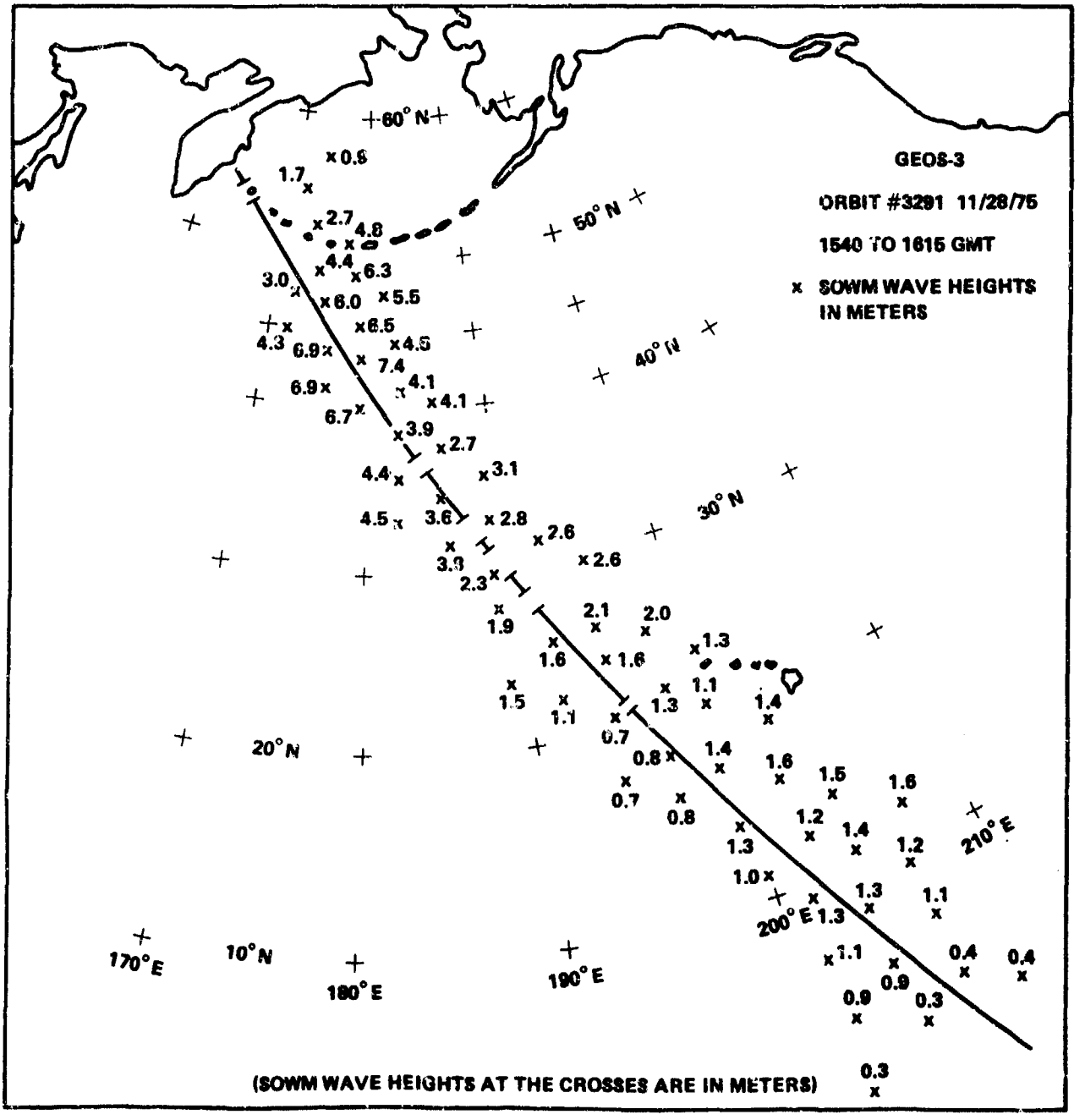

Figure 38 - GEOS-3 Orbit 3291 for 28 November 1975
(From Reference 45)

on station, it probably would be worthwhile to have them stay on station for several weeks so as to obtain additional data. The advantage would be, of course, that wave spectra could be obtained from the records, whereas current remote sensing techniques provide only an estimate of the wave height.

Even if an experiment of the type hypothesized above could be carried out, it would still not be possible to repeat it enough times to obtain the global coverage that was obtained from the spacecraft, SEASAT, during its brief lifetime. The capability to study storms and storm waves in any ocean at any time with a 12-hour separation between observations became a reality with this spacecraft.

The 30 July 1979 issue of the Journal of Geophysical Research (Volume 84 Number B8) describes the scientific results of GEOS-3.[41] Many of these results have to do with geodesy and aspects of plate tectonics and oceanography. However, a considerable section is devoted to the study of the wave heights measured by that spacecraft. Several papers are concerned with the study of the altimeter data as a means of measuring wave heights.[44,45,75,76,77] The theory of the measurements is discussed and six different algorithms are compared for the estimation of the wave height from the altimeter data.[75] These algorithms differ in various details that are explained by the paper. The overall conclusion is that they appear to work equally well. Intercomparisons show differences of the order of 0.5 meter for the various wave height calculations. All six algorithms were compared with measurements by the National Oceanographic and Atmospheric Administration data buoys and the standard deviations ranged from 0.39 meters to 1.67 meters for the different models. The scatter in the plots that compare waves measured with a buoy and measured by the altimeter are as much due to sampling variability effects in the measurement of the waves by the data buoy as they are to the scatter caused by altimetry effects. Each of the wave heights gotten from the data buoys should have a confidence interval on them as discussed elsewhere. One should multiply each of the buoy wave heights by 1.15 and 0.85 approximately to get some idea of the range in which the "true" wave height would fall when estimated from a wave record.

The significant wave heights from various surface truth sources were compared with the GEOS-3 wave heights independently of the other papers in the volume.[44] The mean difference for National Data buoys was 0.24 meters with a standard deviation of 0.53 meters. For nanosecond radar measurements from an aircraft, the difference was 0.16 meters with an 0.59 meter standard deviation. For an altimeter developed by the AAFE program, the mean difference was 0.62 meters and the standard deviation

was 0.71, and combined and weighted according to the number of points, the overall mean difference was 0.34 meters with a standard deviation of 0.61 meters. The scatter diagram (Figure 5 of the cited paper) shows quite good agreement for waves up to 8 meters high.

Quasi-synoptic wave height fields were prepared for the North Atlantic ocean using the GEOS-3 data.[44] At the same time, the initial value specifications for the wave heights, as given by the Spacecraft Meteorology Group, the FNOC SOWM model, and the National Meteorological Center were obtained.

For somewhere between 21 and 25 such fields, it was possible to compare various features of the GEOS-3 wave height fields for the North Atlantic ocean and the wave specification fields. The difference between the highest waves measured by GEOS-3, and the highest waves produced by these three different models was first studied. It was found that the GEOS-3 measurements were on the average higher than the waves in the models. For the FNOC SOWM model, GEOS-3 measured waves that were, on the average, 1.68 meters higher; and the standard deviation about this high measurement was 2.04 meters. For the Spacecraft Meteorological Group product, the GEOS-3 measurements were 4 meters higher with a standard deviation about this value of 1.65 meters. For the National Meteorological Center, the GEOS-3 waves were 3.58 meters higher on the average with a variability of 2 meters above this average. The bias for the SOWM was one third to one half of the bias for the other two methods, and the variability about this bias was comparable. Thus, the overall errors in the SOWM, when comparing SOWM model wave heights with GEOS-3 measured wave heights were much less.

It was found that the location of the high waves, as measured by GEOS-3, differed from the location of the high waves in these various models, that these high wave centers generally were displaced farther north, and that their location has considerable variability, being ± 4 to 7 degrees of latitude. Similarly the locations of the high wave centers were displaced to the east, by several degrees of longitude, and the variability about the correct location was of the order of 10 degrees of longitude. These differences were explained in terms of the errors in the wind field for the initial value specification. Most initial value specifications for numerical weather prediction and for the description of wind fields begin with the preceeding 12 to 24 hour computer-based numerical forecasts of the wind field; and, if such numerical weather forecasts tend to locate low centers in

incorrect places and to produce low centers that are too weak, the overall effect would be such as that observed.

Nevertheless, the SOWM, according to these results, is clearly superior to the other two methods that were compared. The wave heights are much more accurate on an oceanwide scale, and the displacements of the centers of high waves are in each case less than the other two models and have smaller variability. The FNOC specification of the wind fields over the North Atlantic therefore must be more accurate than the specification of the wind fields used by the other two methods.

The waves, as measured by 44 GEOS-3 orbit segments obtained during 1975 and 1976 for both the North Atlantic and the North Pacific, were compared with the operational output of the SOWM, as interpolated from 6 hourly spectral data to the time of the spacecraft pass.[45,78] Every tenth point of the GEOS-3 output was compared with the wave heights determined by the SOWM along the subsatellite track. Some of the subsatellite tracks extended all the way from the Equator to landfall at such places as the Kamchatka Peninsula for the North Pacific. Other orbit segments were rather short. The 44 orbit segments in this study were selected solely on the basis of the fact that they were made available to the investigators by the GEOS-3 program office. The GEOS-3 significant wave heights were compared to the FNOC archived waves.

An example of a subsatellite track and of the SOWM and GEOS heights along it is shown in Figures 38, 39, and 40. An as yet unsolved problem is that of the sampling variability of altimeter wave heights measurements. A tentative band of ±15 percent or ±0.5 meters, whichever is larger, is suggested. The SOWM heights given at the X's have a fine structure, or graininess, that is not apparent in the smoothed wave height fields produced by a contour plotter at FNOC as one of the SOWM products. A question arises as to whether or not a higher resolution, less smoothed height field analysis might be more realistic and whether or not such a field would agree better with altimeter data.

As summarized in Table 7, the highest waves measured by GEOS-3 were 9.0 meters for the 44 orbit segments; the highest waves predicted by the SOWM (for that same orbit segment incidentally) were 11.5 meters. On a point-by-point basis in these comparisons, there were at times very large errors with the SOWM, for example, being 4.7 meters too low for one case and 4.2 meters too high for another. The root mean square error along a given orbit, varied all the way from 0.4 meters to 3.2 meters depending on the orbit. The average of the root mean square errors was for all of

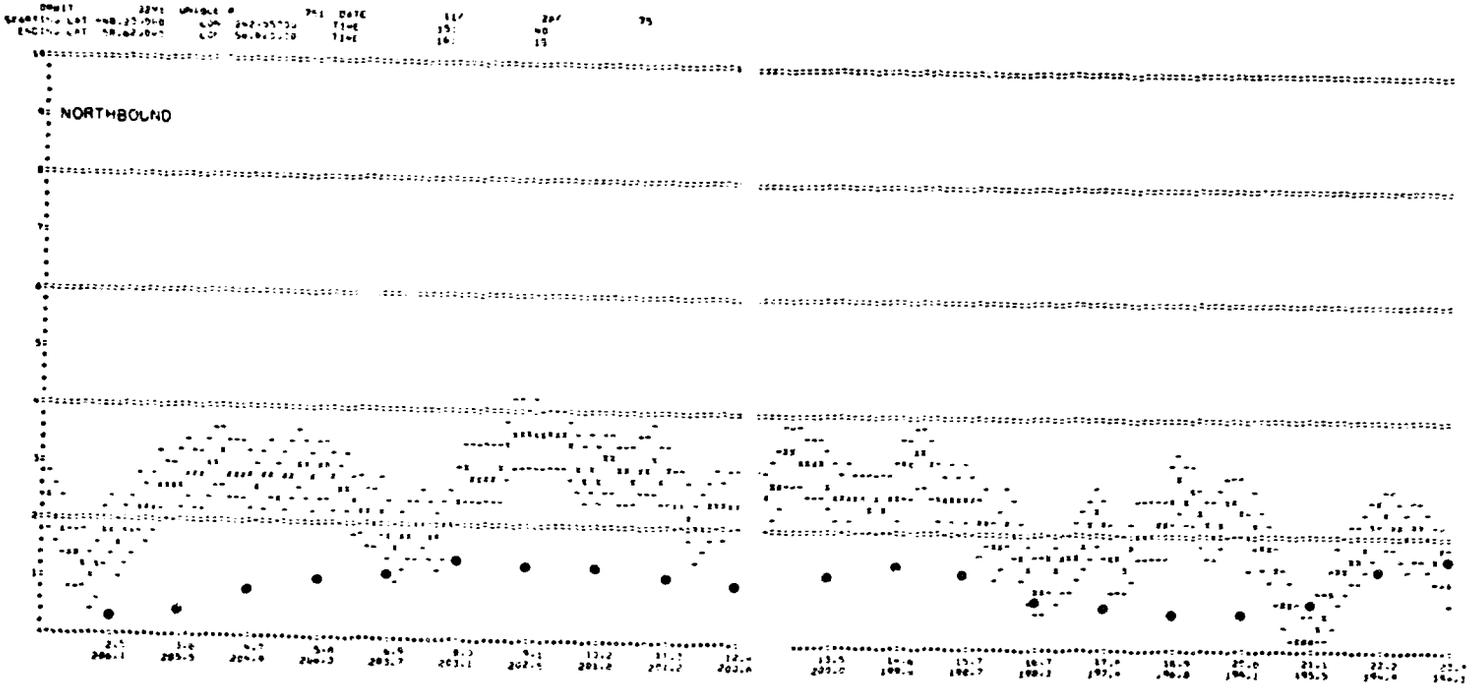

NOTE: The upper number on the horizontal scale is the latitude and the lower is the longitude.

Figure 39 - Spectral Ocean Wave Model Significant Wave Heights (dots) and GEOS-3 Wave Heights (X's) for the Orbit Segment from Revolution 3291 on 28 November 1975 from the Equator to 23 Degrees North (From Reference 45)

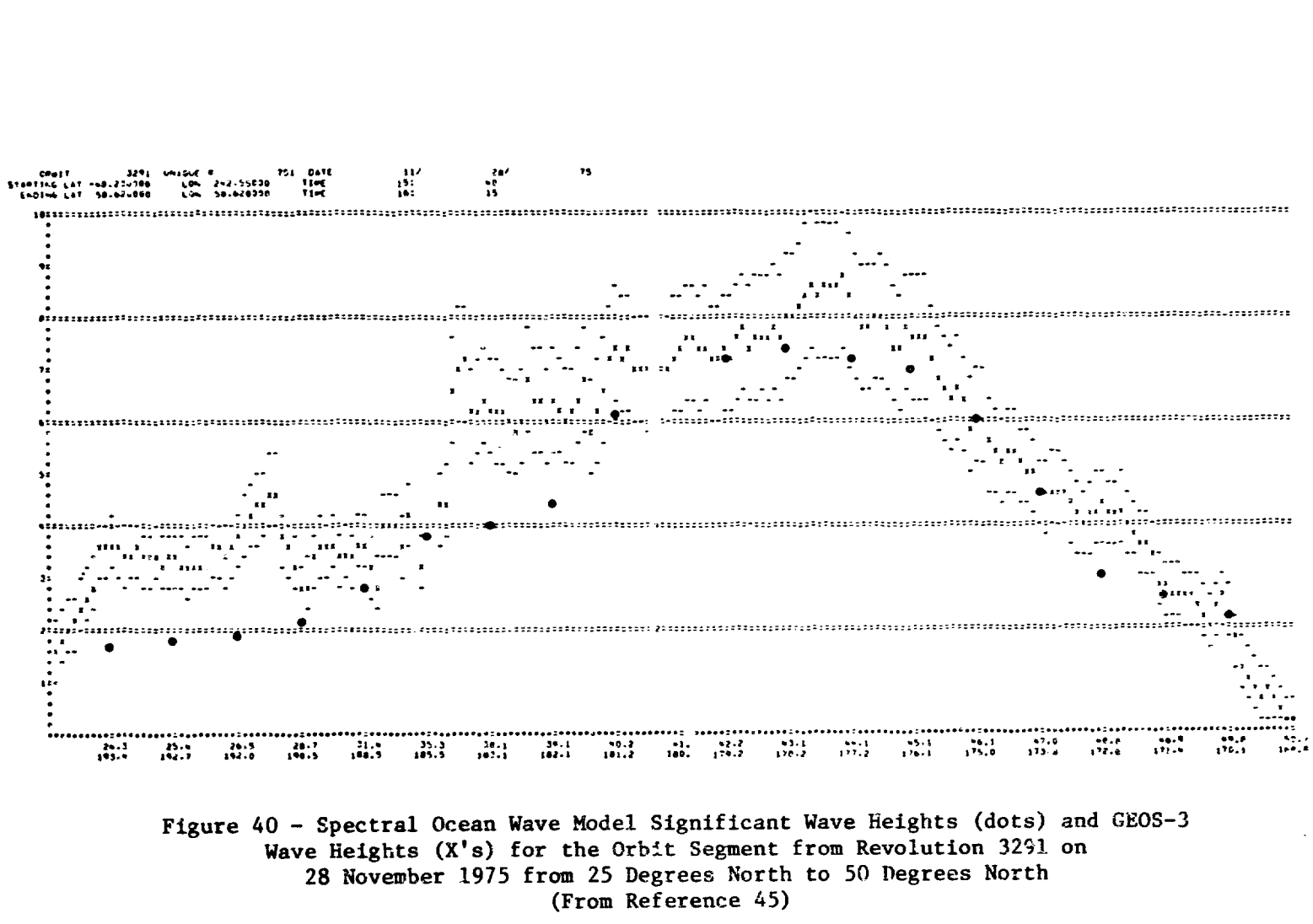

Figure 40 - Spectral Ocean Wave Model Significant Wave Heights (dots) and GEOS-3 Wave Heights (X's) for the Orbit Segment from Revolution 3291 on 28 November 1975 from 25 Degrees North to 50 Degrees North (From Reference 45)

TABLE 7 - A SUMMARY OF 44 GEOS-3 ORBIT SEGMENTS COMPARING SPECTRAL OCEAN WAVE MODEL SIGNIFICANT WAVE HEIGHT WITH ALTIMETER MEASUREMENTS FOR 1975 AND 1976

Orbit	Date (1975)	Number of Points	RMS	Bias	Error	GEOS Range	SOWM Range	Wind	
								GEOS	SOWM
1929	24 Aug.	24	0.8	-0.6	-1.8	0.0-2.8	0.1-1.1		
1991	28 Aug.	36	1.0	-0.2	-2.3	0.0-4.0	0.8-3.7		
2100	5 Sep.	7	0.5	-0.3	-1.2	0.0-1.8	0.2-0.9		
2114	6 Sep.	20	1.3	-1.0	-3.2	0.0-3.8	0.2-1.0	8-11	0-5
2254	16 Sep.	30	1.1	-0.8	-2.6	0.0-4.2	0.1-2.4	12-13	8-10
2318	20 Sep.	10	0.6	0.0	-1.3	0.2-3.0	0.5-1.2		
2658	14 Oct.	9	0.8	-0.5	-1.7	1.0-4.2	1.0-2.5		
		6	3.1	-2.8	-4.7	3.0-7.6	1.0-2.9	18	12
2782	23 Oct.	11	0.7	-0.1	-1.2	0.2-3.2	1.2-3.5	12	10
2812	25 Oct.	28	1.0	-0.8	-2.0	2.6-6.2	2.0-5.0	16	13.5
2827	26 Oct.	26	1.1	-1.0	-2.4	1.8-5.4	1.0-6.9	14	12
2829	26 Oct.	19	0.9	-0.5	-2.1	0.6-5.0	0.6-4.6	15	12
2904	1 Nov.	24	1.2	-0.8	-2.0	0.6-6.0	0.8-4.1	16	13
2919	2 Nov.	12	0.8	-0.5	-1.7	0.2-3.0	0.3-3.2		
2936	3 Nov.	21	0.7	-0.3	-2.3	0.2-6.4	0.3-3.9		
2998	7 Nov.	17	0.9	+0.2	+1.9	2.8-5.4	2.7-5.6	13	15.5
3030	10 Nov.	28	2.0	-1.5	-4.2	0.0-7.0	0.3-3.4	17	10
3075	13 Nov.	21	0.6	-0.4	-1.3	0.0-2.8	0.5-1.6		
3152	18 Nov.	26	1.0	-0.6	-1.9	0.0-4.4	0.2-3.6	11.5	9
3167	19 Nov.	29	1.1	+0.5	+2.6	0.2-4.0	1.3-5.3	14	15.5
3214	23 Nov.	6	1.2	-1.1	-2.0	0.8-3.2	0.8-1.3	12	7.5
3229	24 Nov.	21	0.8	-0.5	-1.6	3.4-7.8	3.9-6.6	17	16
3231	24 Nov.	23	1.1	-0.7	-1.9	0.2-4.8	0.9-4.3	12-13	8
3291	28 Nov.	38	1.4	-1.0	-2.3	0.0-8.8	0.3-7.4	20	19
3430	8 Dec.	17	1.4	+0.3	+2.6	0.6-4.8	0.9-6.0		
3524	15 Dec.	12	0.6	-0.2	-1.0	0.0-3.8	0.2-2.7		
3539	16 Dec.	19	0.9	-0.2	-1.5	0.0-2.4	0.2-1.8		
3554	17 Dec.	18	0.6	+0.1	+1.3	0.2-2.6	1.3-2.4		

Heights are in meters and winds in meters per second. The 'error' is the largest of the indicated number of points.
(From Reference 45).

TABLE 7 (Continued)

Orbit	Date (1975)	Number of Points	RMS	Bias	Error	GEOS Range	SOWM Range	Wind	
								GEOS	SOWM
3586	19 Dec.	12	2.5	-2.0	-4.0	2.4-7.6	1.3-5.3		
3645	23 Dec.	42	1.3	-0.8	-3.8	0.0-8.0	0.0-8.7	19.5	15
Total		529							

Orbit	Date (1976)	Number of Points	RMS	Bias	Error	GEOS Range	SOWM Range	Wind	
								GEOS	SOWM
4576	27 Feb.	12	1.1	-0.4	-2.0	0.0-6.2	0.5-5.1		
4593	28 Feb.	12	0.9	-0.7	-2.2	0.2-4.4	0.5-2.5		
4608	29 Feb.	19	1.0	-0.2	-2.4	0.6-7.0	1.2-5.9		
4623	1 Mar.	7	0.5	+0.1	-0.8	0.2-5.4	0.2-4.9		
4978	26 Mar.	11	1.2	+0.5	+0.3	0.0-5.8	1.6-7.1		
5025	30 Mar.	46	0.9	-0.2	--	1.4-7.4	1.3-9.5		
			2.5	+2.4	+3.0			17	21
5149	7 Apr.	10	3.2	+2.6	+4.2	3.6-9.0	5.0-11.5	18	22
5164	9 Apr.	9	1.8	+1.6	+2.7	1.2-8.4	2.4-9.6		
5258	15 Apr.	19	1.0	+0.2	+2.2	0.0-3.2	0.3-2.6		
6295	27 June	14	0.9	-0.7	-1.6	1.2-4.6	0.9-4.1		
6479	10 July	37	0.7	-0.4	+1.6	0.0-3.8	0.2-5.3		
6481	11 July	19	0.7	-0.3	-1.8	0.0-2.8	0.3-2.7		
6635	21 July	45	1.0	-0.6	-2.5	0.0-4.2	0.3-2.7	13.5	11
6883	8 Aug.	12	0.8	-0.6	-1.4	0.0-2.2	0.2-1.3		
7858	16 Oct.	14	0.4	+0.2	+0.8	0.0-2.0	0.3-1.0		
Total		296							

Heights are in meters and winds in meters per second. The 'error' is the largest of the indicated number of points.
(From Reference 45).

the data 1.1 meters for 1975 and 1.2 meters for 1976 for cases in which the poor specifications were included. With these removed, the root mean square errors were 0.9 meters for both years. There was also a tendency for the SOWM to be biased somewhat too low. Typically, this bias would be from -0.5 to -1 meter. Were this bias removed so that the standard deviation about each orbit segment was computed, the standard deviations would have been considerably under 1 meter.

For a number of orbit segments the SOWM could be considered to be a bust, and for others the bias was consistently too high or too low. This was interpreted to be the result of poor wind fields. The last two columns indicate what wind speed would correspond to the fully developed SOWM heights and what wind speed would be required to produce the GEOS-3 measurements.

The analysis techniques of Reference 78 were used to study additional GEOS-3 passes.[71] The procedures of Reference 78 were considerably simplified because the wave height contour fields generated by FNOC were obtained; and these wave height contour fields were compared with the wave heights estimated by GEOS-3. This eliminated a difficult and expensive numerical computation which recovered the wave spectra along the subsatellite track from the spectral output of the SOWM and located those wave heights within an assigned distance of the track, for comparison with the GEOS-3 heights. The results were comparable to the previous results in that similar bias and root mean square errors were obtained. Table 8 summarizes these results. A number of other results were obtained, some of which are given below. Figure 48 shows histograms of the root mean square errors for both of these studies including five "outriders" in Reference 78.

Figure 41 shows a scatter diagram of the highest wave in a given orbit segment as measured by GEOS-3 as compared with the highest wave predicted by the SOWM for that same orbit segment. In general, the highest measured waves were higher than those predicted. According to Reference 71:

"A regression equation and correlation coefficient were calculated for this diagram. They were

$$\text{GEOS-3}_{max} = 0.9852\ \text{SOWM}_{max} + 0.8743\ (\text{m}) \qquad (52)$$

Correlation coefficient = + 0.935

TABLE 8 - STATISTICAL SUMMARY OF ORBITS OBTAINED IN 1977-1978
(from Dooley 1978, Reference 71)

Orbit	Date	Pts H1/3	Pts H1/3	RMS H1/3	RMS H1/3	Bias H1/3	Bias H1/3	Error H1/3	Error H1/3	GEOS Range H1/3	GEOS Range H1/3	SOWM Range
13224	10/30/77	33	31	0.65	0.50	-0.19	-0.16	-1.80	-1.42	1.99 to 5.01	2.38 to 4.55	1.37 to 5.36
13229	10/31/77	24	22	1.43	1.32	-1.21	-1.22	-2.28	-1.87	1.34 to 4.34	2.15 to 3.61	0.55 to 2.50
13268	11/02/77	11	9	1.18	0.76	-0.40	-0.27	-1.94	-1.45	1.80 to 5.40	2.41 to 3.63	2.17 to 3.56
13267	11/02/77	24	17	1.21	1.19	-0.50	-0.61	-2.21	-2.09	0.00 to 4.69	0.44 to 4.51	0.91 to 4.66
13276	11/03/77	23	20	0.99	0.83	-0.71	-0.73	-2.00	-1.69	0.00 to 5.22	0.81 to 4.91	0.17 to 4.09
13282	11/03/77	26	24	1.02	0.79	-0.63	-0.65	-1.85	-1.38	0.00 to 5.79	1.42 to 4.87	1.00 to 4.01
13285	11/03/77	15	13	1.51	1.47	-1.38	-1.42	-2.33	-2.19	1.35 to 3.31	2.02 to 2.99	0.80 to 1.85
13320	11/06/77	11	9	1.26	1.05	-1.04	-1.00	-2.44	-1.54	0.00 to 2.79	1.06 to 2.57	0.00 to 1.55
13444A	11/15/77	31	30	1.60	1.51	0.06	0.10	2.95	-2.47	0.00 to 3.92	0.15 to 3.62	1.01 to 3.64
13444B	11/15/77	32	31	0.85	0.63	-0.29	-0.36	1.78	1.49	0.00 to 3.93	0.56 to 3.30	0.77 to 2.40
13446	11/15/77	27	25	0.56	0.31	-0.10	-0.09	-1.24	-0.90	0.00 to 2.07	0.01 to 1.64	0.01 to 1.32
13449	11/15/77	27	26	1.21	1.09	0.19	0.16	2.56	2.45	0.54 to 4.38	1.56 to 3.66	0.86 to 4.55
13450	11/15/77	41	40	1.00	0.86	0.13	0.18	2.22	1.38	0.00 to 7.14	0.03 to 6.74	1.87 to 5.71
13453	11/15/77	19	19	1.04	0.68	-0.30	-0.33	-2.40	-1.51	0.06 to 3.79	0.30 to 3.44	0.44 to 2.80
13458	11/16/77	32	30	1.21	1.13	-0.16	-0.17	-2.39	-1.99	0.00 to 3.67	0.29 to 3.16	0.96 to 2.66
13460	11/16/77	26	25	0.99	0.65	-0.05	-0.08	-2.25	-1.32	0.77 to 6.50	2.13 to 6.12	1.38 to 5.36
13461	11/16/77	26	23	1.09	0.94	0.87	0.88	2.14	1.56	0.00 to 2.15	0.04 to 1.37	0.68 to 2.49
13464	11/16/77	36	36	1.32	1.17	-0.39	-0.38	-2.55	-2.30	0.00 to 5.29	0.53 to 4.85	1.89 to 2.74
13467	11/16/77	22	21	0.69	0.44	-0.03	-0.10	1.85	-0.89	0.00 to 2.65	0.26 to 2.43	0.59 to 2.07
13472	11/17/77	32	32	1.11	1.03	0.72	0.73	2.35	2.10	0.00 to 3.49	0.37 to 3.31	1.09 to 3.16
13475	11/17/77	33	31	0.88	0.60	0.37	0.35	1.67	1.31	0.00 to 2.65	0.08 to 1.89	0.04 to 1.84
13478	11/17/77	31	31	1.10	1.01	-0.28	-0.27	-2.42	-1.96	0.13 to 3.88	1.11 to 3.38	1.18 to 3.17

TABLE 8 (Continued)

Orbit	Date	Pts H1/3	Pts H1/3	RMS H1/3	RMS H1/3	Bias H1/3	Bias H1/3	Error H1/3	Error H1/3	GEOS Range H1/3	GEOS Range H1/3	SOWM Range
13481	11/17/77	58	57	1.59	1.48	-0.67	-0.66	-5.12	-4.23	0.11 to 7.40	0.39 to 6.51	1.02 to 5.98
13489	11/18/77	27	26	0.98	0.90	0.81	0.84	1.77	1.56	0.00 to 2.44	0.12 to 2.32	1.13 to 2.52
13490	11/18/77	11	10	1.22	1.03	-0.58	-0.58	-2.39	-2.10	0.14 to 4.89	0.66 to 4.60	0.75 to 3.00
13492	11/18/77	30	30	1.08	0.95	-0.54	-0.52	-2.29	-1.84	0.57 to 3.92	1.31 to 3.07	0.68 to 2.49
13495	11/18/77	15	13	1.03	0.84	-0.07	-0.14	-1.89	-1.53	3.63 to 10.01	4.79 to 9.47	4.40 to 8.12
13649	11/29/77	33	32	1.26	1.01	0.59	0.48	2.83	2.18	0.89 to 4.58	1.47 to 3.42	1.90 to 4.74
13663	11/30/77	29	26	1.13	1.04	0.68	0.71	2.63	1.93	0.95 to 3.58	1.74 to 3.02	2.00 to 3.95
15202	3/19/78	14	11	1.18	1.06	-0.38	-0.69	-2.04	-1.86	0.32 to 4.19	1.36 to 3.73	1.25 to 3.15
15209	3/20/78	25	23	1.92	1.71	0.65	0.71	-3.64	2.77	3.15 to 14.19	5.78 to 11.79	1.86 to 11.90
15223	3/20/78	24	22	1.55	1.48	1.11	1.22	2.66	2.28	3.81 to 9.93	4.06 to 9.82	5.00 to 10.10
15227	3/21/78	20	18	0.93	0.81	-0.57	-0.57	-1.98	-1.60	1.41 to 4.01	1.91 to 3.93	1.24 to 3.12
15230	3/21/78	14	10	1.03	0.91	-0.77	-0.68	-1.73	-1.39	0.00 to 4.09	0.73 to 3.58	0.00 to 3.85
15241	3/22/78	26	22	1.31	1.11	-0.22	0.04	-2.23	1.75	2.09 to 9.65	2.30 to 8.61	0.50 to 8.03
15258	3/23/78	12	9	1.13	1.07	0.44	0.79	2.12	1.50	1.56 to 5.17	3.15 to 4.86	0.00 to 5.80
15361	3/30/78	32	30	1.22	1.12	-0.03	0.04	-3.23	1.93	1.03 to 7.95	1.81 to 7.30	1.10 to 8.31
15400	4/02/78	21	19	1.15	1.06	-0.67	-0.65	-2.60	-2.41	1.19 to 6.66	2.20 to 6.13	1.05 to 5.95
15414	4/03/78	27	25	0.90	0.76	0.18	0.24	-1.85	-1.30	0.80 to 4.65	1.19 to 4.11	1.00 to 3.60
15421	4/03/78	26	24	1.00	0.81	0.17	0.14	3.00	1.69	0.00 to 5.17	1.02 to 4.83	0.75 to 4.10
15485	4/08/78	10	8	1.67	1.26	-0.70	-0.82	-2.56	-2.24	0.00 to 5.76	1.53 to 5.44	0.55 to 4.40
15499	4/09/78	11	7	1.09	0.70	0.01	0.51	-2.15	1.01	1.44 to 4.61	3.00 to 3.87	0.91 to 4.80
15527	4/11/78	10	8	1.30	1.25	1.19	1.19	2.00	1.74	2.80 to 4.36	3.16 to 3.96	3.80 to 5.00

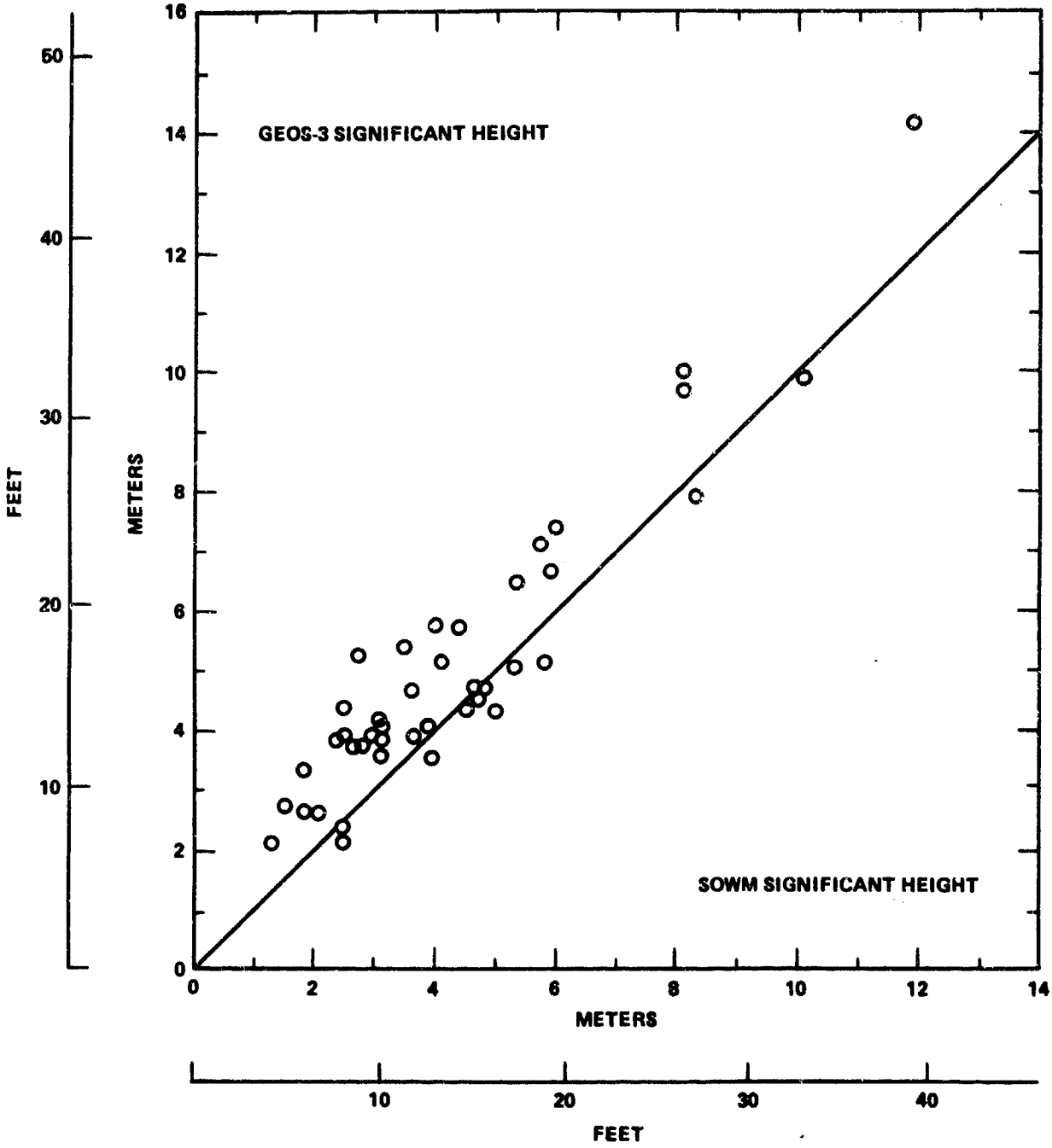

Figure 41 - The Scatter of the Spectral Ocean Wave Model Value and Highest GEOS-3 Value for Each Orbit Segment
(From Reference 71)

Some solutions are:

$SOWM_{max}$	1.0	5.0	7.0	10.00 m
$GEOS\text{-}3_{max}$	1.86	5.80	7.77	10.73 m

The (percentage) accuracy of the SOWM appears to increase with increasing height."

A portion of the summary of this research is quoted below.[71]

"The absolute magnitude of the largest error was found to average at 2.32 meters and have a standard deviation of 0.63 meters. The 95 percent confidence interval for the mean value was 2.13 meters to 2.51 meters. The percentage value of the error decreased with increasing wave height. A significant amount of the largest errors was caused by short spatial variations in GEOS-3 wave heights (47 percent). Comparing SOWM to smooth GEOS-3 values showed a twenty-one percent (21 percent) decrease in the average absolute magnitude of the largest errors.

"A maximum shown by SOWM was found within four degrees of latitude of a GEOS-3 maximum about 72 percent of the time. The position of a SOWM minimum was within 4 degrees of latitude of a GEOS-3 minimum 72 percent of the time.

"The correlation coefficient between the highest SOWM value and highest GEOS-3 value in each segment was +0.935.

"A climatological study of the model showed that in the Pacific the Tropics were overpredicted,* mid-latitudes were underpredicted, and wide variations occurred in the higher latitudes.

"In the Atlantic, the values in the Tropics were influenced by the Caribbean region but tended to be overpredicted south of 17.5°N.** The SOWM underspecified from 17.5°N to about 30.0°N, and then alternated high and low to about 45.5°N. The higher latitudes showed wide variations just as the Pacific values.

"The types of errors outlined above can be largely attributed to errors in the wind field specification, especially in the higher

*In the Pacific by +0.4 meters. The root mean square errors were over 1 meter.
**By +0.2 meters.

latitudes. Given more accurate wind reports in the higher latitudes, the observed latitudinal variation in root mean square errors and biases can be expected to be reduced significantly. Scarcity of surface observations in this region will cause wide variations in errors between points in the oceans."

VERIFICATION OF SIGNIFICANT WAVE HEIGHTS BY MEANS OF WAVE HEIGHTS MEASURED WITH A RADAR ALTIMETER ON SEASAT

SEASAT altimeter wave height measurements have been compared with the SOWM product as generated by FNOC during 1978.[9] A total of 18 orbit segments of SEASAT altimeter data for the Atlantic and Pacific oceans at various times were examined. Of these, two were for a pass over a tropical cyclone near the Phillipine Islands. Special techniques from Reference 9 were used to try to predict the waves for the tropical cyclone. The SOWM wave climatology does not have this capability, and there are no waves due to tropical cyclones in it. These two orbit segments are not included in the statistics to follow for this reason. However, the data that were obtained are presented in order to show an area in which the SOWM could be improved.

Of the remaining 16 orbit segments, four were for strong offshore flow off Labrador. The waves that were involved in the verification therefore occurred in Davis Strait, Baffin Bay, and the Labrador Sea. The comparisons were made between the significant wave height contour fields produced as FNOC and the SEASAT altimeter data. There is a question in the mind of the writer as to the adequacy of this contouring procedure for this particular set of four orbit segments. Therefore, they have been left out of this analysis.

There remain 12 orbit segments. Five of these were for strong north-south flow over the Atlantic Ocean; four were for weather situations over the Gulf of Alaska; and three were for a trade wind surge. The segments were picked in order to test the ability of the SOWM to specify waves correctly under these conditions.

There were very high waves in the North Atlantic for the case study involving strong north-south flow. As examples, the sea surface isobaric patterns for 6 October 1978 at 00z and 12z are shown in Figures 42a and 42b. The strong north-south flow occurs to the south of Greenland and to the west of Nova Scotia, at about the center of the North Atlantic ocean on an east-west basis.

The wave height fields produced by the SOWM are shown for the same times in Figure 43. For 00z the subsatellite track for SEASAT passes nearly over the high

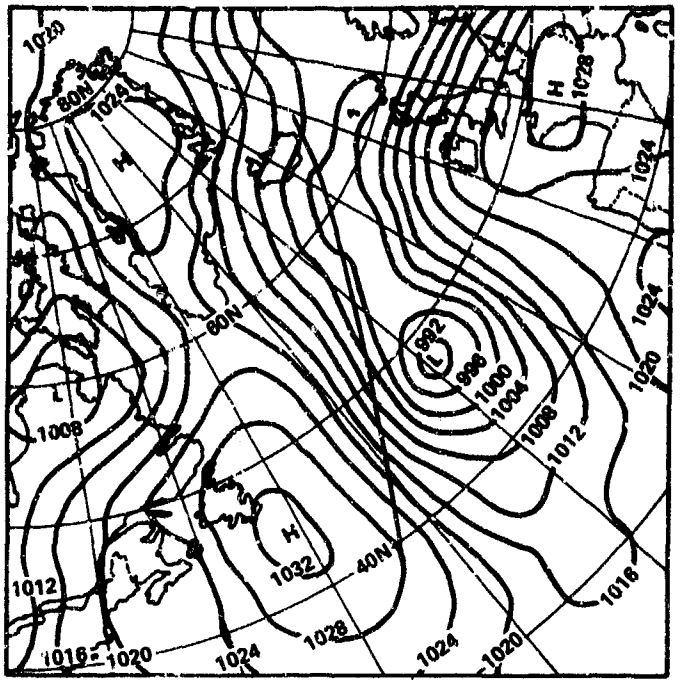

Figure 42a - 0000Z 6 October 1978

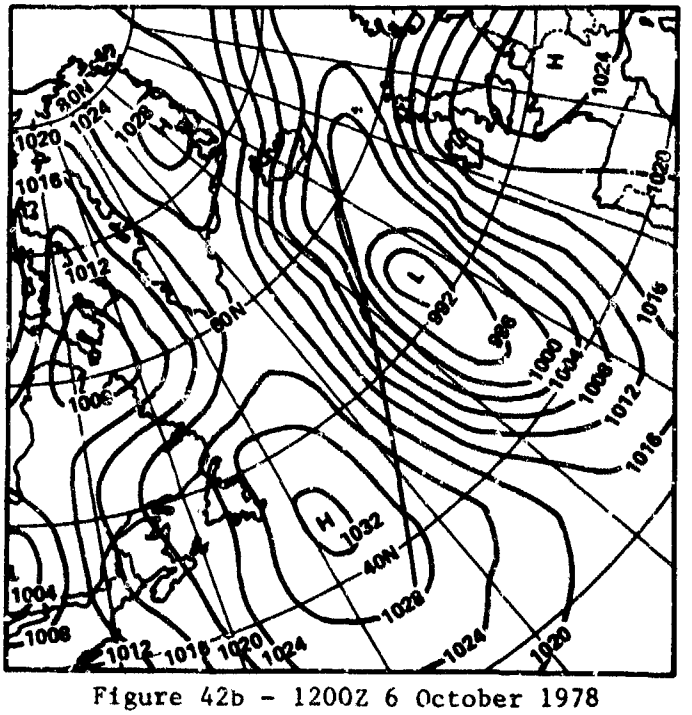

Figure 42b - 1200Z 6 October 1978

Figure 42 - Sea Level Pressure Analyses with Ground Track of SEASAT Revolution 1446 Superimposed
(From Reference 9)

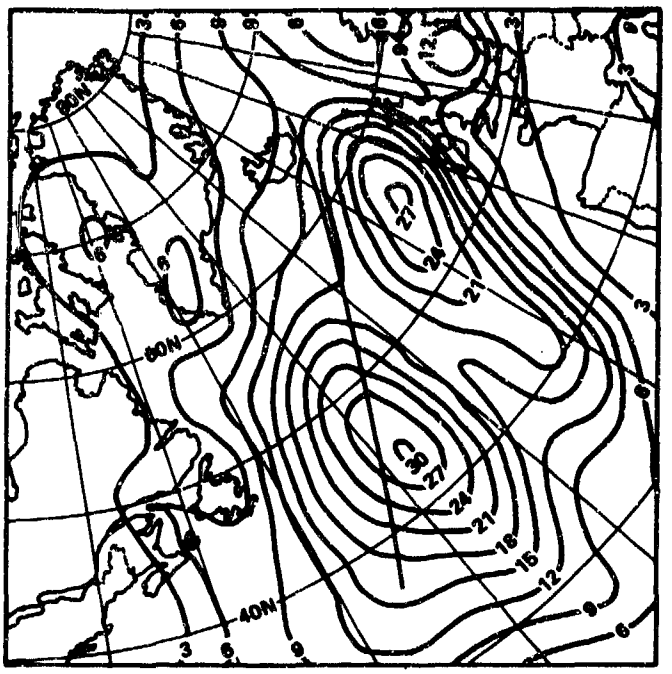

Figure 43a - 0000Z 6 October 1978

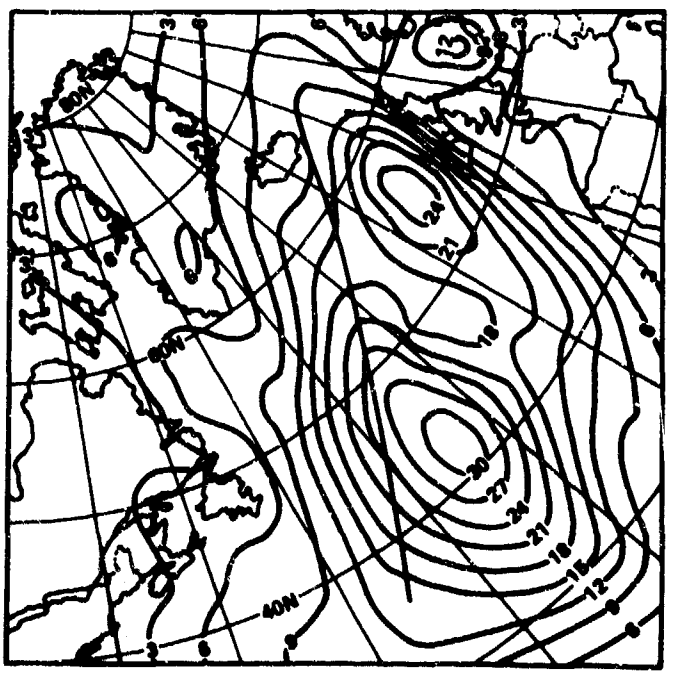

Figure 43b - 1200Z 6 October 1978

Figure 43 - Spectral Ocean Wave Model Analyses with Ground Track of SEASAT Revolution 1446 Superimposed (From Reference 9)

center for waves at that time, which was a small closed contour for 30-foot waves centered in the area of the strong north-south flow. Twelve hours later this contour for 30-foot waves (9.1 meters) has increased in area and shifted southward. The spacecraft orbit occurred at about 0330z, and the SOWM fields for these two conditions twelve hours apart were interpolated to 0330z. Values from the SOWM field were read off at every latitude intersection with the subsatellite track and compared to the SEASAT significant wave heights. The result is shown in Figure 44 where the SEASAT wave heights are shown by the dots and the SOWM heights are shown by the Xs. The largest difference is -1.8 meters, where the SOWM predicted a value that is much too low compared to what was measured by the spacecraft. It is to be noted that from 39 degrees to 40 degrees north, a mere 60 nautical miles (111 kilometers) (plus whatever is needed to correct for the east-west component) the significant wave heights measured by SEASAT increased from 4.2 meters to 7.7 meters.

More of the same is shown in Figures 45a and 45b. The sea surface isobaric pattern is shown in the first part of this figure and the SOWM significant wave height contours are shown in the second. The spacecraft orbit occurred approximately 40 minutes after the synoptic time and this difference in time was neglected. The graphs for the SOWM and the SEASAT measurements are shown in Figure 46. The agreement is quite good from about 45° north to 50° north where a sharp decrease in wave height from about 6 meters to about 3 meters is tracked quite well. The largest descrepancy between SEASAT and SOWM, is at 55° north, where the SOWM was 1.4 meters too low.

The last illustration for this study (Figure 47) is for orbit segment 1163 over the Equatorial Pacific for 16 September 1978, which occurred roughly at 08z. The measurements were compared with the SOWM product for 06z. The largest descrepancy is 1.2 meters with the SOWM being too low at this point 12° north.

The 12 orbit segments described above are summarized in Table 9. The highest significant wave height predicted by the SOWM along the subsatellite track and the highest significant wave height measured by the spacecraft are shown for each orbit segment. The largest error for a point by point comparison is shown, both in meters and feet. The bias is simply the average value of the difference with regard to sign between the SOWM and SEASAT values for the number of points involved. A plus sign in either of these two columns means that the SOWM was high compared to SEASAT and conversely. The final column is perhaps the most useful. It represents the sum of the squares of the differences between the SOWM and the SEASAT values divided

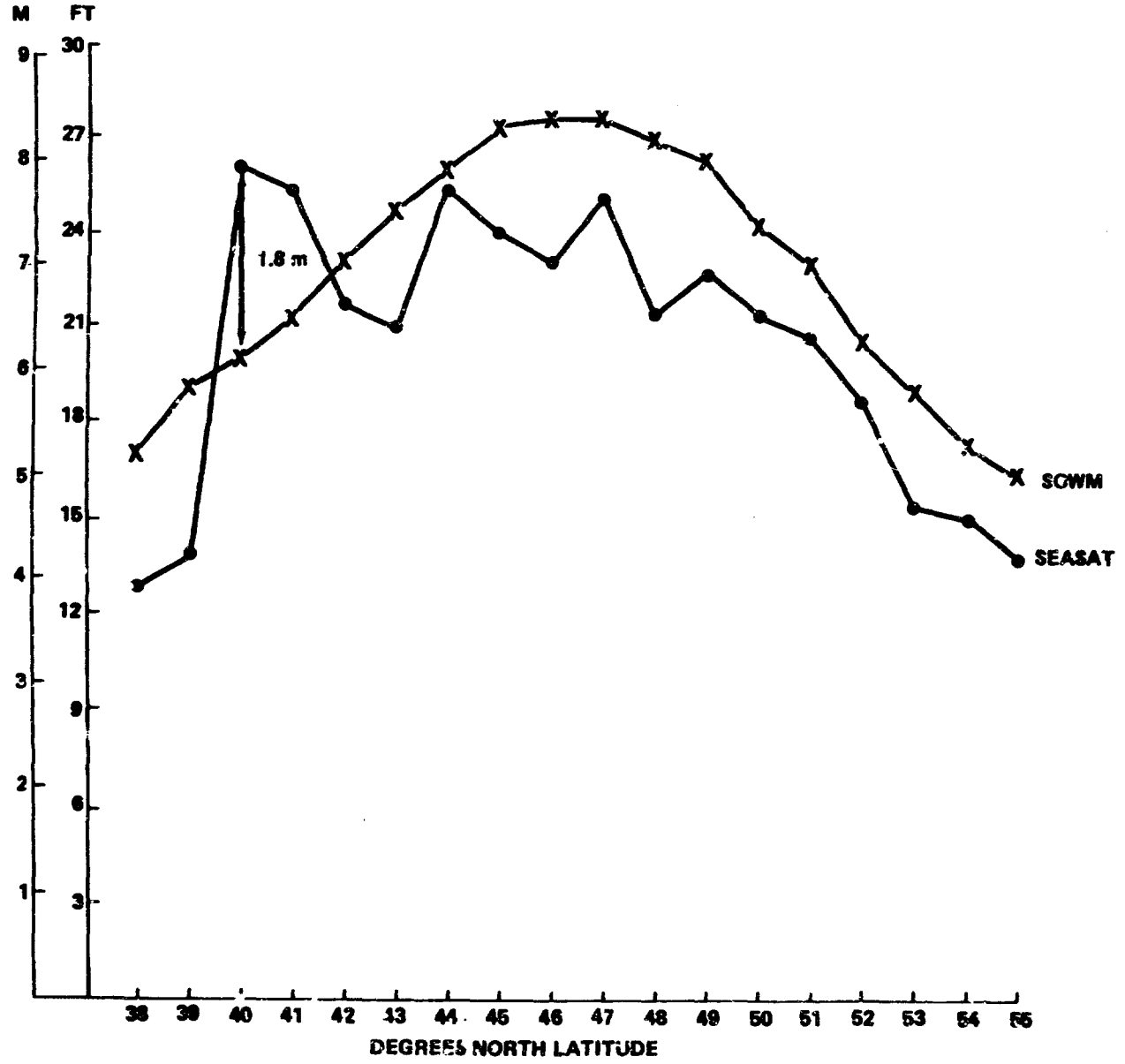

Figure 44 - SEASAT and Spectral Ocean Wave Model Significant Wave Heights for Revolution 1446 on 6 October 1978 from Iceland to 38 Degrees North, 45 Degrees West

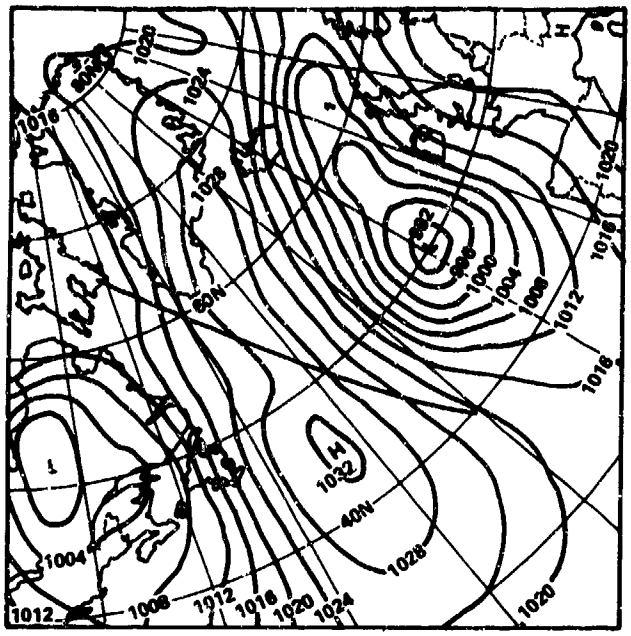

Figure 45a - Sea Level Pressure Analysis

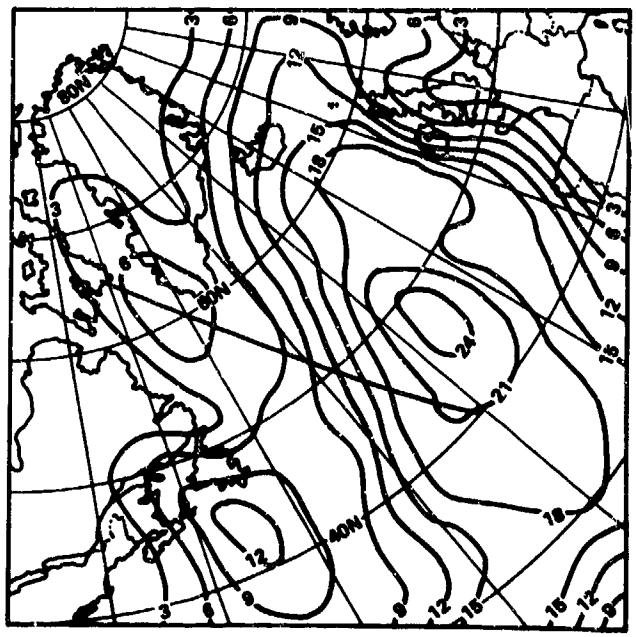

Figure 45b - Spectral Ocean Wave Model Analysis
(Height in feet)

Figure 45 - Sea Level Pressure and Spectral Ocean Wave Analyses for 120oz 7 October 1978 with Ground Track of SEASAT Revolution 1466 Superimposed (From Reference 9)

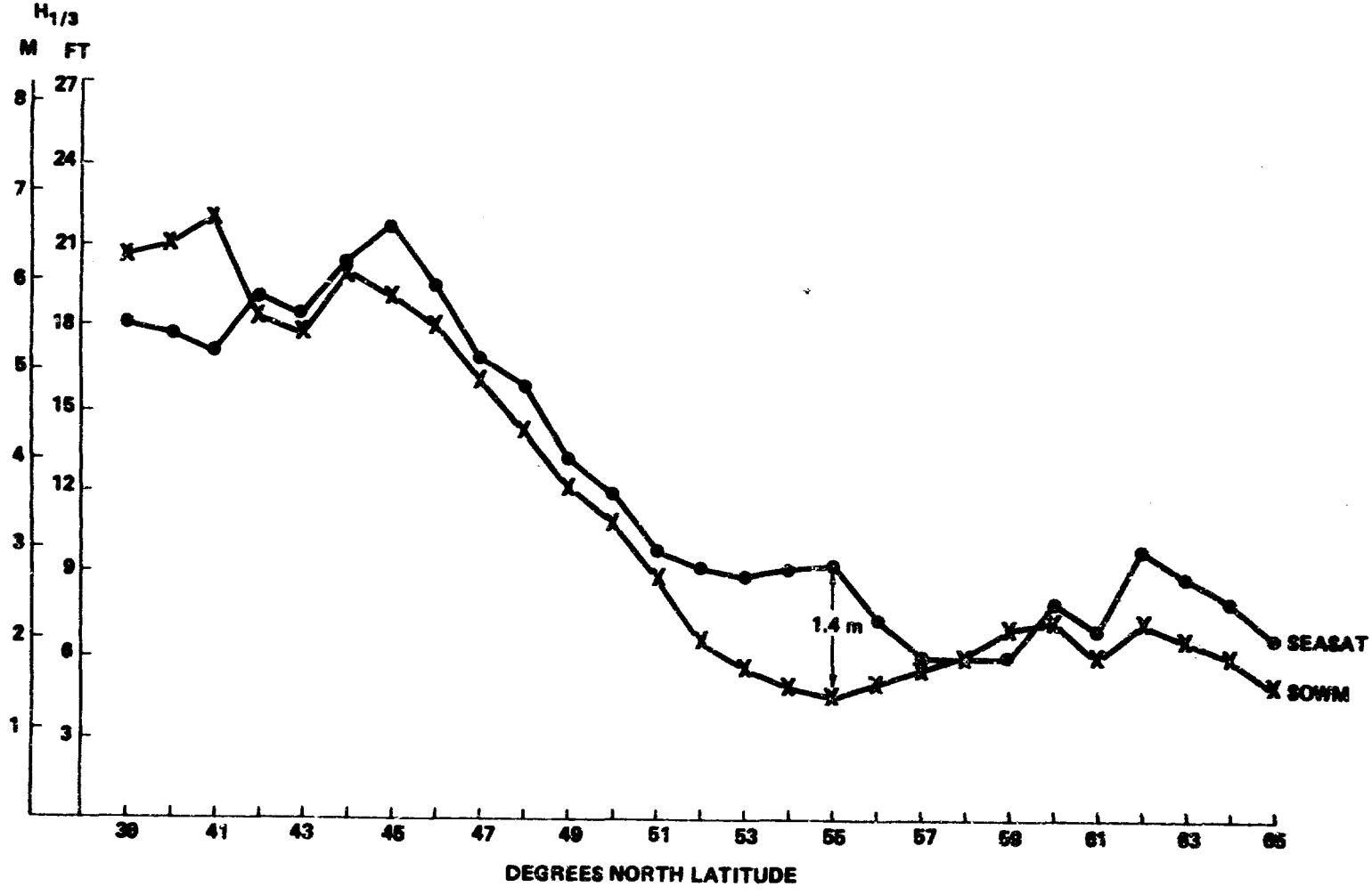

Figure 46 - SEASAT and Spectral Ocean Wave Model Significant Wave Heights for Revolution 1466, 12z 7 October 1978 Over the North Atlantic from Davis Straight to 39 Degrees North, 30 Degrees West

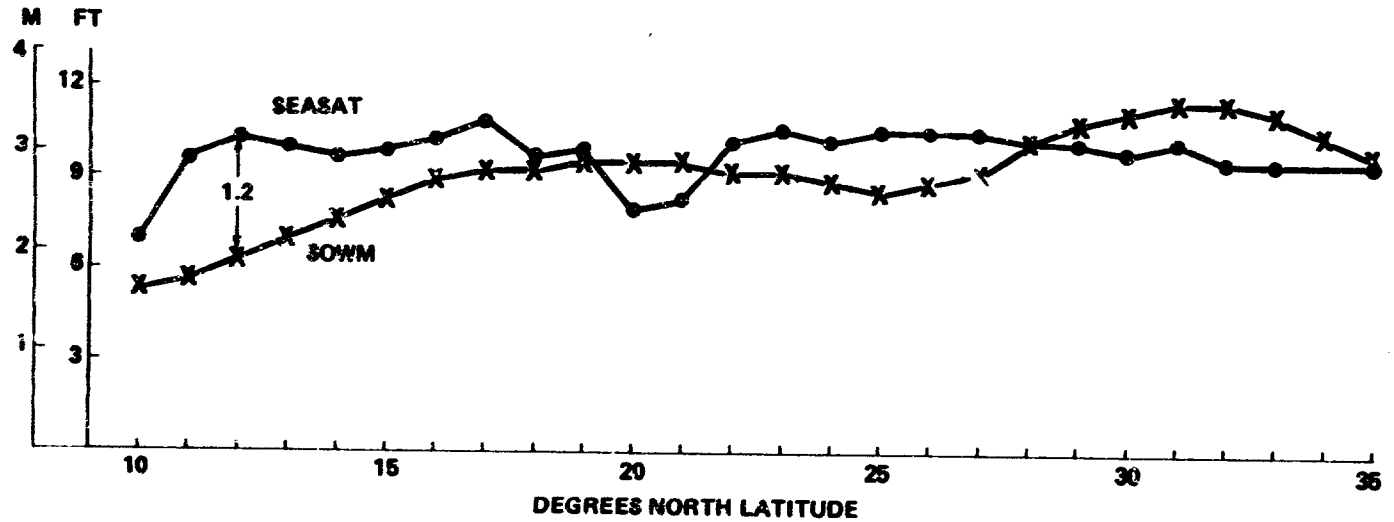

Figure 47 - SEASAT and Spectral Ocean Wave Model Significant Wave Heights for Revolution 1163 Over the Equatorical Pacific for 08z 16 September 1978

TABLE 9 -- A COMPARISON OF SEASAT ALTIMETER SIGNIFICANT WAVE HEIGHT MEASUREMENTS WITH SPECTRAL OCEAN WAVE MODEL NOWCASTS DURING SEPTEMBER AND OCTOBER 1978
(Note: Values are in meters with the conversion to feet or inches in parenthesis)

Revolution	Date	Time	Location	Number of Points	Highest Waves		Largest Error	Bias	RMS
					SOWM	SEASAT			
1149	9/15	09z	Equatorial Pacific	26	3.6 (11.8)	3.0 (9.8)	±0.9 (3.0)	+0.05 (2 in.)	0.62 (2.0)
1163	9/16	08z	Same as 1149	26	3.5 (11.5)	3.3 (10.8)	+0.9 (3.0)	+0.01 (0 in.)	0.54 (1.8)
1170	9/16	18z	Same as 1149	26	3.8 (12.5)	3.2 (10.5)	+1.1 (3.6)	+0.07 (3 in.)	0.56 (1.8)
1292	9/25	09z	Vancouver to 25°N, 145°W	20	3.0 (9.8)	3.5 (11.5)	-1.7 (5.6)	+0.12 (5 in.)	0.64 (2.1)
1298	9/25	13z	Alaska to 28°N, 124°W	26	3.4 (11.2)	3.4 (11.2)	-1.5 (2.3)	-0.07 (3 in.)	0.82 (2.7)
1335	9/28	10z	Same as 1292	20	5.1 (16.7)	4.4 (14.4)	+1.2 (3.5)	+0.09 (4 in.)	0.61 (2.0)
1341	9/28	19z	Same as 1298	26	4.4 (14.4)	4.1 (13.4)	-1.2 (3.9)	-0.15 (6 in.)	0.55 (1.8)
1437	10/5	12z	Greenland to 50°N, 30°W	11	5.2 (17.1)	6.1 (20.0)	-2.0 (6.6)	-0.20 (8 in.)	0.78 (2.6)
1446	10/6	12z	Iceland to 38°N, 45°W	18	8.4 (27.6)	7.9 (25.9)	+1.8 (5.9)	+0.70 (27 in.)	1.09 (3.6)
1466	10/7	12z	Davis Strait to 40°N, 30°W	27	6.7 (22.0)	6.8 (22.3)	-1.4 (4.6)	+0.34 (1.1 ft)	0.64 (2.1)
1480	10/8	12z	Same as 1437	11	5.3 (17.4)	5.1 (16.7)	+1.6 (5.2)	-0.50 (1.6 ft)	0.98 (3.2)
1489	10/9	0z	Same as 1446	18	2.9 (9.5)	3.9 (12.8)	-1.1 (3.6)	-0.51 (1.7 ft)	0.65 (2.1)
							Average	-0.004 0	0.73 (2.4)

by the total number of points. All but one of the values are less than 1 meter. One can note that SEASAT revolution 1446 with a bias of plus 0.7 meters has the largest root mean square difference.

As with the preceeding studies, the wave heights along a particular orbit segment are highly correlated. For this reason, the biases and the root mean square differences were averaged without regard to the number of points involved in the orbit segment. Thus, the 11 points for revolution 1437 with the 0.78 root mean square difference has as much weight as the 27 points for revolution 1466.

There does not seem to be any substantial bias between the SEASAT and the SOWM wave heights according to this limited data set. The overall root mean square difference is a little more than 0.7 meters.

The cited study gave indications that the SEASAT altimeter wave heights may have been biased slightly too high, by 0.5 meters. This particular matter is not easily settled. A study by French scientists indicates there is no bias in the SEASAT altimeter wave heights when compared with ship observations including ocean weather ships with Tucker recorders in the North Atlantic.[42] The particular computational procedure (or algorithm) that is used to produce a significant wave height from the altimeter wave form is under investigation, and two different algorithms may have been used in these particular studies.

Histograms of the root mean square errors (or perhaps differences) for the values given in Tables 7, 8, and 9 are shown in Figures 48 and 49. The range of the values has decreased substantially from the first to the last of the three studies. "Busts" are missing in the last study.

TYPHOON WAVES

Figure 50 illustrates the results of two passes over typhoon Lola, one for 27 September 1978 (revolution 1317) and the other for 29 September 1978 (revolution 1346). For the first of these two passes the typhoon was located to the east of the Phillipine Islands. For the second, it had moved across the Phillipine Islands and entered the South China Sea. For both orbit segments, the largest error was 1.8 meters with the SOWM product being too high in both cases. Not much can be said, at the moment, about the differences for revolution 1317, but the behavior of the SEASAT altimeter wave heights for revolution 1346 again shows this interesting feature of a 2-meter increase in wave height over approximately one degree of longitude that is not tracked by this tropical cyclone model.

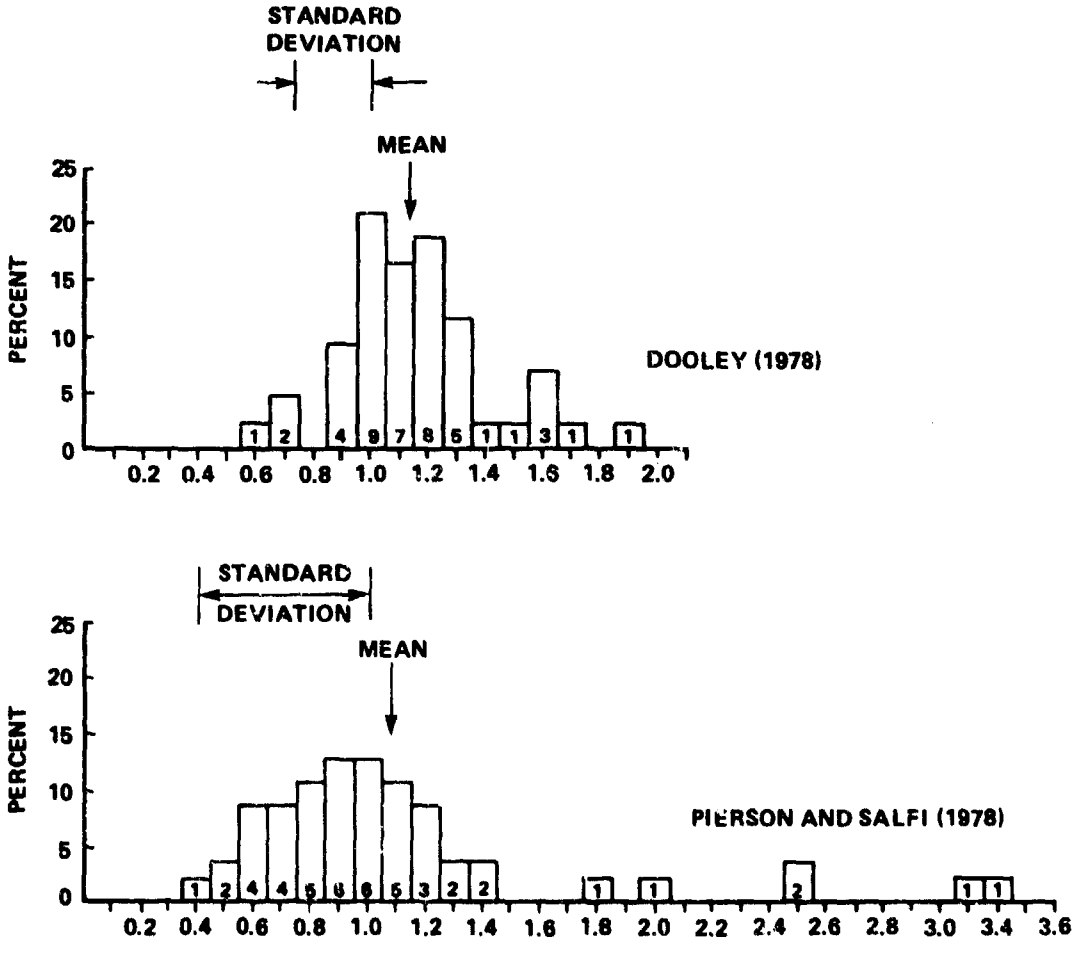

Figure 48 - Histograms of the Distribution of the Root Mean Square Errors Showing the Mean and Standard Deviation for Each Comparison (After Reference 70)

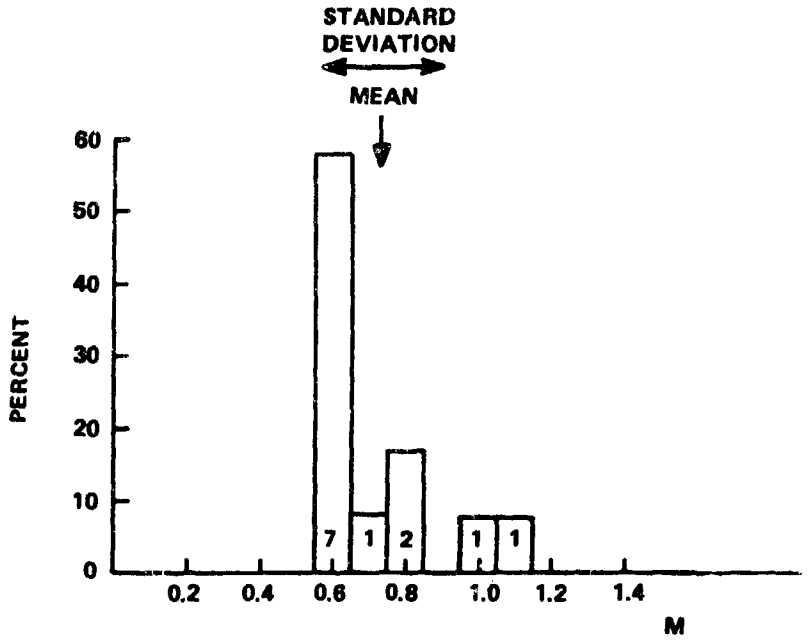

NOTE: Data from Ocean Data Systems Incorporated Report.

Figure 49 - A Histogram of the Distribution of the Root Mean Square Errors for the Spectral Ocean Wave Model Compared to SEASAT Altimeter Significant Wave Heights, Showing the Mean and Standard Deviation (Reference 9)

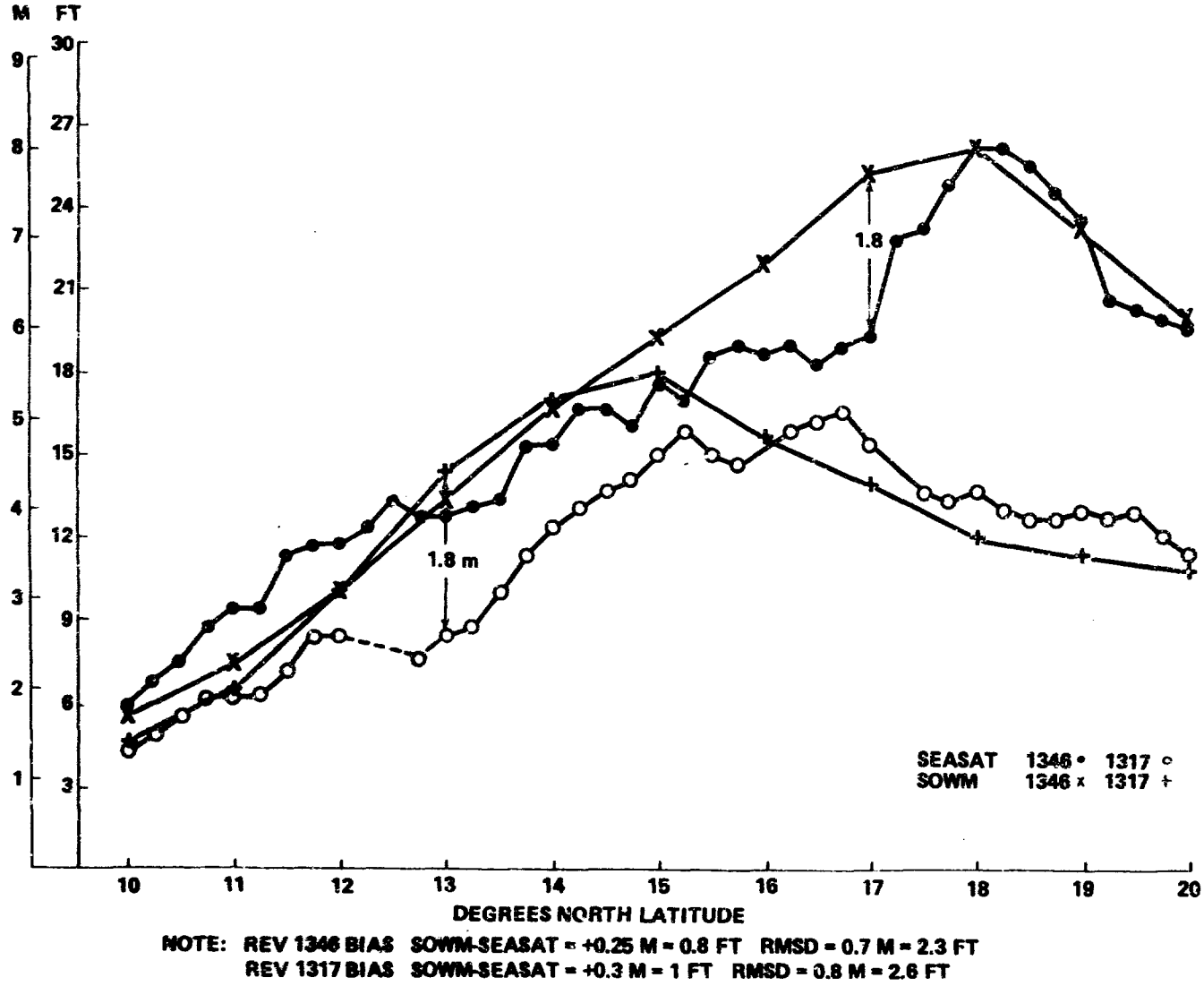

Figure 50 - SEASAT and Spectral Ocean Wave Model Heights for Typhoon Lola

ADDITIONAL INFORMATION FROM SEASAT

The altimeter significant wave height measurements from SEASAT have also been used to study the accuracy of the DSA model.[42] In this study, two orbit segments for 30 September 1978 are particularly revealing. The first (Figure 51) is for an orbit segment which took place at 04z on that date. The wave height measurements are compared with the sea surface synoptic pressure field for 00z. This rather short orbit segment, roughly from the southern tip of Greenland, to Labrador as shown on the Figure, has a very interesting shape. From point A as shown on the synoptic analysis, to point B, a distance of 130 nautical miles (241 kilometers), the wave height decreases from about 8.8 meters to 3.5 meters. It stays at this value for a distance of 108 nautical miles (200 kilometers) and then increases again to about 8.5 meters. For 12 hours later, a second orbit segment is shown in Figure 52 again passing over Baffin Bay and Davis Strait. Over a distance of 32 nautical miles (59 kilometers), the wave height increases on a north-bound pass from about 7.5 meters to 12 meters. Three other orbit segments illustrate similar sudden changes.[42]

Another interesting feature of these graphs is the jitter in the trace of the significant wave height. There is some element of sampling variability in significant wave height measurements by an altimeter on a spacecraft that varies depending upon the methods of data reduction and the length of time the altimeter wave form is averaged as a function of distance along the subsatellite track. These questions have not been resolved, but clearly there is some uncertainty, or some effect of sampling variability, in these measurements, just as there is in records that obtain the variation of sea surface elevation as a function of time at a fixed point.

It is now possible to refer to the previous figures that illustrated altimeter data for spacecraft passes over various wave fields that have been compared with the SOWM product. If, indeed, the waves in nature can vary by these large amounts over these relatively short distances, then the grid point spacing and the resolution of the SOWM are inadequate to track them. One can note for example, for the pass over typhoon Lola that roughly the same thing happened over just a few tens of nautical miles as one approached the peak of 8 meters. Similarly, for revolution 1446, in Figure 44, a very sharp increase in wave height over one degree of latitude was indicated between 39 degrees and 40 degrees north. The resolution of the SOWM is not adequate to treat these variations, even with a greatly enhanced ability to

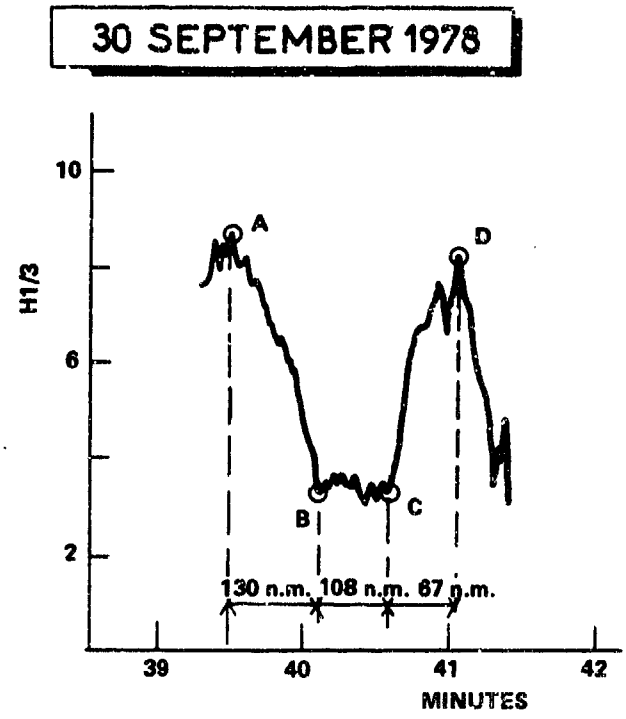

Figure 51a - SEASAT Waveheight (0439z to 0442z)

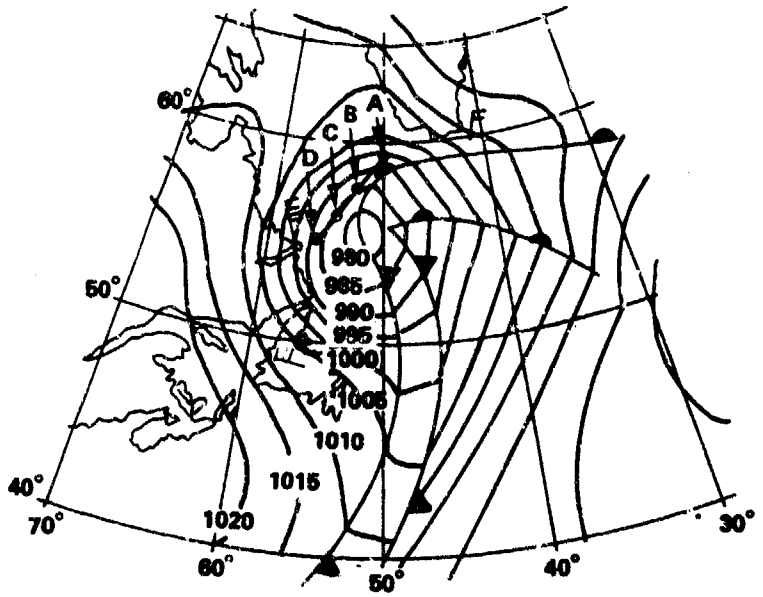

Figure 51b - Surface Pressure Analysis 0000z

Figure 51 - SEASAT Data for 30 September 1978, 00GMT

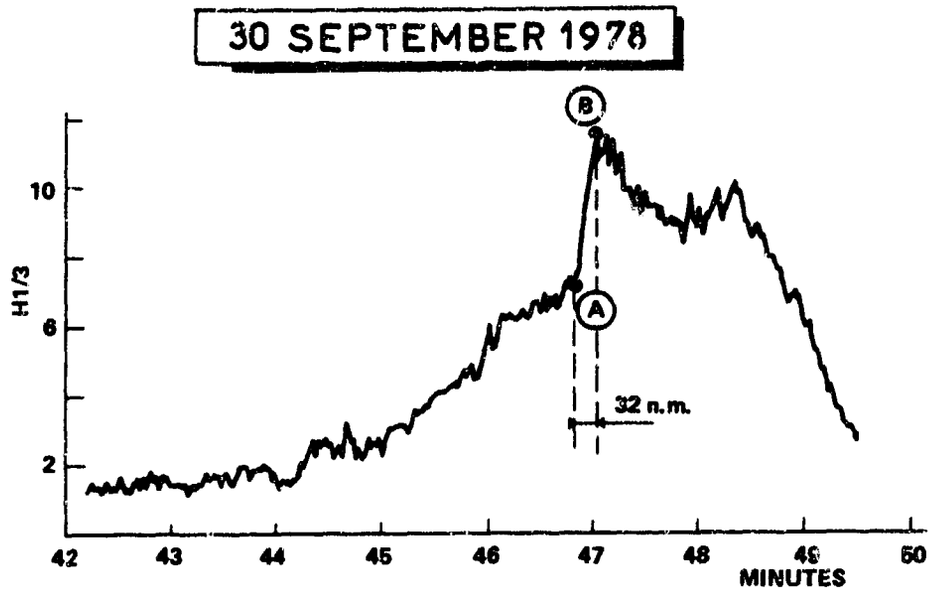

Figure 52a - SEASAT Waveheight (1242z to 1249z)

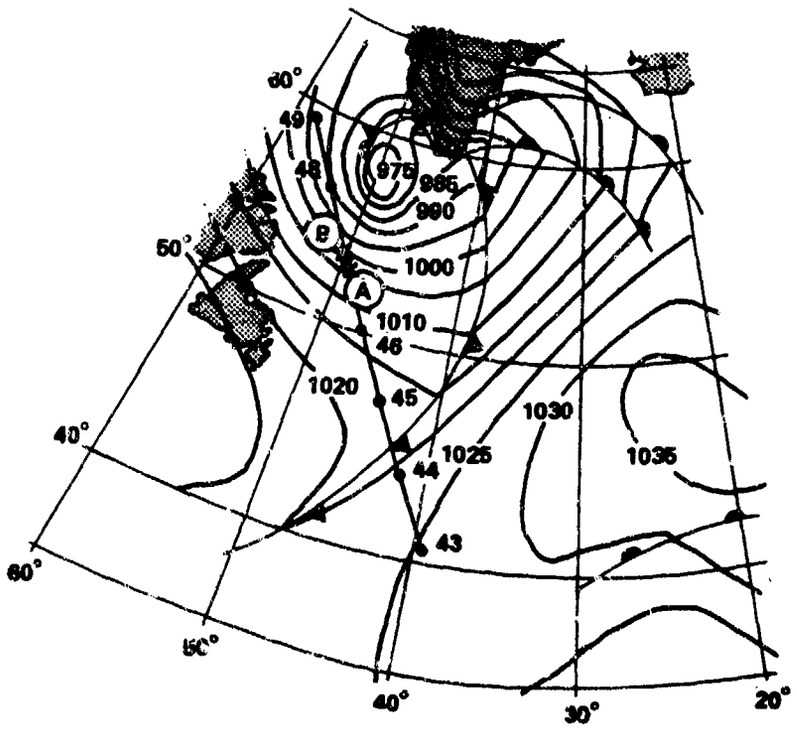

Figure 52b - Surface Pressure Analysis 1200z

Figure 52 - SEASAT Data for 30 September 1978, 12GMT

treat the discontinuity function that was described previously. It is extremely doubtful whether or not higher resolution in space and time and in the frequency direction spectrum would yield results that would show these sharp variations in wave height from point to point in midocean. They must be caused in part by details of the wind field that cannot possibly be detected by means of the conventional network of transient ships and data buoys for the Northern Hemisphere oceans.

This should not in any way detract from the value from the SOWM, both as a forecast tool and for a wave climatology. It simply means that there are additional elements of uncertainty in the behavior of the waves that are not resolvable at the present state of the art.

SUMMARY OF THE RESULTS OF ALTIMETER MEASUREMENTS OF WAVE HEIGHTS AS COMPARED TO THE SPECTRAL OCEAN WAVE MODEL PRODUCTS

Table 10 shows a summary of the results, discussed above. There have been a total of 99 orbit segments of varying lengths, some extending from the Equator to landfall in either ocean. There have been 2210 points, roughly spaced one degree of latitude apart, used to compare the SOWM product with the spacecraft measurements. The total represents approximately 132,000 nautical miles (244,000 kilometers) of travel over the oceans for wave height measuring purposes. Much more data are available from SEASAT that could profitably be used in a further study of the SOWM.

This table must be interpreted with care. The significant wave heights from the SOWM were those obtained from the day-to-day operational output of the SOWM. The winds that were used to drive the model need not necessarily have corresponded to the winds from the climatology used to generate the waves of the climatology. The data in the climatology for the Atlantic were all produced by means of the climatological wind data. The data in the climatology for the Pacific through 1971 used the climatologically generated wind data. Thereafter, the spectra and winds from the operational FNOC product were used.[68]

A study of the FNOC operational product in terms of these spacecraft measurements, which cover a period from 1975 through 1978, provides information on this product as it evolved during the above four years. Further studies would be needed to compare the climatological product, where possible, with altimeter wave height measurements.

Operational systems are not static. During the one and a half to two year period from 1977 to 1978, the winds were modeled at FNOC by increasingly more

TABLE 10 - SUMMARY OF COMPARISONS OF THE SPECTRAL OCEAN WAVE MODEL WITH ALTIMETER WAVE HEIGHT MEASUREMENTS

	Orbits	Points	Root Mean Square*		Bias*		Absolute Magnitude of the Largest Error*	
			Average	Standard Deviation	Average	Standard Deviation	Average	Standard Deviation
Pierson & Salfi (1978) GEOS-3	44	898	1.09 (3.6)	0.60 (2.0)	-0.29 (1.0)	0.91 (3.0)	2.19 (6.9)	0.91 (3.0)
Dooley (1978) GEOS-3	43	1057	1.15 (3.8)	0.27 (0.9)	-0.12 (0.4)	0.59 (1.9)	2.32 (7.6)	0.63 (2.1)
ODSI (1980) SEASAT	12	255	0.73 (2.4)	0.17 (0.6)	0 (0)	0.31 (1.0)	1.50 (4.9)	0.39 (1.3)
Totals (or Pooled)	99	2210	0.99 (3.2)	0.35 (1.1)	-0.14 (0.5)	0.60 (2.0)	2.00 (6.6)	0.64 (2.1)

*Values are in meters with feet in parentheses.

realistic techniques.[68] The 1975-1976 GEOS-3 data were obtained prior to these changes.[78] The 1977-1978 GEOS-3 data were obtained during these changes.[71] The SEASAT data were obtained after these changes.[9]

For these orbit segments, the root mean square difference between the spacecraft measurement and the SOWM product, varied from 0.73 to 1.15 meter, averaged over the entire data set involved. These averages had standard deviations that in turn varied from 0.17 to 0.6 meter. The bias was a few tenths of a meter too low for the grand average, essentially zero, and the standard deviations of the bias varied from 0.91 to 0.31 meter.

Each orbit segment had a maximum error, either positive or negative. The average value of the largest error varied from 2.3 meters to 1.5 meters with standard deviations of 0.63, 0.91, and 0.39 meters.

All of these data are pooled in the last row of the table. Each of the three investigations is given equal weight instead of weighing them according to either the number of orbit segments or the total number of points. The average of the root mean square difference is 0.99 meter with a standard deviation of 0.35 meter. The bias is -0.14 meter with a standard deviation of 0.6 meter, and the average magnitude of the largest error is 2.0 meters with a standard deviation of 0.64 meter. An average composed of sample values from different populations can be used to detect the differences between the populations. In Table 10, the errors of different types show a strong tendency to be larger for the earlier comparisons and smaller for the later comparisons. With standard deviations as well as averages considered, there has been a definite improvement in the operational SOWM product error statistics from 1975 to 1978.

The SEASAT results can be interpreted as the current operational quality of the SOWM. For an arbitrary line drawn across a SOWM wave height field in the wave specification, or nowcast, mode, roughly simulating the subsatellite track of a spacecraft, the waves along that line will differ from the correct waves by practically a zero amount with reference to the average along that segment. The root mean square difference between the measured waves along that line and the SOWM will be somewhere between 0.90 and 0.56 meters two-thirds of the time. Somewhere along that track there will be one large error between 1.9 meters and 1.1 meters, two-thirds of the time; and, roughly one-sixth of the time, the error will be larger than 1.9 meters.

The inherent inability of current meteorological wind field analysis systems and of the SOWM, with reference to its resolution, to detect and specify large and sudden variations in wave height over short distances as detected by the altimeters should be made known to the users of the SOWM as an uncertainty in the waves that are forecasted or specified. It will then be possible for these users to take these effects into consideration for whatever use the product is to have.

In the next section on the verification of frequency spectra, similar results will be documented for the time histories of wave heights at a point. These results show that the variability from hour-to-hour of the waves is larger than that which can be specified by the SOWM. These two features, one as a function of distance along a line and the other as a function of time at a point, are complementary. They must be taken into consideration in the use of these data for climatological purposes.

VERIFICATION OF THE FREQUENCY SPECTRA OF THE SPECTRAL OCEAN WAVE MODEL

INTRODUCTION

In the description of the development of the SOWM, an essential first requirement was stated to be the ability to estimate the spectrum of the waves. This ability first became available when a classical paper entitled "The Sampling Theory of Power Spectrum Estimates" by J.W. Tukey was presented at a symposium at Woods Hole.[11] Prior to that time, although a great many things had been done concerning time series, the overall procedure for interpreting time series was not clear. There were some scientists who preferred to work with the covariance function and a few who had some idea of the concept of a variance spectrum such as S.O. Rice.[79] There was no way available to take a time history of a randomly fluctuating quantity and interpret a spectrum computed from that data.

The title of Tukey's paper is the essence of the problem of verifying wave spectra. The subject of the title is <u>sampling theory</u>, which means that in the author's mind this was the critical problem that needed to be solved. The problem was solved in this paper; and subsequent works clarified the concept even further, leading to the idea of cross spectra (cospectra and quadrature spectra) and bispectra. However, until the sampling theory for these estimates becomes understood, the computation of power spectra could not be undertaken with confidence as to how the spectra should be interpreted.

A SIMPLIFIED ANALOGY FOR THE PREDICTION OF RANDOM EVENTS

The frequency spectrum of ocean waves at a fixed point on the ocean for a given time interval of measurement can never be predicted exactly. There will always be some difference between what is predicted by a model such as the SOWM and what is computed (estimated) from an ocean wave record. In earlier sections of this paper, every once in a while words like estimated spectrum, or estimates, have been used in the description of wave spectra. To estimate something in a statistical sense is a very precise procedure.[80] The term arises in the many excellent text books on the subject, such as Mood, Graybill, and Boes.[81]

The concepts that are involved in the estimation of ocean wave spectra from ocean wave time histories are highly abstract. In order to provide some intuitive feeling for nonstatisticians of the concepts involved, the following is a very brief exposition of a much simpler problem.

Consider the very simple problem of tossing a coin five times as a start. A schematic representation for the probability of heads and tails for five successive tosses is given by

$$\begin{aligned}(H(\tfrac{1}{2}) + T(\tfrac{1}{2}))^5 = \frac{1}{32}\ &(HHHHH + (HHHHT + HHHTH + \ldots) \\ &+ (HHHTT + HHTHT + \ldots..) + (HHTTT + HTHTT + \ldots) \\ &+ (HTTTT + \ldots.) + TTTTT)\end{aligned} \tag{53}$$

If the binomial form representing this probability is expanded into all of its terms, and if the commutation of the multiplication operation is prohibited, so that HT does not mean the same as TH, the result will be 32 terms as above. The $(\tfrac{1}{2})^5$ can be factored out front. Each term represents a unique sequence of events. For example, there is one chance in 32 of having all five heads. There is exactly one chance in 32 of getting three heads, a tail, and a head in that order, and so on.

If someone were to ask the reader to predict, before the coin was tossed five times, which of these 32 possibilities would occur, he would have no choice but to pick one of them and he would have one chance in 32 to be correct. These odds are not particularly good.

A similarity would be the numbers game in New York City where the player picks a three digit number between 000 and 999 and pays $1. If his number comes up, by

whatever technique it is picked, the player gets back $500. The only sure thing in that particular game is that if $10 million are spent on chances during a given time interval, about one tenth of one percent of the players will get back $5 million, plus or minus a few hundred thousand.

Now suppose that the order in which the heads and tails appear does not matter. The terms in Equation (53) can be grouped, and the result is then

$$(H(\tfrac{1}{2}) + T(\tfrac{1}{2}))^5 = \frac{1}{32}\,(H^5 + 5H^4T + 10H^3T^2 + 10H^2T^3 + 5HT^4 + T^5) \qquad (54)$$

Now, if one were asked to predict the number of heads and tails that would come up, a much safer prediction would be three heads and two tails. This prediction has 10 chances in 32 of being correct. Note that something must happen in both of these examples and the sum of all of the probabilities is one.

Now consider the act of tossing 100 coins, as an extension of Equations (53) and (54), as in

$$(H(\tfrac{1}{2}) + T(\tfrac{1}{2}))^{100} = (H^{100} + 100H^{99}T + 4950H^{98}\,T^2 + \ldots\ldots + T^{100}) \cdot (\tfrac{1}{2})^{100} \qquad (55)$$

If the left hand side of this equation were expanded in full, in the same way that Equation (53) was expanded, there would have to be 2^{100} completely different terms, each with a probability of $(\tfrac{1}{2})^{100}$. The probability is less than one chance in more than 10^{30} that a particular sequence of heads and tails will occur. The probability of getting exactly 50 heads and 50 tails in any order is very small. It is given by

$$P(50\ \text{Heads}) = \frac{100!}{50!\ 50!}\,(\tfrac{1}{2})^{100} \qquad (56)$$

To claim that the SOWM is capable of predicting either the significant wave height or the spectrum of the waves exactly is essentially as foolish as claiming that one is able to predict the exact number of heads that will come up when 100 coins are tossed. Both are virtually impossible, except for the fact that one never goes beyond ±0.05 meter for wave height in a model that is essentially continuous.

There are, however, events that can be predicted when a coin is tossed N times. For example, from the theory of probability, the expected number of heads is equal to the number of tosses times the probability of a head, which is N/2 as shown by

$$E(H) = NP = N/2 \tag{57}$$

Also the variance of the expected number of heads is given by Equation (58) where, for a coin $P = \frac{1}{2}$. The square root of the variance is the standard deviation, which yields Equation (59).

$$VAR(H) = NP(1-P) = N/4 \tag{58}$$

$$SD = N^{\frac{1}{2}}/2 \tag{59}$$

If one were to compute all of the terms in Equation (55) that would be analogous to Equation (54), there would be 101 terms that add to one. The plot of these values as points on a line as the number of heads goes from 100 to 0, or from 0 to 100, would look very much like the famous and usually misunderstood bell-shaped curve; that is, the normal probability density function.

For purposes of illustration, therefore, it is possible to treat this example as if it were a sample from a normal population and to be a little imprecise for the exact values of the probabilities that are involved. For example, there is about a 95 percent chance (or a 0.95 probability) that a sample drawn from a normal population with the above expected value and standard deviation will lie within the range from the expected value minus twice the standard deviation to the expected value plus twice the standard deviation. This is indicated by

$$P(N/2 - N^{\frac{1}{2}} < \text{Number of heads} < N/2 + N^{\frac{1}{2}}) = 0.95 \tag{60}$$

For $N = 100$, this becomes Equation (61) or (62)

$$P(40 < \text{Number of Heads} < 60) = 0.95 \tag{61}$$

$$P(0.4 < \frac{\text{Number of Heads}}{100} < .6) = 0.95 \tag{62}$$

Now, a very nice prediction can be made. If a coin is tossed 100 times, the number of heads will be between 40 and 60. Even more interestingly, the ratio of the total number of heads to the total number of tosses, will be between 0.4 and

0.6. This prediction has a 95 percent chance of being correct. It would be a nice bet to make if one could get even money each time it was made.

Very interesting things happen if 10,000 tosses of the coin are considered. There are 95 chances in 100 that the total number of heads that come up will be somewhere between 4900 and 5100. The ratio of the total number of heads to the total number of tosses will be somewhere between 0.49 and 0.51 for this case. This would be a nice bet to make at even money. If one wants to be somewhat more conservative, change the values to 0.48 and 0.52. The probability of this happening would be very close to, but not exactly equal to, one.

With a few minor modifications of the concepts involved, one could consider that the probability of obtaining a success was unknown. An example might be a very large urn containing a mixture of black and white marbles, with an unknown percentage of white ones. Upon reaching in and drawing out a handful of marbles, the problem then becomes that of determining the ratio, or the percentage, of the white marbles compared to both kinds in the urn. A statement similar to the last equation can then be derived.

THE ESTIMATION OF FREQUENCY SPECTRA AND SIGNIFICANT WAVE HEIGHTS

In an oversimplified way, the above example illustrates the significance of the paper by Tukey. Through this paper it was possible for the first time to obtain an equation analogous to Equation (62). The difference is that the equation has the form given by Equation (63), where the upper and lower bounds can be computed from the known degrees of freedom of the spectral estimate and the value of the estimate.

$$P(S_L(f_i) < S(f_i) < S_U(f_i)) = 0.90 \tag{63}$$

Typically, for the estimation of spectra, the righthand side is picked to be 0.9 and the two numbers that result as the bounds of the inequality are called the 90 percent fiducial confidence interval. The correct interpretation of such an equation is that the true value of the spectrum would be found to lie between these two bounds nine chances in ten. If a spectrum from a very long time history of the waves for unchanging conditions could be computed (by analogy to tossing a coin many millions of times and calculating the ratio of the number of heads to the total number of times so as to get very close to one half) the result would be the "true" value.

As will be explained in what follows, the calculation of a spectrum is not a simple exercise. There are severe limitations on the information contained in an ocean wave time history of twenty minutes duration. If a wave spectrum is estimated, it is possible to obtain Equation (63) for each of the values of the estimated spectrum and to draw one curve lying above and one lying below the plotted points. These two curves enclose the true spectrum of the waves (that would in principal be obtained if a much longer time history could be gotten) nine times out of ten. Some investigators use narrower ranges and other probabilities, such as 0.5. The closeness of such intervals gives them a certain degree of confidence (which is unwarranted). They are, in essence, taking a chance of being wrong half the time.

Unfortunately, for the spectra predicted by the SOWM, with the spectral band widths that are used, a twenty minute (1200 second) long ocean wave time history (or due to Fast Fourier Transforms, 1024 seconds) which has been the standard recording length for most wave data, does not provide very good spectral estimates. Typically, the estimate does not tell one the true value of the spectrum within a factor of approximately two. For example, one can multiply the estimated value of the spectrum by 2/3 to obtain the lower curve (for the narrow frequency bands) and by 4/3 to obtain the upper curve. The ratio of the two is a factor of two, and the true spectrum lies somewhere between these two values nine times out of ten.

Suppose that a large number of wave time histories at locations corresponding to grid points of the SOWM are obtained and that each of these is processed to provide estimates of the wave spectra and their 90 percent confidence intervals. Then the spectra predicted by the SOWM can be expected to fall between the upper and lower confidence intervals of these estimated spectra nine times out of ten if the model and the winds are correct. There will be five spectral values out of each hundred for which the bounds of the confidence interval will fall below the SOWM value and five out of a hundred for which they will be above.

The SOWM spectra can only be evaluated in a statistical sense. One cannot predict the number of heads that will come up when a hundred coins are tossed, and one cannot predict the exact values for the ocean wave spectra that would be estimated from wave records and compared with the SOWM, or, for that matter, any other wave model.

The question might be asked "Why bother to verify the SOWM spectra against spectral estimates that are only good to within a factor of two?" The answer lies in the comments and remarks made in the description of the fully developed spectrum

and its variability. It also lies in the very large range of spectral values that occur for the frequencies of interest in the SOWM as the waves vary in height from under a meter to more than 15 meters. To get the spectra correct to within a factor of two is almost good enough. In fact, it is difficult to do.

However, there is a dilemma here. The theories that are available are for stationary gaussian processes, and with minor ifs, ands, and buts, for any stationary process, such as ocean waves, which are mildly non-gaussian. The concepts that are used all involve picking a sample so many minutes in length from a long time history that does not change its properties. If the ocean waves at a particular point on the ocean never changed their statistical properties, there would be no problem in forecasting. The corrections, modifications, and conceptual changes in wave record treatment required upon introduction of the idea that the spectra are changing as a function of time are very difficult and have not yet been fully addressed.

The total area under the frequency spectrum is the variance of the time history. This quantity is related to the significant wave height as defined previously for relatively narrow band spectra. Because the estimated spectra have this property of sampling variability, the total area under the spectra also has sampling variability. Therefore, not even the significant wave height is a precisely defined quantity that can be computed from an ocean wave record, or from the spectrum of that ocean wave record. The significant wave height has sampling variability also.

It is possible to write an equation similar to Equation (63) that puts a confidence interval on the significant wave height estimated from an ocean wave height time history by means of a spectrum. This confidence interval typically ranges from ±10 percent to ±30 percent of the significant wave height that is estimated depending upon the details of the spectral shape.

In the material that has been presented so far, notably missing has been any description of the sampling variability of the data that have been used to "verify" the SOWM. This problem will be addressed in what follows for both frequency spectra and significant wave heights; then, the material in the preceeding section on the verification of significant wave heights will be reinterpreted, along with additional data on significant wave heights.

There is another, perhaps equally shocking, concept that is a corollary of the idea of sampling variability. Weather Ship J, operated by the British for many

years, has faithfully obtained ocean wave time histories once every 6 hours and at special times, once every hour, for many, many years at a particular latitude and longitude of the North Atlantic ocean. Suppose that for this entire time, Weather Ship J had had an identical twin, with an identical ocean wave recorder on it and that it had been stationed at a point on a circle, with a two mile radius away from the true J with the exact location picked at random on that circle. Suppose that also this twin ship had taken a wave record starting and ending at exactly the same time as the one at J for this entire period.

Consider the pairs of estimated spectra that were obtained by these two ships. The consequences of the concept of sampling variability are that the spectra estimated from these two time histories would not agree with each other. There would be times when one spectral estimate for a particular frequency would be 30 to 40 percent higher than the estimate for that same frequency in the second spectrum. There would be other times when the reverse would occur. There would be times when a spectral band in the first spectrum would be twice as high as in the other spectrum. A probabilist would be able to take the theories that have been developed and make a great many predictions about how these spectra would differ, one from the other, for many, many pairs.

A corollary is that the significant wave heights obtained at these two locations could differ by as much as 10, 15, or 20 percent, at times, for measurements made at exactly the same time.

The SOWM has grid points several hundreds of nautical miles apart. Those unfamilar with sampling variability concepts would ask, "Why not measure waves on a grid spacing of 2 nautical miles (3.7 kilometers) over the North Atlantic Ocean?" Apart from the cost of such an operation, it would hardly be worthwhile because one would then be measuring sampling variability effects and not the true variability of the waves (most of the time) that one really wishes to predict.

These statements have to be modified somewhat on the basis of the kind of spatial distribution found by the altimeter on SEASAT as illustrated in the preceeding section. However, it is possible to go too far in the resolution of the grid to be used for wave forecasting and hindcasting, and it is possible to misinterpret wave measurements because of the effect of sampling variability. This problem becomes particularly difficult when waves are changing with time, as they actually do. It is not an easy task to sort out a true change in the spectrum from a change brought about by sampling variability. This is one of the major objections to the

techniques that led to the development of the JONSWAP spectrum, which will be explained later.[64]

Incidentally, there will always be doubters as to sampling variability effects. It might be very interesting, just for once, to locate five or six ocean wave recorders all properly calibrated on a square grid of points, perhaps 2 nautical miles apart, at some place on the North Atlantic ocean, and obtain simultaneous wave records. A great many statisticians would be shocked indeed if the spectra from these time histories were identical.

The first step in obtaining an estimate of a spectrum of a time history is to digitize the time history at intervals of Δt seconds as shown in Equation (64). The value of Δt should be small enough so that the Nyquist frequency does not produce any aliasing.

A standard procedure is to make a fast Fourier transform of the data contained in Equation (64) which consists of N points where $2^q = N$.

$$\eta(o),\ \eta(\Delta t),\ \eta(2\Delta t),.....\eta((n-1)\Delta t) \tag{64}$$

It is assumed that the record is periodic with a period of $N\Delta t$, which is the equivalent of the statements in

$$\eta(N\Delta t) = \eta(o),\ \eta((N+p)\Delta t) = \eta(p\Delta t) \tag{65}$$

This set of points has a mean which is assumed to be zero or corrected so that it will be zero, and the variance is given by

$$\bar{\eta} = \frac{1}{N} \Sigma\ \eta(p\Delta t) = 0 \tag{66}$$

$$\hat{VAR}(\eta) = \frac{1}{N} \Sigma\ (\eta(p\Delta t))^2 \tag{67}$$

The operation of obtaining a fast Fourier transform yields a representation of the same N points as given by Equation (68)

$$\eta(p\Delta t) = \sum_{n=1}^{N/2} a_n \cos \frac{2\pi np\Delta t}{\tau} + b_n \sin \frac{2\pi np\Delta t}{\tau} \tag{68}$$

where $\tau = N\Delta t.$

Incidentally, it is not absolutely essential to do a fast Fourier transform. For a fast Fourier transform N is some integer power of two. If the number of points in the time series differs from this, the Fourier transform can be calculated by brute force, but it turns out to be much more expensive. Typically therefore, most investigations are made today with some set of values given by 2^q.

The values of a_n and the b_n that are obtained in this way, are the complete equivalent of the time series values in the representation given by Equation (64). The information in the data has been transformed from the time domain to the frequency domain. With these 2^q values for the trigonometric coefficients, one can go back and recover exactly the number in Equation (64). Therefore, no information has been lost by this procedure.

The lowest frequency that goes with this set of coefficients, a_1 and b_1, is given by $1/N\Delta t$ and the highest frequency is given by $1/2\Delta t$. The highest frequency is called the Nyquist, or the folding, frequency.

From the point of view of the spectral analysis of an ocean wave time history or any other property of ocean waves such as the orbital motions and the potential function, there is too much information in the set of numbers that define the uniquely determined coefficients, a_n and b_n. The information is smoothed and by so doing the original record is no longer recoverable. What might be done at this stage of the game with an ocean wave time history has been rather thoroughly discussed in Reference 82.

However, continuing, the two coefficients for a particular frequency can be squared and summed to obtain Equation (69). For this kind of random process that fairly well describes ocean waves, this new number has a Chi Square distribution with 2 degrees of freedom. Its expected value is given by Equation (70) and the probability density function is given by Equation (71).

$$C_n^2 = \tfrac{1}{2}(a_n^2 + b_n^2); \quad n=1 \text{ to } N/2 \tag{69}$$

$$E(C_n^2) = S_n = \int_{(n-\frac{1}{2})/\tau}^{(n+\frac{1}{2})/\tau} S(f)dt \tag{70}$$

$$P(C_n^2)\, d\, C_n^2 = \exp\,(-\, C_n^2/S_n)\, d\, C_n^2/S_n \tag{71}$$

This value of C_n^2 is very erratic when repeated calculations of it for the same n, but for different time histories, are considered. The probability that it will be near its expected value is rather small, and, in fact, the 90 percent confidence interval about its expected value is found by multiplying a particular estimate by 0.334 and 19.42.

The idea behind spectral estimation is to smooth a number of these values of C_n^2 to obtain more stable numbers at a less dense spacing on the frequency axis for the study of the properties of the waves. This smoothing operation is indicated by Equation (72) where δ_p is a weight factor.

$$S(f_n) = \sum_{n-r}^{n+r} \delta_p \, C_p^2 \cdot \tau \tag{72}$$

In particular, if the values of δ_p are all equal as indicated by Equation (73), this consists of just averaging the values of C_n^2 over 2r + 1 values and plotting the resulting average at the central frequency of this range.

$$\delta_p = 1/(2r + 1) \tag{73}$$

There are, of course, many other ways to do the smoothing operation. Just as long as the δ_p satisfy certain criteria relative to preserving the total variance, they can have many different values. Also, it is not necessary just to estimate the spectrum at a set of nonoverlapping frequencies. This smoothing operator could be applied twice as frequently to obtain double the number of points on the frequency axis. All of these various techniques are possible today, because of the ability to carry out the fast Fourier transform operation.

From a theoretical point of view, the procedure is indicated by Equation (74), where whatever choice of the weight factors made and applied to the fast Fourier transform is equivalent to a convolution of the weighting function with a true function for the spectrum as indicated in this equation. Clearly a wide variety of weight functions could be chosen. The output of the convolution will be more or less a smooth version of the input under many conditions.

The point of this discussion is that the choice of weight functions and smoothing operators is more or less irrelevant because of the sampling variability of

these estimates. The true values of the spectrum are really not known to within a range of about a factor of two. For this reason, minor fluctuations in the shape of the spectrum usually do not have any meaning because of this large uncertainty.

$$S_c(f) = \int S(f')\, w(f-f')\, d\, f' \tag{74}$$

SMOOTHED SPECTRAL ESTIMATES

Given the N/2 values of C_n^2, suppose that 2r + 1 values are combined with unit weights centered on a frequency, f_n, and covering a certain frequency band. If the spectrum is slowly varying enough over the frequency band, then the 2r + 1 values of C_n^2 combine as Chi Square variables each with 2 degrees of freedom to yield a Chi Square variable with 4r + 2 degrees of freedom, but with an unknown parameter equal to the "true" or expected value of the spectrum as integrated over the frequency band.

If $S(f_n)\Delta f$ is this expected value and if $\hat{S}(f_n)\Delta f$ is the value computed from the sum as the estimate, then the ratio, $D\hat{S}(f_n)/S(f_n)$, is Chi Square distributed with (4r+2 = D) degrees of freedom.

From standard tables, the values of Chi Square, such that this random variable will exceed α_D with a probability of 0.05 (say) and will be less than β_D (say) with a probability of 0.95, can be found so that Equation (75) can be assigned numerical quantities.

$$P\left(\alpha_D < \frac{D\,\hat{S}(f_n)}{S(f_n)} < \beta_D\right) = 0.90 \tag{75}$$

Some algebra yields

$$P\left(\frac{D\,\hat{S}(f_n)}{\beta_D} < S(f_n) < \frac{D\,\hat{S}(f_n)}{\alpha_D}\right) = 0.90 \tag{76}$$

If D for example is 30, $\alpha_D = 18.5$ and $\beta_D = 43.8$ so that

$$P(0.685\,\hat{S}(f_n) < S(f_n) < 1.622\,\hat{S}(f_n)) = 0.90 \tag{77}$$

and the ratio of 1.622 to 0.685 is 2.37. Everything is known in this equation as a number except $S(f_n)$. The equation states that the probability is 0.90 that interval

defined by the two numbers in the parenthesis will enclose the true value of the spectrum at f_n.

A 17-minute, 4-second wave record digitized once per second has a Nyquist frequency of 0.5 second^{-1} and has 1024 points. There would be 512 values of C_n^2 (less 1 for zero frequency). The frequencies would be 1/1024, 2/1024, n/1024, ... 512/1024 second^{-1}. Averages centered on f = 16p/1024 for p = 0 to 32 with values at f = 16 (p+½)/1024 weighted one half and assigned at 16p/1024 and 16(p+1)/1024 would yield 33 spectral estimates, each with 32 degrees of freedom (except at 0 and 0.5 Hertz) and confidence intervals nearly equal to those given above.

For p = 5, the frequency is 80/1024 corresponding to a period of 12.8 seconds with bounds of 72/1024 and 88/1024 (periods of about 14.2 and 11.6 seconds). To halve the frequency bands for the same record length requires using f = 8q/1024 as q goes from 0 to 64, and this halves the degrees of freedom. The confidence intervals become even wider. To narrow the confidence intervals by doubling the degrees of freedom for the same record length requires that f = 32r/1024 as r goes from 0 to 16.

For a fixed record length, high resolution sacrifices degrees of freedom and implies wide confidence intervals. Narrow confidence intervals and high degrees of freedom sacrifice spectral resolution.

Further verification of the frequency spectra of the SOWM might benefit from obtaining 35- or even 52-minute long wave records instead of 17-minute long wave records. The lack of stationarity could be investigated theoretically. For a 52-minute record the frequencies can be centered on f = 48S/3072 and there would be 96 degrees of freedom per estimate. The confidence intervals would then become 1.26 and 0.79 in Equation (77) with the upper bound being 60 percent higher than the lower bound.

To estimate a spectrum with a ±10 percent confidence interval requires about 580 degrees of freedom, and a record about 5 hours long for the same resolution. During 5 hours, the waves will have probably changed their statistical properties, and thus high resolution and narrow confidence intervals are unobtainable for real situations in the time domain.

The points raised above are simply a restatement of the properties of time series. They were clearly and more briefly stated in Reference 80. From page 2 of Reference 80:*

*Underlined words are not emphasized in the original quotation.

"Practically useful answers to these questions may be found by combining results from transmission theory and the theory of statistical estimation. These answers prove to be relatively simple. The only major difficulty in their practical application is the extensiveness of the data required for highly precise estimates. This requirement is an inherent, irrevocable characteristic of such random processes"

A second quotation from page 93 is:

"Clearly, for any specific value to T_n (and number of pieces of record), we can increase frequency resolution (or stability) only by sacrificing stability (or frequency resolution)."

CONFIDENCE INTERVALS ON WAVE HEIGHT

The Chi Square probability density function is derived by considering the sum of the squares of D independent random variables drawn from a normal population with a zero mean and unit variance. After referring a variable to zero mean, which occurs naturally in calculating a fast Fourier transform, it must be scaled by dividing it by the standard deviation for the calculation of the value of Chi Square. The Chi Square distribution has the reproductive property; specifically, if y_{N1} is distributed according to Chi Square with N1 degrees of freedom and if y_{N2} is distributed according to Chi Square with N2 degrees of freedom, then $Y = y_{N1} + y_{N2}$ is distributed according to Chi Square with N1 + N2 degrees of freedom.

An estimated spectrum consists of p numbers typically of the form $\hat{S}(p\Delta f)$ where p varies from zero to, say, m. The first and last values for p = 0 and m have say D/2 degrees of freedom and the estimates for p equal to 1 to m-1 have D degrees of freedom. Conceptually there is some true, but unknown, spectrum, essentially $S(p\Delta f)$, that the values of $\hat{S}(p\Delta f)$ estimate. The sum of the values of $\hat{S}(p\Delta f)$ is an estimate of the variance of the random process as in

$$VAR = \sum_{o}^{m} \hat{S}\,(p\Delta f) = \hat{VAR}(\eta) \tag{78}$$

and in Equation (67). This sum is like a sum of Chi Square distributed random variables except that each term has a different normalizing value.

The exact probability density function for the estimate of the total variance is unknown. However, it can be shown that the total variance is approximately

distributed according to Chi Square with a total number of degrees of freedom (TDF), if the separate spectral estimates are independent, as given in Equation (79). The total number of degrees of freedom can also be called the effective number of degrees of freedom.

$$TDF \cong \frac{D\left(\sum_{o}^{m} \hat{S}(p\Delta t)\right)^2}{\left[\left(\frac{\hat{S}(o) + \hat{S}(m)}{2}\right)^2 + \sum_{1}^{m-1} \left(S(p\Delta t)\right)^2\right]} \tag{79}$$

The proof involves deriving the moment generating function for each estimate and using the fact that moment generating function for a sum is the product of the moment generating functions for the terms in the sum. The resulting moment generating function is then equated to the moment generating function for a Chi Square distribution with an unknown value for the degrees of freedom and a parameter equal to the total variance. Equation (79) results by requiring that the first two moments of the approximating Chi Square distribution equal the first two moments of the correct distribution.

One extreme would be the case where all of the values of $\hat{S}(p\Delta f)$ are equal (or nearly equal). The numerator of Equation (79) would equal Dp^2 and the denominator would equal p so that TDF would equal Dp or N, the total number of points in the sample. This never happens for actual ocean wave time histories, but the result is the equivalent of drawing an independent sample of size N from a zero mean normal population with an unknown variance. A total number of observations equal to 1024, if they were independent, would yield 90 percent confidence intervals of about 1.07 and 0.93 times the estimated variance.

The other extreme would be to find all but one of the values of C_n^2 in Equation (69) to be zero. The total degrees of freedom would be 2 no matter how long the time history. Narrow band swell can approach this condition.

Typically, the total degrees of freedom for an ocean wave time history about 20 minutes long can range from about 50 to 150. The time correlation between the points in the time history makes each value less useful in estimating the variance than would be an independent observation from a normal distribution. The appropriate constants in an equation similar to Equation (77) are given by

$$10^{+(1/TDF)^{\frac{1}{2}}}$$

and

$$10^{-(1/TDF)^{\frac{1}{2}}}$$

for the 90 percent confidence interval for large enough values.

Thus

$$P\left[10^{-(1/TDF)^{\frac{1}{2}}}\,\hat{VAR} < VAR < 10^{+(1/TDF)^{\frac{1}{2}}}\,\hat{VAR}\right] = 0.90 \tag{80}$$

Since

$$H_{1/3} = 4\,(VAR)^{\frac{1}{2}} \tag{81}$$

it follows that Equation (82) holds.

$$P\,(\alpha_{0.05}\,\hat{H}_{1/3} < H_{1/3} < \beta_{0.95}\,\hat{H}_{1/3}) = 0.90 \tag{82}$$

where

$$\alpha_{0.05} = \left[10^{-(1/TDF)^{\frac{1}{2}}}\right]^{\frac{1}{2}} \tag{83}$$

and

$$\beta_{0.95} = \left[10^{+(1/TDF)^{\frac{1}{2}}}\right]^{\frac{1}{2}} \tag{84}$$

If the estimated significant wave height was 10 meters, and if TDF equaled 50, then Equation (82) yields

$$P(8.50 < H_{1/3} < 11.77) = 0.90 \tag{85}$$

and the wave height is not known to within 3.27 meters (plus or minus about 1.6 meters or 16 percent), even if it is estimated to be 10 meters.

For 150 total degrees of freedom, the corresponding equation is Equation (86), and there is almost a 2-meter spread.

$$P(9.10 < H_{1/3} < 10.99) = 0.90 \tag{86}$$

The verification efforts for the SOWM and for comparisons of altimeter wave height measurements with waves recorded by ships and data buoys, as described previously, did not take these considerations into account. Ways to do so will be described shortly.

A RESTATEMENT OF A SPECTRAL OCEAN WAVE MODEL FORECAST

Suppose that the SOWM spectral predictions were perfect, and that in particular the one in Table 5 was perfect. Suppose that a ship near that grid point measured the waves with a wave recorder for 25 minutes and 36 seconds on the date and time indicated, and that the data were digitized at a Δt of 1.5 seconds to obtain 1024 measurements. Suppose that the spectrum was resolved into 60 frequency bands with a Δf of 180^{-1}. Each band would have about 17 degrees of freedom. Let the values of $\hat{S}(f_i)$ be computed from the time series of recorded values to be compared to the values tabulated in Table 5; and let the significant height be computed according to the appropriate equation.

Equation (75) becomes

$$P\left\{8.67 < \frac{17\ \hat{S}(f_i)}{S\ (f_i)} < 27.6\right\} = 0.90 \tag{87}$$

for the lowest seven frequencies, and, hence, for $f_i = 0.039$

$$P\ (0.576 < \hat{S}\ (0.039) < 1.83) = 0.90 \tag{88}$$

For $f_i = 0.044$

$$P\ (15.67 < \hat{S}\ (0.044) < 49.89) = 0.90 \tag{89}$$

For $f_i = 0.05$

$$P\ (19.33 < \hat{S}\ (0.05) < 61.55) = 0.90 \tag{90}$$

and so on. For $f_i = 0.081$ there are 34 degrees of freedom and roughly (for 30 degrees of freedom)

$$P\ (9.60 < \hat{S}\ (0.081) < 22.7) = 0.90 \qquad (91)$$

and so on.

The total degrees of freedom are found from Equation (79) except that $S(f_i)$ and not $\hat{S}\ (f_i)$ is used. There are 142 degrees of freedom.

Therefore, because the significant wave height from the SOWM is 55.5 feet

$$P\ (50.4 < H_{1/3} < 61.1) = 0.90 \qquad (92)$$

Thus the wave record obtained by the ship will yield estimates of the spectrum such that nine times out of ten each of the fifteen values calculated from the wave record will be between the bounds illustrated above for four of the bands. The significant wave height will lie between 50.4 and 61.1, nine times out of ten.

This is really all that the SOWM can predict. The ship could actually experience waves considerably higher or considerably lower than 55 feet. The actual values could be quite different from those predicted from Table 5. Yet, in a very real sense, the prediction is still correct.

Were the SOWM actually perfect and had a fleet been present near the grid point, some of the ships would have experienced higher waves and some lower. Had 20 spectra been estimated from 20 different wave records, the averages of these spectra would have 340 degrees of freedom. The average of the spectra would have been within ±13 percent of the SOWM spectrum, nine times out of ten.

The total degrees of freedom would have been such that the average of the variances of the individual wave records would have yielded a significant wave height between 53 and 58 feet (nine times out of ten).

To go further, the chance that all 15 values of $\hat{S}(f_i)$ would lie between the calculated bounds for one 25-minute wave record is $(0.9)^{15}$, or 0.206; the chance that 14 out of the 15 would, is $1.5\ (0.9)^{14}$, or 0.343; the chance that 13 out of the 15 would is $(1.5)\ (0.7)\ (0.9)^{13}$, or 0.267; the chance that 12 out of the 15 would, is $(0.5)\ (0.7)\ (1.3)\ (0.9)^{12}$, or 0.129; and, because these values sum to 0.945, the chance that 11 or fewer would is 0.055.

One time in 20, the significant wave height calculated from this hypothetical wave record would exceed the upper bound calculated for this example. Yet the SOWM was assumed to be perfect. The ship captain that experienced this condition might well conclude that the forecast was wrong.

Thus, there is an element of randomness, or unpredictability, in ocean wave forecasts that must be understood by those who produce the forecasts and those who verify the forecasts. This element of randomness can be treated either by predicting, as above, the amount by which an observation made at a verification time can differ by chance from the prediction or by analyzing the verification data in terms of fiducial confidence intervals on the estimates of the spectra and wave heights that they provide.

Because the SOWM is clearly not a perfect wave specification and forecasting model, there will be discrepancies between what it predicts and what the observations show. Because the observations inherently have large sampling variability, the inconsistencies of the SOWM, or of any other model, are difficult to identify, isolate, and correct.

The literature on wave forecasting models rarely, if ever, mentions these considerations with reference to the problem of verification, and the development of the model. Some authors seem both disappointed and surprised (and perhaps even embarrassed) when the wave heights and frequency spectral predicted by their model do not verify perfectly.

COMMENTS

When Tukey first discovered these techniques of power spectral estimation, the fast Fourier transform was unavailable.[11] It was discovered a number of years later. For this reason the estimation of wave spectra during the early days of the study of ocean waves was based on a number of equations operating on the time series that effectively ended up doing the same thing as Equation (74), but that did it in a different way.[80] These operations were all variations of roughly the same scheme. They consisted of lagging the time series with itself and taking the products of lagged sums over that part of the series that still overlapped to form an estimate of the covariance function; that is, the correlation of the time history will itself delayed by an integer number of Δt's. The covariance function would be computed for perhaps 10 or 20 percent of the length of the original record. It would be an even function of the lag, and it could be expanded as an even function about the origin. The Fourier transform of this covariance function was then computed in order to obtain a raw estimate of the spectrum. The difficulty with this particular procedure was that the weight functions that result are negative for some values. Typically one could obtain, for rapidly varying spectra, a negative estimate of the

variance in a given frequency band. A negative estimate of a variance is highly disconcerting. Tukey showed that a linear combination of three such estimates by any one of several weighting procedures would usually eliminate these negative side lobes in the weight function and produce a series of spectral estimates as the function of frequency that had many desirable properties. These weight functions were roughly triangular in shape and overlapped adjacent frequency bands. References and details of these types of procedures are contained in various sources such as References 80, 15, and 83.

Two of the smoothing operators that were used were called Hanning and Hamming. They yield ever so slightly different spectral estimates.

Other spectral estimates guaranteed absolutely no negative side lobes. These very fine techniques in the pre-fast Fourier transform era were concerned with problems for which the spectral estimates could vary over perhaps four orders of magnitude as a function of frequency. They were concerned, for example, with whether or not very low values were contaminated by leakage in the spectral filters from the high values. Most of these problems are no longer as pressing as they were at that time because of the ability to carry out fast Fourier transforms. An investigator who is interested in functions of time that can have frequency content that varies over several orders of magnitude need only to be concerned today with the number of significant figures that are carried in the original time series. Round off and truncation errors can produce a white noise background such that extremely low values of the spectrum are hidden by this white noise background.

SPECTRAL OCEAN WAVE MODEL FREQUENCY SPECTRA VERSUS PARAMETRIC REPRESENTATIONS

The literature to date has had a number of papers by various authors that have been concerned with other ways to estimate spectra and with fitting spectra by means of a set of parametric curves. For various reasons, objections can be raised to the JONSWAP spectrum on this basis and to the efforts to fit ocean wave spectra by a six parameter family of curves. A six parameter representation, for example, is not much of an improvement over the 15 values that define a SOWM spectrum as a function of frequency. Even if it is successful and is capable of defining the shape of the spectrum as well as the original SOWM values, nothing much has been achieved because one still has to apply the spectrum to whatever practical application is required over a continuous range of frequencies. The real problems of applying SOWM products to problems in naval architecture lie in how well (and in what sense) the SOWM spectra verify, in whether or not the frequency resolution is adequate for possible

resonance phenomenon and in taking into the account the effects of wave direction as well as the variations of the spectra as a function of frequency. The progress in this direction achieved in Reference 70 is most impressive.

EXAMPLES OF THE VERIFICATION OF BOTH SIGNIFICANT WAVE HEIGHTS AND FREQUENCY SPECTRA IN TERMS OF SAMPLING VARIABILITY CONSIDERATIONS FOR MODELS SIMILAR TO THE SPECTRAL OCEAN WAVE MODEL

Efforts were made to develop the SOWM using the concepts just described, at least in principal. With the techniques then available for getting a wind field and for a developmental version of the SOWM, data such as those in Figure 53 were studied as also described in Reference 84. The four 6-hourly specifications for 3 days (17, 18, and 19 December 1959) are compared with estimates of the spectra computed from wave records obtained by the Tucker shipborne wave recorder.[13,14]

Two predicted spectra were compared with the spectrum estimated from a wave record for each time. The histogram-like plot shows the predicted (hindcast or specified) spectra, and the estimated spectrum plus its upper 95 percent and lower 5 percent confidence intervals are graphed by connecting the estimates by straight lines.

Also tabulated are the significant wave heights that were predicted and estimated and the 90 percent confidence intervals on the estimates. These numbers are hard to read so they are repeated in Table 11 except that only the best of the two heights is used. The height predicted by the model can fall in any one of four locations in the table relative to the estimated height and its 5 percent and 95 percent values for the confidence interval.

The 90 percent confidence interval on the estimate of the significant wave height encloses the "true" value of the wave height 9 times out of 10 by definition. One time out of 10 it does <u>not</u>*. If the significant wave heights of a wave hindcasting (specification or forecasting) model are contained within the 90 percent confidence interval of a significant wave height estimated from an ocean wave time history nine times out of ten, then the model is doing very well indeed.

For this particular test case, eight of the 12, (67 percent) of the hindcast heights verified in this sense. There ought to have been about 11. Thus, the model did not do well.

If the estimated height and the predicted height are compared in the usual way, the bias is +1.75 feet and the root mean square difference is 4.14 feet.

---

*Be careful! What does this statement mean?

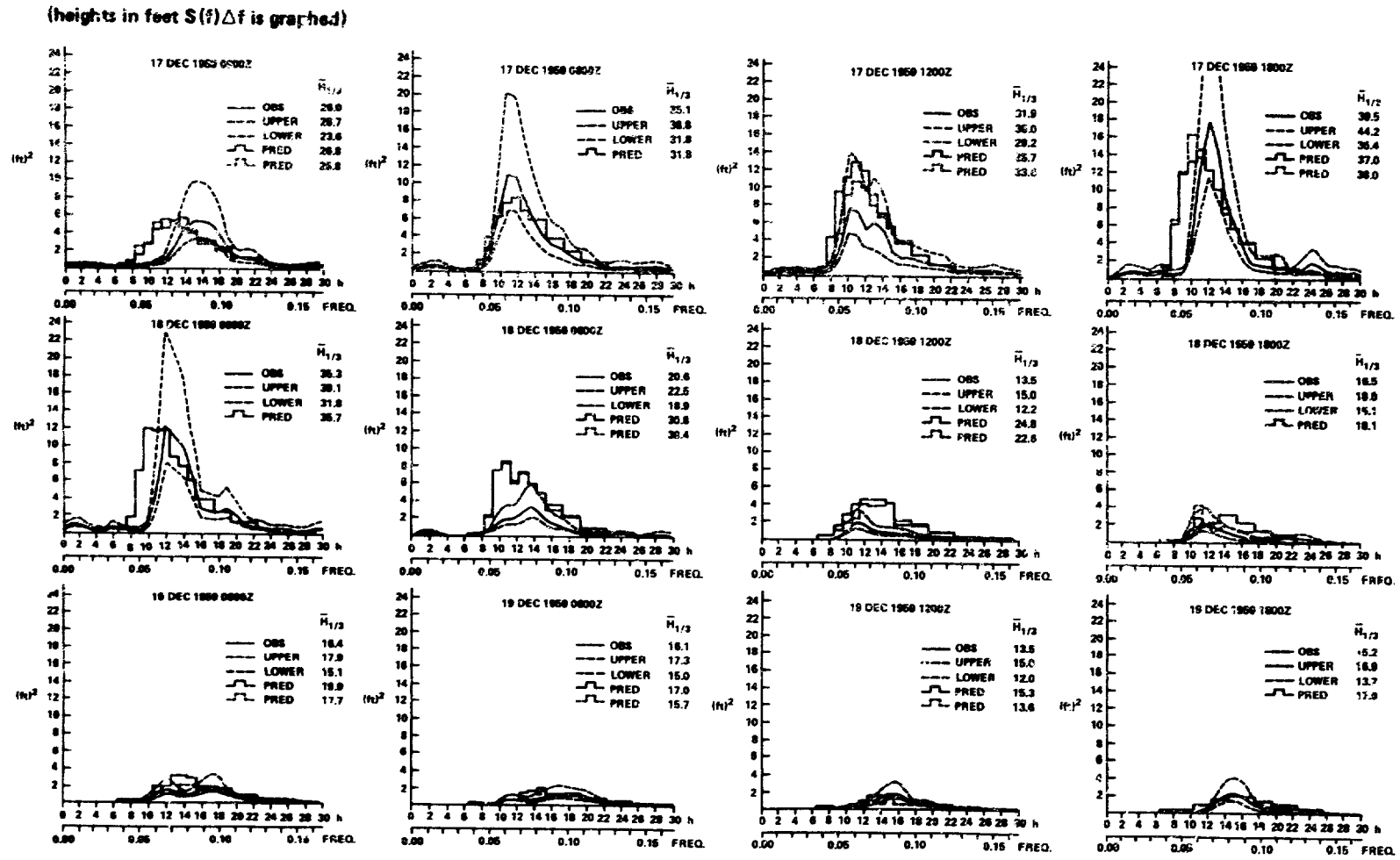

Figure 53 - A Sequence of Observed and Hindcasted Spectra for the Dates and Times Shown
(From Reference 84)

TABLE 11 - EXAMPLE OF SIGNIFICANT HEIGHT VERIFICATIONS DURING THE DEVELOPMENT OF THE SPECTRAL OCEAN WAVE MODEL

(Wave Heights in Feet)

17 December 1959	Verify	Predicted	Lower	Predicted	Estimated	Predicted	Upper	Predicted	Predicted-Estimated	Range Upper-Lower
00z	yes		23.6		26.0	26.8	28.7		+0.8	5.1
06z	yes		31.8	31.8	35.1		38.8		-3.3	7.0
12z	yes		29.2		31.9	33.6	35.0		+1.7	5.8
18z	yes		35.4	38.0	39.5		44.3		-1.5	8.8
18 December 1959										
00z	yes		31.8		35.3	35.7	39.1		+0.4	7.3
06z	no		18.9		20.6		22.5	30.4	+9.8	3.6
12z	no		12.2		13.5		15.0	22.6	+9.1	2.8
18z	no		15.1		16.5		18.0	18.1	+1.6	2.9
19 December 1959										
00z	yes		15.1		16.4	16.4	17.7		0.0	2.6
06z	yes		15.0	15.7	16.1		17.3		-0.4	2.3
12z	yes		12.0		13.5	13.6	15.0		+0.1	3.0
18z	no		13.7		15.2		16.9	17.9	+2.7	3.2

Bias = +1.75 feet

RMS = 4.14 feet

Clearly the root mean square value could have been fairly large even if all of the heights had verified!

Even though some of the heights verified, the spectra sometimes did not verify. The low frequencies in the first predicted spectrum are much too high and the spectral values are nowhere near the upper and lower bounds of the estimated spectrum. The second predicted spectrum verifies extremely well. The third runs consistently too high, and so on.

The predicted heights range from 38 feet to 13.6 feet implying that one predicted spectrum will have 7.8 times the area under it than the lowest. The estimated heights range from 39.5 feet to 13.6 feet so that the areas under the estimated spectra varied by a factor of 8.4. The highest and the lowest waves and the next highest and the lowest spectra were predicted fairly well.

The current SOWM specifications in this climatology produced at FNOC are available for December 1959. It would be interesting to redo this study, because a very long series of spectral estimates are available.[14] The wind field analyses should be better and the final version of the SOWM described in the first part of this paper is substantially different from the version that was tested in this example.

During SKYLAB it was thought that wave data might be an important part of the study of S193, which was the radar on the spacecraft. Fortunately this turned out not to be the case for measuring winds over the ocean.[37] However, to meet this contingency, 20-minute long ocean wave time histories were obtained every hour when SKYLAB would be anywhere near Weather Ship J.[85] These records were spectrally analyzed and the results were compared with hindcasts generated with a wave model much more nearly like the current SOWM.[53]

The significant wave heights were estimated from the wave records obtained each hour. Wave hindcasts were made for every 6 hours.

Some of the results are shown in Figure 54. The circled dots are the estimated wave heights and the jagged lines above and below are the 90 percent confidence intervals.

The diamonds are the hindcasted wave heights. Weather Ship J is not exactly at a grid point of the model but lies within a triangle of three grid points. The spectra at these three grid points were recovered. A plane was put through the three values for each frequency direction component for the three points and the location of J on this plane was found to compute by interpolation the value of $S(f_i,\theta_j)$

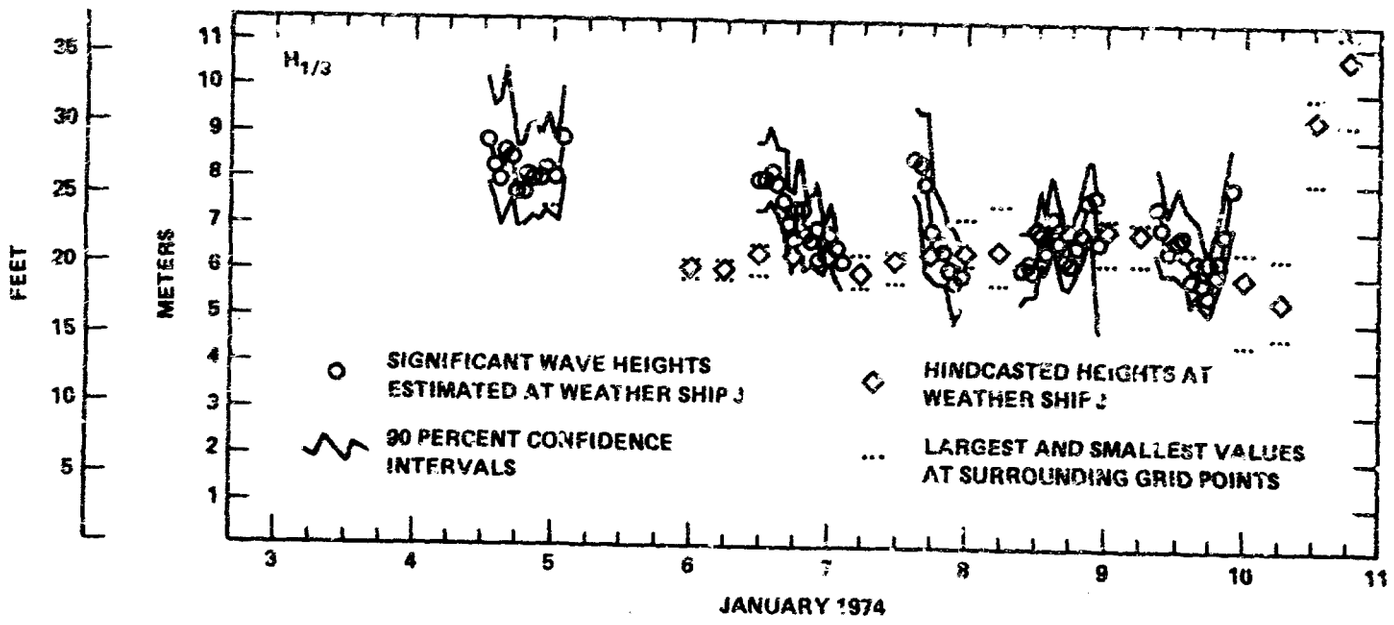

Figure 54 - Significant Wave Heights Estimated at Weather Ship J, Their 90 Percent Confidence Intervals, the Hindcasted Heights at J, and the Largest and Smallest Values at Surrounding Grid Points
(From Reference 37)

for the location of the ship. The significant wave height was then computed from this interpolated spectrum. The result is shown as the diamonds in Figure 54. The horizontal dots above and below the diamonds represent the highest and lowest significant heights for the three grid points of the model that surround the weather ship. The gradients of wave height (and hence even more for spectra) over one grid distance are thus quite large.

For 4 to 5 January 1974, the estimated wave heights fluctuate erratically, but a horizontal line at about 8.3 meters could fit the estimates equally well. For 6 to 7 January, a marked decrease in wave height over the 15 hours of data is required for any smooth curve between the confidence intervals, and similarly for 7 to 8 January.

The jagged behavior on 8 January may or may not be real. The waves almost surely first decrease and then increase on 9 January.

The hindcasts miss part of this erratic variation and seem to be much smoother than the estimates. This similarity as a function of time at a fixed point to the variation of the waves as a function of distance along a line in the altimeter data is a feature of waves that is not currently predictable for reasons given above.

It was possible to compare nine wave height hindcasts as shown in Table 12. Four of the nine (instead of about eight of the nine) fell within the 90 percent confidence intervals of the wave height estimate. Yet, computed the usual way the bias was only -0.06 meters and the root mean square error was only 0.83 meters. Ways to interpret root mean square errors when there is an effect of sampling variability in the estimates used to verify a wave forecasting (specification) model will be illustrated later. There is clearly a minimum (not zero) value that can be achieved because of the effect of sampling variability. A wave model that consistently verified to within ±5 percent of wave heights computed from 20 minute long wave records is obviously a fraud. The model would have to have extrasensory perception!

The interpolated spectra from the model were compared to the estimated spectra as shown in Figure 55. The histogram-like plot is the model spectrum. The circled points are the estimates from a time history and the vertical lines with bars at the top and bottom are the 90 percent confidence intervals. All but the last confidence interval enclose the model spectrum value so that this spectrum verifies quite well. The computed wave height from the model compares well with the observed (estimated) wave height from the wave record differing from it by -0.75 meters.

TABLE 12 - VERIFICATION OF A MODEL SIMILAR TO THE SPECTRAL OCEAN WAVE MODEL AT WEATHER SHIP J DURING SKYLAB

(Wave Height in Meters)										
	Verify	Pred.	Lower	Pred.	Est.	Pred.	Upper	Pred.	Pred.-Est.	Range
6 Jan 74										
12z	No	6.20	7.13		7.99		8.22		-1.77	1.09
18z	Yes		6.00	6.17	6.74		7.72		-0.57	1.72
7 Jan 74										
00z	No	6.17	6.37		6.92		7.60		-0.75	1.23
18z	Yes		6.05	6.48	6.86		7.94		-0.38	1.89
8 Jan 74										
12z	No		5.52		6.11		6.86	7.01	+0.90	1.34
18z	No		5.62		6.21		6.95	7.03	+0.82	1.33
9 Jan 74										
00z	Yes		6.15		6.69	7.02	7.36		+0.33	1.21
12z	Yes		6.07		6.72	6.84	7.55		+0.12	1.48
18z	No		5.10		5.60		6.22	6.36	+0.76	1.12

Bias = -0.06 meters

RMS = 0.83 meters (33 inches)

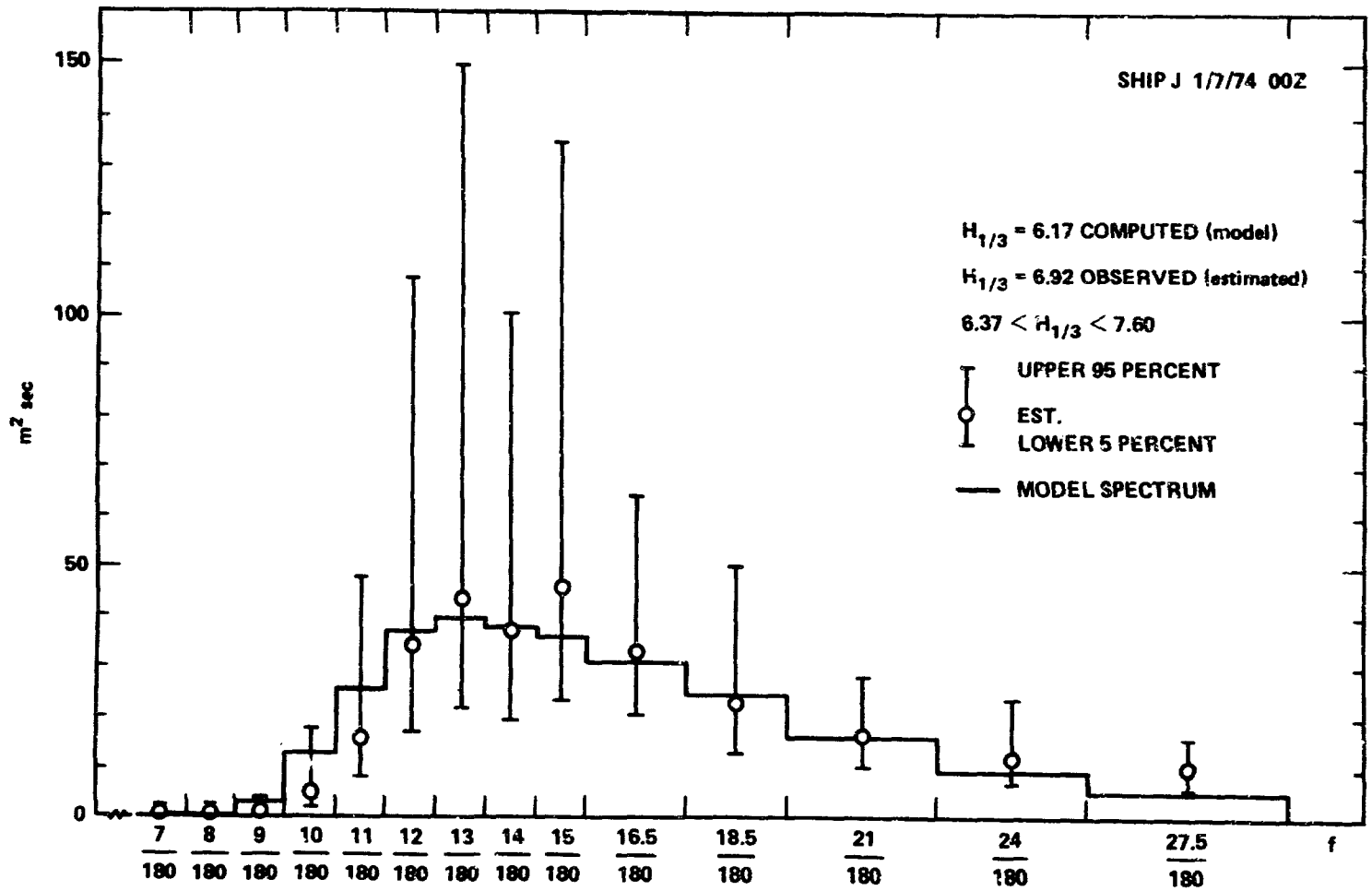

Figure 55 - Spectral Verification for Weather Ship J for 7 January 1974 at 00z

The model height did not fall within the confidence intervals for the estimated height despite the good spectral agreement.

From figures such as Figure 55 for the nine available spectra, a count was made as to whether or not the confidence interval of the estimated spectrum enclosed the model spectrum. The results are shown in Table 13. The first two bands essentially contained no spectral variance and the model predicted that they would not as shown by the ones in the table. Band 3 was fairly good, but bands 4 and 5, which were near the sharp increase in the spectrum, were not predicted well.

Out of a possible 126 spectral bands for the model, 104 bands or 83 percent, fell within the 90 percent confidence intervals of the spectral estimates. There should have been about 113 bands (90 percent). Even with this criterion, the model was not quite good enough.

There are statistics involved with the statistics of this table. The number of ones has a binomial distribution with a sample size of 126 and a probability of 0.9. The expected value of the number of ones is 113.4 and the standard deviation is about 3.37, so that 95 times in 100, the number of ones should fall between 106.7 and 120.1. Because only 104 successes were obtained, the number of successes is somewhat less than what could occur by chance (but not completely unreasonable).

The spectra for this series are also available.[53] If the SOWM hindcasts cover the above period, a comparison along these same lines would be beneficial.

The last example of this section is for a model developed to hindcast hurricane waves in the Gulf of Mexico.[51] The grid points were 20 nautical miles apart, the time step was one hour, wave refraction effects were incorporated for shallow water, and many aspects of the model were similar to the SOWM. The spectra were resolved into 24 direction bands instead of 12.

Figure 56 shows significant wave height in feet as a function of time at three locations during Hurricane Camille. The solid and dashed lines represent the model values at two grid points. The points are the estimated wave heights at the locations shown near the grid points and the 90 percent confidence intervals.

Wave heights estimated from wave records at Station 1, which is about halfway between the two plotted grid points, agree with the model values during the last part of the plotted period. If the wave heights at Station 1 were the average of the heights at the two grid points, then the model could be said to verify within the 90 percent confidence interval at seven of the 15 times for which the heights were estimated.

TABLE 13 - NUMBER OF TIMES 90 PERCENT FIDUCIAL CONFIDENCE INTERVAL OF SPECTRAL ESTIMATE ENCLOSED SPECTRAL HINDCAST FOR 14 SPECTRAL BANDS AT WEATHER SHIP J

Hit Ratio J												
f	Band	1/6/74		1/7/74		1/8/74		1/9/74			Sum	Percent
		12z	18z	00z	18z	12z	18z	00z	12z	16z		
1/25.7	1	1	1	1	1	1	1	1	1	1	9	100
1/22.5	2	1	1	1	1	1	1	1	1	1	9	100
1/20.0	3	1	1	1	1	0	1	1	1	0	7	78
1/18.0	4	0	1	1	1	0	0	0	1	0	4	44
1/16.4	5	1	1	1	0	0	1	1	0	1	6	67
1/15.0	6	1	1	1	0	0	1	1	1	1	7	78
1/13.8	7	1	0	1	0	1	1	1	1	1	7	78
1/12.9	8	1	1	1	1	1	1	1	1	1	9	100
1/12.0	9	1	1	1	1	1	1	0	1	1	8	67
1/10.9	10	1	1	1	1	1	1	1	1	1	9	100
1/9.7	11	1	1	1	1	0	0	1	1	1	7	78
1/8.6	12	0	1	1	1	1	1	1	1	0	7	78
1/7.5	13	1	1	1	0	1	1	1	1	1	8	89
1/6.5	14	0	1	0	1	1	1	1	1	1	7	78
Sum		11	13	13	10	9	12	12	13	11	104	
Percent		79	93	93	71	64	86	86	93	79		83

Figure 56 - Significant Wave Height as a Function of Time at Three Locations During Hurricane Camille

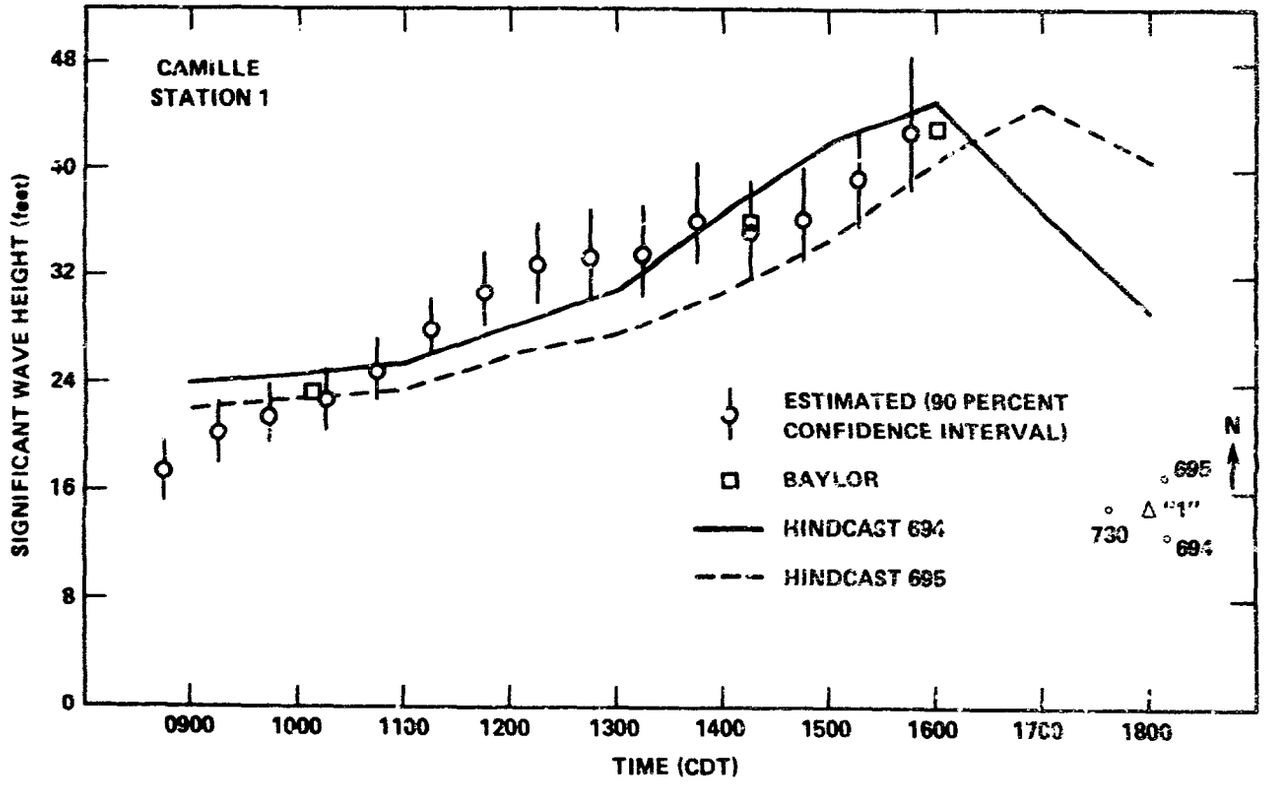

Figure 56a - Comparison of Measured and Hindcast Significant Wave Height at Station 1 for the Hurricane Camille Historical Wind Field Hindcast (From Reference 51)

Figure 56 (Continued)

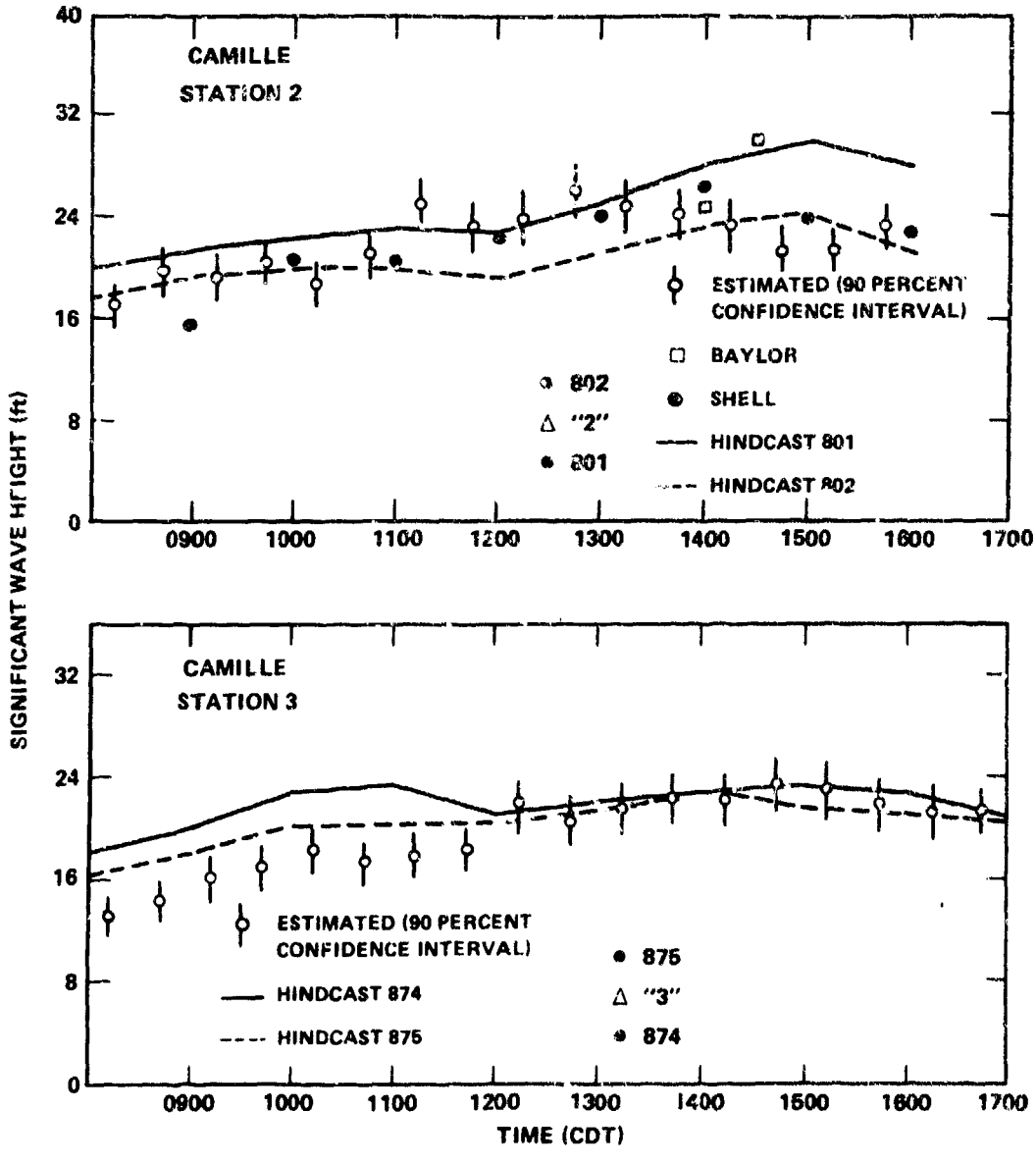

Figure 56b - Time Histories of Measured and Hindcast Significant Wave Height at Stations 2 and 3 for the Hurricane Camille Hindcast
(From Reference 51)

For Station 2, with grid point 801 as the verification of the hindcast, eight out of 16 verify, and for Station 3, with the average of 874 and 875 used as the model hindcast, 10 out of 18 verify. The estimates of the wave height vary much more smoothly for these data than they did for the preceeding SKYLAB study.

Figures 57 and 58 show verifications of three frequency spectra of hurricane waves during Camille. Figure 57 shows a spectrum plotted in a way that is somewhat deceptive based on the discussion of Figure 36. However, if only the values at the frequencies corresponding to the circled points are studied for the estimated spectrum and its confidence intervals, it is seen that the model spectrum falls everywhere within the confidence intervals. There are 12 successes out of 12 tries. The estimated wave height is 43.13 feet with a confidence interval of 48.3 to 39.02 feet (a range of 9.28 feet) and the model predicted 44.88 feet.

For the other two spectra, in Figure 58, there are 22 successes out of 24 tries, so that for all three spectra there are 34 successes out of 36 tries or 94 percent success, which is just about right. The confidence intervals on the estimate of the height enclose the predicted height for both spectra.

Since only 25 out of 49 heights appear to verify in Figure 56 (or 51 percent, instead of 90 percent), the model clearly could be improved. The verification of the spectra for peak wave conditions at the various stations was, in general, quite good. Note that in all three of the spectral comparisons, the peak of the estimated spectrum was higher than the peak of the model spectrum.

VERIFICATION OF THE SPECTRAL OCEAN WAVE MODEL CLIMATOLOGICAL PRODUCTS AS COMPARED TO ESTIMATED SPECTRA AND SIGNIFICANT WAVE HEIGHTS IN TERMS OF SAMPLING VARIABILITY

The SOWM spectra specified by the operational version have been compared with estimated spectra during the development of the model.[3,86] Because the wind fields have been improved and because the present SOWM differs from the models described above in some of its details (as described at the end of the Propagate section) these comparisons cannot be used to evaluate its present accuracy.[71,87]

The statistical procedures that have just been illustrated can be applied to the large set of spectral analyses that are available[14,88] so as to provide an extensive set of comparisons for spectra and significant wave heights. The data of Reference 72 are all potentially capable of being interpreted in ways similar to the examples given above.

It is possible to make a preliminary analysis of 15 comparisons based on plots of spectra given in Reference 70 as graphed in Figure 59. The times for the data

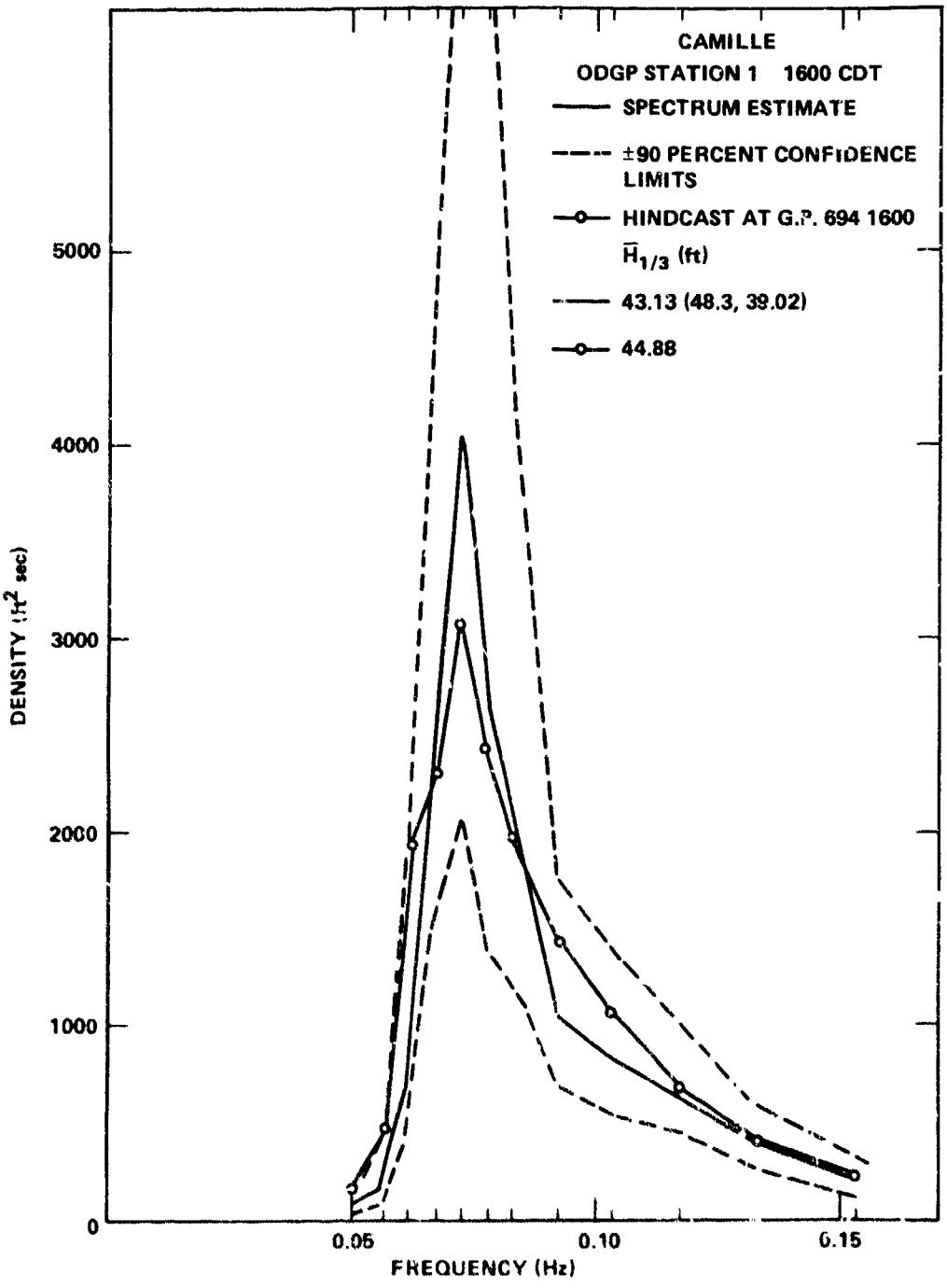

Figure 57 - Wave Spectrum Verification for Hurricane Camille (From Reference 51)

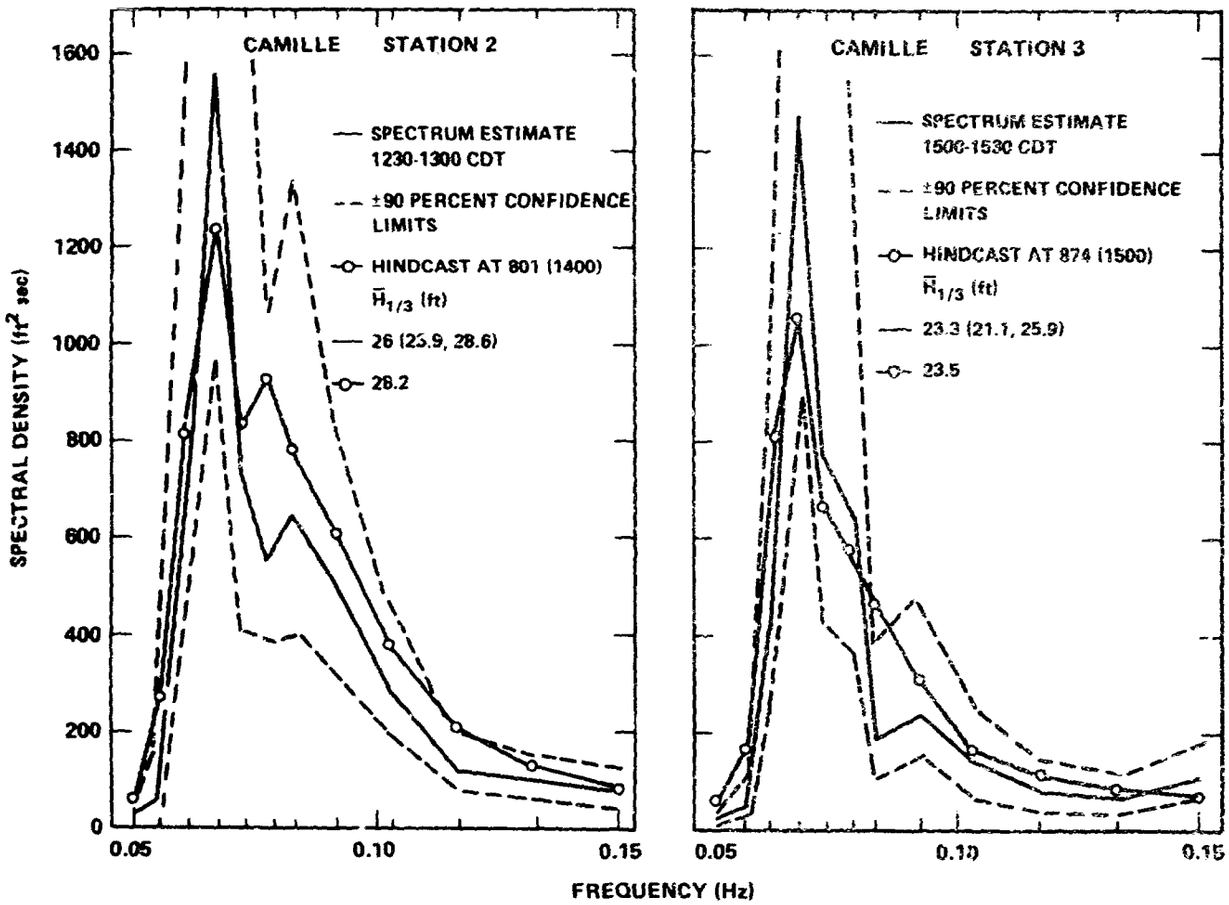

Figure 58 - Wave Spectra Verifications for Hurricane Camille
(From Reference 51)

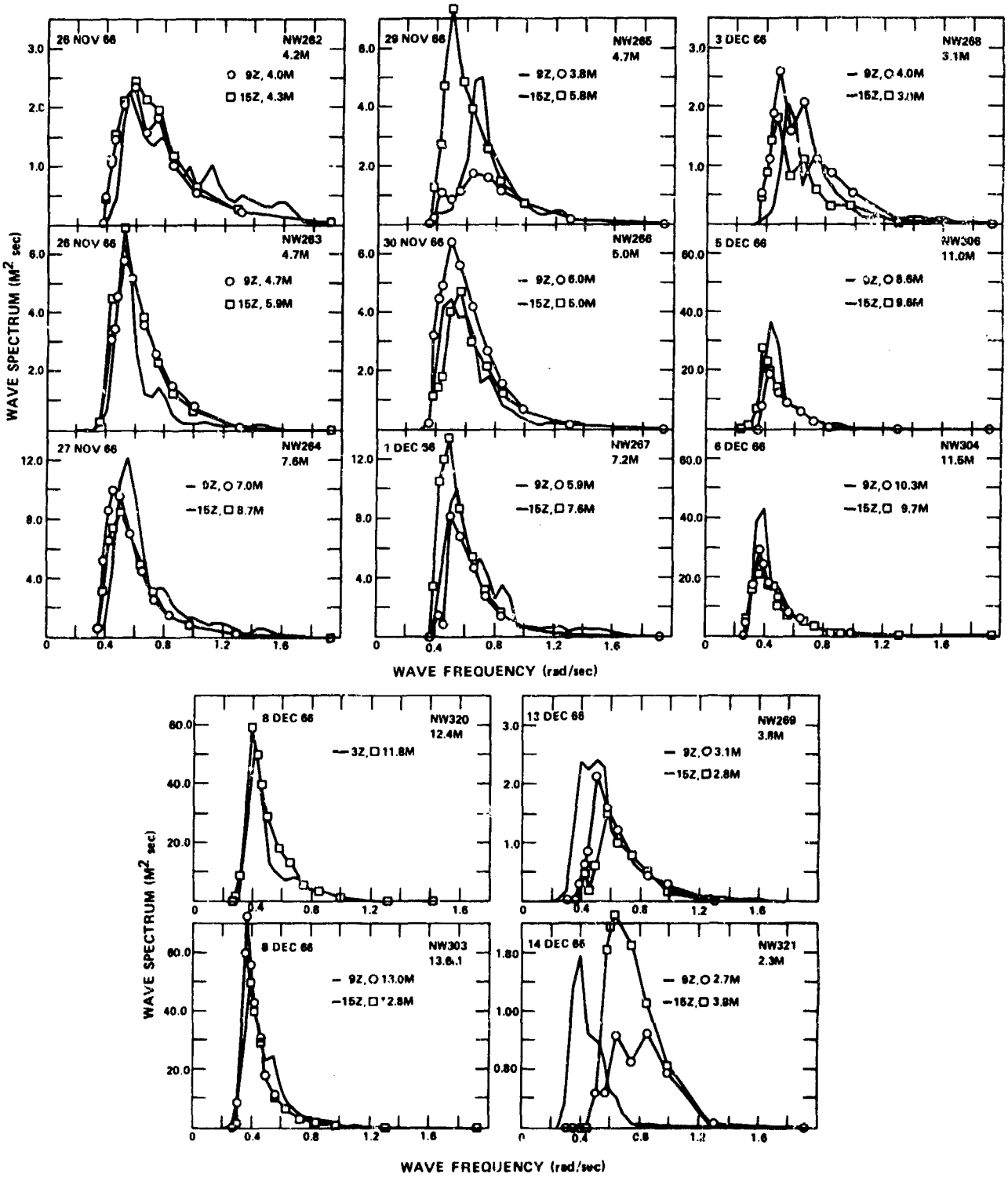

Figure 59 - Comparison of Station India and Grid Point 128 Point Spectra for 25 November to 14 December 1966 Storm
(From Reference 70)

increase reading from top to bottom and then from left to right so that the three plots in the left hand column correspond to 25, 26, 27 November 1966, and so on. Each date (except 8 December 1966) shows two SOWM spectra connected by circles and squares for 09z and 15z and an estimated spectrum, based on data tabulated in Reference 88 for 12z along with the significant wave heights corresponding to each spectrum.

The SOWM spectra are not synoptic with the estimated spectra. This immediately introduces an additional problem especially in view of the results graphed in Figure 54. For comparison with the estimated spectra, the SOWM spectra at the synoptic time need not necessarily be the one obtained by a linear interpolation of the two SOWM products, one 3 hours before and one 3 hours after the time of the estimated spectra.

Similarly, interpolating the heights (which is the equivalent of connecting the points in Figure 13 by straight lines) implies a spectrum that would not be obtained by interpolating the spectra linearly in Figure 59.

The vertical axes on these spectra are in units of meters^2 seconds and the horizontal axes are in radians seconds^{-1}. The scale on the first one is from 0 to 3; for the second, it is from 0 to 6; and then, ordered in time, the scales are 0 to 12, 0 to 6, 0 to 6, 0 to 12, 0 to 3, 0 to 60, 0 to 60, 0 to 60, 0 to 60, 0 in 3, and 0 to 1.8. In contrast to Figure 53, where all scales are the same and the spectra grow and shrink, the scales in Figure 59 grow and shrink and the spectra all look somewhat the same. In fact, if the spectra for NW 320 on 8 December and NW 321 on 14 December were plotted on the same graph, the peak of the first would be 33 times higher than the peak of the second, and the area under the first spectrum would be 29 times the area under the second.

Table 14 is an attempt to score these 13 cases in a way similar to those done above. For each day except 8 December three times are shown. The SOWM predictions are for 09z and 15z. The significant height estimates and confidence intervals are for 12z. The SOWM height predictions have been interpolated linearly to 12z and tabulated in parentheses. Each prediction falls in one of four possible columns relative to the estimated wave height and its upper and lower 90 percent confidence interval. If it is less than the lower or greater than the upper the prediction does not verify. Of the 37 possibilities, 17 verify in this sense. For the 13 days involved, at least one of three verified 11 times. The interpolated height verified six out of 11 times. Were the SOWM rerun for interesting synoptic situations such

TABLE 14 - A COMPARISON OF SPECTRAL OCEAN WAVE MODEL SIGNIFICANT WAVE HEIGHTS AND SPECTRAL WITH WAVES AT STATION INDIA DURING PART OF NOVEMBER AND DECEMBER 1966

(Heights in Meters)

Date 1966		V	Verify	Pred.	Lower	Pred.	Est.	Pred.	Upper	Pred.	Range	6-Hour Change	NW	ΔH	P	HFT*
25 Nov	09		Y			4.00										
	12	3	Y		3.9	4.15	4.2		4.5		0.6	+0.3	252	-0.05	Y	L
	15		Y					4.3								
26 Nov	09		Y			4.70										
	12	6	N		4.2		4.7		5.2	(5.3)	4.0	+1.2	253	+0.60	Y	H
	15		N							5.9						
27 Nov	09		Y			7.00										
	12	12	N	(6.85)	6.9		7.6		8.3		1.4	-0.3	257	-0.75	N	C
	15		N	6.70												
29 Nov	09		N	3.80												
	12	6	Y		4.3		4.7	(4.8)	5.2		0.9	+2.0	255	+0.10	N	C
	15		N							5.8						
30 Nov	09		N							6.0						
	12	6	Y		4.6		5.0	(5.5)	5.6		1.0	-1.0	256	+0.50	Y	C
	15		Y					5.0								
01 Dec	09		N	5.90												
	12	12	Y		6.6	(6.75)	7.2		7.9		1.3	+1.7	257	-0.45	Y	C
	15		Y					7.6								
03 Dec	09		N							4.0						
	12	3	N		2.9		3.1		3.4	(3.5)	0.5	-1.0	258	+0.40	Y	C
	15		Y			3.00										

*See text for interpretation of P and HFT.

TABLE 14 (Continued)

Date 1966		V	Verify	Pred.	Lower	Pred.	Est.	Pred.	Upper	Pred.	Range	6-Hour Change	NW	Δh	P	HFT*
05 Dec	09		N	8.6												
	12	60.0	N	(9.1)	9.3		11.0		12.4		3.1	+1.0	305	-1.90	Y	C
	15		Y			9.6										
06 Dec	09		Y			10.3										
	12	60.0	N	(10.00)	10.2		11.5		13.0		2.8	-0.6	304	-1.50	Y	C
	15		N	9.7												
08 Dec	03	60.0	Y		11.1	11.8	12.4		13.9		2.8	X	320	-0.60	Y	C
08 Dec	09		Y			13.0										
	12	60.0	Y		12.2	(12.8)	13.6		15.1		2.9	-0.4	303	-0.80	Y	C
	15		Y			12.6										
13 Dec	09		N	3.1												
	12	3.0	N	(2.85)	3.4		3.8		4.1		0.7	-0.5	259	-0.95	N	C
	15		N	2.6												
14 Dec	09		N							2.7						
	12	1.8	N		2.0		2.3		2.5	(3.15)	0.5	+0.9	321	+0.85	?	?
	15		N							3.6						

Total Y (Yes) = 17

Total N (No) = 20

Bias = -0.35 meter

RMS = 0.88 meter

Number 1 of 3 (or more) correct = 11 out of 13

Number interpolated correct = 6 out of 11

*See text for interpretation of P and HFT.

as this one, the question arises as to how often the SOWM wave heights would verify for the results of that time step that produced the 12z values.

An alternate way of scoring is to compute the difference between the interpolated predicted height and the estimated height as tabulated in the ΔH column. The bias for this kind of verification is 0.35 meter and the root mean square value is 0.88 meter. Clearly, these quantities are misleading because they contain the effect of sampling variability in the estimated wave heights that cannot be predicted and that therefore should not be used in assessing the errors of the SOWM.

The last two columns attempt a qualitative judgement as to how well the spectra verify. The P refers to the peaks of the spectra and the HFT refers to the high frequency tail. A Y (Yes) for the peak means that a typical 90 percent confidence interval is judged to enclose the SOWM peaks, an N means it would not or that the frequency content as low frequencies is not correct. The asterisk on the N for NW 29 means that the 12z SOWM spectrum could easily have verified if it were available. The question mark for 14 December is there to point out that, if this spectrum were drawn to the same scale as the set of three for 8 December, it would appear to verify quite well. The SOWM has predicted that the spectral values are all very low compared to those earlier in the period for this particular time. The HFT column (for High Frequency Tail) shows whether the SOWM is too low (L) too high (H) or close (C) to the estimated spectrum for high frequencies compared to typical confidence intervals for the higher frequencies. The overall fit at high frequencies is good except for the first two spectra and the last spectrum. More quantitative results would require a table similar to Table 13.

THE SEPARATION OF SPECTRAL OCEAN WAVE MODEL ERRORS FROM SAMPLING VARIABILITY EFFECTS

The sampling variability of an ocean wave record produces deviations from the spectra and wave heights predicted by the SOWM. There is an irreducible minimum below which the differences between the SOWM predictions and the spectra and wave heights obtained from wave records cannot be reduced. Let H_S be the SOWM significant height; H_E, the significant height estimated from a wave record; and H_T be the "true" value of the significant height. Then

$$\frac{1}{N} \Sigma \, (H_S - H_E)^2 = \frac{1}{N} \Sigma \, ((H_S - H_T) - (H_E - H_T))^2$$

$$= \frac{1}{N} \Sigma \, (H_S - H_T)^2 - 2 \, \frac{1}{N} \Sigma \, (H_S - H_T) \, (H_E - H_T) + \frac{1}{N} \Sigma \, (H_E - H_T)^2 \qquad (93)$$

The lefthand side of Equation (93) is the usually computed quantity. Various values for it have been given in preceeding sections. The first term in the right-hand side is the "true" error of the SOWM. The second term is more or less liable to be nearly zero because sampling variability will make the second term in the product alternately positive and negative so that the sum will tend to zero.

The last term can be estimated. The estimate of the significant wave height is an estimate of the "true" value. The variance of the wave record has an approximate Chi Square distribution with a TDF given by Equation (79). The Chi Square variable, u, for a large number of degrees of freedom is such that $\sqrt{2u} - \sqrt{2k-1}$ (where k is degrees of freedom) is a unit variance, zero mean normal variable. The 90 percent range for the significant wave height, given the upper 95 percent value and the wave height, will be normally distributed because of this relationship. The standard deviations of the estimates of the significant wave height can be estimated from

$$SD = \frac{1}{1.65} (H_U - H_E) \tag{94}$$

Thus, from Table 15, the lefthand side of Equation (93) and the last term on the righthand side can be found. This yields

$$0.88 = \frac{1}{N} \Sigma (H_S - H_T)^2 + 0.31 \tag{95}$$

For the 13 values given in the table, where the SOWM height is the interpolated value for all but one entry, it then follows that

$$\frac{1}{N} \Sigma (H_S - H_T)^2 = 0.59 \text{ (meters)}^2 \tag{96}$$

and that

$$H_S = H_T \pm 0.75 \text{ meters} \tag{97}$$

About 35 percent of the variability of the waves when comparing the SOWM to wave height is explained, in terms of variance, by the sampling variability of wave measurements, or estimates, and the remaining difference of 65 percent is attributable to errors of the SOWM for this example.

TABLE 15 - ERROR BUDGET FOR SPECTRAL OCEAN WAVE MODEL SIGNIFICANT WAVE HEIGHTS DURING PART OF NOVEMBER AND DECEMBER 1966

Date 1966	$H_{1/3}$ SOWM	$H_{1/3}$ Est.	$H_{1/3}$ Upper	$H_U - H_E$	TDF	SD	$H_S - H_E$
25 Nov	4.15	4.20	4.50	0.30	278	0.18	0.05
26 Nov	5.30	4.70	5.20	0.50	130	0.30	0.60
27 Nov	6.85	7.60	8.30	0.70	171	0.42	0.75
29 Nov	4.80	4.70	5.20	0.50	130	0.30	0.10
30 Nov	5.50	5.00	5.60	0.60	103	0.36	0.50
01 Dec	6.75	7.20	7.90	0.70	154	0.42	0.45
03 Dec	3.50	3.10	3.40	0.30	155	0.18	0.40
03 Dec	9.10	11.00	12.40	1.40	92	0.85	1.90
06 Dec	10.00	11.50	13.00	1.50	88	0.91	1.50
08 Dec	11.80	12.80	13.90	1.50	102	0.91	0.60
08 Dec	12.80	13.60	15.10	1.50	66	0.91	0.80
13 Dec	2.85	3.80	4.10	0.30	230	0.18	0.95
14 Dec	3.15	2.30	2.50	0.20	191	0.12	0.85

As computed from the table

$\frac{1}{N} \Sigma (H_S - H_E)^2 = 0.88$ and $\frac{1}{N} \Sigma (H_E - H_T)^2 = 0.31$, Therefore $\frac{1}{N} \Sigma (H_S - H_T)^2 = 0.57$.

This example must be worked out for a much larger sample, preferably for actual instead of interpolated SOWM heights before stable values can be found. However, the example, at least, shows that a part of the differences between the SOWM and the estimated wave heights is explainable in terms of sampling variability.

THE VERIFICATION OF SWELL

Little data are available to verify the swell heights and the swell spectra of the SOWM, plus usually a local sea, in subtropical highs, the trade wind areas and, for example, off the coasts of California and North Africa. One study of the SOWM spectra near Trinidad showed that the swell in the model behaved realistically and yielded graphs similar to those obtained from actual wave data[89,90] such that the distance to and the general location of the generation area can be found. Also, for the area studied, most of the spectral variance of the waves locally was imported as swell and less than half was produced by the local wind.

There is concern about the angular granularity of the SOWM and its effects on swell. Because the climatology has already been produced with the current model any corrections for errors introduced in this way will have to be after the fact.

THE JONSWAP SPECTRA

The spectrum of a fetch-limited sea would be like one of the curves in Figure 5 according to the SOWM. The family of fetch-limited spectra is quite variable when the controlling form of a fully developed sea as an upper bound, which varies considerably as a function of wind speed, is considered. The variation of the wind over a fetch also complicates the interpretation of fetch effects.

In this context, objections to the JONSWAP spectral parameterization procedures have been raised.[65] A major point that was made was that scaling spectra according to f/f_m, where f_m is the spectral peak, biases the data and the wave model. If a spectrum is actually fairly smooth for three or so bands across its peak, picking that spectral estimate that is the highest practically always guarantees that it will be an overestimate. Further use of such a model is then bound to yield misleading results.

The figures that compare model spectra with estimated spectra in preceeding sections often show an estimated peak that exceeds the model peak. Had other wave records been available from nearby locations within the scale of the model, the peaks in the spectral estimate would shift back and forth over several spectral bands and each estimate would have the appearance of being more peaked than the

model spectrum. This type of variability ought to be treated in the applications of the model to particular problems and not built into the model.

The phenomenon of overshoot and the nonlinear transfer function used in some wave models can both be data processing artifacts instead of actual physical phenomenon. Further research in these problem areas is needed.

THE VERIFICATION OF FREQUENCY DIRECTION SPECTRA

No data are available for the routine verification of spectra such as those given in Tables 5 and 6. There have been data obtained during the past 20 years of a scientific nature that could be used for verification purposes, but this has not been done.

If the frequency-direction spectra were badly in error, the frequency spectra and the hour-by-hour wave height variations that have been illustrated would not have verified well. The general accuracy of the frequency-direction spectra can be inferred by default in this way. Nevertheless, a verification effort for the SOWM spectra is needed, especially for the purpose of the development of improved forecast models.

AN ASSESSMENT OF THE SPECTRAL OCEAN WAVE MODEL WAVE CLIMATOLOGY

The SOWM wave climatology differs from all previous open ocean compilations of wave data that have been used to understand the wave environment. These previous compilations were based on wave heights and periods as reported by transient ships by means of the World Meteorological Organization's (WMO) code.[91]

These ship reports have become increasingly questioned. A few years ago the code was changed, and, prior to that time, waves with heights of 5 meters and 10 meters were overreported compared to their actual frequency of occurrence because of peculiarities of the code. For the same reason, waves over 10 meters were not sufficiently reported. Recent studies indicate both a bias and a large scatter when ship reports are compared to wave measurements made by a national data buoy.[9]

A single period, of any value, is hardly a valid description of a wave system. There are many different kinds of "periods" that can be computed from a frequency spectrum such as the "period" associated with a spectral peak and at least two different "periods" that can be computed from the spectrum. Although various ways to convert ship reports of wave heights and wave periods to spectra have been pro-

posed, none of them can possibly preserve the information in an actual wave spectrum or in the spectra specified by the SOWM.

Ship reports of wave heights and periods also include a provision for reporting both sea and swell. The instructions in the WMO code are hardly adequate for differentiating between sea and swell, and the reports for the swell group usually show that the observers cannot properly separate sea and swell.

Also, ship reports are concentrated on the international shipping lanes so that vast areas of the oceans are rarely visited by a ship. The current available ship report statistics for some of the ocean areas may be unreliable because of poor sample size. For the SOWM, these same ships are used to determine the meteorological fields to be used to compute the waves. These meteorological fields can, in general, be interpolated and extrapolated into areas with no data more accurately than can the corresponding wave fields. Thus by its very nature, the SOWM provides a uniform coverage. There are, however, probably some areas for which the SOWM may be biased because of the lack of ship reports to define the wind field.

A comparison of SOWM height distributions with a conventional climatology shows that the SOWM calls for a higher incidence of high waves.[70] This difference appears to be both realistic and correct. The Institute of Oceanographic Sciences has published numerous compilations of wave statistics based on measurements made by the Tucker shipborne wave recorder.[92] A comparison of the SOWM statistics with these data could provide a calibration point for the SOWM climatology.

The available statistics on comparisons of the SOWM with wave data of various kinds all suggest a negligible bias for the SOWM of at most a few tenths of a meter. The root mean square differences between the SOWM and wave height measurements have ranged from 1.20 meter through 1.00 meter and as low as 0.80 meter. A part of this root mean square difference is the result of sampling variability and so the errors of the SOWM for middle latitudes may actually be as low as 0.7 to 0.8 meter.

The limited amount of data that have been used to verify the SOWM frequency spectra show that the SOWM tracked the variations in the estimated spectra fairly realistically. Much more needs to be done in the area of the verification of frequency spectra, especially in view of the effects of the improved wind fields and the FNOC modification, which was described at the end of the section on Propagate, on the performance of the model. Ways to verify frequency spectra have been illustrated. The data must be interpreted with great care.

Despite concern at the beginning with the accuracy of the winds that are used in the SOWM, the available data do not seem to show that rather large root mean square errors in the winds (even after correction) have generated large root mean square errors in the waves. From about 1976 onward, it was not necessary to correct the FNOC winds in the way that was described in the section on the verification of the winds. A possible explanation may be that the errors in the winds have oscillated above and below the correct values both in space and time and that the integrating effect of the SOWM calculations on the input winds has yielded output waves nearly in accord with reality.

Two last precautions are required before ending this analysis. They are concerned with the verification of swell and with the variability of the waves that has been observed over both small spatial distances and short time intervals. Both of these features require further scientific study and analyses; and both have been discussed in various sections of this paper. Care should be taken that the wave climatology have built in factors of protection against errors that may be introduced into it because of these effects.

ACKNOWLEDGMENT

The contents of this report do not necessarily reflect official Navy or DTNSRDC policy.

The responsibility for all statements of fact rests with the author.

REFERENCES

1. Pierson, W.J., L.J. Tick, and L. Baer, "Computer-based Procedures for Preparing Global Wave Forecasts and Wind Field Analyses Capable of Using Wave Data Obtained by a Spacecraft," Proceedings of the Sixth Naval Hydrodynamics Symposium Publication, ACR-136, Office of Naval Research, Department of the Navy, Washington, D.C. (1966)

2. Salfi, R.E., "Operational Computer-Based Spectral Wave Specification and Forecasting Models," Report for SPOC/NESS/NOAA, CUNY Inst. of Mar. and Atmos. Sci., City Coll. of the City Univ. of N.Y. (1974) (Available from Spacecraft Oceanography Group, National Oceanic and Atmospheric Administration, Washington, D.C.).

3. Lazanoff, S.M. and N. Stevenson, "An Evaluation of a Hemispheric Operational Wave Spectral Model," Tech Note 75-3, Fleet Numerical Weather Center, Monterey, Calif. (1975)

4. Pierson, W.J., G. Neumann, and R.W. James, "Practical Methods for Observing and Forecasting Ocean Waves by Means of Wave Spectra and Statistics," H.O. Publication 603, U.S. Navy Hydrographic Office, Washington, D.C. (1955)

5. Baer, L., "An Experiment in Numerical Forecasting of Deep Water Ocean Waves," LMSC-801296, Lockheed Missile and Space Co., Sunnyvale, Calif. (1962) (Also Ph.D. Thesis, N.Y. Univ.).

6. Gelchi, R. and P. Chavy, "Seven Years of Routine Numerical Wave Prediction with the D.S.A. 5 Model," in Favre, A. and K. Hasselmann, Editors, Turbulent Fluxes Through the Sea Surface, Wave Dynamics and Prediction, Plenum Press, 677 pp. (1978)

7. Lazanoff, S.M. and N.M. Stevenson, "A Twenty Year Northern Hemisphere Wave Climatology," in Favre, A. and K. Hasselmann (1978): Editors. Turbulent Fluxes Through the Sea Surface, Wave Dynamics and Prediction, Plenum Press, 677 pp. (1978)

8. Barnhart, C.L. (Editor), "Thorndike-Barnhart Comprehensive Desk Dictionary, Country Life Press. (1951)

9. Anonymous, "Forecast Impact Study: To Study the Effects of Quality Environmental Data on Numerical Analysis and Forecast Model," Final Technical Report Task 5 Significant Wave Heights Comparisons, Ocean Data Systems Inc., Report Prepared for Jet Propulsion Laboratory. (1980)

10. Miles, J.W., Comments on Reference 1, page 529 of ACR-136. (1966)

11. Tukey, J.W., "The Sampling Theory of Power Spectrum Estimates." Symposium on Application of Autocorrelation Analysis in Physical Problems. Woods Hole, June 13, 1949, NAVEXOS O-735, Office of Naval Research (1949)

12. Pierson, W.J., and W. Marks, "The Power Spectrum Analysis of Ocean-Wave Records." Trans. Amer. Geophys. Un., Vol. 33, No. 6, pp. 834-844. (1952)

13. Tucker, M.J., "A Shipborne Wave Recorder." Trans. Inst. Naval Arch., Vol. 98, pp. 236-250 (London). (1956)

14. Moskowitz, L., W.J. Pierson, and E. Mehr, "Wave Spectra Estimated From Wave Records Obtained by the OWS Weather Explorer and the OWS Weather Reporter, I, II and III." Prepared for the U.S. Naval Oceanogr. Office. School of Engineering and Science, New York University. (1962, 1963, 1965)

15. Neumann, G., and W.J. Pierson, "Principles of Physical Oceanography," Prentice-Hall, 545 pp. (1966)

16. Thomasell, A. and J.G. Welsh, "Studies of the Specification of Surface Winds over the Ocean." Travelers Research Center, Prepared for U.S. Naval Oceanographic Office. (1963)

17. Cardone, V.J., "Specification of the Wind Field Distribution in the Marine Boundary Layer for Wave Forecasting." Rep. JR-69-1, Geophysics Science Lab., New York Univ. (1969)

18. Kinsman, B., "Wind Waves, Their Generation and Propagation on the Ocean Surface." Prentice-Hall. (1965)

19. Cote, L.J., et al, "The Directional Spectrum of a Wind Generated Sea as Determined from Data Obtained by the Stereo Wave Observation Project." Meteor Pap., Vol. 2, No. 6, 88 pp., New York Univ. Press. (1960)

20. Longuet-Higgins, M.S., "The Effects of Non-Linearities on Statistical Distributions in the Theory of Sea Waves." J. Fluid Mech., 17(3), pp. 450-480. (1963)

21. Tayfun, M.A., "Narrow Band Nonlinear Sea Waves." J. Geophys. Res., Vol. 85, No. C3, pp. 1548-1552. (1980)

22. Kuo, Y.Y., H. Mitsuyasu and A. Masuda, "Experimental Study on the Phase Velocity of Wind Waves." Part I, Laboratory Wind Waves Res. Inst. Appl. Mech., Kyushu Univ., Vol. XXVII, No. 83, pp. 1-19. Part 2, Ocean Waves, Ibid, No. 84, pp. 47-66. (1979)

23. Pierson, W.J. and L. Moskowitz, "A Proposed Spectral Form for Fully Developed Wind Seas Based on the Similarity Theory of S.A. Kitaigorodskii." J. Geophys. Res., Vol. 69, No. 24, pp. 5181-5190. (1964)

24. Moskowitz, L., "Estimates of the Power Spectrums for Fully Developed Seas for Wind Speeds of 20 to 40 Knots." J. Geophys. Res., Vol. 69, No. 24, pp. 5161-5179. (1964)

25. Pierson, W.J., "The Interpretation of Wave Spectrums in Terms of the Wind Profile Instead of the Wind Measured at a Constant Height." J. Geophys. Res., Vol. 69, No. 24, pp. 5191-5203. (1964)

26. Stacy, R.A., "Spectral Analyses of High Frequency Gravity Waves Generated by a Hurricane." Ph.D. Thesis, School of Engineering and Science, New York University. (1974)

27. Mitsuyasu, H. and T. Honda, "The High Frequency Spectrum of Wind Generated Waves." J. Oceanograph. Soc. Japan, Vol. 30, No. 4, pp. 2942. (1974)

28. Phillips, O.M., "On the Generation of Waves by Turbulent Wind." J. Fluid Mech., Vol. 2, No. 5, pp. 417-445. (1957)

29. Miles, J.W., "On the Generation of Surface Waves by Shear Flow." Part 1, J. Fluid Mech., Vol. 3, pp. 185-204, (1957). Part 2, J. Fluid Mech., Vol. 6, pp. 568-582, (1959). Part 3, J. Fluid Mech., Vol. 6, pp. 583-598, (1959). Part 4, J. Fluid Mech., Vol. 13, pp. 433-448, (1962).

30. Phillips, O.M., "The Dynamics of the Upper Ocean." Cambridge University Press, 261 pp. (1966)

31. Inoue, T., "On the Growth of the Spectrum of a Wind Generated Sea According to a Modified Miles-Phillip's Mechanism and its Application to Wave Forecasting." TR-67-5, Geophysical Sciences Laboratory Report, New York University, School of Engineering and Science. (1967)

32. Hasselmann, K., "On the Nonlinear Energy Transfer in a Gravity Wave Spectrum." Part 1, J. Fluid Mech. 12: 481-500. Part 2, Ibid 5: 273-281, (1963), Part 3, Ibid 15: 385-398, (1962).

33. Hasselmann, K., Comments on Reference 1, page 530 of ACR-136. (1966)

34. Barber, N.F. and F. Ursell, "The Generation and Propagation of Ocean Waves and Swell." Phil. Trans. Roy. Soc. A., Vol. 240, pp. 527-560. (1948)

35. Snodgrass, F.E., et al., "Propagation of Ocean Swell Across the Pacific," Phil. Trans. Roy. Soc., Ser A, 259, pp. 431-497. (1966)

36. Ewing, G.C., (Editor) "Oceanography from Space," Reference No. 65-10, Woods Hole Oceanographic Institution. (1965)

37. National Aeronautics and Space Administration, "Skylab EREP Investigations Summary," NASA SP-399. (1978)

38. Science, Vol. 204, No. 4400, pp. 1405-1423. Eight papers on SEASAT by various authors. (1979)

39. Barrick, D.E., J. Wilkerson, et al., (Editors) "SEASAT Gulf of Alaska Workshop II Report," NASA Jet Propulsion Laboratory Rept. 622-107. (1980)

40. Businger, J., R. Stewart, et al., (Editors) "SEASAT-Jasin Workshop," 18-26 March 1980, Jet Propulsion Laboratory.

41. "Journal of Geophysical Research," Vol. 84, No. B8, devoted to articles describing the scientific results of GEOS-3.

42. Queffeulou, P., A. Braun and C. Brossier, "A Comparison of SEASAT Derived Wave Height with Surface Data," in Oceanography from Space, J.F.R Gower (Editor) Plenum Press. (1981)*

43. Beal, R.C., "Spaceborne Imaging Radar Monitoring of Ocean Waves," Science Vol. 208, No. 4450, pp. 1373-1375. (1980)

44. Parsons, C.L., "GEOS-3 Wave Height Measurements: An Assessment During High Sea State Conditions in the North Atlantic." J. Geophys. Res., Vol. 84, No. B8, pp. 4011-4020. (1979)

*The figures used here do not appear in the reference cited. They were in the original draft, and copies were provided by Dr. Queffeulou.

45. Pierson, W.J. and R.E. Salfi, "A Brief Summary of Verification Results for the Spectral Ocean Wave Model (SOWM) by Means of Wave Height Measurements Obtained by GEOS-3." J. Geophys. Res., Vol. 84, No. B8, pp. 4029-4040. (1979)

46. Wellick, R.E., "Atmospheric Prediction Model Survey." Final Report for JFL, Ocean Data Systems, Inc. (1976)

47. Gunther, H., W. Rosenthal, and K. Richter, "Application of the Parametrical Surface Wave Prediction Model to Rapidly Varying Wind Fields During JONSWAP 1973." J. Geophys. Res., Vol. 84, No. C8, pp. 4855-4865. (1979)

48. Golding, B.W., "A Depth Dependent Wave Model for Operational Forecasting," in Favre, A. and K. Hasselmann (1978) Editors. Turbulent Fluxes Through the Sea Surface, Wave Dynamics and Prediction, Plenum Press, pp. 593-606. (1978)

49. Weare, T.J. and B.A. Worthington, "A Numerical Model Hindcast of Severe Wave Conditions for the North Sea," in Favre, A. and K. Hasselmann (1978) Editors. Turbulent Fluxes Through the Sea Surface, Wave Dynamics and Prediction, Plenum Press, pp. 617-628. (1978)

50. Cavaleri, L. and P. Malanotte Rizzoli, "A Wind-Waves Prediction Model in the Adriatic Sea," in Favre, A. and K. Hasselmann (1978) Editors. Turbulent Fluxes Through the Sea Surface, Wave Dynamics and Prediction, Plenum Press, pp. 629-646. (1978)

51. Cardone, V.J., W.J. Pierson, and E.G. Ward, "Hindcasting the Directional Spectra of Hurricane-Generated Waves." Journal of Petroleum Technology, pp. 385-394. (1976)

52. Adamo, L.C., L. Baer, and J.P. Hosmer, "Icosahedral-gnomonic Projection and Grid of the World Ocean for Wave Studies." J. Geophys. Res., Vol. 73, No. 16, pp. 5125-5132. (1968)

53. Salfi, R.E. and W.J. Pierson, "A Verification Study of Hindcasted Wave Spectra Based on Wave Data from Weather Ships J and K and Wind Data Obtained for December 1973 and January 1974 during Skylab." Report for SPOC/NESS/NOAA, CUNY Inst. of Mar. and Atmos. Sci., City Coll. of the City Univ. of N.Y., (1977) (Available from Spacecraft Oceanography Group, National Oceanic and Atmospheric Administration, Washington, D.C.)

54. Forristall, G.Z., "On the Statistical Distribution of Wave Heights in a Storm." J. Geophys. Res., Vol. 83, pp. 2353-2358. (1978)

55. Longuet-Higgins, M.S., "On the Distribution of the Heights of Sea Waves; Some Effects of Nonlinearity and Finite Band Widths." J. Geophys. Res., Vol. 85, No. C3, pp. 1519-1523. (1980)

56. Kitaigorodskii, S.A., "Application of the Theory of Similarity to the Analysis of Wind Generated Wave Motion as a Stochastic Process," Izv. Akad. Nauk. SSSR Ser. Geophys., Vol. 1, pp. 105-117, (1961) (English Edition pp. 73-80).

57. Pierson, W.J., "Comments on a paper by O.M. Phillips in Ocean Wave Spectra, proceedings of a Conference, Prentice-Hall, Englewood Cliffs, pp. 179-190. (1963)

58. Barnett, T.P., "On the Generation, Dissipation and Prediction of Ocean Wind Waves," J. Geophys. Res., Vol. 73, pp. 513-529. (1968)

59. Snyder, R.L. and C.S. Cox, "A Field Study of the Wind Generation of Ocean Waves." Institute of Marine Science, U. of Miami and Scripps Institution of Oceanography, 40 pp. + figures and appendices. (1965)

60. Darbyshire, J., "An Investigation of Storm Waves in the North Atlantic Ocean." Proc. Roy. Soc. A, Vol. 230, No. 1183, pp. 560-569. (1955)

61. Darbyshire, J., "A Further Investigation of Wind Generated Waves," Deut Hydrogr. Zeit Band 12 Heft 1, pp. 1-13. (1959)

62. Comments by O.M. Phillips at a wave forecasting conference.

63. Lamb, H., "Hydrodynamics," 6th Edition, Dover Publications, 738 pp. (1945)

64. Hasselmann, K., D.B. Ross, P. Muller and W. Sell, "A Parametric Wave Prediction Model." J. Phys. Oceanogr., Vol. 6, No. 2, pp. 200-228. (1976)

65. Pierson, W.J., Comments on "A Parametric Wave Prediction Model." J. Phys. Oceanogr., Vol. 7, No. 1, pp. 127-134. (1977)

66. Hasselmann, K., D.B. Ross, P. Muller and W. Sell, Reply, J. Phys. Oceanogr., Vol. 7, No. 1, pp. 134-137. (1977)

67. Salfi, R.E., "Spectral Ocean Wave Model Data Base Management System, Technical Description and Computer Program Documentation," Tech. Rept. Prepared in the Department of Energy, Contract DE-AC05-78ET20488, CUNY Inst. Marine and Atmos. Sci., The City College. (1980) (Also available from DTNSRDC.)

68. Lazanoff, S.M. and J. Kaitala, Data and information provided through a personal communication.

69. Cummins, W.E. and S.L. Bales, "Extreme Value and Rare Occurence Wave Statistics for Northern Hemispheric Shipping Lanes." Proceedings Fifth SNAME Ship Technology and Research (STAR) Symposium, Coronado, (June). (1980)

70. Bales, S.L., W.E. Cummins and E.N. Comstock, "Potential Impact of Twenty Years Hindcast Wind and Wave Climatology on Ship Design," Paper presented at 17 Sept. 1980 meeting of the Chesapeake Section of the Society of Naval Architects and Marine Engineers. (1980)

71. Dooley, A.L., "The Use of Geodynamic Experimental Ocean Satellite (GEOS-3) Measurements of Significant Wave Height in a Verification Study of the Spectral Ocean Wave Model (SOWM) at Fleet Numerical Weather Central." Ph.D. Thesis, New York University, 203 pp. (1978)

72. Chen, H.T., H.H. Chen and D. Hoffman, "The Implementation of the 20-Year Hindcast Wave Data in the Design and Operation of Marine Structures." OTC paper 3644, 11th annual OTC conference, April 30-May 3, 1979, 9 pp. (1979)

73. Greenwood, J.A., A. Nathan, et al., "Radar Altimetry from a Spacecraft and its Potential Applications to Geodesy." Remote Sensing of Environ. Vol. 1, No. 1, pp. 59-70. (1969).

74. Greenwood, J.A., A. Nathan, et al., "Oceanographic Applications of Radar Altimetry for a Spacecraft." Remote Sensing of Environ. Vol. 1, No. 1, pp. 71-80. (1969)

75. Fedor, S.L., T. Godbey, J.F.R. Gover, R. Guptill, G. Hayne, C. Eufenach, and E.J. Walsh, "Satellite Altimeter Measurements of Sea State-An Algorithm Comparison." J. Geophys. Res., Vol. 84, No. B8, pp. 3991-4002. (1978)

76. Walsh, E.J., "Extraction of Ocean Wave Height and Dominant Wavelength from GEOS-3 Altimeter Data." J. Geophys. Res., Vol. 84, No. B8, pp. 4003-4010. (1979)

77. Priester, R.W. and L.S. Miller, "Estimation of Significant Wave Height and Wave Height Density Function Using Satellite Altimeter Data." J. Geophys. Res., Vol. 84, No. B8, pp. 4021-4026. (1979)

78. Pierson, W.J., and R.E. Salfi, "Verification Results for the Spectral Ocean Wave Model (SOWM) by Means of Significant Wave Height Measurements Made by the GEOS-3 Spacecraft." NASA Contract Rep. NCR-62089, 234 pp., (1978) (Available from National Technical Information Service, Springfield, Va.)

79. Rice, S.O., "Mathematical Analysis of Random Noise." Bell System Technical Journal, Vol. 23, pp. 282-332 (1944) and Ibid, Vol. 24, pp. 46-156. (1945)

80. Blackman, R.B. and J.W. Tukey, "The Measurement of Power Spectra from the Point of View of Communications Engineering." Bell System Tech. Jour. Jan. and March, Vol. 37. (1958)

81. Mood, A.M., F.A. Graybill and D.C. Boes, "Introduction to the Theory of Statistics," Third Edition, McGraw Hill, 564 pp. (1974)

82. Dalzell, J.F., "The 'Input-Output' Approach to Seakeeping Problems - Review and Prospects; Seakeeping 1953-1973," T and R Symposium S-3, The Society of Naval Architects and Marine Engineers. (1973)

83. Jenkins, G.M. and D.G. Watts, "Spectral Analysis and its Applications." Holden-Day, 525 pp. (1968)

84. Pierson, W.J., "The Theory and Applications of Ocean Wave Measuring Systems at and Below the Sea Surface, on the Land, From Aircraft and From Spacecraft." NASA Contractor Report NASA CR-2646. (1976)

85. Data provided by J.A. Ewing of the Institute of Oceanographic Sciences.

86. Hayes, J.G., "Operational Wave Forecasting with the Ocean Wave Spectral Model." The Technical Exchange Conference, El Paso, Texas. (1976)

87. Based on a copy of the program for the presently operational version provided by Commander D. Honhart.

88. Hoffman, D. and M. Miles, "Analysis of a Stratified Sample of Ocean Wave Records at Station India." SNAME, Technical and Research Bulletin No. 1-35 (May). (1976)

89. Sylvester, W.B., "A SOWM Swell Verification Study: Extratropical Winter Storm Forcing of the Wave Climate in the East of the Southern Caribbean Chain," Ph.D. Thesis, New York University. (1978)

90. Munk, W.H., Comments in Ocean Wave Spectra, pp. 158-160, Prentice-Hall. (1963)

91. Hogben, N. and F.E. Lumb, "Ocean Wave Statistics." London, Her Majesty's Stationary Office. (1967)

92. Draper, L., "Waves at Dowsing Light Vessel." Institute of Oceanographic Sciences, Report No. 31, December (as just one example). (1976)

INITIAL DISTRIBUTION

Copies	
2	CNO
	1 NOP-952
	1 R. James
1	ASN (RAST)/S. Hawkins
2	NAVMAT
	1 ONT/0724/CAPT Young
	1 JCM-5-106/R. Hall
11	NAVSEA
	1 SEA 03R N. Kobitz
	1 SEA 321 R. Keane
	1 SEA 3213 E. Comstock
	1 SEA 3213 W. Sandberg
	1 SEA 3213 W. Louis
	1 SEA 06R C. Smith
	1 SEA 61R4 H. Demattia
	1 SEA 61433 F. Prout
	1 SEA 61433 O. White
	1 SEA 63R3 F. Romeno
	1 SEA A. Franceschetti
1	ONR 480
2	CNOC
	1 CAPT Hughes
	1 J. Ownbey
2	NOSC
	1 Lib
	1 8143/R. Eastley
2	NUSC
	1 Lib
	1 3711/J. Lee
1	NAEC/Lib
1	NADC/Lib
1	NATC/Lib
4	NSWC
	1 Dahlgren/Lib
	1 K44/R. Carson
	1 White Oak/Lib
	1 G41/W. Walker

Copies	
1	NCSC/Lib
1	CEL/Lib
2	NRL
	1 Lib
	1 L. Moskowitz
2	NORDA
	1 Lib
	1 R. Hollman
3	NAVOCEANO
	1 N00 Lib
	1 3431/O. Von Zweck
	1 3431/D. Smith
3	FNOC
	1 CAPT P. Petit
	1 S. Lazanoff
	1 J. Zuver
3	NOCD/Asheville
1	NEPRF
2	PMTC
	1 Lib
	1 32532/R. Deviolini
1	NAVPGSCOL/Lib
3	USNA
	1 Lib
	1 R. Bhattacharyya
	1 M. McCormick
1	NAVSAFECEN
4	USCG
	1 Lib/5-2
	1 G-MMT/12/W. Cleary
	1 G-DMT-1/54/D. Walden
	1 G-MMT-4/82/P. Cojeen
1	Maritime Administration Div. of Ship Design

Copies

1 NTSB/R. Johnson

12 NOAA
- 1 AMOL D. Russ
- 1 AMOL J. Overland
- 1 NESS P. Deleonibus
- 1 NESS J. Sherman
- 1 NHEML P. Black
- 1 NOS Lib
- 1 NOS H. Frey
- 1 NWS L. Baer
- 1 NWS Lib
- 1 NWS G. Flittner
- 1 EDIS/NEAD J. Bishop
- 1 NDBO K. Steele

4 NASA
- 1 AAEO W.L. Jones
- 1 WALLOPS N. Huang
- 1 WALLOPS R. Stanley
- 1 GODDARD F. Jackson

1 USGS/E. Escowitz

1 JPL/A. Loomis

1 EPA/D. Jones

1 NCC/Lib

1 CERC/Lib

1 WES/Lib

1 ABS/H. Chen

1 APL/O. Conrad

1 MPR Associates/F. Sellars

1 ORI

1 Science Applications Inc./A. Kerwin

1 Rockwell International/L. Liong

1 Boeing Marine Systems/D. Stark

1 Bell Helicopter/P. O'Reilly

Copies

1 Sikorsky Aircraft/F. Camaratta

1 Ocean Routes, Inc./N. Stevenson

2 Exxon Production Research Co.
- 1 K. Lambrakos
- 1 E. Lacour

1 Mobile Research & Development Corp./W. Spring

1 Shell Development Co./E. Ward

1 McDonnel Douglas Corp./F. Dubois

1 Gulf Research & Development Co. O. Oakley

1 Amocco Production Co. Research Center

1 Cities Service Co./K. Schaudt

1 Maritech, Inc./L. Vassilopoulos

1 Designers and Planners, Inc. W. Reuter

1 Hoffman Maritime Consultants D. Hoffman

1 Field Research Lab/R. Stacy

1 Marine Environments Corp. M. Earle

1 Ocean Weather, Inc./V. Cardone

1 Tetra Tech/M. Brandsma

1 Brown and Root, Inc./H. Chen

1 Hydronautics, Inc./Lib

1 Environmental Research and Technology Corp./J. Hayes

1 The Glosten Associates, Inc. B. Hutchison

Copies	
20	CUNY/W. Pierson/Lib
1	U of Michigan/Lib
1	U of Delaware/Lib
2	U of California 1 Lib 1 R. Paulling
2	Webb Institute of Naval Arch. 1 Lib 1 E. Lewis
2	U of Florida 1 Lib 1 D. Harris
1	MIT/Engr Lib
1	Scripps Institution of Oceanography T. Barnett
1	Johns Hopkins U/O. Phillips
1	U of Washington/R. Brown
1	U of Kansas/R. Moore
1	Institute of Storm Research J. Freeman
12	DTIC
1	Scott E. Dillion 9009 Linton St. Silver Spring, MD 20901
1	Edward V. Lewis 97 Plymouth Drive, North Glen Head, New York 11545
1	Dr. M. St. Denis 6750 Hawaii Kai Drive #1301 Honolulu, Hawaii 98625
1	Dr. B. Kinsman Riva, MD 21140

Copies	
1	Dr. D. Chelton JPL 4800 Oak Grove Dr. Pasadena, CA
1	Dr. C.C. Bates 136 West La Pintura Green Valley, AZ 85614
1	NMI/Lib

CENTER DISTRIBUTION

Copies	Code	Name
1	117	
1	15	W. Morgan
1	152	
1	154	
1	156	
1	1561	G. Cox
1	1561	A. Baitis
1	1561	S. Bales
30	1561	
10	5211.1	Reports Distribution
1	522.1	Unclassified Library (C)
1	522.2	Unclassified Library (A)